Interrogating the Role of Cocaine-Generated Silent Synapses in the Regulation of Cocaine-Associated Memory Dynamics

by

William James Wright

B.S., Wofford College, 2015

Submitted to the Graduate Faculty of the

Dietrich School of Arts and Sciences in partial fulfillment

of the requirements for the degree of

Doctor of Philosophy

University of Pittsburgh

2021

UNIVERSITY OF PITTSBURGH

DIETRICH SCHOOL OF ARTS AND SCIENCES

This dissertation was presented

by

William James Wright

It was defended on

June 30, 2021

and approved by

Dr. Oliver Schlüter, Associate Professor, Neuroscience

Dr. Susan Sesack, Professor, Neuroscience

Dr. Mary Torregrossa, Associate Professor, Psychiatry

Dr. Caroline Runyan, Assistant Professor, Neuroscience

Dr. Sachin Patel, Professor, Psychiatry, Vanderbilt University

Dissertation Director: Dr. Yan Dong, Professor, Neuroscience

Interrogating the Role of Cocaine-Generated Silent Synapses in the Regulation of Cocaine-Associated Memory Dynamics

William James Wright

University of Pittsburgh, 2021

Drug addiction is an acquired behavioral state that develops progressively through repeated drug experience and is characterized by maladaptive and compulsive behavior associated with drug seeking and taking. Cravings and subsequent drug seeking are often precipitated by the reactivation of memories associated with drug use, which are formed between various external stimuli, or cues, and the rewarding and pleasurable experience of taking the drug. As such, drug addiction is often conceptualized as a pathological form of memory that drives maladaptive behavior. This has spurred intensive investigation into the neural substrates underlying drug-associated memories, with the ultimate goal of targeting these substrates to disrupt drug seeking behaviors. To explore the synaptic underpinnings of cocaine-associated memories, we studied AMPA receptor (AMPAR)-silent excitatory synapses, which are generated in the nucleus accumbens (NAc) by cocaine experience. These synapses functionally mature during withdrawal through the recruitment of AMPARs and contribute to subsequent cocaine seeking behavior, indicating these synapses contribute to the encoding of cocaine-associated memories and behaviors. In this dissertation, we have further investigated the role of cocaine-generated silent synapses in the encoding of cocaine-associated memories by examining their role in regulating the natural dynamics of cocaine-associated memories. Our results demonstrate that dynamic changes in the functional state of cocaine-generated synapses contributes to the natural destabilization and

reconsolidation of cocaine-associated memories following memory retrieval, and that disrupting these synaptic dynamics impairs subsequent cocaine seeking behaviors. In addition, we also demonstrate that cocaine-generated synapses contribute to the recruitment and activation of neurons within the NAc associated with cocaine seeking behavior during withdrawal, suggesting they may contribute to the encoding of cocaine-associated memories at the circuit level. Collectively, these findings provide further support to the hypothesis that cocaine-generated synapses serve as discrete synaptic substrates underlying aspects of cocaine-associated memories and behaviors.

Table of Contents

List of Figures

Preface

Graduate school has been both one of the most fulfilling as well as one of the most challenging periods of my life. I would like to take this opportunity to express my gratitude to all those who have helped me along the way, for I would not have made it where I am today without them. First, I would like to thank my mentor and dissertation advisor, Dr. Yan Dong. Yan has been a great mentor to me, giving me great independence and space to allow for my scientific growth, while at the same time always challenging me to continuously push me forward. I am grateful for this balanced combination of freedom and guidance that has allowed me to develop into an independent scientist with my own unique perspectives. I would also like to thank my whole committee, Drs. Oliver Schlüter, Susan Sesack, Mary Torregrossa, and Caroline Runyan, for their advice, guidance and feedback, as well as Dr. Sachin Patel for his time and effort in serving as my outside examiner. I also owe a great deal of gratitude to members of the Dong lab who have helped me through the years with their support and friendship. In particular, I would like to thank Drs. Nicholas Graziane and Allen Li. Lastly, I would like to thank my friends and family for their support over the past six years, without which the work in this dissertation would not be possible. I would especially like to thank Dr. Becca Krall, who was always there for me, as well as my parents, for their lifelong care and support.

1.0 Introduction: Maladaptive Learning and Memory Underlying Addiction

Portions of this chapter are adapted from the following manuscripts:

Wright, W.J. & Dong Y. (2020) Psychostimulant-induced adaptations in nucleus accumbens glutamatergic transmission. ***CSHL Perspectives in Medicine****, in press*.

The nervous system is an extraordinary and complex organ system that serves to guide an organism's behavior and maximize survival. Perhaps one of the most striking features of the nervous system compared to other organ systems is its incredible adaptability. Throughout an organism's lifetime, experiences continually shape and reshape the structure and function of the nervous system. These plasticity processes are quite diverse and can range in nature from the highly rapid and transient (e.g. neural gain modulation) to the slow and extremely long-lasting (e.g. circuit remodeling). Yet, almost all of these processes ultimately allow for the modification of behavioral output. Such behavioral adaptation is essential to meet the survival demands in the ever-changing environments organisms live in, and thus plasticity mechanisms are critical for the normal functioning of the nervous system. However, the engagement of these plasticity mechanisms by extreme experiences can go awry and lead to maladaptive behavioral states. One such maladaptive state is drug addiction.

Drug addiction is an acquired behavioral state that develops progressively through repeated drug experience and is characterized by maladaptive and compulsive behavior associated with drug seeking and taking (Koob and Volkow, 2010; Lüscher et al., 2020). Repeated exposure to drugs of abuse induces numerous physiological adaptations throughout the body. These can include the emergence of tolerance to the drug's effects as well as the development of physical

dependence for the drug (Koob and Volkow, 2010; Wise, 1987; Wise and Koob, 2013). While tolerance and physical dependence undoubtedly contribute to the escalation and continuation of drug use, they are relatively transient and can be overcome with periods of forced abstinence. However, the preoccupation and craving for the drug persists through abstinence long after the symptoms of physical withdrawal have subsided, and it is these persistent cravings that serve as the primary drivers for subsequent relapse in drug use (Gawin and Kleber, 1986; Hyman, 2005; Pickens et al., 2011).

Craving and drug seeking are often precipitated by the reactivation of memories associated with drug use, which are formed between various external stimuli, or cues, and the rewarding and pleasurable experience of taking the drug (Everitt and Robbins, 2005; Hyman, 2005; Milton and Everitt, 2012; Torregrossa and Taylor, 2016). As such, drug addiction is often conceptualized as a pathological form of memory that drives maladaptive behavior. Indeed, drug addiction shares many common plasticity mechanisms underlying natural learning and memory, and exhibit typical memory dynamics, including memory acquisition, consolidation, retrieval-induced destabilization, and reconsolidation (Everitt and Robbins, 2016; Kauer and Malenka, 2007; Kelley, 2004; Torregrossa and Taylor, 2013; Wolf, 2016a). This has led to the neuroadaptation theory, which postulates that drugs of abuse harness cellular mechanisms that underlie general learning and memory processes to form addiction-related memories (Hyman et al., 2006a). As a result, a major focus of the addiction research field over the past two decades has been to identify neural adaptations induced by drugs of abuse that alter the function of reward and motivational circuits to promote addiction-related behaviors, with the ultimate hope of targeting them to decrease seeking and usage. However, despite much exciting progress in delineating the neurobiological underpinnings of drug addiction, the discrete and selective substrates underlying drug-associated

memories remains unclear. In this thesis, I attempt to interrogate the function of a specific synaptic population that may represent a selective substrate underlying drug seeking behaviors.

1.1 The Neural Basis of Learning and Memory

At its core, memory is the storage of information that can subsequently be retrieved and utilized at a later time. From a computational viewpoint, memory can also be viewed simply as the persistence of information encoding states over time (Chaudhuri and Fiete, 2016). Such memory systems will also ideally have additional features such as 1) the existence of a sufficient number of states, 2) different states should be sufficiently separable and robust to noise/interference, and 3) the states must be accessible and retrievable given appropriate inputs (stimuli or cues). However, setting up, retaining, and retrieving such states in a biological system is an incredibly daunting task given that biological substrates are inherently transient, decaying over various timescales, and as a result the brain must construct enduring states from temporary building blocks (Chaudhuri and Fiete, 2016).

Understanding how the brain overcomes this significant challenge to produce memory has long been a central goal of neuroscience research and many psychological and physiological theories have been proposed about how memory is achieved. One of the most prominent theories currently is the ‘Engram Theory’, first proposed by Richard Semon over a century ago, which postulates that a given memory is encoded in the brain by a select set of persistent structural and functional changes, termed the memory trace or ‘engram’ (Josselyn et al., 2015; Josselyn and Tonegawa, 2020; Semon, 1921; Tonegawa et al., 2015). Subsequent theories have posited that these persistent changes lead to the formation of cellular assemblies, or neural ensembles, whose

coordinated activity dynamics form representations of information or experiences, which can be reactivated later for the retrieval of these representations (Frankland et al., 2019; Hebb, 1949; Josselyn and Tonegawa, 2020). The remodeling of synaptic connections between neurons by experience has long been theorized to underlie the formation and retention of memory traces (Hebb, 1949; Ramon y Cajal, 1894), such that a collection of these synapses may form a so-called 'synaptic engram' (Josselyn et al., 2015). On the other hand, recent research has focused extensively on sparse neural populations that are selectively activated during the formation and retrieval of a memory, which are hypothesized as engram neurons (Josselyn and Tonegawa, 2020). While debate persists (Langille and Gallistel, 2020; Titley et al., 2017), I support the theory that that the activities of neural ensembles are driven by remodeled synaptic connectivity within the circuit, and, as such, synapses are likely the underpinning units supporting neural ensembles to encode specific memory traces (Poo et al., 2016).

1.1.1 The Role of Synapses and Synaptogenesis in Memory Encoding

By definition, memory engrams are the *changes* that experience induces within the brain to encode experiences. In most cases, neurons exist long before a given memory is formed, so their existence per se does not represent the engram. Rather, some neurons undergo functional changes by 'tuning' their activity to encode experience, and thus become engram neurons functionally. However, this is complicated by observations that individual neurons have multiple functions beyond memory encoding. For example, the activity of hippocampal neurons simultaneously encodes multiple representations, including both continuous spatial information as well as discrete, explicit experiences (Sun et al., 2020a; Tanaka et al., 2018). Furthermore, beyond other non-memory related functions, the same engram neurons often also contribute to multiple memories

(Cai et al., 2016; Rashid et al., 2016; Yokose et al., 2017). Such overlap may be even greater than documented by most studies using early immediate gene (IEG)-dependent methods to statically label engram neurons (Cruz et al., 2014; Khalaf et al., 2018; Reijmers et al., 2007; Sun et al., 2020b), as *in vivo* recording studies suggest the encoding of experience can be distributed across a substantially larger population of neurons (Grewe et al., 2017; Kyriazi et al., 2020; Stefanini et al., 2020). While overlaps between engram neurons may provide a mechanism underlying memory linkage or generalization (Cai et al., 2016; Yokose et al., 2017), they will also lead to interference between memories (Rashid et al., 2016). Thus, engram neurons per se are not likely basic units encoding separable memory traces. Rather, neurons likely operate as multifunctional units and it is their temporal dynamics in combination with other neurons, instead of just which neurons are activated, that generate unique network activity patterns representing a given experience (Gonzalez et al., 2019; Ju and Bassett, 2020; Kyriazi et al., 2018; Ruff et al., 2018; Sussillo, 2014; Yuste, 2015). Therefore, the fundamental neural substrates of a memory should be the long-term adaptations within neurons that drive circuit dynamics encoding an experience and allow for these dynamics to be reactivated and recapitulated. Given that the temporal output of neurons *in vivo* is largely governed by synaptic inputs, long-term synaptic changes that are induced by an experience fit such a profile.

Established synaptic connectivity dictates neural activity dynamics, but it also constrains the range of possible activity patterns within a circuit, and such constraints can limit learning capacity (Oby et al., 2019; Sadtler et al., 2014). Thus, generation of novel circuit activity patterns to encode new experiences likely requires substantial modification of the synaptic connectivity within the circuit. Since it's discovery, synaptic plasticity has been extensively studied, with a vast number of types and mechanisms having been identified (Bliss and Lomo, 1973; Huganir and

Nicoll, 2013; Malenka and Bear, 2004), and there is substantial evidence that synaptic plasticity contributes to learning (Abdou et al., 2018; Hayashi-Takagi et al., 2015; Nabavi et al., 2014; Penn et al., 2017; Rogan et al., 1997; Stuber et al., 2008; Takahashi et al., 2003; Tye et al., 2008; Whitlock et al., 2006; Zhou et al., 2017). However, traditional formulations of models of synaptic plasticity, which emphasize scaling the strength, or weight, of pre-existing synapses in response to precise, coincident spiking activity, have significant limitations in their capacity to encode multiple, behaviorally relevant memories over extended periods of time (for review and discussion see (Magee and Grienberger, 2020)

Theoretical studies modelling memory encoding in artificial neural networks highlight one of the main failings of these plasticity models, namely the occurrence of spontaneous fluctuations in synaptic strength driven by spurious neural activity within the neural network. Such spontaneous fluctuations lead to rapid degradation of the precise synaptic weights encoding a given memory, resulting in catastrophic forgetting (French, 1999; Fusi, 2002; Fusi and Abbott, 2007). Critically, similar spontaneous fluctuations in synaptic strength are also well documented in *in vitro* and *in vivo* experimental observations (for review see (Ziv and Brenner, 2017), indicating these theoretical findings extend to the biological reality. Alternatively, if information is primarily encoded in the patterns of connectivity within circuits, instead of in precise synaptic weights, then fluctuations in strength at individual synapses should have minimal consequence on memory storage. Such a connectivity-based memory encoding schema is supported by recent computational studies, where the formation and elimination of synaptic connections within the circuit significantly increased memory encoding capacity and precision, eliminating catastrophic forgetting, when compared to the modification of synaptic weights alone (Knoblauch et al., 2014; Knoblauch and Sommer, 2016). Interestingly, modification of connectivity patterns also increases

the number of functionally separate neuronal ensembles that can be stably formed, retained, and reactivated within a given neuronal population, similar to the sparse ensembles of engram neurons observed in animals (Josselyn and Tonegawa, 2020; Knoblauch and Sommer, 2016). While remodeling connectivity patterns via generation and elimination of synapses is likely more metabolically costly, such a cost is predicted from modeling work to actually favor modularity within a circuit, which can boost sparse encoding to reduce interference between memories and ultimately increase memory capacity (Ellefsen et al., 2015). Lastly, remodeling the connectivity patterns between neurons qualitatively has the greatest capacity to reshape circuit activity dynamics by altering the ability of neurons to communicate with one another, dramatically changing co-activity patterns (Chklovskii et al., 2004). Thus, despite several unresolved questions, the remodeling of circuit connectivity patterns may serve as a fundamental mechanism underlying the encoding of novel information and memory formation. In contrast, the adjustment of synaptic weights may modulate previously encoded information and incorporate it into the memory trace, which is particularly important when considering that few experiences in adulthood are completely novel and new memories almost always incorporate previously learned information. In other words, synaptic strength may regulate the value or weight of information, while the pattern of synaptic connectivity encodes specificity of the information. This is supported by observations that novel experiences trigger synaptogenesis in the cortex, while re-experiencing them modifies synaptic strength (Hofer et al., 2008).

Although traditionally less extensively focused on, the remodeling of synaptic connectivity patterns is a prevalent form of plasticity throughout the brain (Chklovskii et al., 2004; Holtmaat and Svoboda, 2009). During the induction of long-term potentiation (LTP) and long-term depression (LTD), which are traditionally associated with the scaling of synaptic strength,

synaptogenesis and synaptic elimination also occur, respectively (Bastrikova et al., 2008; Engert and Bonhoeffer, 1999; Hasegawa et al., 2015; Maletic-Savatic et al., 1999; Tominaga-Yoshino et al., 2008; Wiegert and Oertner, 2013). During learning, there is also extensive synaptogenesis and synaptic elimination observed *in vivo*, which are strongly correlated with and causally implicated in memory formation and retention (Chen et al., 2015; Cichon and Gan, 2015; Cole et al., 2012; Fu et al., 2012; Hayashi-Takagi et al., 2015; Holtmaat et al., 2006; Lai et al., 2012; Parkhurst et al., 2013; Vetere et al., 2011; Xu et al., 2009; Yang et al., 2009). In addition, the formation of engram neuron ensembles is also associated with synaptogenesis (Choi et al., 2018; Ryan et al., 2015), and the natural reactivation of these engram neurons during memory retrieval is dependent on this pattern of synaptic connectivity (Roy et al., 2016; Roy et al., 2017b; Ryan et al., 2015), indicating synaptogenesis is critical for engram formation and retention. Importantly, synapses that are generated by an experience are likely to encode information that is specific to that experience. In this case, different groups of encoding synapses co-existing on the same neuron may allow a single neuron to contribute to multiple memories. This scenario is supported by observations that distinct memories are associated with the generation of different populations of synapses on the same neuron, and disrupting the function of one synaptic population impairs only its associated memory and not others (Abdou et al., 2018; Cichon and Gan, 2015; Yang et al., 2014). Such an arrangement could allow for the segregated activation of different synaptic populations and selective feature storage in a single neuron (Cichon and Gan, 2015; Losonczy et al., 2008). Thus, experience-generated synapses may selectively encode a given memory and help drive experience-specific activity dynamics, even in neurons contributing to multiple memories.

The above discussion supports a hypothesis that a memory can be selectively encoded in a specific population of synapses, or a synaptic ensemble, that is generated *de novo* during learning,

similar to previously proposed models (Chklovskii et al., 2004; Holtmaat and Caroni, 2016; Rogerson et al., 2014). Therefore, in searching for the substrates underlying non-overlapping memory traces, we should strive to identify specific sets of synapses. Such synapses will likely have several key characteristics, including 1) they are generated by the learning experience, 2) they critically contribute to subsequent memory recall, and 3) changes in their functional state influence the natural dynamics of a memory.

1.1.2 The Dynamic Nature of Memory Encoding

The formation, storage, and retrieval of memory across time is highly dynamic in nature. Following the initial learning event, memories must undergo a period of consolidation, where the memory becomes stabilized in the brain to allow for its long-term storage (Dudai, 2004, 2012). The process of consolidation occurs over various timescales, from hours to days, as well as at various levels, from molecular to inter-region circuits. Furthermore, during consolidation the neural underpinnings of the memory may change substantially (Asok et al., 2019; Johansen et al., 2011; Klinzing et al., 2019; Tonegawa et al., 2018). Following consolidation and storage, memories continue to be susceptible to modification whenever they are reactivated, when the memory is transiently destabilized and made labile, before it is consolidated once again, or reconsolidated. In addition, other process such as extinction and active forgetting can also influence memory storage and reactivation (Davis and Zhong, 2017; Dunsmoor et al., 2015). Therefore, to understand the neural basis of memory we must also understand how memories change over time.

Consolidation processes serve to stabilize the representation of memories within the brain (Dudai, 2012), and as these representations are dependent on molecular functions to brain-wide

activity dynamics, these process occur at various levels. Molecular mechanisms underlying the consolidation of memory at the synaptic and cellular level have been extensively studied (for reviews see (Alberini and Kandel, 2014; Bailey et al., 2015; Kandel et al., 2014), and generally involve long-lasting molecular adaptations. Briefly, consolidation requires alterations in gene transcription and chromatin structure (Chen et al., 2020; Marco et al., 2020; Rao-Ruiz et al., 2019) as well as *de novo* protein translation (Shrestha et al., 2019; Shrestha et al., 2020), which are thought to induce long-lasting changes in cellular and synaptic function, such as the formation and stabilization of new synapses (De Roo et al., 2008b; Tanaka et al., 2008), which is critical for consolidation (Cole et al., 2012). Indeed, many of the genes upregulated during consolidation are associated with synaptogenesis, synaptic plasticity, and neurotransmission (Chen et al., 2020; Rao-Ruiz et al., 2019). For example, memory consolidation is dependent on the upregulation of the transcription factor CREB, which regulates the transcription of synaptogenic proteins and is sufficient to drive synaptogenesis (Marie et al., 2005; McClung and Nestler, 2003; Murphy and Segal, 1997). Accumulating evidence suggests that these transcriptional and translational processes, and other signal transduction pathways, are critical for the formation and strengthening of synaptic connections involved in memory encoding (Alberini and Kandel, 2014; Asok et al., 2019; Bailey et al., 2015; Johansen et al., 2011; Kandel et al., 2014).

However, in addition to processes directly involved in synaptic remodeling, consolidation also engages processes that serve to stabilize synapses. For example, learning induces the expression of the IEG Arc/Arg3.1, which is specific to activated neurons and synapses (Guzowski et al., 1999; Han et al., 2007; Kelly and Deadwyler, 2002; Link et al., 1995; Lyford et al., 1995; Steward et al., 1998; Steward and Worley, 2001), and is essential for memory consolidation (Guzowski et al., 2000; Plath et al., 2006; Ploski et al., 2008). In addition, Arc/Arg3.1 is also

essential for the maintenance, but not the induction, of LTP *in vitro* and *in vivo* (Guzowski et al., 2000; Messaoudi et al., 2007; Plath et al., 2006). While Arc/Arg3.1 has several functions regulating synapses, these effects are most likely mediated by the actin cytoskeleton, specifically through its inhibition of cofilin, a small actin severing molecule whose inhibition stabilizes the actin cytoskeleton (Cingolani and Goda, 2008; Huang et al., 2007; Ploski et al., 2008) (but see (Bramham, 2008; Bramham et al., 2008) for discussion other functional roles of Arc). During synaptogenesis and LTP, there is an increase in actin polymerization driving morphogenesis and potentiation (Okamoto et al., 2004; Zito et al., 2004), which is subsequently stabilized (Star et al., 2002). Critically, the actin cytoskeleton serves to stabilize the synaptic structural and functional adaptations (Fukazawa et al., 2003; Honkura et al., 2008; Krucker et al., 2000; Rex et al., 2009; Rex et al., 2010), and thus the storage of the memory.

Another stabilizing factor that is critical for memory consolidation is the constitutively active PKC isoform, PKMζ (for review see (Sacktor, 2011). PKMζ is critical for the maintenance of functional and structural synaptic modification (Madroñal et al., 2010; Pastalkova et al., 2006; Ron et al., 2012) as well as for memory consolidation (Serrano et al., 2008; Shema et al., 2011; Shema et al., 2007) but see (Volk et al., 2013). PKMζ serves to stabilize the cytoskeletal structure and receptor content at synapses (Calabrese and Halpain, 2005; Migues et al., 2010; Ron et al., 2012), which is most likely mediated by its role in clustering PSD-95 at the synapse (Shao et al., 2011). PSD-95 is critical for the maturation and stabilization of synapses, including newly generated synapses (Cane et al., 2014; De Roo et al., 2008a; Ehrlich et al., 2007; El-Husseini et al., 2000; Huang et al., 2015a; Meyer et al., 2014; Yusifov et al., 2021), and is critical for long-lasting memories (Elkobi et al., 2008; Fitzgerald et al., 2019; Migaud et al., 1998). Thus, one of

the key functions of consolidation processes at the cellular level is to stabilize synaptic remodeling, including newly formed connections (**Figure 1**).

However, other consolidation processes appear to transform the representation of the memory in the brain (Dudai et al., 2015). One such transformation occurs during the phenomenon of systems consolidation, where memory is initially encoded in one brain region and then gradually transferred to another for long-term storage (see for reviews (Dudai, 2012; Klinzing et al., 2019; Squire et al., 2015; Tonegawa et al., 2018). Systems consolidation has been extensively studied for hippocampal-dependent memories, where memories are initially encoded in the hippocampus and then gradually transferred to the cortex. However, similar systems consolidation processes can occur for other types of memories, such as fear conditioning (Do-Monte et al., 2015; Penzo et al., 2015).

The mechanisms underlying systems consolidation are still quite unclear, however, recent studies have demonstrated that during the initial encoding cortical neurons are activated and 'tagged' (Lesburguères et al., 2011; Tse et al., 2011). This tagging involves epigenetic and transcriptional modification (Lesburguères et al., 2011; Tse et al., 2011; Zovkic et al., 2014), similar to what is observed in cellular consolidation. Following this 'tagging' there is the progressive generation and maturation of new synaptic connections in these neurons, which are necessary for the long-term consolidation of the memory (Aceti et al., 2015; Kitamura et al., 2017; Lesburguères et al., 2011; Restivo et al., 2009; Vetere et al., 2011). This synaptogenesis is also associated with the remodeling of cortical activity dynamics and the formation of cortical engram neuron ensembles (DeNardo et al., 2019; Kitamura et al., 2017; Takehara-Nishiuchi and McNaughton, 2008). Interestingly, the progressive maturation of synapses in cortical ensembles coincides with the loss of synapses in the hippocampus (Kitamura et al., 2017; Restivo et al., 2009),

which corresponds with the loss of memory dependence on the hippocampus. Thus, it appears mechanisms regulating the formation and maturation of new synaptic connections are also involved in systems consolidation, however, with a temporal delay, that results in the migration of memory storage within the brain.

After stabilization during consolidation, memories remain malleable. This is particularly true during recall when the memory is reactivated. During reactivation, memories can be transiently destabilized, where they become labile once again, before they are re-stabilized through another round of consolidation, termed reconsolidation (Dudai, 2012; Nader, 2015; Tronson and Taylor, 2007). The destabilization of memory is thought to provide a mechanism that allows memory content to be updated, which is supported by observations that destabilization appears to occur only when new information (e.g. outcome change) is present during reactivation (Morris et al., 2006; Pedreira et al., 2004; Rodriguez-Ortiz et al., 2008; Winters et al., 2009). Indeed, memory destabilization and reconsolidation has been demonstrated to allow for memory updating in some cases (Flavell et al., 2011; Fukushima et al., 2014; Haubrich et al., 2015; Lee, 2008; Monfils et al., 2009; Schiller et al., 2010; Sevenster et al., 2013).

Compared to consolidation, the mechanisms underlying destabilization and reconsolidation are less well characterized, particularly at the level of the synapse (for review see (Tronson and Taylor, 2007). Evidence suggests that memory destabilization requires glutamatergic signaling and the activation of NMDARs, particularly GluN2B-containing NMDARs (Lopez et al., 2015; Mamou et al., 2006; Milton et al., 2013; Wang et al., 2009). The activation of NMDARs subsequently engages parallel processes that lead to destabilization. One process necessary for destabilization is synaptic protein degradation, mediated by ubiquitination and proteasome activity (Lee et al., 2008; Shehata et al., 2018). Concurrently, NMDAR activation triggers AMPAR

endocytosis at the synapse (Clem and Huganir, 2010; Hong et al., 2013; Lopez et al., 2015; Rao-Ruiz et al., 2011), which are then degraded (Ferrara et al., 2019; Shehata et al., 2018). There is conflicting evidence about the precise dynamics of AMPAR trafficking following memory reactivation, with some reporting only internalization and a resultant synaptic weakening (Doyère et al., 2007; Li et al., 2013b; Lopez et al., 2015; Rao-Ruiz et al., 2011; Shehata et al., 2018), while others report an exchange of typical GluA2-containing calcium impermeable AMPARs (CI-AMPARs) for atypical GluA2-lacking calcium permeable AMPARs (CP-AMPARs) (Clem and Huganir, 2010; Hong et al., 2013). However, *in vivo* studies primarily support the synaptic weakening scenario (Abdou et al., 2018; Doyère et al., 2007; Shehata et al., 2018). Importantly, there is some evidence that this synaptic weakening may occur preferentially at synapses encoding the memory (Abdou et al., 2018; Doyère et al., 2007), although this is difficult to discern as experiments assessed relatively large populations of synaptic inputs. In addition, to alterations in synaptic AMPAR content, there may also be structural changes at synapses as actin dynamics have also been implicated (Rehberg et al., 2010). Together, these findings indicate that during reactivation, synapses are weakened through the internalization and degradation of AMPARs, possibly accompanied by other processes (e.g. actin depolymerization) (**Figure 1**). This may reset the synapse back to a labile and more modifiable state, allowing for the synapse to be altered and allow for memory updating. This is supported by recent findings that AMPAR internalization is necessary for memory updating during reconsolidation (Ferrara et al., 2019; Rao-Ruiz et al., 2011).

Following memory reactivation reconsolidation mechanisms are also engaged. Similar to consolidation, reconsolidation also requires transcription and translation in a time-dependent manner (Da Silva et al., 2008; Huynh et al., 2014; Nader et al., 2000; Sangha et al., 2003). There is some evidence that consolidation and reconsolidation may involve some different processes (e.g.

Zif268, C/EBP, BDNF) (Alberini, 2005; Lee et al., 2004; Taubenfeld et al., 2001; von Hertzen and Giese, 2005), however, these differences may be dependent on differences in brain regions and behavioral procedures (Jones et al., 2001; Milekic et al., 2007; Penke et al., 2014; Radiske et al., 2017). Regardless if consolidation and reconsolidation are truly distinct physiological processes, the mechanisms underlying reconsolidation appear to have the same end result as those involved in consolidation.

Several key signaling pathways critical for memory reconsolidation play an important role in regulating AMPAR trafficking and synaptic stabilization. For example, PKA, ERK, and CaMKII have all been identified to play a role in memory reconsolidation (Duvarci et al., 2005; Kelly et al., 2003; Miller and Marshall, 2005; Rich et al., 2016; Tronson et al., 2006), all of which regulate the trafficking of AMPARs to the synaptic surface (Esteban et al., 2003; Hayashi et al., 2000; Malinow et al., 1989; Zhu et al., 2002). Therefore, it appears one of the functions of signaling pathways triggered during reconsolidation is to regulate the re-insertion of AMPAR at the synapse after their initial internalization during the destabilization of the memory. This is supported by findings that disrupting reconsolidation leads to persistently weakened synaptic transmission (Abdou et al., 2018; Lopez et al., 2015; Shehata et al., 2018). In addition, reconsolidation, similar to consolidation, also appears to promote synaptic stabilization. For example, memory reactivation triggers Arg/Arg3.1 expression in neural ensembles (Han et al., 2007; Han et al., 2009; Lacagnina et al., 2019) and is necessary for memory reconsolidation (Chia and Otto, 2013; Maddox and Schafe, 2011). Similar to consolidation, these effects may in part be due to Arc's regulation of the actin cytoskeleton via the LIMK-cofilin pathway (Lunardi et al., 2018; Medina et al., 2020;

Rehberg et al., 2010), and re-stabilize the synapse. Thus, one of the roles of reconsolidation appears

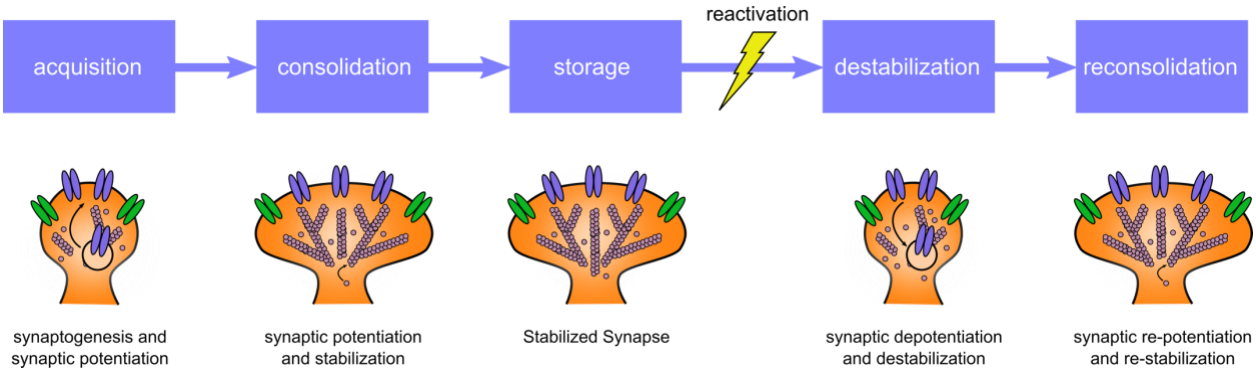

Figure 1. Natural Memory Dynamics and Hypothesized Synaptic Adaptations

Schematic detailing the natural dynamics of memories and the hypothesized synaptic adaptations based on previous findings reviewed in the main text. During the acquisition of a memory there is there is the initial phase of synaptogenesis and synaptic potentiation. These processes continue during consolidation and are stabilized, with actin polymerization likely playing an important role in this stabilization. Once the synapses are stabilized the memory becomes stored in a stable state. Following reactivation during recall, the memory is destabilized and made labile. This corresponds with the depotentiation and destabilization of synapses via the internalization of AMPARs and other processes, such as actin depolymerization. Then during memory reconsolidation synapses are re-potentiated and re-stabilized.

to be the re-stabilization of synapses after they have been destabilized and potentially modified following memory reactivation and updating (**Figure 1**).

Another process that can occur following consolidation, specifically for associative memories, is extinction. During extinction, repeated presentations of the conditioned stimulus without the unconditioned stimulus leads to an attenuation in the behavioral expression of the memory. However, unlike reconsolidation, extinction is generally thought to result from the formation of a new, competing memory, rather than from the modification of the original memory. This idea has originated from observations that similar to other forms of learning, extinction also undergoes phases of acquisition, consolidation, and retrieval, while the original memory is left

intact (for review see (Milad and Quirk, 2012; Quirk and Mueller, 2008)). This is supported by findings showing that extinction is associated with synaptogenesis and synaptic potentiation (Herry and Garcia, 2002; Knackstedt et al., 2010; Lai et al., 2012; Sutton et al., 2003; Trouche et al., 2013). More recent studies have also demonstrated that extinction is mediated by distinct engram neural ensembles (Lacagnina et al., 2019; Warren et al., 2016; Zhang et al., 2020) and is associated with the generation of novel population activity dynamics representing the new association, rather than reversing to the original representation (Grewe et al., 2017). However, there is also evidence that extinction may reverse some of the synaptic adaptations underlying the original memory (Hartley et al., 2019; Lai et al., 2018; Rich et al., 2019a, b), although it is difficult to discern if these adaptations are indeed occurring in the same synapses. As such, extinction may not solely be the formation of a new, competing memory, but also influence aspects of the original memory trace (Dunsmoor et al., 2015).

1.2 Neural Mechanisms Underlying Drug Addiction

Memories that serve to drive the continuation of addiction are associative in nature, where external stimuli associated with drugs of abuse serve to promote behaviors to seek and take the drug. One prominent example of associative memory is classical, or Pavlovian, conditioning, where a previously neutral stimulus (e.g. auditory tone) or environmental context becomes associated with a biologically relevant unconditioned stimulus (US; e.g. foot shock) through repeated pairings (Pavlov, 1927). This transforms the previously neutral stimulus into a conditioned stimulus (CS), such that its presentation alone can trigger a conditioned response, similar to the behavioral response to the US. Another example of associative memory is operant,

or instrumental, conditioning, where an association is made between a behavioral response (e.g. lever press) and a positive or aversive outcome (e.g. food delivery) (Skinner, 1938). This association results in behavioral modification, such as increasing or decreasing behavioral responding to obtain or avoid the associated outcome. The principles of both Pavlovian and operant conditioning are highly relevant for drug-associated memories, where external stimuli become associated with the drug of abuse and its subsequent presentation can serve to drive behaviors to seek and take the drug.

Several models have been developed to recapitulate these associative memory processes in rodents (Belin-Rauscent and Belin, 2012; Marchant et al., 2013). Conditioned place preference (CPP) is one relatively simple model, where rodents receive non-contingent drug injections in one chamber of a multi-chamber box, resulting in the formation of an association between the chamber and the effects of the drug (for review see (McKendrick and Graziane, 2020)). This contextual association leads to subsequent approach behavior towards and increased time spent in the drug-paired chamber, which is used as a behavioral readout of the drug-associated memory. However, a significant limitation of CPP is the absence of volitional drug seeking and taking, and thus it lacks a critical aspect of the human condition. This limitation is overcome by operant drug self-administration models (Belin-Rauscent and Belin, 2012; Epstein et al., 2006; Marchant et al., 2013), where animals are trained to generate a behavioral response (e.g. lever press) to obtain the drug, typically through intravenous administration. Drug administration in these models is also often paired with an additional associative cue (e.g. cue light), resulting in complex associations between the cue, behavioral action, and the drug experience.

There are numerous variants of these self-administration models that have differences during periods of abstinence and subsequent seeking tests (for review see (Marchant et al., 2013)).

These variants each have advantages and disadvantages in examining different aspects of addiction. For example, the widely adopted extinction-reinstatement model has animals undergo operant extinction during abstinence, where they are allowed to press the lever in the absence of drug delivery or cue presentation, resulting in the extinction of the operant response (e.g. lever pressing) and the context. After extinction, reinstatement of seeking can be triggered by the presentation of the drug-associated cue, priming exposure to the drug, or stress, which manifests as a reemergence of operant responding (e.g. lever pressing) despite the absence of the drug. This model is advantageous in that it can allow different aspects of drug-associated memories to be isolated, such as associations related to the cue versus the context. However, as extinction involves additional learning and neural adaptations as discussed above, this can make it difficult to identify neural substrates underling the drug-associated memory versus the extinction memory (Roberts Wolfe et al., 2019; Roberts-Wolfe et al., 2018; Sutton et al., 2003). In addition, there are some views that operant extinction does not accurately replicate the experience of human patients (Epstein et al., 2006; Marchant et al., 2013).

Other self-administration models employ a period of force abstinence, rather than extinction procedures, before testing for seeking behavior in a similar manner as the extinction-reinstatement model. One such model is the incubation of craving model, where under prolonged self-administration conditions, there is a progressive increase in craving, assessed by the level of seeking behavior, during prolonged forced abstinence (Grimm et al., 2001; Pickens et al., 2011). This model has several advantages, such as the lack of influence of extinction learning on observed neural adaptations, while also modeling increases in drug craving during withdrawal, which is seen in human patients (Gawin and Kleber, 1986; Li et al., 2016; Parvaz et al., 2016). However, during the seeking test it can be difficult to discern what variables are driving behavioral responding.

These and other models have been leveraged to great extent in the interrogation of the neural substrates underlying drug-associated memories and drug seeking behaviors. While these models have been utilized to study a variety of different drugs of abuse, the following discussion and this dissertation will focus mostly on the mechanisms underlying cocaine seeking, which may have some similarities and differences to other drugs of abuse.

1.2.1 The Role of the Mesoaccumbal System in Drug Seeking Behaviors

Early studies established that activity in specific regions of the brain is sufficient to drive motivated behaviors, such that animals will work for electrical self-stimulation of these regions, even in the face of aversive consequences (Olds, 1958). Subsequent studies identified the dopaminergic mesolimbic pathway as a critical circuit in driving these motivated behaviors (Fibiger et al., 1987; Koob et al., 1978; Phillips and Fibiger, 1978; Wise and Rompre, 1989). The mesolimbic pathway consists of the ventral tegmental area (VTA) projections to the nucleus accumbens (NAc), in addition to the various inputs and outputs they receive and send respectively (for review see (Sesack and Grace, 2010)) (**Figure 2)**.

The VTA consists primarily of dopaminergic neurons (~60%), but also consists of GABAergic and glutamatergic populations, which project locally and to downstream regions (for review see (Morales and Margolis, 2017). Furthermore, some populations of dopaminergic neurons have also recently been found to co-release glutamate and/or GABA (Stuber et al., 2010; Tecuapetla et al., 2010; Tritsch et al., 2012). In addition to the NAc, the VTA sends extensive projections throughout the brain, including to other brain areas critically involved in the regulation of motivated behavior, such as the basolateral amygdala (BLA) and medial prefrontal cortex (mPFC) (Sesack and Grace, 2010). The activity of dopaminergic neurons plays a critical role in

reinforcement learning and motivational processes (Schultz, 2007, 2016), with their various activity dynamics encoding variables such as reward prediction errors (RPEs) and value (Cohen et al., 2012; Eshel et al., 2015; Hamid et al., 2015; Howe et al., 2013; Mohebi et al., 2019; Schultz et al., 1997) (but see (Kim et al., 2020)), which are thought to contribute to learning and motivation respectively (Berke, 2018; Cagniard et al., 2006; Saunders et al., 2018; Steinberg et al., 2013). While the influence of glutamatergic and GABAergic signaling cannot be discounted (Root et al., 2014; Wang et al., 2015; Zell et al., 2020), these behavioral effects are thought to be mediated primarily through dopaminergic signaling, which can influence neural excitability, presynaptic release, and synaptic plasticity (for review see (Surmeier et al., 2007; Tritsch and Sabatini, 2012)).

Exposure to drugs of abuse, as well as their predictive cues, increases dopaminergic transmission in downstream target regions, such as the NAc and mPFC (Di Chiara and Imperato, 1988; Moghaddam and Bunney, 1989; Phillips et al., 2003; Stuber et al., 2004; Stuber et al., 2005), and this dopaminergic signaling in these regions plays a critical role in the acquisition of drug seeking behaviors (for reviews see (Kelley, 2004; Kelley and Berridge, 2002; Volkow et al., 2017; Wise, 2004; Wise and Rompre, 1989). However, dopaminergic signaling does not appear to always be essential for drug seeking behavior once it has been established, such that infusions of dopamine antagonists in the NAc does not influence the reinstatement of cocaine seeking (Cornish and Kalivas, 2000; McFarland and Kalivas, 2001) (but see (Saunders et al., 2013). This may suggest that one of the critical roles of dopaminergic signaling from the VTA is to serve as a teaching signaling during the learning phase of drug self-administration, whereby dopamine may regulate synaptic plasticity in downstream areas to encode and consolidate drug-related associations (Mameli et al., 2009).

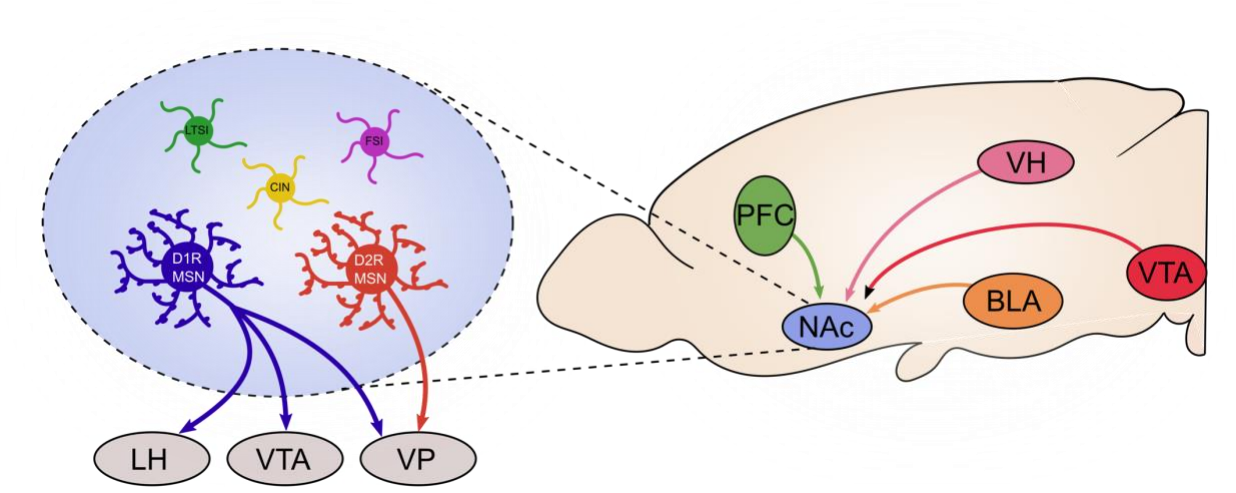

Figure 2. The Mesoaccumbal Circuitry

A simplified schematic showing the major inputs and outputs of the nucleus accumbens (NAc). The central pathway in the mesoaccumbal circuit are dopaminergic projections from the ventral tegmental area (VTA) to the NAc. The NAc receive major glutamatergic inputs from the medial prefrontal cortex (mPFC), ventral hippocampus (VH), and basolateral amygdala (BLA). Within the NAc, the output neurons are MSNs, which comprise the vast majority of neurons within the NAc. MSNs are subdivided into D1R- and D2R-expressing MSNs, which differentially project to the lateral hypothalamus (LH), VTA, and ventral pallidum (VP). Inhibitory fast-spiking interneurons (FSIs) and low-threshold spiking interneurons (LTSIs) as well as cholinergic interneurons (CINs) also form local connections within the NAc.

One of the major downstream targets of the VTA is the NAc within the ventral striatum. The NAc serves as a key node within the neural circuits regulating motivational and reward seeking behaviors, where it is anatomically positioned as an interface between limbic and motor systems to prioritize and translate motivational signals into behavioral output (Mogenson et al., 1980). Similar to dorsal regions of the striatum, the NAc is made up primarily (~90%) of GABAergic medium spiny neurons (MSNs), which project to downstream regions such as the ventral pallidum (VP), VTA, hypothalamus, substantia nigra (SN), and areas of the brainstem to

mediate the primary functions of the NAc (Chang and Kitai, 1985; Kreitzer, 2009; Sesack and Grace, 2010) (**Figure 2)**. In addition, the NAc consists of a variety of inhibitory and cholinergic interneurons, which also play a role in regulating NAc function (Gonzales and Smith, 2015; Kawaguchi et al., 1995; Schall et al., 2020). The NAc is also subdivided into two main sub-compartments, the core and shell. These two subdivisions receive and send overlapping and divergent afferent inputs and outputs, suggesting to separable functions (Sesack and Grace, 2010).

The role of the NAc and its subdivisions have been extensively studied in the regulation of motivated behaviors, including drug addiction. Despite this extensive study, it remains difficult to precisely define its functional role, with several conflicting findings and/or interpretations, and as a result a unified theory detailing the functional roles of the NAc subdivisions is not yet fully established (for review and discussion see (Floresco, 2015)). Some of the controversy may arise from greater functional heterogeneity in the NAc beyond just the two defined compartments (for example see (Al-Hasani et al., 2015)), such that the NAc may contain many functionally divergent neural clusters (Pennartz et al., 1994).

The most prevailing view of NAc function is that it serves a critical role in reward processing, with the core contributing primarily to conditioned reinforcement and the shell to unconditioned reinforcement (Everitt and Robbins, 2005). However, this is likely an oversimplification of the NAc's function, and is difficult to reconcile with several results showing the NAc is not required for obtaining rewards (Corbit and Balleine, 2011; Corbit et al., 2001; Ito et al., 2004; Yin et al., 2008). Rather accumulating evidence indicates the NAc plays a role in action selection, similar to the dorsal striatum, where it integrates cognitive and emotional information to bias and invigorate specific motivated actions (for reviews see (Floresco, 2015; Nicola, 2007). In particular, the NAc appears to play a critical role in the ability of discrete (e.g.

cues) and spatial (e.g. context) information to select, guide, and invigorate actions to achieve signaled goals, including both approach and avoidance (Ambroggi et al., 2011; Ambroggi et al., 2008; Bravo-Rivera et al., 2014; Bravo-Rivera et al., 2015; Corbit et al., 2001; Di Ciano et al., 2001; Floresco et al., 2018; Ghazizadeh et al., 2012; McGinty et al., 2013; Nicola et al., 2004; Parkinson et al., 1999). Studies have also begun to delineate functional differences in the core and shell subdivisions, with the core being found to play a role in directing approach towards goals, while the shell suppresses other actions to stay on task (Ambroggi et al., 2011; Feja et al., 2014; Ghazizadeh et al., 2012; Saunders and Robinson, 2012; Stopper and Floresco, 2011). There is additional evidence that the core may preferentially utilize discrete cues to shape behavioral actions, while the shell utilizes primarily spatial and contextual information (Bossert et al., 2007; Chaudhri et al., 2009; Fuchs et al., 2004b; Fuchs et al., 2008; Ito and Hayen, 2011; Ito et al., 2004; Ito et al., 2008). One interpretation of these two lines of evidence together is that the shell serves to guide the direction of behavior within the environment, and when its function is impaired it may lead to unrewarded actions.

One prominent theory through which the NAc initiates and guides behavior in response to external stimuli is the incentive salience theory (Berridge, 2007), which postulates that dopamine transmission within the NAc attributes incentive salience to stimuli that in turn motivates and invigorates actions towards them. While there are some shortfalls with this theory (for discussion see (Floresco, 2015)), there is substantial evidence that the NAc plays a role in encoding the value and outcome associated with external stimuli. *In vivo* recording studies have demonstrated that neurons throughout the NAc encode value and outcome-related information associated with reward and drug predictive cues (Atallah et al., 2014; Day et al., 2010; Gmaz et al., 2018; Goldstein et al., 2012; Nicola et al., 2004; Ottenheimer et al., 2018; Roesch et al., 2009; Saddoris and Carelli,

2014; Schultz et al., 1992; Setlow et al., 2003; Sugam et al., 2014; West and Carelli, 2016). In terms of the core and shell, however, there appear to be subtle differences in the representation of outcomes. There is some evidence that the core may encode action- and cost-related information associated with the outcome (Morrison and Nicola, 2014; Sugam et al., 2014), while the shell may encode value-related information (Sugam et al., 2014; West and Carelli, 2016). This is supported by findings demonstrating the shell is critical for determining differences in value between rewards (Dalton et al., 2014; Stopper and Floresco, 2011). These and other findings indicate the NAc encodes value- and outcome-related information pertaining to predictive cues, likely taking the form of an associative memory, which is then utilized to guide decision making and action selection (Averbeck and Costa, 2017).

In the context of addiction, the NAc plays a role in promoting drug-seeking behaviors, especially after periods of abstinence (Kalivas et al., 2005; Lüthi and Lüscher, 2014; Wolf, 2016a). As mentioned earlier, extensive evidence has identified glutamatergic transmission within the NAc as a critical mediator. The first wave of evidence came from studies of locomotor sensitization, a phenomenon where repeated drug exposure results in the enhancement of drug-induced locomotion. In cocaine-sensitized rats inhibiting AMPARs in the NAc decreased locomotion to basal levels, eliminating the sensitized component, whereas infusing AMPAR agonists into the NAc without drug challenge is sufficient to induce the expression of locomotor sensitization (Pierce et al., 1996). Subsequent studies extended these findings to self-administration models, where inhibiting AMPARs in the NAc decreases the reinstatement of cocaine seeking after extinction (Cornish and Kalivas, 2000; McFarland and Kalivas, 2001; Xie et al., 2012), with some evidence suggesting the core and shell may preferentially contribute to cue- and context-induced seeking respectively (Fuchs et al., 2004a; Fuchs et al., 2008; Ito et al., 2004; Ito et al., 2008).

Interestingly, the NAc also plays a role in refraining from cocaine seeking if animals have undergone extinction training (Peters et al., 2008a), indicating the NAc may contribute to the formation of extinction-related memories in addition to drug-associated memories.

The NAc receives glutamatergic input from a number of upstream regions, such as the BLA, mPFC, and ventral hippocampus (vHipp), which are thought to convey different types of information to the NAc (for review see (Sesack and Grace, 2010)(**Figure 2**). In general, the BLA projection conveys information related to discrete cues, as well as valence, to promote cue-induced reward seeking (Ambroggi et al., 2008; Stuber et al., 2012), while the hippocampus projection conveys spatial and contextual information to promote context-induced reward seeking (Britt et al., 2012; Ito et al., 2008; Lansink et al., 2009; Trouche et al., 2019). The mPFC transmits more complex information relating to several modalities, including discrete cues, spatial and context, and response inhibition to influence reward seeking (Ghazizadeh et al., 2012; Ishikawa et al., 2008; Kim et al., 2017; Murugan et al., 2017; Otis et al., 2017). This information, along with reward-related information from the VTA, is thought to be integrated within the NAc, where individual neurons receive highly convergent inputs (French and Totterdell, 2002; French and Totterdell, 2003; Xia et al., 2020), and it is then utilized to form value and outcome representations. Importantly, each of these projections is also critically implicated in promoting cocaine seeking behavior following abstinence (Di Ciano, 2004; McFarland et al., 2003; Sjulson et al., 2018; Stefanik and Kalivas, 2013; Stefanik et al., 2012; Zhou et al., 2019). Interestingly, the prelimbic (PL) and infralimbic (IL) subdivisions of the mPFC, which primarily project to the core and shell subdivisions of the NAc, have somewhat opposing effects on cocaine seeking, such that activation of the PL promotes, whereas activation of the IL suppresses, cocaine seeking (Cameron et al., 2019; McFarland et al., 2003; Peters et al., 2008a; Stefanik et al., 2012). However, the role of the

IL in suppressing seeking appears to be dependent on extinction learning (Augur et al., 2016; Peters et al., 2008b), and as such the IL inputs may play a role in encoding new cue and context associations that compete with older ones.

The NAc projects to numerous downstream areas, with some of the most prominent pathways projecting to the VTA, SNr, VP, and LH (for review see (Sesack and Grace, 2010))(**Figure 2**). NAc outputs to these different brain regions have differential effects on drug seeking behaviors. Outputs to the VP, which also encodes reward-associated information (Ottenheimer et al., 2018; Richard et al., 2016; Richard et al., 2018), appears to be the primary pathway driving drug seeking, with its inactivation suppressing cocaine seeking behaviors (McFarland and Kalivas, 2001; Pardo-Garcia et al., 2019; Stefanik et al., 2013). In contrast, NAc outputs to the LH suppress consummatory behaviors (Maldonado-Irizarry et al., 1995; O'Connor et al., 2015; Stratford and Kelley, 1999) and may also play an important role in the extinction of drug seeking behaviors (Gibson et al., 2018; Millan et al., 2010). Projections back to the VTA may also influence ongoing behavior via disinhibition of dopaminergic neurons (Bocklisch et al., 2013; Yang et al., 2017). In addition, this projection may play an important role in the recruitment of dopamine neurons projecting to other striatal areas (Willuhn et al., 2012), which is thought to be critical for the transition to compulsive drug seeking (Everitt and Robbins, 2005, 2016; Lüscher et al., 2020).

The output neurons of the NAc can be subdivided into those that express D1-like (D1 and D5) dopamine receptors (D1R-MSNs) and those that express D2-like (D2, D3, D4) dopamine receptors (D2R-MSNs) (Gerfen et al., 1990). In general, these two MSN subtypes have opposing effects on reward seeking behaviors, with D1R-MSNs promoting, and D2R-MSNs suppressing, reward and drug seeking (Bock et al., 2013; Heinsbroek et al., 2016; Kravitz et al., 2012; Lobo et

al., 2010; Pardo-Garcia et al., 2019). However, such a dichotomous role in behavioral regulation should not be taken in the extreme sense. Growing evidence from the dorsal striatum strongly indicates that the activity of both D1R- and D2R-MSNs is important for sculpting appropriate learned behaviors (Cui et al., 2013; Geddes et al., 2018; Jin et al., 2014; Lee et al., 2020; Markowitz et al., 2018; Meng et al., 2018; Tecuapetla et al., 2016). This also appears to be true within the NAc for guiding reward seeking behaviors, where both D1R- and D2R-MSNs appear important for CPP and discriminative learning (Calipari et al., 2016; Iino et al., 2020; Sjulson et al., 2018). Furthermore, D1R-MSNs can also have opposing effects on behavior depending on their localization and projection patterns (Al-Hasani et al., 2015; Gibson et al., 2018). Thus, while D1R- and D2R-MSNs are capable of opposing each other, their activity is highly coordinated for the successful execution of behavior.

The reviewed findings highlight the importance of the NAc in regulating drug seeking behaviors. The circuitry regulating these behaviors are complex and widespread, with different regions likely performing different processes. The NAc is a critical node within this circuitry, where these diverse forms of information converge and are integrated with one another. This may result in the formation of unique associative representations or memories. For example, the BLA is critical for the formation of CS-US associations and may be sufficient for maintaining such associative memories. However, as this associative information is transmitted to the NAc new information, such as context and value, may become incorporated, forming a more multifaceted associative memory. Furthermore, the NAc may serve as an important link between upstream regions, such as the BLA and mPFC, to downstream areas that ultimately produce behavioral responses. Together, this indicates the NAc as a key brain regions that contributes to the encoding of the complex memories associated with drug use.

1.2.2 Cocaine-Induced Excitatory Synaptic Plasticity in the Nucleus Accumbens

Drugs of abuse, including cocaine, have been extensively shown to induce synaptic adaptations throughout circuits regulating motivated behaviors, including the amygdala, mPFC, dorsal striatum, and VTA (Kauer and Malenka, 2007; Lüscher and Malenka, 2011; Nestler and Lüscher, 2019; Wolf, 2016a). However, one of the most studied regions has been the NAc, which undergoes a number of different functional adaptations following exposure to cocaine. Synaptic strength can be modified through presynaptic (e.g. release probability) and/or postsynaptic mechanisms (e.g. number of receptors). Both types of synaptic adaptations have been identified within the NAc after cocaine exposure, however, it is less clear how presynaptic plasticity contributes to cocaine seeking. Therefore, I will focus on postsynaptic adaptations (for discussion of presynaptic plasticity see (Wright and Dong, 2020)).

After withdrawal from non-contingent cocaine exposure, AMPAR-mediated glutamatergic synaptic strength in NAc MSNs is persistently increased (Boudreau and Wolf, 2005; Kourrich et al., 2007). Subsequent studies extended these findings to self-administration models (Anderson et al., 2008; Conrad et al., 2008; Gipson et al., 2013b; Ortinski et al., 2012), albeit with some distinct differences. In addition to quantitatively upregulating AMPARs, cocaine exposure also leads to qualitative changes in AMPARs within the NAc. In naïve animals, the vast majority (~95%) of AMPARs in NAc MSNs contain GluA2 subunits and are calcium impermeable (CI-AMPARs). However, following long-term withdrawal from cocaine self-administration, GluA2-lacking AMPARs, which are calcium permeable (CP-AMPARs) are expressed and accumulate (Conrad et al., 2008; Wang et al., 2018). In general, the accumulation of CP-AMPARs is more reliably detected after more intensive and prolonged self-administration conditions that result in the progressive intensification of cocaine seeking, or the incubation of craving, during withdrawal, but

not after non-contingent exposure or shorter self-administration procedures (McCutcheon et al., 2011b; Purgianto et al., 2013). However, there is growing evidence that CP-AMPARs may also accumulate under these conditions, but is perhaps limited to specific synaptic populations (Pascoli et al., 2014; Shukla et al., 2017; Terrier et al., 2016). Subsequent studies have shown that this synaptic potentiation is critical for cocaine seeking behaviors following withdrawal (Lee et al., 2013; Loweth et al., 2014; Ma et al., 2014; Pascoli et al., 2014; Wang et al., 2018; Zhou et al., 2019), demonstrating a causal role of synaptic remodeling within the NAc for the persistence of drug-induced behavioral modification.

Several mechanisms have been identified to drive cocaine-induced synaptic potentiation within the NAc, which share many similarities to the induction and expression of traditional LTP (Malenka and Bear, 2004). For example, NMDARs, which are critical for LTP induction (Kauer et al., 1988; Morris et al., 1986), have been shown to be critical for cocaine-induced synaptic potentiation in the NAc (MacAskill et al., 2014). In addition to NMDARs, dopaminergic signaling also likely plays a critical role in the upregulation of AMPARs in the NAc. Activation of D1Rs phosphorylates and promotes synaptic insertion of AMPARs in the NAc (Chao et al., 2002a; Chao et al., 2002b; Mangiavacchi and Wolf, 2004). Furthermore, self-stimulation of dopamine neurons is sufficient to upregulated NAc AMPARs, mimicking the effects of cocaine (Pascoli et al., 2015). Given that dopaminergic signaling is significantly modulated by cocaine, and plays a role in the acquisition of drug seeking behaviors, dopamine likely serves as a teaching signal to induce synaptic remodeling that ultimately leads to the long-term behavioral modification underlying persistent drug seeking. This is supported by observations that cocaine's effects of AMPAR composition is dependent on its ability to increase dopamine levels (Brown et al., 2010). Furthermore, enhanced VTA dopaminergic signaling to the NAc is critical for AMPAR

upregulation in MSNs after repeated cocaine exposure (Mameli et al., 2009). Thus, activation of NMDARs and dopamine receptors appear to be important initial steps in the upregulation of AMPARs in the NAc and acquisition of drug seeking behaviors.

Intracellular signaling pathways coupled to NMDARs and dopamine receptors likely serve as mediators regulating changes in AMPAR trafficking and stabilization induced by cocaine exposure. Two prominent pathways linked to cocaine-induced synaptic plasticity involve CaMKII and cAMP-PKA signaling. Calcium influx through open NMDARs activates CaMKII, which phosphorylates the c-terminal domain of the GluA1 subunit of AMPARs at Ser831, resulting in the synaptic targeting and stabilization of GluA1-containing AMPARs (Barria et al., 1997; Hayashi et al., 2000; Lee et al., 2003; Lu et al., 2010; Poncer et al., 2002). CaMKII has also been demonstrated to promote the enlargement of dendritic spines and stabilize synaptic structure (Lee et al., 2009; Okamoto et al., 2007; Robison et al., 2013). After withdrawal from cocaine, the basal level of active CaMKII is elevated in the NAc, corresponding with the increased expression of synaptic AMPARs (Boudreau et al., 2009; Ferrario et al., 2011). Conversely, inhibition of CaMKII impairs the acquisition of cocaine and amphetamine self-administration as well as the reinstatement of drug seeking after withdrawal (Anderson et al., 2008; Loweth et al., 2013). As such, CaMKII signaling likely plays an important role in regulating drug-induced synaptic remodeling that underlies subsequent behavioral adaptation.

D1R activation results in increased cAMP production and PKA activity, while D2R activation can suppress it (Surmeier et al., 2007; Tritsch and Sabatini, 2012). Given cocaine and its associated cues trigger phasic dopamine release in the NAc (Phillips et al., 2003; Stuber et al., 2005), there is likely dynamic changes in PKA activity within the NAc during self-administration acquisition, as has recently been shown for food-reward learning (Lee et al., 2020). Indeed, the

inhibition of NAc D1R-cAMP-PKA signaling pathway impairs the acquisition of cocaine self-administration and other cocaine-associated learning, suggesting a critical role of this pathway (Anderson et al., 2008; Caine et al., 2007; Pisanu et al., 2015; Self et al., 1998). While PKA activity is typically transient (Tang and Yasuda, 2017), cocaine self-administration has been found to increase basal PKA activity in the NAc, which persists through withdrawal (Lu et al., 2003). Importantly, inhibition of NAc PKA results in long-lasting impairments in cocaine seeking and the consolidation of cocaine CPP (Cervo et al., 1997; Lynch and Taylor, 2005). These long-term behavioral effects may stem from PKA-mediated upregulation of GluA1-containing AMPARs (Esteban et al., 2003; Mangiavacchi and Wolf, 2004). Interestingly, PKA-mediated trafficking of GluA1-containing AMPARs results in their insertion primarily to extrasynaptic sites, followed by translocation to the synaptic sites upon activation of NMDAR-CaMKII signaling (Esteban et al., 2003; Gao et al., 2006; Passafaro et al., 2001; Sun et al., 2005), suggesting cross-talk between NMDAR-CaMKII and D1R-cAMP-PKA signaling pathways in driving cocaine-induced synaptic potentiation.

In addition to the direct activation of signaling pathways that regulate AMPAR trafficking, such as CaMKII and PKA, other pathways that mediate longer lasting changes in transcription and translation are also activated by cocaine exposure. For example, cocaine exposure activates ERK (Boudreau et al., 2007; Ferrario et al., 2011) and CREB (Mattson et al., 2005). Both ERK and CREB regulate the transcription and translation of several proteins involved in synaptic plasticity and synaptogenesis (Derkach et al., 2007; McClung and Nestler, 2003). Furthermore, ERK and CREB have been demonstrated to contribute to cocaine-induced synaptic plasticity within the NAc, as well as to long-lasting adaptations to drug seeking behavior (Brown et al., 2011a; Carlezon et al., 2005; Lu et al., 2006; Pascoli et al., 2013). These, and other epigenetic and transcriptional

adaptations likely play a critical role in the long-term synaptic remodeling of NAc circuitry contributing to the persistence of drug-seeking behaviors (for reviews see (Carlezon et al., 2005; Dong and Nestler, 2014; Lu et al., 2006; Nestler and Lüscher, 2019).

While the synaptic adaptations discussed thus far primarily pertain to experience-dependent and Hebbian-like plasticity mechanisms, there is also evidence that homeostatic plasticity mechanisms contribute to cocaine-induced synaptic remodeling. Homeostatic plasticity is the adjustment of synaptic strength or membrane excitability, which often interact with one another, up or down to maintain a stable functional output of neurons in response to "unexpected" changes (Davis, 2013; Turrigiano, 2008). For example, changes in synaptic input induce changes in the membrane excitability of MSNs to compensate, and vice versa, which is termed "synapse-membrane homeostatic cross talk" (SMHC) (Ishikawa et al., 2009). In the NAc, GluN2B-containing NMDARs serve as 'sensors' of overall synaptic strength, which is conveyed through coupled CaMKII signaling to regulate membrane excitability (Wang et al., 2018). Following cocaine exposure, GluN2B-NMDARs are upregulated (Brown et al., 2011a; Huang et al., 2009), which generates a false signal of an increased synaptic strength and triggers a decrease in membrane excitability via SK2 channel upregulation (Wang et al., 2018). This decrease in neuronal excitability subsequently leads to synaptic strengthening through the accumulation of CP-AMPARs, and importantly, disrupting this process impairs cocaine seeking behaviors after withdrawal. Therefore, homeostatic plasticity mechanisms are also important for the development of long-term behavioral adaptation driving persistent cocaine seeking.

As discussed above, the NAc receives excitatory inputs from several different brain regions, each of which conveys different types of information to ultimately influence behavior. Recent optogenetic studies have demonstrated that following withdrawal from cocaine exposure,

glutamatergic synapses on MSNs originating from the mPFC, BLA, vHipp, and PVT are all potentiated to some extent (Britt et al., 2012; Joffe and Grueter, 2016; MacAskill et al., 2014; Pascoli et al., 2014; Pascoli et al., 2013; Terrier et al., 2016; Zhou et al., 2019). The mechanisms and features of these potentiated synapses, however, differ from one another. For example, IL-to-NAc synapses are potentiated in part through the upregulation of CP-AMPARs, while in contrast PL-to-NAc synapses are potentiated primarily via upregulation of CI-AMPARs (Ma et al., 2014; Pascoli et al., 2014; Pascoli et al., 2013). Similar to IL inputs, the potentiation of BLA-to-NAc projections is also associated with the synaptic incorporation of CP-AMPARs (Lee et al., 2013; Ma et al., 2016; Terrier et al., 2016). In contrast, potentiation of neither vHipp-to-NAc synapses nor PVT-to-NAc synapses is associated with CP-AMPARs (Neumann et al., 2016b; Pascoli et al., 2014). Importantly, the potentiation of these different inputs to the NAc differentially influences cocaine seeking behaviors. Reversing cocaine-induced synaptic strengthening of mPFC-to-NAc synapses via optogenetic induction of LTD impairs subsequent cocaine seeking (Pascoli et al., 2014). However, the PL and IL projections have differential effects, with depotentiation of PL-to-NAc synapses reducing cocaine seeking behavior, whereas weakening IL-to-NAc synapses enhances seeking (Ma et al., 2014). Reversing or preventing cocaine-induced strengthening of either BLA-to-NAc or vHipp-to-NAc synapses also decreases cocaine seeking behaviors (Lee et al., 2013; Pascoli et al., 2014; Zhou et al., 2019), which may be due to compromises in cue- and contextual associations respectively. In contrast to these other pathways, disrupting transmission at PVT-to-NAc synapses does not affect cocaine seeking after withdrawal (Neumann et al., 2016b). This may suggest PVT-to-NAc projections contribute to other aspects associated with drug use, such as their aversive qualities (Zhu et al., 2016).

In addition to pathway-specific synaptic remodeling, evidence also indicates that cocaine exposure may differentially remodel synapses onto D1R- and D2R-MSNs. Most studies thus far have found that cocaine-induced synaptic strengthening primarily occurs in D1R-MSNs (Bock et al., 2013; Dobi et al., 2011; Pascoli et al., 2014; Pascoli et al., 2013; Zhou et al., 2019), which is consistent with the prominent role of D1Rs in regulating AMPAR trafficking discussed above. This appears to occur at synapses receiving inputs from the BLA, mPFC, vHipp, and PVT (Joffe and Grueter, 2016; MacAskill et al., 2014; Pascoli et al., 2014; Zhou et al., 2019). Furthermore, cocaine-induced synaptic strengthening may also be selective for D1R-MSNs that specifically project to the VP versus those projecting to the VTA (Baimel et al., 2019). In contrast to D1R-MSNs, different studies have reported mixed findings on cocaine-induced synaptic modification in D2R-MSNs, with some reporting no changes (Pascoli et al., 2014), potential weakening (Kim et al., 2011), and strengthening (Bock et al., 2013; Terrier et al., 2016). These different findings may be due to differences in in cocaine exposure and self-administration procedures. Regardless, however, it appears cocaine exposure primarily strengthens synapses on D1R-MSNs, which may ultimately serve to drive cocaine seeking behaviors.

1.2.3 Mechanisms and Functions of Cocaine-Generated Silent Synapses

Extensive evidence has demonstrated that cocaine exposure triggers synaptic plasticity and remodeling within the NAc, which is thought to underlie a key substrate underlying aspects of cocaine-associated memories. As is often the case with synaptic plasticity, these adaptations are most commonly conceptualized as the modification of pre-existing functional synapses. However, as discussed earlier, simply modifying the weights of pre-existing synapses may have limited capacity for the long-term encoding and storage of memories. Instead the generation of new

functional synapses may provide fundamental substrates for the encoding of cocaine-associated memories.

During brain development, immature excitatory synapses often contain only NMDARs without functionally stable AMPARs, and are thus called AMPAR-silent synapses (Kerchner and Nicoll, 2008). After development, the rate of synaptogenesis and number of silent synapses decline to low levels (Durand et al., 1996; Petralia et al., 1999), but synaptogenic capacity remains throughout adulthood to contribute to experience-induced synaptic remodeling (Holtmaat and Svoboda, 2009). Under many learning conditions, new excitatory synapses are generated in the adult brain, which, similar to nascent silent synapses seen during development, often have an initially thin or filopodia-like postsynaptic structure, and then undergo gradual enlargement (Holtmaat et al., 2006; Knott et al., 2006), a process corresponding to functional maturation via incorporation of AMPARs (Matsuzaki et al., 2004). Similar generation of silent synapses has been observed during fear conditioning and likely other learning processes (Ito et al., 2015; Ito and Morozov, 2019; Suvrathan et al., 2013). Thus, silent synapse-based synaptogenesis may serve as a basic and generalized strategy for certain learning processes to remodel related neural circuits for memory encoding.

Exposure to cocaine and amphetamine increases the density of dendritic spines on NAc MSNs (Robinson et al., 2001; Robinson and Kolb, 1997, 1999), suggesting synaptogenesis. Mirroring these findings, cocaine exposure also induces the generation of silent synapses in NAc MSNs (Brown et al., 2011a; Huang et al., 2009; Koya et al., 2012; Whitaker et al., 2016). Several features of these cocaine-generated silent synapses are consistent with nascent, immature synapses; 1) they are enriched in GluN2B-containing NMDARs (Brown et al., 2011a; Huang et al., 2009; Wang et al., 2021), a hallmark of immature glutamatergic synapses (Kirson and Yaari,

1996; Monyer et al., 1994; Tovar and Westbrook, 1999), 2) the majority of cocaine-generated silent synapses are not due to AMPAR internalization at pre-existing synapses, as blocking AMPAR endocytosis does not prevent silent synapse generation (Graziane et al., 2016), 3) cocaine-induced generation of silent synapses is correlated with a selective increase in thin and filopodia-like spines (Graziane et al., 2016), and preventing silent synapse generation abolishes these cocaine-induced effects on spine densities (Wang et al., 2020). These results argue that cocaine-generated silent synapses are a discrete set of new synapses related to cocaine experience.

The mechanisms governing experience-induced synaptogenesis in the adult brain are complex and remain incompletely understood (Südhof, 2018; Waites et al., 2005). To date, several mechanistic processes underlying cocaine-induced generation of silent synapses have been characterized, which share many similarities to those implemented during developmental synaptogenesis (Dong and Nestler, 2014) (**Figure 3**). One key process identified involves the upregulation of CREB activity, as well as other transcriptional pathways, which promote the transcription of synaptogenic proteins (McClung and Nestler, 2003) and drives the generation of silent synapses (Brown et al., 2011a; Grueter et al., 2013; Marie et al., 2005). Another essential process is the synaptic insertion of GluN2B-containing NMDARs (Huang et al., 2009; Wang et al., 2021)(**Figure 3**), an NMDAR subtype critically involved in synaptogenesis and silent synapse generation during both development and adulthood (Chung et al., 2017; Gambrill and Barria, 2011; Nakayama et al., 2005; Tovar and Westbrook, 1999). A recent study has also suggested that GluA2-containing AMPARs are inserted simultaneously with GluN2B-NMDARs during the initial generation of synapses following cocaine experience. However, these AMPARs are unstable and quickly internalize, resulting in an AMPAR-silent state shortly after (Wang et al.,

2021)(**Figure 3**). Such a two-step process is again reminiscent of synaptogenesis during

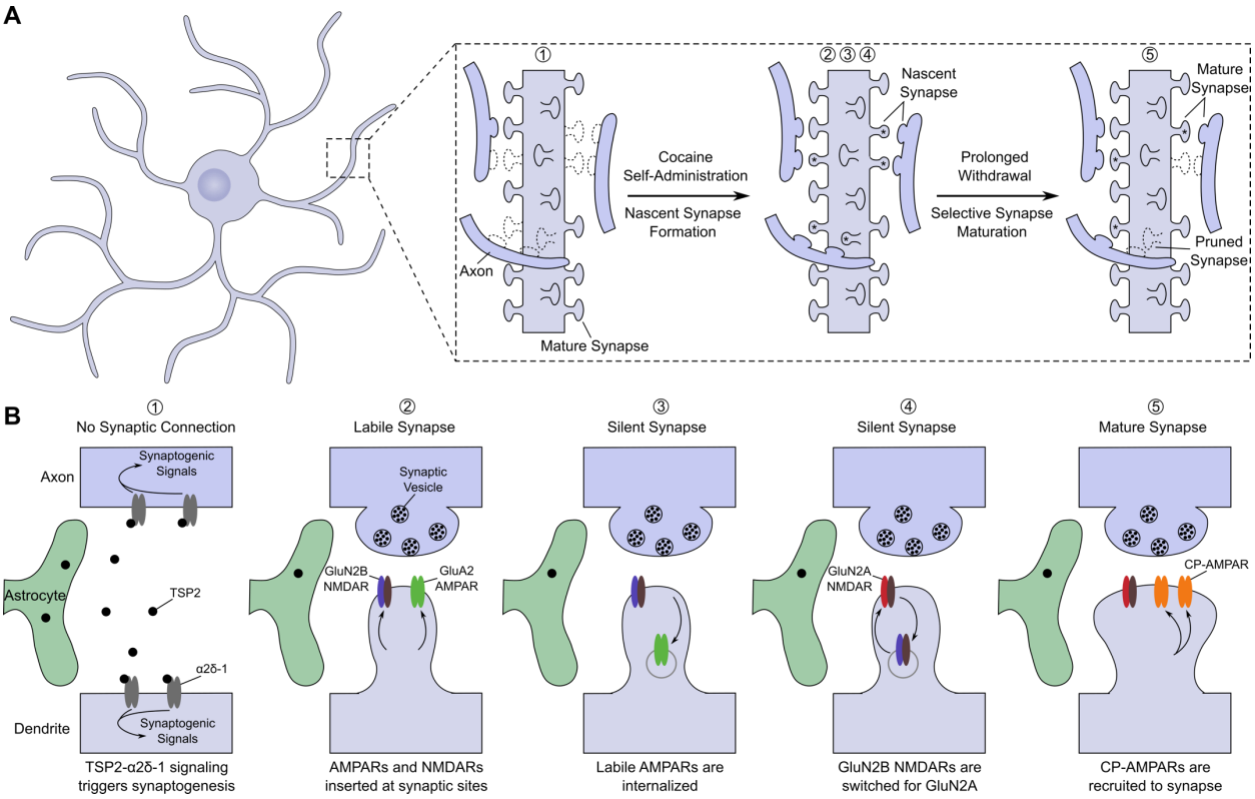

Figure 3. Cocaine-Induced Generation of Silent Synapses in the NAc

(A) Schematic depiction of synaptogenesis in a MSN within the NAc during and following cocaine self-administration. During self-administration training, nascent, immature synapses are generated along the dendritic arbor, forming new connections. During withdrawal, some of these synapses mature into functional synapses, while others are presumably pruned away. Numbers correspond to the stages depicted in panel B. **(B)** Illustration of the stages of cocaine-induced synapse generation and maturation. During cocaine self-administration, astrocytes release TSP2, which binds to neuronal α2δ-1 receptors, triggering synaptogenic processes. This leads to the generation of new synapses, which contain both GluN2B-containing NMDARs and GluA2-containing AMPARs. These AMPARs, however, are highly labile and are shortly internalized, resulting in silent synapses containing only NMDARs. During early withdrawal, GluN2B-containing NMDARs are replaced with GluN2A-containing NMDARs. This is critical for the subsequent functional maturation of the synapse mediated by the recruitment of CP-AMPARs to the synapse.

development, where AMPARs and NMDARs are transported to nascent synapses, but AMPARs are highly labile and readily removed (Groc et al., 2006; Washbourne et al., 2002; Xiao et al., 2004).

In addition to neuronal mechanisms, cocaine-induced generation of silent synapses also requires an astrocyte-mediated synaptogenic signaling pathway. Specifically, cocaine experience induces astrocytic release of thrombospondin-2, which, in turn, activates its neuronal receptor α2δ-1, promoting silent synapse generation in the NAc (Wang et al., 2020) (**Figure 3**). This and other astrocytic pathways have been critically implicated in synapse generation, maintenance, and elimination during both development and adulthood (for reviews see (Allen and Eroglu, 2017; Eroglu and Barres, 2010)). The signals downstream of α2δ-1 receptor activation driving cocaine-induced synaptogenesis have yet to be delineated, however, one interesting candidate are small Rho-GTPases, which dynamically regulate the actin cytoskeleton to influence synaptic generation, stabilization, and plasticity (for reviews see (Hedrick and Yasuda, 2017; Hering and Sheng, 2001; Koleske, 2013; Nishiyama and Yasuda, 2015; Yasuda, 2017). Indeed, α2δ-1 synaptogenic functions have been linked with Rac1 activity (Risher et al., 2018), as has cocaine-induced synaptogenesis (Dietz et al., 2012b), suggesting a potential link between α2δ-1 and Rac1 in the generation of silent synapses by cocaine experience.

After cocaine experience, silent synapses do not exist for long, but return to basal levels after several days of withdrawal (Huang et al., 2009; Lee et al., 2013). In general, nascent synapses follow two possible fates: 1) to mature and be incorporated into the existing circuitry, or 2) to be eliminated. The first scenario is supported by observations that the increase in spine density following cocaine experience persists through withdrawal, and importantly, it is accompanied by a conversion of thin/filopodia-like spines to mushroom-like spines, suggesting synaptic maturation

(Graziane et al., 2016). Furthermore, the disappearance of silent synapses corresponds with an upregulation of AMPARs, specifically atypical CP-AMPARs, and blocking CP-AMPARs unmasks the matured silent synapses after withdrawal (Lee et al., 2013; Ma et al., 2014; Ma et al., 2016).

Recent results have begun to identify key mechanistic steps underlying the functional maturation of cocaine-generated silent synapses (**Figure 3**). First, it appears that GluN2B-containing NMDARs regulate the rate of maturation. During development, GluN2B-NMDARs at nascent glutamatergic synapses inhibit AMPAR insertion, maintaining the synapses in their AMPAR-silent state (Adesnik et al., 2008; Gray et al., 2011), and subsequent synaptic maturation through AMPAR stabilization coincides with a switch from GluN2B to GluN2A (Chavis and Westbrook, 2001; Cohen-Cory, 2002; Monyer et al., 1994). Mirroring this developmental process, GluN2B-NMDARs at cocaine-generated synapses are replaced with non-GluN2B-NMDARs during cocaine withdrawal, presumably by GluN2A-NMDARs, and this replacement is required for the maturation of cocaine-generated synapses, such that disrupting this process keeps cocaine-generated synapses in an immature, silent state (Huang et al., 2009; Wang et al., 2021). Second, the recruitment and stabilization of AMPARs at newly matured silent synapses during cocaine withdrawal appears to require coordinative interactions between PSD scaffold proteins. MAGUKs, particularly PSD-95, stabilize synaptic AMPARs within the PSD, while genetic deletion of PSD-95 results in high basal levels of silent synapses in the adult brain (Béïque et al., 2006; Cane et al., 2014; Ehrlich et al., 2007; El-Husseini et al., 2000; Favaro et al., 2018; Huang et al., 2015a; Meyer et al., 2014). Upon PSD-95 knockout or knockdown, cocaine experience still generated silent synapses in NAc MSNs, suggesting intact generation processes, however, these synapses do not

mature after prolonged withdrawal, indicating failed insertion and/or stabilization of AMPARs (Shukla et al., 2017).

One interesting observation about the maturation of cocaine-generated silent synapses is that it occurs with a delay following the cessation of drug use, typically emerging after 7-10 days of abstinence (Huang et al., 2009; Lee et al., 2013). This is similar to the time course of synaptic strengthening seen in NAc MSNs (see previous section) (Boudreau et al., 2007; Kourrich et al., 2007). Given that silent synapses are highly plastic synapses and key substrates for the expression of long-term potentiation (Arendt et al., 2013; Chung et al., 2017; Isaac et al., 1995; Liao et al., 1995; Morita et al., 2013; Nakayama et al., 2005; Poncer and Malinow, 2001; Shi et al., 2001; Suvrathan et al., 2013), it is possible that the maturation of silent synapses underlies a significant proportion of synaptic potentiation observed during the withdrawal from cocaine.

Cocaine-associated memories and behaviors are multi-faceted, containing information related to unconditioned responses, contextual and discrete cues, value, actions, and outcomes. Cocaine-generated silent synapses and the resulting circuit remodeling contribute to some, but not all, aspects of the cocaine-associated memories. Preventing cocaine-induced generation of silent synapses in the NAc does not prevent the acquisition of cocaine self-administration, suggesting that NAc silent synapses are not involved in unconditioned stimulus-driven instrumental learning (Wang et al., 2020). This is consistent with previous findings that the NAc does not contribute to the acquisition of cocaine self-administration, nor instrumental learning during goal-directed behaviors (Corbit et al., 2001; Ito et al., 2004; Jonkman and Everitt, 2011). Rather, as discussed earlier, the NAc contribute to the encoding of value and outcomes associated with conditioned stimuli. Consistent with this viewpoint, in animals trained to self-administer cocaine, which normally exhibit robust cocaine seeking behavior after prolonged drug withdrawal, preventing

NAc silent synapse generation during self-administration, or weakening these synapses after their maturation, impairs cocaine seeking after forced withdrawal, as well as cue-induced reinstatement of seeking after extinction (Lee et al., 2013; Ma et al., 2014; Ma et al., 2016; Wang et al., 2020). Furthermore, these manipulations do not affect learning to extinguish cocaine seeking in the absence of conditioned cues, nor the general motivation to obtain cocaine (Wang et al., 2020), suggesting cocaine-generated synapses in the NAc may preferentially encode conditioned associations contributing to the overall cocaine memory.

As discussed above, NAc MSNs receive convergent glutamatergic projections from several limbic and paralimbic areas, with each projection though to transmit different information related to the cocaine experience. Cocaine-generated silent synapses have been detected in all projections examined thus far, including the BLA, PL and IL subdivisions of the mPFC, and PVT (Lee et al., 2013; Ma et al., 2014; Neumann et al., 2016b), and may be present in other projections, such as the vHipp, that have not yet been investigated. Early evidence suggests that cocaine-generated synapses in different projections may contribute differentially to cocaine-related behaviors. For example, silent synapses receiving inputs from the BLA and PL promote cocaine seeking after withdrawal, while in contrast those receiving input from the IL suppress this behavior (Lee et al., 2013; Ma et al., 2014). These divergent effects, in combination with the previous findings discussed earlier, raises the possibility that cocaine-generated synapses within different NAc afferents receive different types of information, such as discrete and spatial cues, to the same NAc MSNs where they may be integrated. Thus, cocaine-generated synapses dispersed in different afferents may collectively form a synaptic ensemble that encodes a broader multifaceted representation of the cocaine experience.

1.3 Summary and Dissertation Goals

It has become increasingly clear that the formation of maladaptive memories associated with drug use is a critical component of addiction, particularly in driving relapse after periods of abstinence. This has spurred intensive investigation to identify the neural substrates underlying drug-associated memory and the persistence of drug seeking behavior. Given the long-theorized role of synapses and synaptic plasticity in the encoding of memories, much focus has been placed on examining synaptic adaptations within the brain's reward circuitry. One node within this circuitry that has received particular attention is the NAc, which plays a critical role in driving persistent drug seeking after withdrawal. Extensive evidence indicates that the strengthening of excitatory synaptic inputs to the NAc underlies persistent cocaine seeking and may form the substrates for aspects of cocaine-associated memories. However, despite this progress, most studies have been constrained to the changes assessed from functionally heterogeneous neuronal and synaptic populations that are broadly implicated in reward responses rather than unique to drug addiction. For example, it has been shown that cocaine self-administration potentiates vHipp inputs to D1R-MSNs to promote subsequent seeking (Pascoli et al., 2014; Zhou et al., 2019). However, potentiated vHipp transmission to NAc D1-MSNs also promotes seeking for natural rewards (LeGates et al., 2018). Thus, this adaptation is still rather broad to be considered a selective substrate underlying cocaine seeking, as these different memories would likely involve different subsets of synapses within this projection. To precisely manipulate cocaine-associated memories and behaviors, it is important to identify discrete synaptic substrates that are specific for such memories.

Recent studies have identified a population of immature, AMPAR-silent synapses that are generated within the NAc by cocaine experience through synaptogenesis. Importantly, following

their functional maturation during withdrawal, this discrete synaptic population has been demonstrated to contribute to subsequent cocaine seeking, possibly through the encoding of conditioned associations. Given that these synapses are generated by cocaine experiences, thus likely encoding information relatively selective and specific for cocaine, and contribute to subsequent behavioral recall after withdrawal, these cocaine-generated synapses may represent a specific population of synapses, or a synaptic ensemble, that selectively encodes aspects of cocaine memories. The goal of this dissertation is to continue to delineate how this population of cocaine-generated synapses in the NAc contributes to the encoding of cocaine-associated memories. Specifically, I aim to determine if changes in the functional state of cocaine-generated synapses underlies the natural dynamics of cocaine-associated memories, namely destabilization and reconsolidation, which is expected if these synapses indeed encode cocaine-associated memories. In addition, I also aim to determine how cocaine-generated synapses shape population activity dynamics of NAc MSNs contributing to the encoding cocaine seeking behaviors.

Utilizing a combination of behavioral, electrophysiological, and optogenetic approaches, I show that the reactivation of cocaine-associated memories triggers a transient re-silencing of cocaine-generated synapses within the NAc, followed by their re-maturation, and that this process contributes to the reconsolidation of cocaine-associated memories (Chapter 2). Furthermore, I identify the small GTPase Rac1 as a molecular switch that regulates the stability of cocaine-generated synapses, which can be targeted to control synaptic states and behavior (Chapter 3). Lastly, I demonstrate that cocaine-generated synapses contribute to the recruitment and activation of neurons within the NAc associated with cocaine seeking behavior (Chapter 4). These results provide further support that cocaine-generated synapses serve as discrete synaptic substrates underlying aspects of cocaine-associated memories and behaviors.

2.0 Cocaine-Generated Silent Synapses Regulate Cocaine-Associated Memory Destabilization and Reconsolidation

This Chapter is adapted from portions of the published manuscript:

Wright, W.J., Graziane, N.M., Neumann, P.A., Hamilton, P.J., Cates, H.M., Fuerst, L., Spenceley, A., Mackinnon-Booth, N., Iyer, K., Huang, Y.H., Shaham, Y., Schlüter, O.M., Nestler, E.J., & Dong, Y. (2020) Silent synapses dictate cocaine memory destabilization and reconsolidation. ***Nature Neuroscience,*** 23(1); 32-46.

2.1 Overview

Cocaine-associated memories are persistent, but upon retrieval they become temporarily destabilized and vulnerable to disruptions, followed by their reconsolidation. To explore the synaptic underpinnings of these memory dynamics, we studied AMPAR-silent excitatory synapses, which are generated within NAc MSNs by cocaine self-administration and subsequently mature after prolonged withdrawal through the recruitment of AMPARs, echoing the acquisition and consolidation cocaine-associated memories. We show that upon memory retrieval after prolonged withdrawal, the matured cocaine-generated synapses within the NAc transiently become AMPAR-silent once again, followed by their re-maturation approximately 6hrs later, defining the onset and termination of the destabilization window of cocaine-associated memories. These synaptic dynamics involved the bidirectional trafficking of CP-AMPARs as well as changes in spine morphology. Preventing the re-maturation of cocaine-generated silent synapses within the destabilization window resulted in a significant decrease in subsequent cocaine-seeking behavior.

These findings indicate that the functional states of cocaine-generated synapses regulate the dynamic state of cocaine-associated memories.

2.2 Introduction

Consuming drugs of abuse produces drug-associated memories, which promote subsequent drug seeking and relapse (Hyman et al., 2006a). Similar to other forms of memory (Dudai, 2012; Nader and Hardt, 2009), previously formed and consolidated drug-associated memories can be retrieved upon re-exposure to cues and contexts associated with earlier drug experience (Torregrossa and Taylor, 2016). Upon retrieval, drug-associated memories are transiently destabilized and become susceptible to disruption, before the memories are then reconsolidated and made stable once again (Fuchs et al., 2009; Lee et al., 2005; Lee et al., 2006; Miller and Marshall, 2005; Rich et al., 2016; Wells et al., 2011). Without knowing the precise neural substrates underlying drug-associated memories and their dynamics, aggressive, but nonspecific, amnestic manipulations, such as protein synthesis inhibitors or beta-adrenergic receptor inhibitors, within, but not outside of, the destabilization window effectively compromise drug-associated memories and reduce subsequent drug seeking in rodent models (Lee et al., 2005; Lee et al., 2006; Miller and Marshall, 2005; Otis et al., 2013; Torregrossa and Taylor, 2016). However, nonspecific manipulations with more tolerable regimens fail to demonstrate consistent anti-relapse efficacy in human drug users (Dunbar and Taylor, 2017; Jobes et al., 2015; Lonergan et al., 2016). These findings highlight the therapeutic potential of using natural memory destabilization processes for anti-relapse treatments, but also indicate a need to identify precise neural and molecular substrates encoding drug-associated memories and their dynamics that can be targeted.

Synapses are likely fundamental cellular units encoding memory traces within the brain. In search of a specific set of synapses encoding cocaine-associated memories, we have focused on MSNs within the NAc, which play an important role in several forms of drug-associated memories, including cue- and context-induced cocaine seeking, a behavioral readout driven by associative cocaine memories (Cruz et al., 2013; Wolf, 2016b). The function of NAc MSNs is driven by excitatory synapse arising from several cortical and subcortical projections, with each input thought to mediate specific aspects of behavioral responses. Amongst such heterogeneous synapses emerges a unique population, which is generated *de novo* by cocaine experience, and is thus cocaine specific. These synapses are formed within several NAc projections at relatively low levels, but have common cellular features that distinguish them from other synapses. Namely, they are nascent, immature excitatory synapses that contain NMDAR without stable AMPARs, and are thus AMPAR-silent (Brown et al., 2011a; Dong and Nestler, 2014; Huang et al., 2009; Isaac et al., 1995; Koya et al., 2012; Lee et al., 2013; Liao et al., 1995; Ma et al., 2014; Neumann et al., 2016b; Whitaker et al., 2016). After generation during cocaine self-administration training, these silent synapses functionally mature over time by recruiting CP-AMPARs, and this maturation and strengthening process contributes to the further enhancement, or incubation, of subsequent cocaine seeking (Lee et al., 2013; Ma et al., 2014; Ma et al., 2016). These results led to our hypothesis that the functional states of cocaine-generated silent synapses regulate the dynamics of cocaine-associated memories. To test this hypothesis, we examined the role of NAc silent synapses in retrieval-induced destabilization and subsequent reconsolidation of cocaine memories. We trained rats in the cocaine self-administration procedure to establish associative cocaine memories, and then re-exposed them to cues and context associated with drug use after prolonged withdrawal, which induces the retrieval and destabilization of cocaine-associated memories. Using this

approach, we found that the matured cocaine-generated transiently become AMPAR-silent and weakened once again following memory retrieval, before they re-mature and re-strengthen approximately 6hrs later. Furthermore, disrupting the re-maturation process impaired subsequent cocaine-seeking behaviors, indicating impaired reconsolidation. These findings indicated that the functional state of cocaine-generated synapses regulates key aspects of cocaine-associated memories and their dynamics.

2.3 Methods

2.3.1 Subjects

Male Sprauge-Dawley rats (postnatal day 35-40 with 130-150g body weight on arrival) (Charles River) were used in all experiments. Rats were singly housed on a 12hr light/dark cycle (light on/off at 7:00/19:00) with food and water available *ad libitum*. Rats were allowed to habituate their housing cages for approximately 1-2 weeks before catheter surgery. All rats were used in accordance with protocols approved by the Institutional Care and Use Committee at the University of Pittsburgh.

2.3.2 Catheter Implantation

Catheter implantation surgery for self-administration was performed as described previously (Lee et al., 2013; Mu et al., 2010a). Briefly, a silastic catheter was inserted into the right jugular vein by 2.5 cm, and the distal end was led subcutaneously to the back between the scapulae.

Catheters were constructed of silastic tubing (length, 10 cm; inner diameter, 0.0508 cm; outer diameter, 0.09398 cm) and attached to a commercially available Vascular Access Button (Instech). Rats were allowed to recover for approximately 5 days following surgery, during which their wellbeing and weight were monitored. During the recovery period, the catheter was flushed daily with 1 ml kg^{-1} heparin (10 U ml^{-1}) and gentamicin antibiotics (5 mg ml^{-1}) in sterile saline to minimize potential infection and catheter occlusion.

2.3.3 Self-Administration Apparatus

All behavioral experiments were conducted in operant conditioning chambers enclosed within sound attenuating cabinets (Med Associates). Each chamber (29.53 x 24.84 x 18.67 cm^3) contains an active and an inactive nose poke hole, a food dispenser, a conditioned stimulus light within each nose poke hole and a house light. No food or water was provided in the chamber during the training or testing session.

2.3.4 Intravenous Cocaine Self-Administration Training

Cocaine self-administration training began approximately 5 days after catheter implantation. On day 1, rats were placed in the self-administration chamber for an overnight training session on a fixed ratio 1 reinforcement schedule. Nose poking in the active hole resulted in a cocaine infusion (0.75 mg kg^{-1} over 3-6 secs) and illumination of the conditioned stimulus light inside the nose poke hole as well as the house light. The conditioned stimulus light remained on for 6 secs, whereas the house light was illuminated for 20 secs, during which any additional nose pokes were counted but resulted in no cocaine infusions. After the 20 sec timeout period, the

house light was turned off, and the next nose poke in the active hole resulted in a cocaine infusion. Nose pokes in the inactive hole had no reinforced consequences, but were recorded.

Rats first underwent one overnight training session, approximately 12 hrs long, to facilitate acquisition. Only rats that received at least 80 cocaine infusions during the overnight session were allowed to proceed to the 5 day cocaine self-administration training regimen (< 2% of rats failed to meet criteria). The same, or similar, self-administration procedures/standards were used in our previous studies (Lee et al., 2013; Ma et al., 2014; Ma et al., 2016). Rats then underwent 5 days cocaine self-administration training, where they underwent the same cocaine self-administration procedure described above for 2hrs daily. After the fifth day of training, rats were placed back in their home cages and remained there during the subsequent withdrawal days. Cocaine-trained rats that failed to meet the self-administration criteria (≥ 15 infusions per session, 70% active-to-inactive nose poke response ratio) were excluded from further experimentation and analysis.

2.3.5 Withdrawal Phase

Rats were returned to their home cage after each self-administration training session. After the 5 day procedure, the rats were singly housed in their home cage for drug withdrawal, with food and water available *ad libitum*. Withdrawal day 1 was operationally defined as 20-26 hours after the last session of cocaine self-administration training. Withdrawal day 45 was operationally defined as 40-48 days after the last session of cocaine self-administration training.

2.3.6 Memory Retrieval

Memory retrieval sessions were performed in the same manner as the cocaine seeking test procedure as detailed below, except that the retrieval session lasted 10-15 min.

2.3.7 Cocaine Seeking Test

Cocaine seeking was assessed in an extinction test (1 hr) conducted after 1 day or 45 days of withdrawal from cocaine self-administration. During the extinction test session, rats were placed back in the operant chamber, where active nose pokes resulted in contingent delivery of the conditioned stimulus light cues, but not cocaine. The number of nose pokes to the active hole was used to quantify cocaine seeking. Nose pokes to the inactive hole were also recorded.

2.3.8 GluA1 Peptide

The peptide TGL (SSGMPLGATGL) was used to interfere with GluA1 subunit-containing AMPAR trafficking. A similar peptide AGL (SSGMPLGAAGL) was used as the control for TGL. The AGL peptide has a single difference in amino acid sequence that prevents it from interacting with the c-terminal domain of the GluA1 subunit and interfering with its trafficking. (Lin et al., 2010). These two peptides were conjugated with a trans-activating transcriptional activator (TAT) sequence (GRKKRRQRRRPQ), to facilitate intracellular delivery, resulting in TAT-pep1-TGL (GRKKRRQRRRPQSSGMPLGATGL) and TAT-pep1-AGL (GRKKRRQRRRPQSSGMPLGAAGL). TAT-pep1-TGL and TAT-pep1-AGL were custom made from GenScript.

2.3.9 Cannulation Surgery and Peptide Injections

For peptide injections, on withdrawal day 35, rats (350-400g) were bilaterally implanted with guide cannulae (PlasticsOne) targeting the NAc shell (in mm: anterior-posterior (AP), +1.60; medial-lateral (ML), ±1.00; dorsal-ventral (DV), -6.80), which were secured to the skull using dental cement. On withdrawal day 45, at specified time points (e.g. 2hr or 6hr) after cue re-exposure and memory retrieval, rats were lightly anesthetized with isoflurane gas and peptide (30μM) was infused through 32-gauge needles extending 1 mm beyond the cannula into the NAc shell (in mm: anterior-posterior (AP), +1.60; medial-lateral (ML), ±1.00; dorsal-ventral (DV), -7.80). For electrophysiology experiments, 1μl per side (30 pmol per side) was injected to maximize peptide spread throughout the recording area. For behavioral experiments, 0.5μl per side (15 pmol per side) was injected to minimize potential spread of the peptide outside of the NAc shell, which may confound interpretation of results. Peptide was infused at a rate of 200 nl min^{-1}, and the infusion needle was left in place for at least 5 min to minimize backflow. Based on injections of EvansBlue dye, 1μl infusions diffused throughout the NAc shell and into the NAc core, and 0.5μl infusions were confined to within the NAc shell. In addition, previous studies using similar TAT-conjugated peptides confirm that the vast majority of neurons within the infusion area take up the peptide (Brebner et al., 2005). For electrophysiology experiments, to ensure that recordings were made from MSNs within the infusion area, all recordings were made within the ~200-μm radius from the center of the injection site, an area well within the boundaries covered by the infusion. The injection sites of each rat for behavioral tests were assessed by injecting 0.5μl of EvansBlue dye using the same procedures for peptide injections after behavioral testing was complete. Rats were subsequently decapitated under deep isoflurane anesthesia and coronal slices (300 μm thick) containing NAc were prepared on a VT1200S vibratome (Leica) in PBS. Localizations of

EvansBlue dye were determined visually and recorded. Rats with inaccurate injections were excluded from data analysis.

2.3.10 Preparation of Acute Brain Slices

Rats were decapitated following isoflurane anesthesia. For NAc-containing slices, coronal slices (250 μm thick) containing the NAc were prepared on a VT1200S vibratome (Leica) in 4 °C cutting solution containing (in mM): 135 N-methyl-d-glutamine, 1 KCl, 1.2 KH_2PO_4, 0.5 $CaCl_2$, 1.5 $MgCl_2$, 20 choline-HCO_3 and 11 glucose, saturated with 95%O_2/5%CO_2 and pH adjusted to 7.4 with HCl. Osmolality was adjusted to 305 mmol kg^{-1}. For hippocampal recordings, transverse slices (400 μm thick) containing the ventral hippocampus were prepared on a VT1200S vibratome (Leica) in 4 °C cutting solution. A small cut was made in the CA3 region to prevent epileptic activities in the CA1 region. Immediately after cutting, slices were transferred and incubated in the artificial cerebrospinal fluid (aCSF) containing (in mM): 119 NaCl, 2.5 KCl, 2.5 $CaCl_2$, 1.3 $MgCl_2$, 1 NaH_2PO_4, 26.2 $NaHCO_3$ and 11 glucose, with the osmolality adjusted to 280–290 mmol kg^{-1}. Slices were placed in the aCSF saturated with 95% O_2/5% CO_2 at 37 °C for 30 min and then held at 20–22 °C for at least 30 min before experimentation.

2.3.11 Electrophysiology Recordings

2.3.11.1 Extracellular Field Recordings

All field recordings were made within the CA1 region of the hippocampus. Before recordings, hippocampal slices were incubated with 200 μM TGL or 200 μM AGL for >1 h. During recordings, slices were superfused with high-divalent aCSF, containing the same ingredients as

the holding aCSF except that 4 mM $CaCl_2$ and $MgCl_2$ were used to replace 2.5 mM $CaCl_2$ and 1.3 mM $MgCl_2$. Recordings were made by placing a recording electrode filled with 2 M NaCl in the stratum radiatum of the CA1. Schaffer collaterals originating from the CA3 were stimulated with a constant-current isolated stimulator (Digitimer), using a monopolar electrode (glass pipette filled with aCSF). Synaptic currents were recorded with a MultiClamp 700B amplifier, filtered at 2.6–3 kHz, amplified five times and then digitized at 20 kHz. A high-frequency stimulation (two 1-s trains at 100 Hz with a 20-s interval, 1.5 times the test current intensity) was used to induce LTP. In experiments involving inhibition of NMDARs, 50 μM (2R)-amino-5-phosphonovaleric acid (APV) was included in the bath.

2.3.11.2 Whole-Cell Recordings

All recordings were made from MSNs located in the medial NAc shell. During recordings, slices were superfused with aCSF, heated to 30–32 °C by passing the solution through a feedback-controlled in-line heater (Warner) before entering the recording chamber. To measure excitatory postsynaptic current (EPSC) responses, electrodes (2–5 MΩ) were filled with a cesium-based internal solution (in mM: 135 $CsMeSO_3$, 5 CsCl, 5 TEA-Cl, 0.4 EGTA (Cs), 20 HEPES, 2.5 Mg-ATP, 0.25 Na-GTP, 1 QX-314 (Br), pH 7.3). Picrotoxin (0.1 mM) was included in the aCSF during all recordings to inhibit $GABA_A$ receptor-mediated currents. Presynaptic afferents were stimulated by a constant-current isolated stimulator (Digitimer), using a monopolar electrode (glass pipette filled with aCSF). Series resistance was typically 7–20 MΩ, uncompensated and monitored continuously during recording. Cells with a change in series resistance >20% were excluded from data analysis. Synaptic currents were recorded with a MultiClamp 700B amplifier, filtered at 2.6–3 kHz, amplified five times and digitized at 20 kHz.

2.3.11.3 Detection of GluN2B-Containing NMDAR Currents

To measure NMDAR-mediated EPSCs, 2,3-dihydroxy-6-nitro-7-sulfamoyl-benzo[f]quinoxaline (NBQX) (5μm) and picrotoxin (0.1 mM) were included in the bath. Recorded neurons were held at −40 mV to partially relieve Mg2+-mediated blockage of NMDARs. Following a 7-min baseline recording, the bath that additionally contained the GluN2B- selective antagonist Ro256981 (200 nM) was switched in. NMDAR EPSCs were continuously recorded as the new bath perfused the slice, but only EPSCs after 8 min were included for data analysis to allow diffusion of Ro256981 into the slice and this use-dependent antagonist to operate. After 10 min of recording, a bath containing APV (50 μM) instead of Ro256981 was switched in to inhibit all NMDARs, which verified that recorded EPSCs were mediated by NMDARs.

2.3.11.4 Detection of CP-AMPARs

To isolate AMPAR-mediated EPSCs, picrotoxin (0.1 mM) and APV (50 μM) were included in the bath. To properly assess the rectification of AMPAR EPSCs, spermine (0.1 mM) was freshly added to the internal solution. AMPAR EPSCs were evoked at progressively depolarized holding potentials (−70 mV to +50 mV with a 10-mV increment) to generate an I–V curve. Twelve responses were recorded at each holding potential and averaged. The rectification index was calculated by comparing the peak amplitude at +50 mV to −70 mV after correction for the reversal potential with the following equation:

$$\text{Rectification index} = (I_{+50} / (50 - E_R)) / (I_{-70} / (70 - E_R))$$

where I is the peak amplitude at either +50 mV or −70 mV, and E_R is the reversal potential of AMPAR EPSCs, which was measured manually for each recorded neuron.

2.3.11.5 Silent Synapse Recordings and Analysis

NAc shell MSNs were randomly selected for recording. The minimal stimulation assay was performed as previously described (Brown et al., 2011a; Graziane et al., 2016; Huang et al., 2009; Isaac et al., 1995; Lee et al., 2013; Liao et al., 1995; Ma et al., 2014; Ma et al., 2016; Neumann et al., 2016b). After obtaining small (~50 pA) EPSCs at −70 mV, the stimulation intensity was reduced in small increments to the point that failures versus successes of synaptically evoked events (EPSCs) could be clearly distinguished. The stimulation intensity and frequency were then kept constant for the rest of the experiment. The amplitudes of both AMPAR and NMDAR ESPCs resulting from single vesicular release are relatively large in NAc MSNs (for example, ~15 pA for AMPAR mEPSCs at −70 mV), which facilitates the judgment of successes versus failures. For each cell, 50–100 traces were recorded at −70 mV, and 50–100 traces were recorded at +50 mV. Recordings were then repeated at −70 mV and +50 mV for another round or two. Only cells with relatively constant failure rates (changes <15%) between rounds were used to assess percentage of silent synapses. We visually detected failures versus successes at each holding potential over 50–100 trials to calculate the failure rate, as described previously (Brown et al., 2011a; Graziane et al., 2016; Huang et al., 2009; Lee et al., 2013; Ma et al., 2014; Ma et al., 2016; Neumann et al., 2016b). We performed this analysis in a blind manner such that a small number of ambiguous responses were categorized in a fully unbiased way.

To quantify percentage of silent synapses, we made two theoretical assumptions: (1) the presynaptic release sites are independent, and (2) release probability across all synapses, including silent synapses, is identical. Thus, the percentage of silent synapses was calculated using the equation: $1 - \ln(F_{-70})/ \ln(F_{+50})$, in which F_{-70} was the failure rate at −70 mV and F_{+50} was the failure rate at +50 mV, as rationalized previously (Liao et al., 1995). Note that in this equation, the

failure rate is the only variable that determines the percentage of silent synapses. The amplitudes of EPSCs are used to present failures or successes, but do not have analytical value. In the cases in which these two theoretical assumptions are not true, the above equation was still used, as the results were still valid in predicting the changes of silent synapses qualitatively as previously rationalized (Huang et al., 2015b; Ma et al., 2014). The amplitude of an EPSC was determined as the mean value of the EPSC over a 1-ms time window around the peak, which was typically 3–4 ms after the stimulation artifact. To assess the percentage of silent synapses, only the rates of failures versus successes, not the absolute values of the amplitudes, were used. At +50 mV, successful synaptic responses were conceivably mediated by both AMPARs and NMDARs, and inhibiting AMPARs by NBQX (5 μM) modestly reduces the amplitudes of EPSCs (Graziane et al., 2016). Despite the effects of NBQX on the amplitudes, the failure rate of synaptic responses at +50 mV was not altered during AMPAR inhibition (Graziane et al., 2016). Thus, in the minimal stimulation assay assessing the percentage of silent synapses, the results will not be affected, whether the synaptic responses at +50 mV are mediated by NMDARs alone or by both AMPARs and NMDARs.

2.3.12 Dendritic Spine Labeling and Imaging

To visualize dendritic spines, MSNs were filled with Alexa 594 dye using single-cell microinjections, and the labeled dendritic spines were quantified as described previously (Dumitriu et al., 2012; Dumitriu et al., 2011). Briefly, the rats were transcardially perfused with ice-cold 1% PFA in 0.1 M phosphate buffer, followed by 4% PFA and 0.125% glutaraldehyde in 0.1 M phosphate buffer. Brains were removed and postfixed in 4% PFA and 0.125% glutaraldehyde in 0.1 M phosphate buffer for 12–14 hrs at 4 °C. Following postfix, the brains were

transferred into 0.1 M PBS and sectioned into 250-μm-thick slices using a VT1200S vibratome (Leica). Cells were filled shortly after slicing (within 4 hrs). Cells within the NAc shell were impaled with a fine micropipette containing 5 mM Alexa 594 hydrazide (Invitrogen) and injected with 1–10 nA of negative current until dendrites and spines were filled. After filling, the slices were mounted in ProLong Gold Antifade (Molecular Probes) on slides for imaging. Spacers (240 μm thick) were placed along the edge of the slide before mounting to avoid compression of the slices by the overlying coverslip and to prevent deformation of spine morphologies.

Images were captured with a Leica TCS SP5 confocal microscope equipped with Leica Application Suite software (Leica). Individually filled neurons were visualized with a 63x oil immersion objective for final verification of their neuronal types (for example, MSNs versus interneurons). Individual dendritic segments were focused on and scanned at 0.69-μm intervals along the z axis to obtain a z-stack. After capture, all images were deconvolved within the Leica Application Suite software. Analyses were performed on two-dimensional projection images using ImageJ (NIH). Secondary dendrites were sampled and analyzed due to their significant cellular and behavioral correlates (Graziane et al., 2016; Robinson and Kolb, 1999). For each neuron, 1–4 (2.1 average) dendritic segments of ~20 μm in length were analyzed. For each group, 4–8 cells per rat were analyzed. NAc shell dendritic spines can be categorized into at least four subtypes: (1) mushroom-like spines, (2) long-thin spines, (3) filopodia-like spines, and (4) stubby spines, however, ue to their morphological and functional similarity, we combined long-thin and filopodia-like spines for data interpretation. Similar to our previous studies (Brown et al., 2011a; Graziane et al., 2016; Wang et al., 2020), we operationally divided spines into three categories: (1) mushroom-like spines were dendritic protrusions with a head diameter >0.5 μm or >2x the spine neck diameter; (2) stubby spines were dendritic protrusions with no discernable head and a length

of ≤0.5 μm; and (3) thin/filopodia-like spines were dendritic protrusions with a length of >0.5 μm and head diameter <0.5 μm or no discernable head. During counting of dendritic spines, spine head diameters were also measured for analysis.

2.3.13 Statistics

All results are shown as mean ± s.e.m. All experiments were replicated in 3–16 rats. All data collection was randomized. All data were assumed to be normally distributed, but this was not formally tested. No statistical methods were used to predetermine sample sizes, but our sample sizes are similar to those reported in previous publications (Graziane et al., 2016; Lee et al., 2013; Ma et al., 2014; Ma et al., 2016; Neumann et al., 2016b; Wang et al., 2020). All data were analyzed offline and investigators were blinded to experimental conditions during the analyses.

Repeated experiments for the same group were pooled together for statistical analysis. For electrophysiology and dendritic spine experiments, the sample sizes are presented as *n/m*, where n is the number of cells and m is the number of rats. For behavioral experiments, the sample sizes are presented as *n*, which is the number of rats. Animal-based statistics were used for all data analyses, except for extracellular field excitatory postsynaptic potential (fEPSP) electrophysiology experiments, in which *n* is the number of recordings. For electrophysiological experiments, we averaged the values of all the cells from each rat to obtain an animal-based mean value for statistical analysis (Graziane et al., 2016; Lee et al., 2013; Ma et al., 2016). For dendritic spine experiments, we averaged individual dendritic segment values from each cell to obtain a cell-based value, and then averaged cell-based values from each rat to obtain animal-based values for statistical analysis (Dumitriu et al., 2012; Dumitriu et al., 2011). Statistical significance was assessed using unpaired t-tests, one-way analysis of variance (ANOVA) or repeated-measures

two-way ANOVA, as specified in the related text. Two-tailed tests were performed for analyses. Statistical significance was set at $P < 0.05$ for all experiments. Statistical analyses were performed in GraphPad Prism (v.8).

2.4 Results

2.4.1 Memory Retrieval Re-Silences Cocaine-Generated Synapses

We trained rats to self-administer cocaine, during which each intravenous infusion was paired with a light cue to form cocaine-cue associations. Consistent with our previous studies (Lee et al., 2013; Ma et al., 2014; Ma et al., 2016), rats acquired cocaine-associated memories after 5 days of self-administration training, which was manifested by cue-induced cocaine seeking on withdrawal day 1 (**Figure 4 a-c**). This cue-induced cocaine seeking 'incubated' during drug abstinence (Grimm et al., 2001) and became significantly greater after 45 days of withdrawal (**Figure 4 a-c**). Thus, cocaine-associated memories are formed during drug self-administration training and are strengthened during prolonged drug withdrawal.

To assess silent synapses after cocaine memory formation and consolidation, we performed the minimal stimulation assay to estimate the percentage of silent synapses among all sampled synapses in NAc shell MSNs (**Figure 5 a,b**). As demonstrated previously, (Huang et al., 2009; Liao et al., 1995), if silent synapses are present in the set of recorded synapses, the failure rate of EPSCs in response to minimal stimulation at +50mV is lower than that observed at -70mV, and based on the differential failure rates, the percentage of silent synapses can be estimated (**Figure**

5 c) (**see Methods**). After 1 day of withdrawal from cocaine self-administration, the percentage of

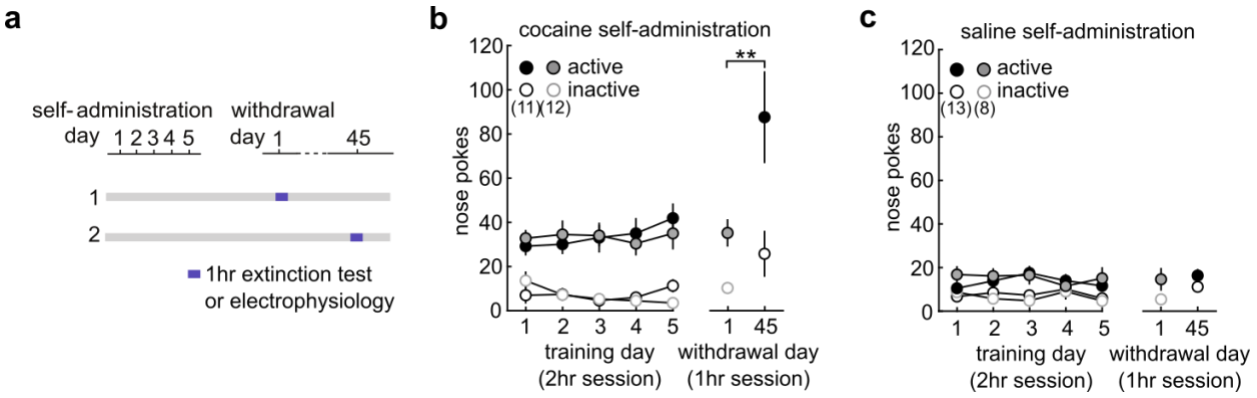

Figure 4. Cue-Induced Cocaine Seeking Behavior

(**a**) Schematic showing experimental timeline. (**b,c**) Summary showing that after cocaine (**b**), but not saline (**c**), self-administration, cue-induced seeking behavior (active nose pokes) was higher on withdrawal day 45 compared to withdrawal day 1 (withdrawal day 1, active = 35.08 ± 5.787, n = 12; withdrawal day 45, active = 87.13 ± 20.367, n = 11; $F_{1,38}$ = 12.27, p = 0.0012, two-way ANOVA; **P < 0.01, Bonferroni post-test)

silent synapses in NAc shell MSNs was significantly increased when compared to saline trained controls (**Figure 5 d,e,i**). Following prolonged (45 days) withdrawal from self-administration, the percentage of silent synapses decreased back to control levels (**Figure 5 f,g,i**). Our previous studies demonstrate that this decrease is partially due to the functional maturation and synaptic strengthening of these silent synapses, during which cocaine-generated synapses recruit CP-AMPARs and become unsilenced, a process that contributes to the heightened cue-induced cocaine seeking after withdrawal (Lee et al., 2013; Ma et al., 2014; Ma et al., 2016). This maturation process is confirmed in our randomly sampled synapses, where application of NASPM (200μM), a selective CP-AMPAR antagonist, restored the percentage of silent synapses to the high levels observed after 1 day of withdrawal from cocaine self-administration (**Figure 5 h,i**). Thus, cocaine

self-administration generates new silent synapses, which subsequently mature after withdrawal via

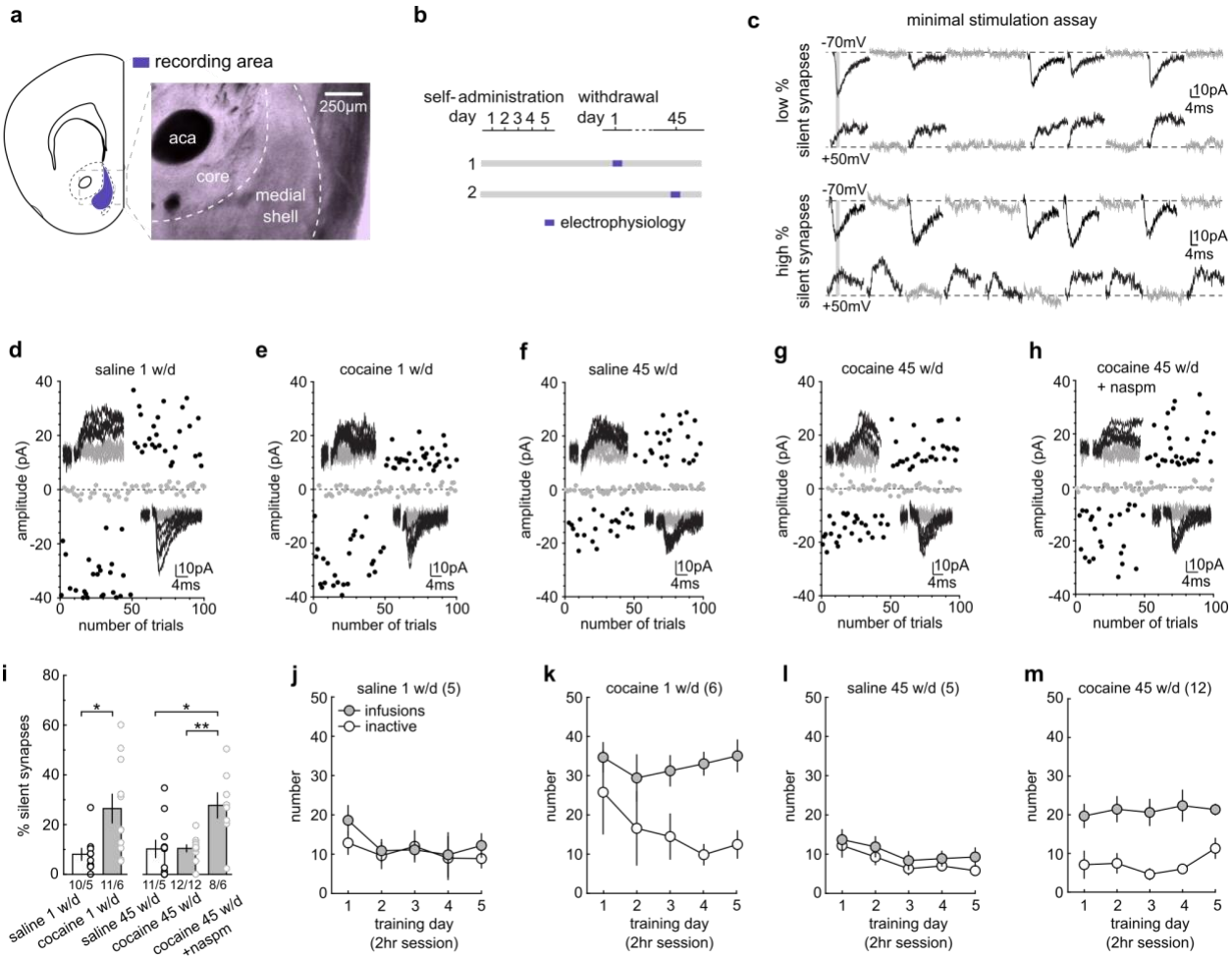

Figure 5. Cocaine-Induced Generation of Silent Synapses

(**a**) Schematic and image showing recording area within the NAc shell. (**b**) Schematic showing the experimental timeline and recording time points. (**c**) Example EPSCs in the minimal stimulation assay, in which failed and successful responses were readily discernable at both −70 mV and +50 mV, and the small versus large failure rate differences between these two holding potentials connote low percentage (top) versus high percentage (bottom) of silent synapses. (**d-h**) EPSCs evoked at -70mV and +50mV (insets) over 100 trials from example recordings for each group (**d**, saline 1 day withdrawal; **e**, cocaine 1 day withdrawal; **f**, saline 45 day withdrawal; **g**, cocaine 45 day withdrawal; **h**, cocaine 45 day withdrawal + naspm). (**i**) Summary showing that the percentage of silent synapses was increased on withdrawal day 1 after cocaine self-administration (saline = 5.93 ± 1.44, n = 5 animals; cocaine = 24.95 ± 7.13, n = 6 animals; $t_9 = 2.38$, $p = 0.04$, two-tail unpaired t-test). On withdrawal day 45, the percentage of silent synapses returned to basal levels, while CP-AMPAR inhibition restored the high percentage of silent synapses (saline

= 11.71 ± 5.35, n = 5 animals; cocaine = 10.53 ± 1.49, n = 11 animals; cocaine naspm = 28.37 ± 4.68, n = 6 animals; $F_{2,19}$ = 8.61, p = 0.0022, one-way ANOVA; *P < 0.05, **P < 0.01, Bonferroni post-test). (**j**-**m**) Self-administration training data for all rats used in electrophysiology experiments.

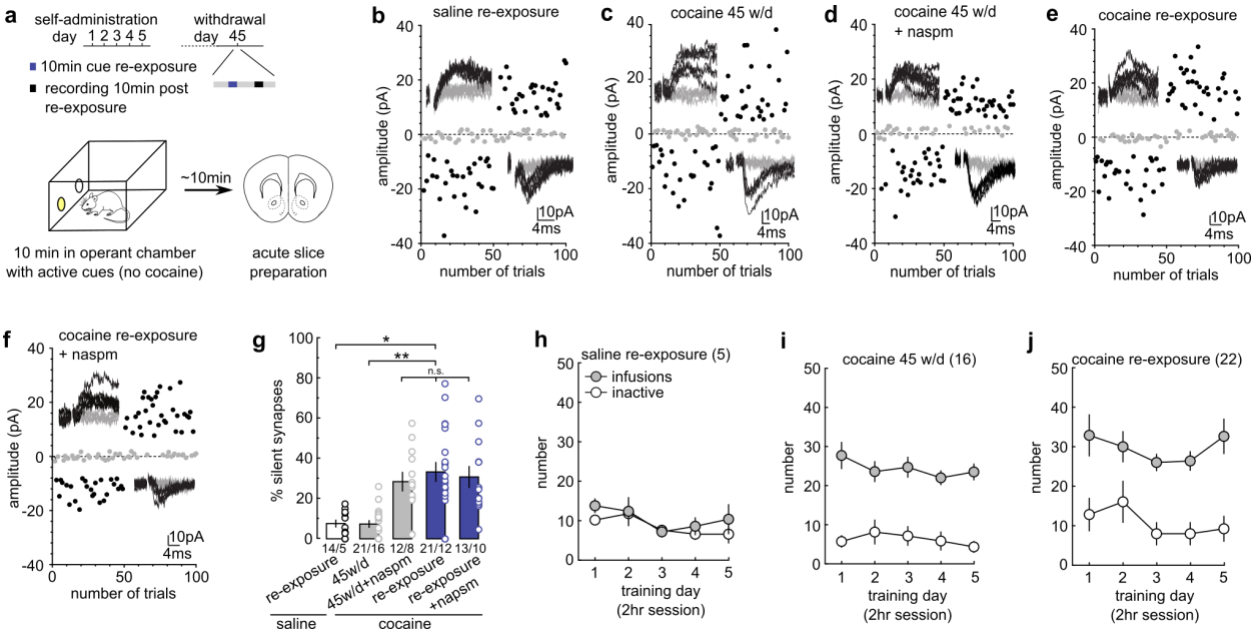

Figure 6. Memory Retrieval Re-Silences Cocaine-Generated Synapses

(**a**) Schematic of experimental timeline. (**b**-**f**) EPSCs evoked at -70mV and +50mV (insets) over 100 trials from example recordings for each group (**b**, saline re-exp; **c**, cocaine 45 withdrawal day; **d**, cocaine 45 withdrawal day + naspm; **e**, cocaine re-exp; **f**, cocaine re-exp + naspm). (**g**) Summary showing that cue re-exposure increased the percentage of silent synapses in cocaine-trained, but not saline-trained, rats on withdrawal day 45, and the effects of NASPM (saline re-exp = 7.74 ± 1.89, n = 5 animals; cocaine 45 w/d = 8.01 ± 1.89, n = 16 animals; cocaine 45 w/d NASPM = 31.31 ± 5.22, n = 9 animals; cocaine re-exp = 32.89 ± 5.41, n = 12 animals; cocaine re-exp NASPM = 29.74 ± 3.85, n = 10; $F_{4,47}$ = 10.11, p < 0.0001, one-way ANOVA; NS > 0.05, *P < 0.05, **P < 0.01, Bonferroni post-test). (**h**-**j**) Self-administration training data for all rats used in electrophysiology experiments.

incorporation of CP-AMPARs, potentially contributing to the formation and consolidation of cocaine-associated memories.

We next examined the effects of cue-induced retrieval and destabilization of cocaine-associated memories on the functional state of cocaine-generated synapses. After 45 days of withdrawal from cocaine self-administration, we briefly (10 min) re-exposed the rats to cocaine-associated cues (discrete and contextual) through an extinction session in the same operant chambers to reactivate and destabilize cocaine-associated memories (Lee et al., 2005). Immediately after cue re-exposure, the rats were analyzed for silent synapses in the NAc shell (**Figure 6 a**). Cue re-exposure had no effect on the percentage of silent synapses in rats previously trained with saline self-administration, indicating that without cocaine-cue pairings, re exposure to the cues does not generated new synapses in the NAc shell (**Figure 6 b,g**). However, the percentage of silent synapses was significantly increased in cocaine-trained rats that underwent cue re-exposure compared to cocaine-trained rats that did not (**Figure 6 c-g**). In addition, the magnitude of this cue re-exposure-induced increase in percentage of silent synapses was comparable to the increase induced by CP-AMPAR inhibition in cocaine-trained rats without cue re-exposure (**Figure 6 d,g**). As the cocaine-generated silent synapses functionally mature by recruiting CP-AMPARs, we speculated that cue re-exposure-induced silent synapses are the mature cocaine-generated synapses that have been re-silenced through the internalization of CP-AMPARs. Consistent with this hypothesis, inhibiting CP-AMPARs did not further increase the percentage of silent synapses in cocaine-trained rats after cue re-exposure, indicating these silent synapses are not a separate population (**Figure 6 f,g**).

While cue re-exposure did not generate new silent synapses in saline-trained rats (**Figure 6 g**), it may do so in cocaine-trained rats, similar to what occurs 1 day after cocaine self-administration. While our results suggesting the internalization of CP-AMPARs argues against

that possibility, we further examined this possibility. Generation of new silent synapses after

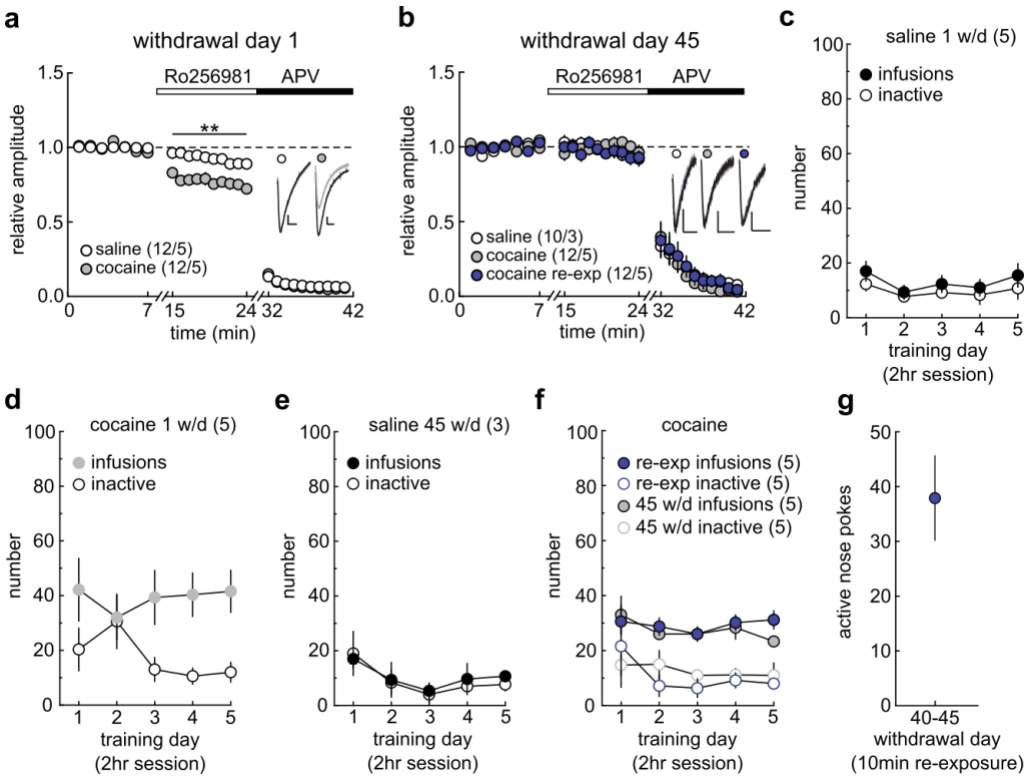

Figure 7. Memory Retrieval Does Not Alter GluN2B-NMDAR Levels

(**a**) Summary showing increased sensitivity to Ro256981 of NMDAR EPSCs in rats 1 d after cocaine self-administration (saline = 0.91 ± 0.03 at 24 min, n = 5 animals; cocaine = 0.74 ± 0.03 at 24 min, n = 5 animals; $F_{26, 104}$ = 7.66, p < 0.0001, two-way repeated-measures (RM) ANOVA; **P < 0.01, Bonferroni post-test). Subsequent application of APV (50 μM) confirmed that currents were mediated by NMDARs. Inset: example NMDAR EPSCs before and during Ro256981 application. (**b**) Summary showing that cue re-exposure did not affect the Ro256981 sensitivity of NMDAR EPSCs in NAcSh MSNs (saline = 0.93 ± 0.03 at 24 min, n = 3 animals; cocaine = 0.92 ± 0.06 at 24 min, n = 5 animals; cocaine re-exp = 0.93 ± 0.05 at 24 min, n = 5; $F_{52, 260}$ = 0.50, p = 0.9984, two-way RM ANOVA). (**c-g**) Self-administration training data (**c-f**) and seeking data during cue re-exposure sessions (**g**) for all rats used in electrophysiology experiments.

cocaine experience involves synaptic insertion of GluN2B-containing NMDARs (Graziane et al., 2016; Huang et al., 2009; Wang et al., 2021). This was confirmed in our current experiments,

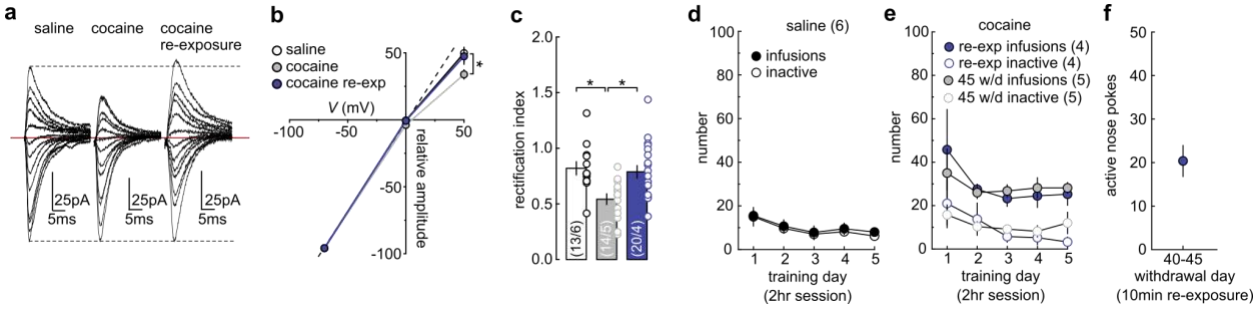

Figure 8. Memory Retrieval Normalizes Synaptic CP-AMPAR Content

(**a**) Example AMPAR EPSCs evoked from holding potentials of −70 mV to +50 mV with 10-mV increments. (**b**) *I–V* curves of AMPAR EPSCs showing rectification in cocaine-trained rats on withdrawal day 45, and the rectification was abolished by cue re-exposure (saline = 52.51 ± 5.68, n = 6 animals; cocaine = 29.98 ± 3.17, n = 5 animals; cocaine re-exp = 43.93 ± 6.01, n = 4 animals; $F_{4,33}$ = 4.15, p = 0.0078, two-way ANOVA; *P < 0.05, Bonferroni post-test). EPSC amplitudes at −70 mV were used to normalize EPSCs at other membrane potentials. (**c**) Summary showing that on withdrawal day 45, the decreased rectification index in cocaine-trained rats was abolished by cue re-exposure (saline = 0.79 ± 0.051, n = 6 animals; cocaine = 0.54 ± 0.041, n = 5 animals; cocaine re-exp = 0.79 ± 0.057, n = 4 animals; $F_{2,12}$ = 8.06, p = 0.006, one-way ANOVA; *P < 0.05, Bonferroni post-test). (**d-f**) Self-administration training data (**d,e**) and seeking data during cue re-exposure sessions (**f**) for all rats used in electrophysiology experiments.

in which NMDAR-mediated EPSCs in the NAc shell exhibited increased sensitivity to the GluN2B-selective antagonist Ro256981 (200 nM) after 1 day withdrawal from cocaine self-administration compared to saline-trained rats (**Figure 7 a**). On withdrawal day 45, the sensitivity of NMDAR EPSCs to Ro256981 declined to low levels (**Figure 7 b**), suggesting that GluN2B-containing NMDARs have been replaced with other NMDAR subtypes, which is consistent with the maturation of silent synapses (Wang et al., 2021). Importantly, cue re-exposure did not alter the low sensitivity of NMDAR-mediated EPSCs to Ro256981 in cocaine-trained rats (**Figure 7**

b), suggesting that cue re-exposure did not trigger GluN2B-mediated *de novo* generation of new

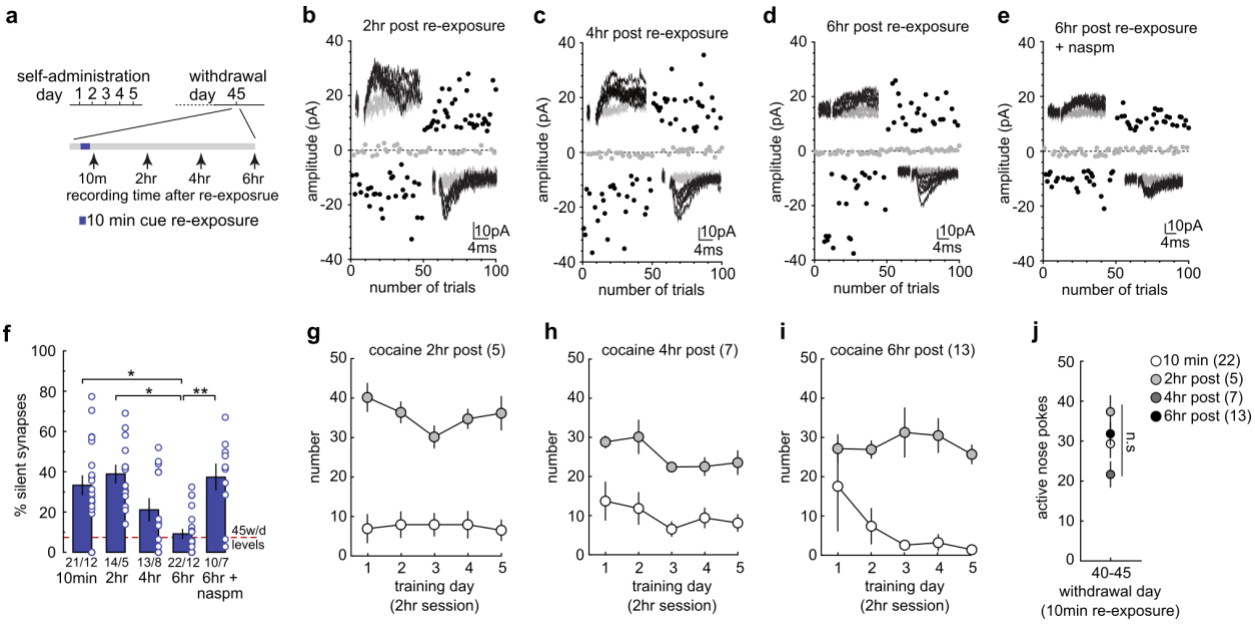

Figure 9. Memory-Retrieval-Induced Silent Synapses Are Transient

(**a**) Diagram showing the time points at which the effects of cue re-exposure on silent synapses were assessed. (**b-e**) EPSCs evoked at -70mV and +50mV (insets) over 100 trials from example recordings for each group (**b**, 2hr post re-exp; **c**, 4hr post re-exp; **d**, 6hr post re-exp; **e**, 6hr post re-exp + naspm). (**f**) Summary showing that after cue re-exposure, the percentage of silent synapses was immediately increased, remained at high levels for a few hours and declined to basal levels by ~6 h, and the declined percentage of silent synapses was restored to high levels by NASPM (10 min = 32.89 ± 5.404, n = 12 animals; 2 h = 37.23 ± 4.86, n = 5 animals; 4 h = 23.62 ± 7.78, n = 8 animals; 6 h = 10.91 ± 3.07, n = 12 animals; 6 h NASPM = 39.47 ± 5.77, n = 7; $F_{4,39}$ = 5.02, p = 0.0023, one-way ANOVA; *P < 0.05, **P < 0.01, Bonferroni post-test). The 10-min data were taken from Figure 3g. Dotted red line represents the average silent synapses level at withdrawal day 45 with no re-exposure. (**g-i**) Self-administration data for rats used in electrophysiology experiments. (**j**) Summary showing no difference in nose poke responding during the 10-min cue re-exposure session in rats in which NAcSh silent synapses were assessed 10 min, 2 hr, 4 hr, and 6 hr after cue re-exposure (10min = 29.45 ± 3.44, n = 22 animals; 2hr = 37.40 ± 3.98, n = 5 animals; 4hr = 21.86 ± 3.12, n = 7 animals; 6hr = 31.92 ± 2.68, n = 13 animals, $F_{3,43}$=1.55, p=0.22, one-way ANOVA, n.s. > 0.05).

silent synapses. While GluN2B-containing NMDARs were not changed by cue re-exposure in cocaine trained rats, we did detect internalization of CP-AMPARs. CP-AMPARs conduct minimal current at depolarized potentials (Cull-Candy et al., 2006; Isaac et al., 2007), and can thus be detected by an increased inward rectification index. In saline trained rats, very low levels of CP-AMPARs are expressed at excitatory synapses on NAc shell MSNs, reflected as a linear current-voltage (*I-V*) relationship of AMPAR EPSCs (**Figure 8 a-c**). After 45 days of withdrawal from cocaine self-administration, AMPAR EPSCs become inwardly rectifying (**Figure 8 a-c**), indicative of CP-AMPAR incorporation at cocaine-generated synapses, as observed previously (Conrad et al., 2008; Lee et al., 2013; Ma et al., 2014). Cue re-exposure, however, normalized this rectification (**Figure 8 a-c**), suggesting the removal of CP-AMPARs. Taken together, these results support a scenario where CP-AMPARs are internalized to mediate the re-silencing of matured cocaine-generated synapses.

Retrieval-induced memory destabilization lasts approximately 6 hrs before reconsolidation is achieved and the memory is re-stabilized (Nader and Einarsson, 2010; Nader et al., 2000). The dynamics of NAc shell silent synapses exhibited a similar time course following cue re-exposure (**Figure 9 a**). Specifically, the percentage of silent synapses remained high 2 hrs and 4 hrs after cue re-exposure, but returned to low levels after 6 hrs (**Figure 9 b-f**). At the 6 hr time point, inhibition of CP-AMPARs by NASPM restored the high percentage of silent synapses (**Figure 9 f**), suggesting that the cue-re-silenced synapses have re-matured through the re-insertion of CP-AMPARs. Thus, the already matured silent synapses are re-silenced and weakened via internalization of CP-AMPARs following cue re-exposure, and then re-mature 6 hrs later. This re-silencing and subsequent re-maturation of cocaine-generated synapses follows the general time course of retrieval-induced destabilization and reconsolidation of cocaine-associated memories.

2.4.2 Spine Morphology Correlates with Memory Destabilization and Reconsolidation

The morphology of dendritic spines is correlated with the maturational state of glutamatergic synapses (Holtmaat and Svoboda, 2009; Kasai et al., 2010). In NAc shell slices, we filled MSNs with Alexa 594 dye and imaged their secondary dendrites, which receive dense glutamatergic inputs (**Figure 10**). NAc shell dendritic spines can be categorized into at least four subtypes: (1) mushroom-like spines, (2) long-thin spines, (3) filopodia-like spines, and (4) stubby spines (**Figure 10**) (**see Methods**) (Graziane et al., 2016). It is thought that mushroom-like spines represent more mature synapses that are enriched in AMPARs, while long-thin and filopodia-like spines are relatively immature synapses with few or no AMPARs (Holtmaat and Svoboda, 2009; Kasai et al., 2010). This relationship is supported by our previous studies examining cocaine-induced silent synapses and dendritic morphology in the NAc shell (Graziane et al., 2016; Wang et al., 2020). Due to their morphological and functional similarity, we combined long-thin and filopodia-like spines for data interpretation.

Similar to previous studies (Graziane et al., 2016; Wang et al., 2020; Wang et al., 2021), on withdrawal day 1 after cocaine self-administration, the density of total spines was increased in cocaine-trained rats compared with saline-trained rats (**Figure 11 a,b**). This increase was primarily attributable to an increase in thin spines (**Figure 11 c,d**) that likely correspond to newly generated silent synapses. We also observed a small increase in the density of stubby spines (**Figure 11 e**), but given their low basal density and small contribution (approximately 4%) to the total spine density change, their role in the generation of silent synapses was considered to be minimal. On

withdrawal day 45, the total spine density remained elevated in cocaine-trained rats compared with

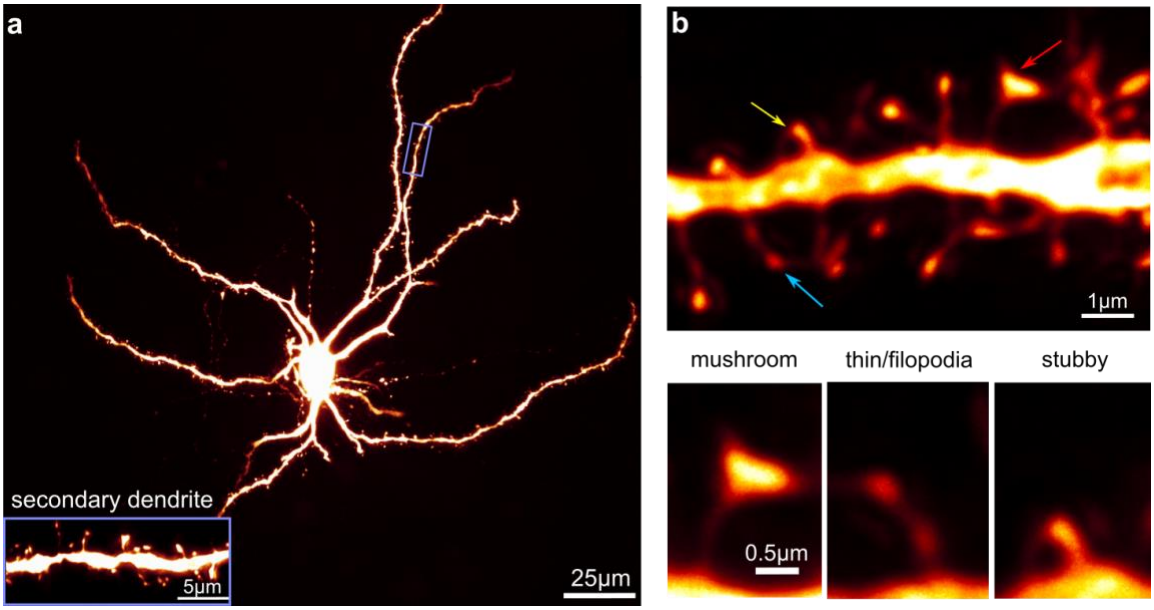

Figure 10. Dendritic Spine Morphology Characterization

(**a**) Example image showing an NAcSh MSN filled with Alexa Fluor 594 dye, and a magnified secondary dendrite (inset). (**b**) Example spiny dendrites (top) and three subtypes of spines (bottom) whose dendritic locations are indicated by arrows; mushroom (red), thin (blue) and stubby (yellow).

saline-trained rats (**Figure 12 a,b**). However, the density of thin spines in cocaine-trained rats returned to levels comparable to saline-trained rats (**Figure 12 c**), while, in contrast, the density of mushroom-like spines was significantly increased in cocaine-trained rats (**Figure 12 d**). The density of stubby spines was also slightly higher in cocaine-trained rats compared with saline-trained rats (**Figure 12 e**). These dendritic spine patterns are consistent with the notion that cocaine-generated silent synapses functionally mature and stabilize by recruiting AMPARs after 45 days of withdrawal.

After 45 days of withdrawal from cocaine self-administration, cue re-exposure did not alter the density of total spines, such that they remained elevated and comparable to cocaine-trained rats

without cue re-exposure (**Figure 12 a,b**). However, following cue re-exposure the density of

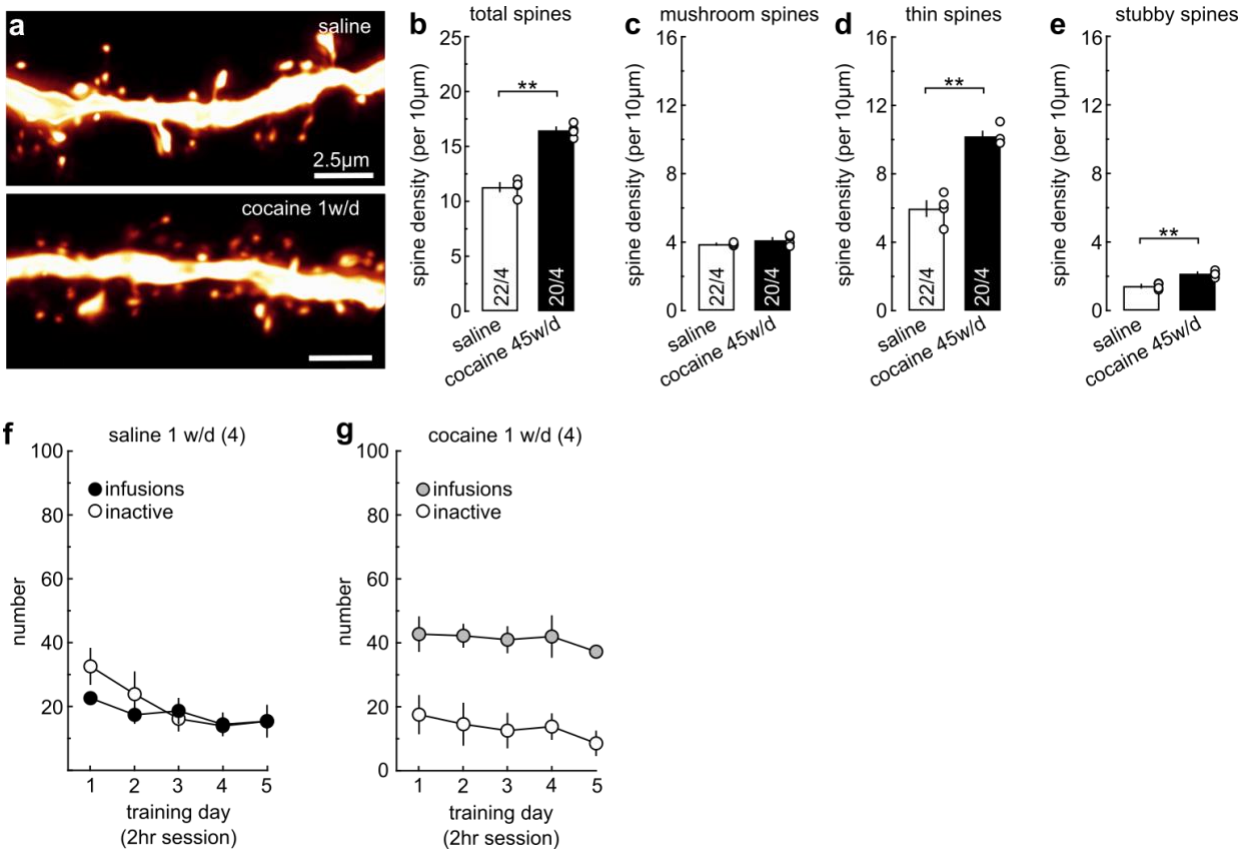

Figure 11. Cocaine-Induced Generation of Thin Spines

(**a**) Example NAc Shell dendrites from saline-trained rats (upper) and cocaine-trained rats (lower) after one day from the 5-day self- administration procedure. Scale bars, 2.5 μm. (**b**) Summary showing that cocaine-trained rats exhibited an increase in the density of total dendritic spines on withdrawal day 1 after cocaine self-administration compared to saline-trained rats (saline = 11.29 ± 0.40, n = 4 animals; cocaine = 16.46 ± 0.298, n = 4 animals, t_6=10.45, p<0.0001, two-tail, unpaired t-test). (**c**) Summary showing no difference in the density of mushroom-like spines between cocaine- and saline-trained rats on withdrawal day 1, there was (saline = 3.89 ± 0.044, n = 4 animals; cocaine = 4.12 ± 0.150, n = 4 animals, t_6=1.41, p=0.21, two-tail, unpaired t-test). (**d**) Summary showing an increase in the density of thin spines in cocaine-trained rats compared to saline-trained rats on withdrawal day 1 (saline = 5.97 ± 0.450, n = 4 animals; cocaine = 10.19 ± 0.292, n = 4 animals, t_6=7.87, p=0.0002, two-tail, unpaired t-test). (**e**) Summary showing an increased in the density of stubby spines in cocaine-trained rats compared to saline-trained rats on withdrawal day 1 (saline = 1.43 ± 0.092, n = 4 animals; cocaine = 2.15 ± 0.092, n = 4 animals, t_6=5.55, p=0.0014, two-tail, unpaired t-test). (**f,g**) Self-administration training data of all rats used for the spine morphology experiments.

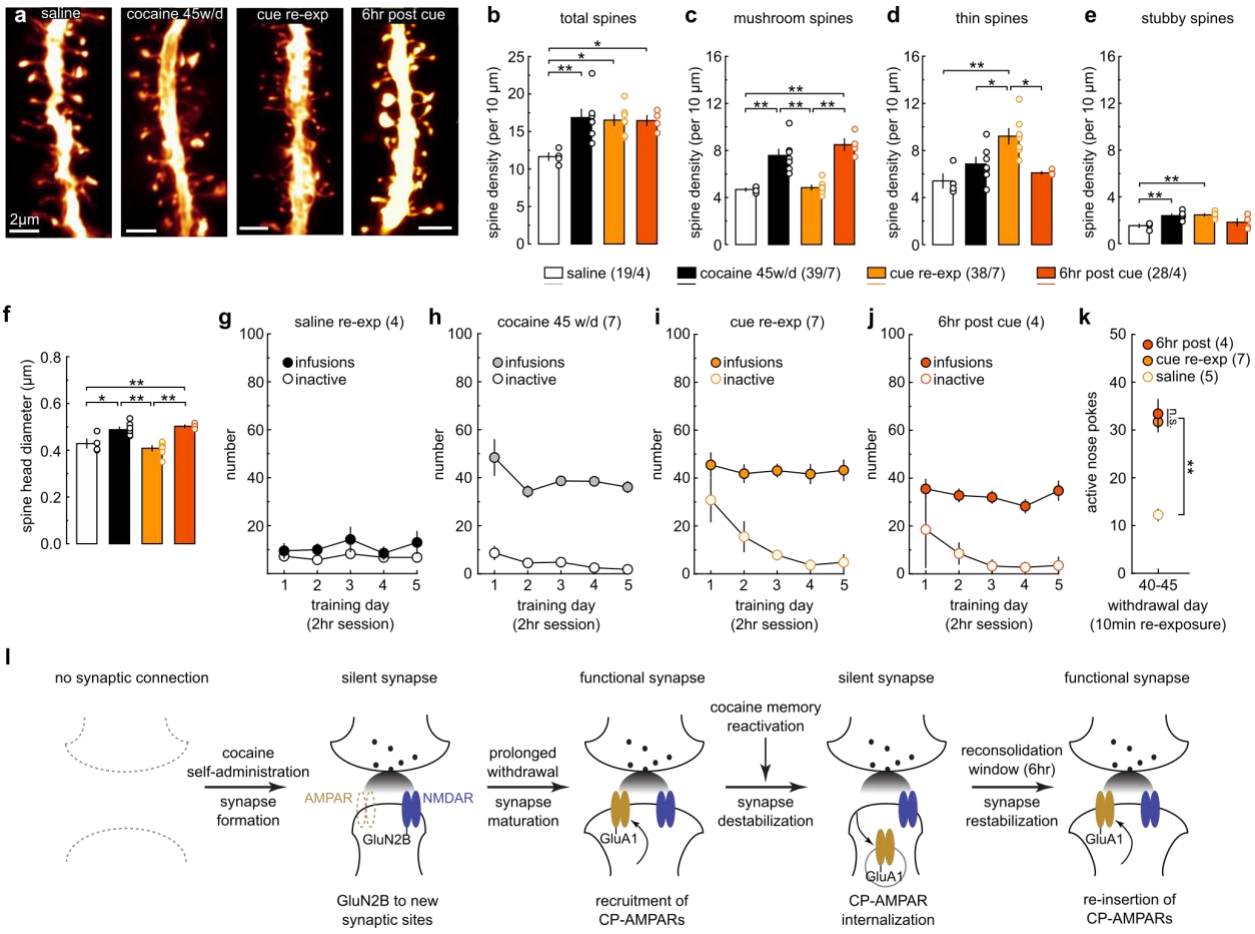

Figure 12. Spine Morphology Correlate with Memory Destabilization and Reconsolidation

(a) Example NAc Shell dendrites from saline-trained rats with cue re-exposure (far left), cocaine-trained rats without (middle left), 10 min after (middle right) and 6 h after (far right) cue re-exposure on withdrawal day 45. **(b)** Summary showing that the density of total spines was increased after 45 d of withdrawal from cocaine compared with saline controls, and this increase was not altered by cue re-exposure and reconsolidation (saline = 11.66 ± 0.49, n = 4 animals; cocaine 45 w/d = 16.86 ± 1.12, n = 7 animals; cocaine re-exp = 16.53 ± 0.716, n = 7 animals; cocaine 6 h post = 16.46 ± 0.665, n = 4 animals; $F_{3,18} = 5.98$, $p = 0.0051$, one-way ANOVA; *P < 0.05, **P < 0.01, Bonferroni post-test). **(c)** Summary showing that the density of mushroom-like spines was increased after 45 d of withdrawal from cocaine compared with saline controls. Cue re-exposure decreased mushroom-like spine density to saline levels, while this cue re-exposure- induced effect disappeared 6 h later (saline = 4.68 ± 0.129, n = 4; cocaine 45 w/d = 7.57 ± 0.531, n = 7; cocaine re-exp = 4.84 ± 0.215, n = 7; cocaine 6 h post = 8.50 ± 0.493, n = 4; $F_{3,18} = 19.86$, $p < 0.0001$, one-way ANOVA; **P < 0.01, Bonferroni post-test). **(d)** Summary showing that the density of thin spines was increased by cue re-exposure in cocaine-trained rats compared with saline-trained rats or cocaine rats without re-exposure. Density

of thin spines normalized 6 h after re-exposure (saline = 5.43 ± 0.598, n = 4 animals; cocaine 45 w/d = 6.86 ± 0.568, n = 7 animals; cocaine re-exp = 9.21 ± 0.643, n = 7 animals; cocaine 6 h post = 6.12 ± 0.107, n = 4 animals; $F_{3,18}$ = 7.89, p = 0.0014, one-way ANOVA; *P < 0.05, **P < 0.01, Bonferroni post-test). **(e)** Summary showing that the density of stubby spines was increased in cocaine-trained rats with or without cue re-exposure, compared with saline-trained rats (saline = 1.56 ± 0.142, n = 4 animals; cocaine 45 w/d = 2.41 ± 0.115, n = 7 animals; cocaine re-exposure = 2.47 ± 0.09, n = 7 animals; cocaine 6 h post = 1.85 ± 0.295, n = 4 animals; $F_{3,18}$ = 8.28, p = 0.001, one-way ANOVA; **P < 0.01, Bonferroni post-test). **(f)** Summary showing an increase in the overall spine head diameter in cocaine-trained rats compared with saline controls. Spine head diameter in cocaine-trained rats decreased to saline levels after cue re-exposure, which normalized 6 h after re-exposure (saline = 0.429 ± 0.019, n = 4 animals; cocaine 45 w/d = 0.488 ± 0.011, n = 7 animals; cocaine re-exp = 0.401 ± 0.011, n = 7 animals; cocaine 6 h post = 0.503 ± 0.005, n = 4 animals; $F_{3,18}$ = 14.67, p < 0.0001, one-way ANOVA; *P < 0.05, **P < 0.01, Bonferroni post-test). **(g-j)** Self-administration training data of all rats used in spine morphology experiments. **(k)** Nose poke responding during the cue re-exposure session of rats used. Cocaine-trained rats exhibited higher levels of nose pokes compared to saline-trained rats. There was no difference in cocaine-trained rats examined 10 min or 6hr after cue re-exposure (saline = 12.25 ± 1.81, n = 4 animals; cue re-exp = 31.71 ± 2.07, n = 7 animals; 6hr post = 33.50 ± 2.99, n = 4 animals, $F_{2,12}$=23.65, p<0.0001, one-way ANOVA; **p<0.01, Bonferroni posttest). **(l)** Schematic illustration depicting the hypothesized dynamics of cocaine-generated silent synapses during acquisition, consolidation, destabilization and reconsolidation of cocaine-associated memories.

mushroom-like spines decreased to lower levels, similar to the saline-trained rats (**Figure 12 c**). This decrease coincided with an increase in the density of thin spines (**Figure 12 d**). Stubby spines were unaffected by cue re-exposure (**Figure 12 e**). The simultaneous downshift in mushroom-like spines and upshift in thin spines suggest that some mature synapses return to a weakened, immature state, consistent with the scenario that matured cocaine-generated synapses are re-silenced after cue re-exposure. Furthermore, 6 hrs after cue re-exposure, the density of mushroom-like and thin spines returned back to levels similar to the cocaine-trained rats without cue re-exposure, also with no change in the density of total spines (**Figure 12 a-e**), suggesting the weakened spines have re-

matured by the end of the destabilization window, which corresponds to the re-maturation of silent synapses and memory reconsolidation.

The diameter of spine heads can also be used as an additional measure of synaptic strength, complementary to the above morphological classification (Matsuzaki et al., 2001). After 45 days of withdrawal from cocaine self-administration, the mean diameter of spine heads was increased compared to saline-trained rats (**Figure 12 f**), indicating overall synaptic strengthening. Following cue re-exposure, the mean diameter of spine heads decreased to saline control levels (**Figure 12 f**), suggesting synaptic weakening or re-silencing. However, 6 hrs after cue re-exposure, the mean diameter of spine heads returned back to the level of cocaine-trained rats without cue re-exposure (**Figure 12 f**), suggesting re-strengthening or re-maturation of synapses.

Based on the above results, we hypothesize that the states of NAc cocaine-generated synapses, including their generation, maturation, re-silencing, and re-maturation, contribute to the encoding, consolidation, retrieval-induced destabilization, and reconsolidation of cocaine-associated memories, respectively (**Figure 12 l**).

2.4.3 Synaptic Re-Silencing Destabilizes Cocaine-Associated Memories

To determine the role of the dynamic re-silencing and re-maturation of cocaine-generated synapses in the destabilization and subsequent reconsolidation of cocaine-associated memories, we adopted a strategy to prevent the re-maturation of silent synapses after cue re-exposure by preventing the re-insertion of CP-AMPARs. Specifically, the small peptide TGL can bind to the c-terminal domain of GluA1 subunits, which is critical for their trafficking and insertion into the synapse, thereby disrupting the synaptic insertion of GluA1-containing AMPARs, which are the predominant population of CP-AMPARs expressed after cocaine self-administration (Conrad et

al., 2008; Lin et al., 2010). We conjugated TGL and its mutant control peptide AGL with a TAT

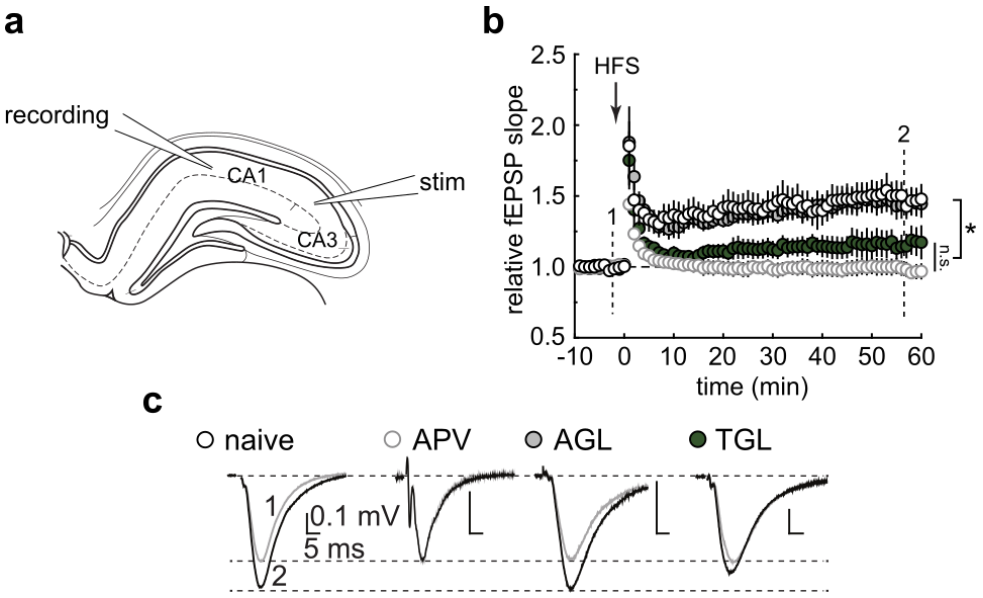

Figure 13. Verification of TAT-TGL Peptide

(**a**) Schematic of the setup for the recording of field EPSPs within hippocampal CA1 and stimulation of Schaffer Collaterals. (**b**) Summarized results showing that this form of LTP, which was sensitive to the NMDAR- selective antagonist APV, was abolished in sliced pre-incubated with TGL, but not AGL (at time 60min: control = 1.48 ± 0.10, n = 8 cells; APV = 0.969 ± 0.05, n = 6 cells; AGL = 1.45 ± 0.092, n = 7 cells; TGL = 1.174 ± 0.113, n = 8 cells, $F_{207, 1725}$=3.07, p<0.0001, two-way RM ANOVA; *p<0.05, Bonferroni posttest, cell-based statistics). (**c**) Example traces for each group before (grey) and after (black) the induction of LTP. Numbers indicate at what time the traces were collected from.

sequence to allow for intracellular delivery *in vivo*. To verify the efficacy of this peptide, we induced a subtype of NMDAR-dependent LTP in hippocampal CA1 (**Figure 13**), the expression of which primarily relies on synaptic insertion of GluA1-containing AMPARs (Hayashi et al., 2000; Zhou et al., 2017). Preincubation of hippocampal slices with TGL, but not AGL, prevented the induction and expression of this GluA1-containing AMPAR-dependent LTP (**Figure 13**), validating this peptide-based approach.

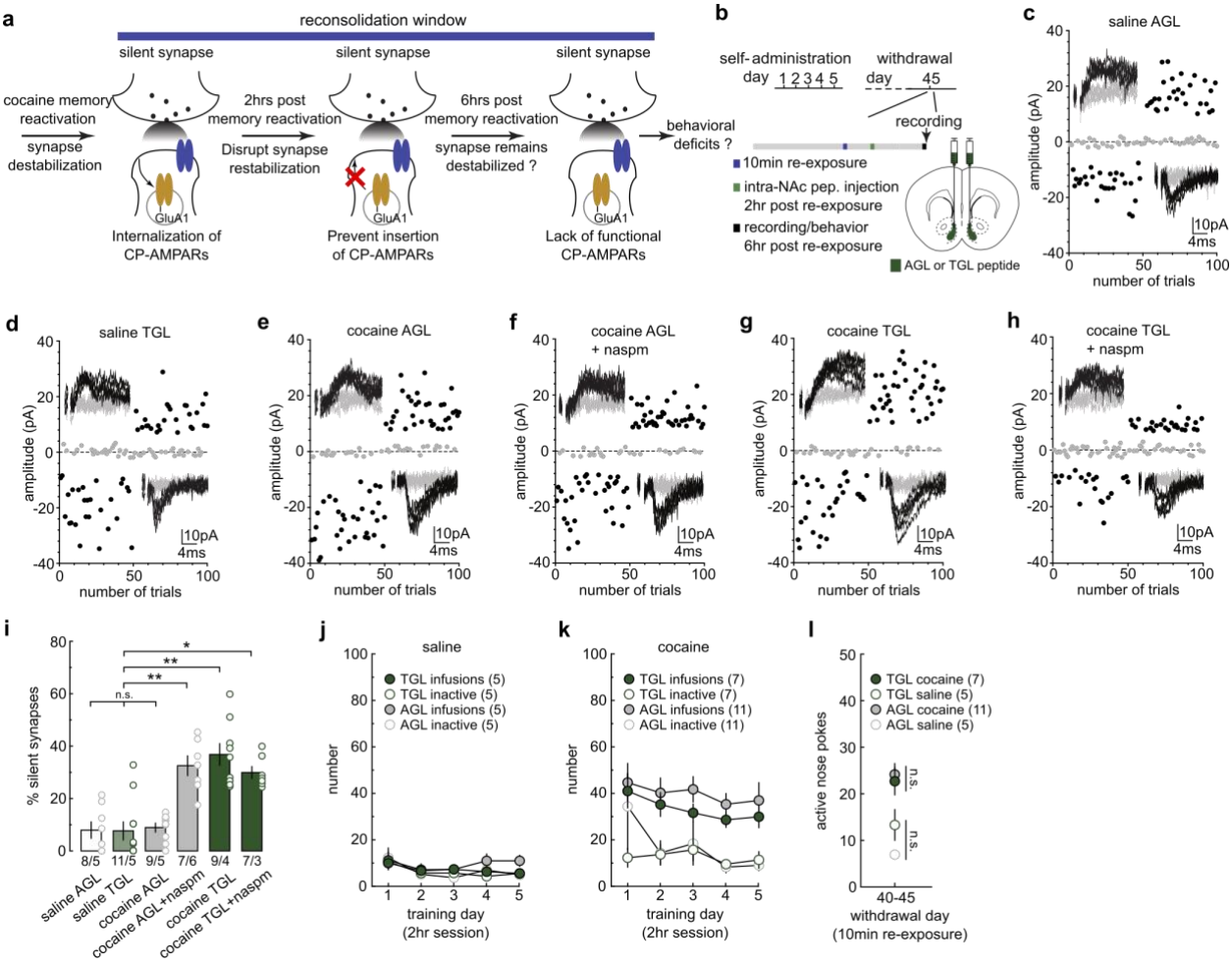

Figure 14. Blocking Synaptic Insertion of CP-AMPARs Maintains Synapses in a Silent State

(**a**) Diagram illustrating the hypothesis that preventing CP-AMPAR re-insertion during the reconsolidation window locks cocaine-generated synapses in the silent state and compromises cue-induced cocaine seeking. (**b**) Diagram showing experimental timeline. (**c**-**h**) EPSCs evoked at -70mV and +50mV (insets) over 100 trials from example recordings for each group (**c**, saline AGL; **d**, saline TGL; **e**, cocaine AGL; **f**, cocaine AGL + naspm; **g**, cocaine TGL; **h**, cocaine TGL + naspm). (**i**) Summary showing that while intra-NAc Shell TGL or AGL did not affect the percentage of silent synapses in saline-trained rats, intra-NAc Shell TGL, but not AGL, maintained the cue re-exposure-induced high percentage of silent synapses in cocaine-trained rats beyond the presumable 6-h destabilization window, and CP-AMPAR inhibition by NASPM did not further affect the percentage of silent synapses (saline AGL = 6.40 ± 3.68, n = 5 animals; saline TGL = 7.06 ± 3.07, n = 5 animals; cocaine AGL = 9.70 ± 1.05, n = 5 animals; cocaine AGL NASPM = 33.76 ± 3.71, n = 6 animals; cocaine TGL = 37.10 ± 3.71, n = 4 animals; cocaine TGL NASPM = 29.70 ± 3.08, n = 3 animals; $F_{5,22} = 14.85$, $p < 0.0001$, one-way ANOVA; NS > 0.05, *P < 0.05, **P < 0.01, Bonferroni post-

test). (**j-k**) Self-administration training data of all rats used in electrophysiology experiments. (**l**) Summary showing no difference in nose poking responding during the 10-min cue re-exposure session in rats presented in Figure 3c-f (saline AGL = 7.00 ± 0.775, n =5 animals; saline TGL = 13.40 ± 3.30, n = 5 animals, t_8=1.89, *p*=0.09, saline-AGL vs saline-TGL; cocaine AGL = 24.00 ± 2.34, n = 11 animals; cocaine TGL = 22.57 ± 2.94, t_{16}=0.38, *p*=0.71, cocaine-AGL vs cocaine-TGL, two-tail, unpaired t-test, n.s. > 0.05).

To attempt to block the re-maturation of cocaine-generated synapses during the destabilization window (**Figure 14 a**), we infused TGL, or AGL as control, (30μM per side) into the NAc shell of rats approximately 2 hrs after cue re-exposure on withdrawal day 45 (**Figure 14 b**), a time point when silent synapses were significantly elevated (**Figure 9**). We then assessed the percentage of silent synapses 6 hrs after cue re-exposure, the time point at which the synapses re-silenced by cue re-exposure have normally re-matured (**Figure 9**). Infusion of either peptide did not alter the percentage of silent synapses in saline-trained rats (**Figure 14 c,d,i**), suggesting these peptides do not by themselves influence the levels of silent synapses. Cocaine-trained rats that receive AGL infusions exhibited a low percentage of silent synapses, which was increased by NASPM application, indicating the expected re-maturation of cocaine-generated synapses occurred (**Figure 14 e,f,i**). In contrast, rats that received TGL infusions exhibited a persistent elevated percentage of silent synapses, and application of NASPM did not further change this percentage (**Figure 14 g-i**), indicating the measured silent synapses are the cocaine-generated silent synapses enriched with CP-AMPARs. Thus, preventing the synaptic insertion of GluA1-containing AMPARs prevents the re-maturation of the re-silenced synapses after cue re-exposure, and locks cocaine-generated synapses in a weakened and destabilized state.

Our subsequent results show that, when administered within the destabilization window, the TGL peptide also prevented the re-enlargement of dendritic spines. Specifically, infusion of

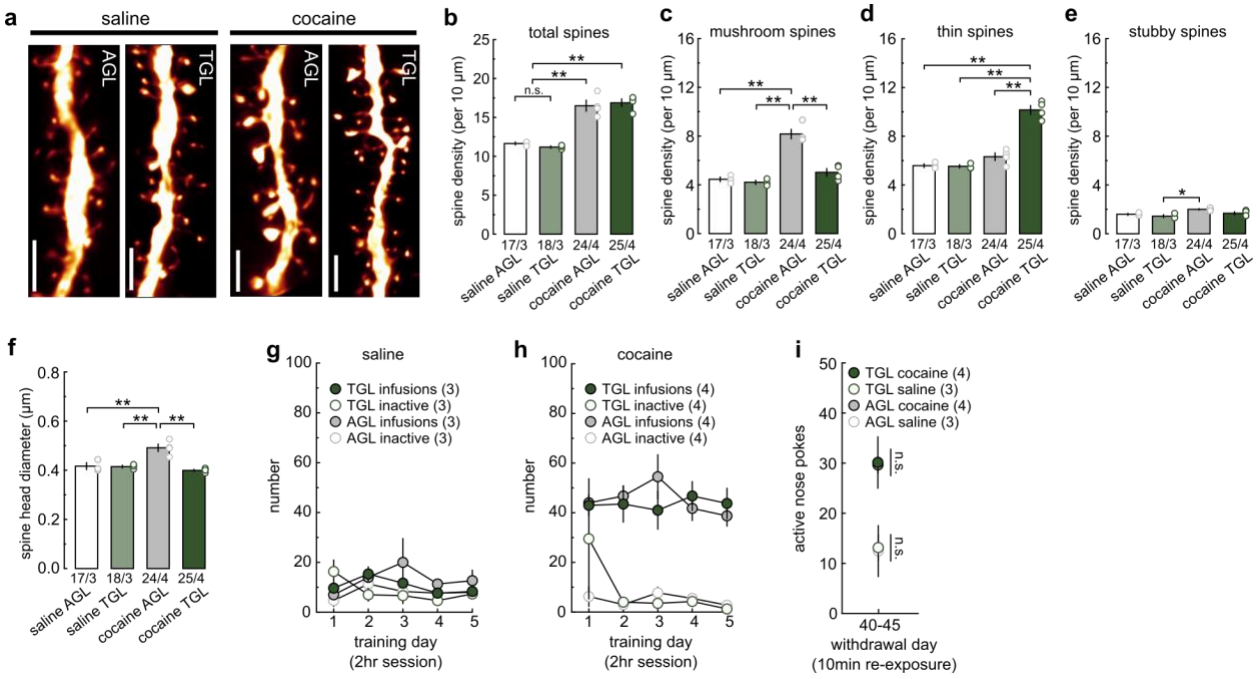

Figure 15. Blocking Synaptic Insertion of CP-AMPARs Maintains Thin Spine Morphology

(**a**) Example NAcSh dendrites from saline-trained rats and cocaine- trained rats with AGL and TGL infusions. Scale bar, 2.5 µm. (**b**) Summary showing that the density of total spines was increased in cocaine-trained rats with either AGL or TGL compared with saline-trained rats (saline AGL = 11.66 ± 0.171, n = 3 animals; saline TGL = 11.20 ± 0.146, n = 3 animals; cocaine AGL = 16.52 ± 0.69, n = 4 animals; cocaine TGL = 16.89 ± 0.488, n = 4 animals; $F_{3,10}$ = 36.01, p < 0.0001, one-way ANOVA; NS > 0.05 **P < 0.01, Bonferroni post-test). (**c**) Summary showing that the density of mushroom-like spines was increased in cocaine-trained rats with AGL compared with saline-trained rats, while TGL treatment normalized mushroom-like spine density to saline levels (saline AGL = 4.46 ± 0.19, n = 3 animals; saline TGL = 4.23 ± 0.163, n = 3 animals; cocaine AGL = 8.18 ± 0.383, n = 4 animals; cocaine TGL = 5.04 ± 0.302, n = 4 animals; $F_{3,10}$ = 38.59, p < 0.0001, one-way ANOVA; **P < 0.01, Bonferroni post-test). (**d**) Summary showing that the density of thin spines was significantly increased in cocaine-trained TGL rats compared with cocaine-trained AGL rats or saline-trained rats (saline AGL = 5.60 ± 0.148, n = 3 animals; saline TGL = 5.54 ± 0.132, n = 3 animals; cocaine AGL = 6.33 ± 0.309, n = 4 animals; cocaine TGL = 10.16 ± 0.363, n = 4 animals; $F_{3,10}$ = 60.80, p < 0.0001, one-way ANOVA; **P < 0.01, Bonferroni post-test). (**e**) Summary showing densities of stubby spines in

saline- and cocaine-trained rats with AGL or TGL treatment (saline AGL = 1.60 ± 0.076, n = 3 animals; saline TGL = 1.45 ± 0.117, n = 3 animals; cocaine AGL = 2.01 ± 0.051 n = 4 animals; cocaine TGL = 1.69 ± 0.118, n = 4 animals; $F_{3,10}$ = 6.32, p = 0.0112, one-way ANOVA; *P < 0.05, Bonferroni post-test). (**f**) Summary showing that the mean spine head diameter was increased in cocaine-trained AGL rats compared with saline-trained rats, while TGL treatment normalized this increase to saline control levels (saline AGL = 0.417 ± 0.013, n = 3 animals; saline TGL = 0.415 ± 0.005, n = 3 animals; cocaine AGL = 0.492 ± 0.015, n = 4 animals; cocaine TGL = 0.400 ± 0.004, n = 4 animals; $F_{3,10}$ = 16.17, p = 0.0004, one-way ANOVA; **P < 0.01, Bonferroni post-test). (**g,h**) Self-administration training data of all rats used in spine morphology experiments. (**i**) Summary showing no difference in nose poking responding during the 10-min cue re-exposure session in rats presented in Figure 3g-l (saline AGL = 12.33 ± 5.04, n =3 animals; saline TGL = 13.00 ± 2.52, n = 3 animals, t_4=0.118, p=0.9116, saline-AGL vs saline-TGL; cocaine AGL = 29.50 ± 1.56, n = 4 animals; cocaine TGL = 30.00 ± 5.12, t_6=0.094, p=0.9285, cocaine-AGL vs cocaine-TGL, two-tail, unpaired t-test, n.s. > 0.05).

the TGL or AGL peptides 2 hrs after cue re-exposure did not change the density of any spine subtypes in saline-trained rats (**Figure 15 a-e**), again demonstrating these peptides do not by themselves alter spine morphology. However, after 45 days of withdrawal from cocaine, the cue re-exposure induced increase in thin spines and decrease in mushroom-like spines, which would otherwise return pre-re-exposure levels 6 hrs later (**Figure 12**), were maintained in the TGL-treated rats (**Figure 15 a-e**). Thus, the spines that were weakened by cue re-exposure in cocaine-trained rats were effectively held in their weakened state by TGL-mediated blockage of GluA1-containing AMPAR trafficking. Consistent with this, the mean diameter of spine heads in cocaine-trained rats treated with TGL was significantly smaller compared to the control rats treated with AGL (**Figure 15 f**). Meanwhile, cocaine-trained rats with either AGL or TGL infusion exhibited higher densities of total spines compared with saline-trained rats, and AGL did not prevent re-maturation of cue re-exposure-induced thin spines (**Figure 15 a-e**). Furthermore, stubby spines were largely insensitive to TGL (**Figure 15 e**).

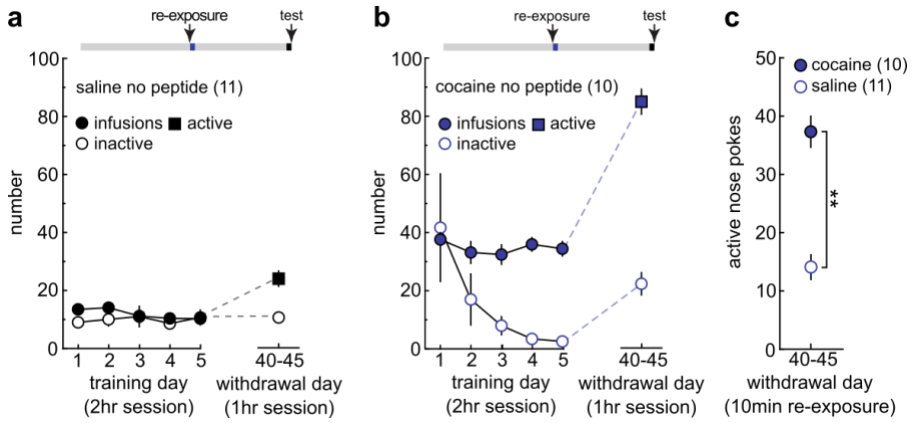

Figure 16. Cocaine Seeking Behavior Remains Elevated 6hrs Post Re-Exposure

(**a,b**) Summary showing that nose poke responding (seeking) in saline (a)- and cocaine (b)-trained rats was not altered when tested 6 hr after cue re-exposure (saline active = 24.18 ± 2.69, n = 11 animals; saline inactive = 10.82 ± 1.16, n =11 animals; cocaine active = 85.20 ± 4.38, n = 10 animals; cocaine inactive = 22.30 ± 3.86, n =11 animals). (**c**) Summary showing that cocaine-trained rats exhibited higher levels of nose poke responding during the 10-min cue re-exposure session compared to saline-trained rats on withdrawal day 45 (saline = 14.33 ± 2.10, n = 11 animals; cocaine = 37.40 ± 2.66, n = 10 animals, t_{17}=6.69, p<0.0001, two-tail, unpaired t-test)

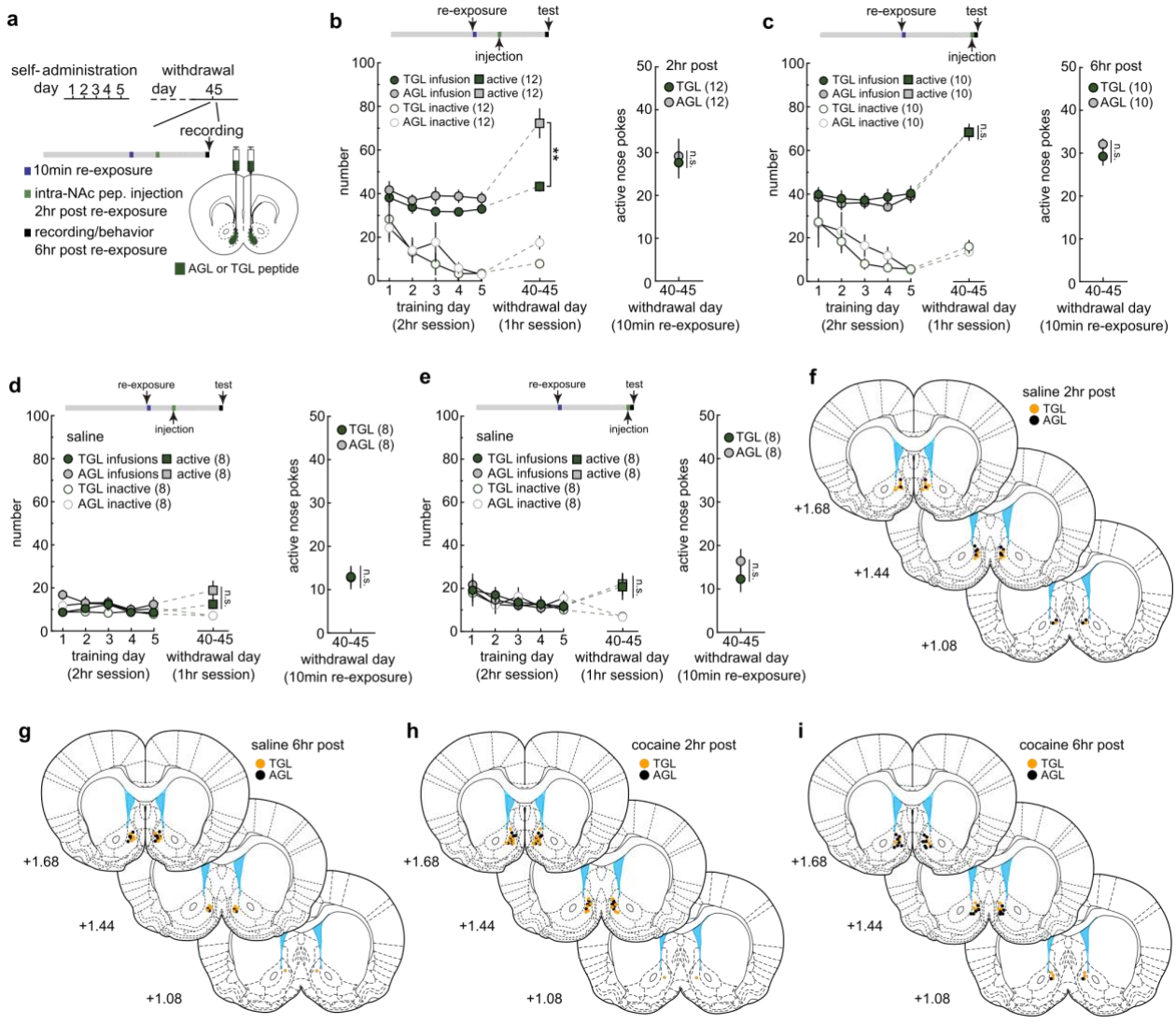

Figure 17. Synaptic Re-Silencing Destabilizes Cocaine-Associated Memories

(**a**) Diagram showing experimental timeline. (**b**) (left) Summary showing that intra-NAc Shell infusion of TGL, but not AGL, at 2 h after cue re-exposure decreased cue-induced cocaine seeking in cocaine-trained rats, measured 6 h after cue re-exposure (AGL active = 72.25 ± 6.68, n = 12 animals; TGL active = 43.25 ± 2.07, n = 12 animals; AGL inactive = 17.58 ± 2.90, n = 12 animals; TGL inactive = 7.92 ± 1.34, n = 12 animals; $F_{1,22} = 12.26$, $p = 0.002$, RM two-way ANOVA, withdrawal day 45 peptide × lever interaction; **P < 0.01, Bonferroni post-test). (right) Summary of nose poke responding during the 10-min cue re-exposure session. Nose poke responding was similar between rats with intra-NAc Shell AGL vs rats with intra- NAc Shell TGL when the peptides were injected 2hr post re-exposure

(AGL = 29.08 ± 3.96, n = 12 animals; TGL = 27.58 ± 3.58, n = 12 animals, t_{22}=0.2811, p=0.7812, two-tail, unpaired t-test). (**c**) (left) Summary showing that rats with intra-NAc Shell infusion of TGL 6 h after cue re-exposure exhibited similar cue-induced cocaine seeking as AGL rats measured 6.5 h after cue re-exposure (AGL active = 68.20 ± 2.87, n = 10 animals; TGL active = 68.20 ± 3.74, n = 10 animals; AGL inactive = 13.30 ± 1.69, n = 10 animals; TGL inactive = 15.70 ± 2.94, n = 10 animals; $F_{1,18}$ = 0.23, p = 0.64, RM two-way ANOVA, withdrawal day 45 peptide × lever interaction). (right) Summary of nose poke responding during the 10-min cue re-exposure session. Nose poke responding was similar between rats with intra-NAc Shell AGL vs rats with intra- NAc Shell TGL when the peptides were injected 6hr post re-exposure (AGL = 32.10 ± 1.20, n = 10 animals; TGL = 29.30 ± 2.01, n = 10 animals, t_{18}=1.196, p=0.2471, two-tail, unpaired t-test). (**d**) (left) Summary showing that intra-NAc Shell infusions of AGL or TGL 2 hr after cue re-exposure did not affect cue-induced nose poke responding in saline-trained rats, measured 6 hr after re-exposure (AGL active = 17.87 ± 4.14, n = 8 animals; TGL active = 12.25 ± 2.07, n =8 animals; AGL inactive = 7.00 ± 1.65, n = 8 animals, TGL in active = 7.00 ± 1.71, n = 8 animals, $F_{1,7}$=4.95, p=0.0614, RM two-way ANOVA, withdrawal day 45 peptide x hole interaction). (right) Nose poke responding during the 10-min cue re-exposure session was also not different between AGL and TGL rats (AGL = 13.00 ± 2.73, n = 8 animals; TGL = 13.00 ± 2.27, n =8 animals, t_{14}=0.000, p=1.00, two-tail unpaired t-test). (**e**) (left) Summary showing that intra-NAc Shell infusions of AGL or TGL 6 hr after cue re-exposure did not affect cue-induced nose poke responding, tested 6.5 hr after cue re-exposure, in saline-trained rats (AGL active = 22.13 ± 4.88, n = 8 animals; TGL active = 20.88 ± 5.92, n = 8 animals; AGL inactive = 6.75 ± 1.37, n = 8 animals; TGL inactive = 7.13 ± 1.46, n = 8 animals, $F_{1,7}$=0.0, p=0.7986, RM two-way ANOVA, withdrawal day 45 peptide x hole interaction). (right) Nose poke responding during the 10-min cue re-exposure session was also not different between AGL and TGL rats (AGL = 16.25 ± 2.72, n = 8 animals; TGL = 12.13 ± 2.91, n = 8 animals, t_{14}=1.036, p=0.3179, two- tail, unpaired t-test). (**f-i**) Diagrams showing the localization of the infusion needle tips for all rats included in the data analysis.

If the re-silencing and re-maturation of cocaine-generated synapses underlie the destabilization and reconsolidation of cocaine memories, preventing their re-maturation should disrupt reconsolidation and decrease the rats' subsequent cue-induced cocaine seeking. To test this idea, we treated cocaine-trained rats with the same peptide procedure used above (**Figure 17 a**),

and measured cocaine seeking 6 hrs after cue re-exposure, a time point at which cocaine seeking was robust in cocaine-trained rats with no peptide infusion (**Figure 16**). Infusion of either TGL or AGL peptides during the destabilization window had no effect on operant behavioral responding in saline-trained rats (**Figure 17 d,e**), indicating minimal off-target effects of these peptides. However, cocaine-trained rats that received TGL infusions exhibited decreased cocaine seeking compared with AGL-treated rats when tested 6 hrs after cue re-exposure, suggesting that preventing the re-maturation of cocaine-generated silent synapses once they are re-silenced during the destabilization window compromises the reconsolidation of cocaine–cue memories (**Figure 17 b**). Note that during the 10-min cue re-exposure, AGL- and TGL-treated rats exhibited similar levels of cocaine seeking, indicating similar initial memory strength and reactivation in these rats before peptide administration. Importantly, when peptides were infused 6 hrs after cue re-exposure, a time point outside of the hypothesized destabilization window, cocaine-trained TGL-treated rats exhibited similarly high levels of cocaine seeking as in cocaine-trained AGL-treated rats, suggesting that once silent synapses have re-matured, cocaine memories become resistant to TGL manipulations (**Figure 17 c**). These results reveal a causal link of the functional dynamics of cocaine-generated synapses to the destabilization and reconsolidation of cocaine memories.

2.5 Discussion

The synaptic mechanisms underlying destabilization and reconsolidation of drug-associated memories remain largely elusive. Our current findings provide such a mechanism, in which the dynamic state of a specific population of synapses, initially generated by cocaine experience, controls the destabilization and reconsolidation of cocaine memories. Furthermore, we

believe these findings provide additional evidence to support the hypothesis that cocaine-generated synapses represent a discrete synaptic ensemble through which key aspects of cocaine-associated memories can be manipulated for therapeutic benefit.

2.5.1 Cocaine-Generated Synapses Regulate Cocaine-Associated Memory Dynamics

Memories are not static, but after their formation and consolidation, stable memories can be destabilized again upon memory retrieval, followed by reconsolidation (Dudai, 2012; Nader and Hardt, 2009). The destabilization not only allows for updating memories in response to changing outcomes, but also provides a therapeutic opportunity to weaken undesirable memories (Lee, 2008; Torregrossa and Taylor, 2013). Although synapses are important memory-encoding substrates, how synapses operate to mediate these memory dynamics has remained quite elusive. New AMPAR-silent excitatory synapses are generated in the NAc when rats acquire cue-conditioned cocaine self-administration, and then mature over prolonged withdrawal as cue-induced cocaine seeking strengthens (Lee et al., 2013; Ma et al., 2014; Ma et al., 2016). Here, we demonstrate that these synapses are re-silenced and weakened upon memory destabilization following memory reactivation, and then re-mature when the memory reconsolidates (**Figures 6-12**). When these synapses are held in the silent state after memory retrieval-induced re-silencing, reconsolidation is compromised, resulting in decreased cocaine seeking (**Figures 13-17**). These findings depict cocaine-generated silent synapses as key cellular substrates underlying the dynamic process of memory destabilization and reconsolidation. As such, cocaine memories, can be mechanistically manipulated through specific underlying populations of synapses during the memory destabilization window, during which these synapses are naturally destabilized and primed for modification.

Evidence from the literature suggests that similar mechanisms may also be involved in the destabilization of other types of memories. Specifically, we observed memory retrieval induced the internalization of CP-AMPARs from cocaine-generated synapses, resulting in their silencing. Studies examining fear memories, have also observed the internalization of AMPARs at excitatory synapses within the BLA following the reactivation and destabilization of conditioned fear memories, and that this process is necessary for memory destabilization to occur (Ferrara et al., 2019; Rao-Ruiz et al., 2011). It remains to be determined if these AMPARs are internalized at specific, memory-encoding synapses, but are consistent with our results and may indicate synaptic silencing may represent a generalized mechanism underlying memory destabilization. However, there are some unique features of cocaine-generated synapses, that may lead to differences in the mechanisms governing their dynamics. Namely, cocaine-generated synapses are enriched with CP-AMPARs, which are typically not present in functionally stable and mature synapses in principle neurons, eventually being swapped for GluA2-containing AMPARs (Guire et al., 2008; Morita et al., 2013; Park et al., 2016; Plant et al., 2006; Shi et al., 2001). The persistence of CP-AMPARs following cocaine experience may be due to dysregulation of mechanisms regulating their translation, trafficking, and degradation (Loweth et al., 2018; Loweth et al., 2014; Scheyer et al., 2014; Werner et al., 2018) (for discussion and review see (Wright and Dong, 2020)). This may ultimately result in some differences in the underlying mechanisms regulating memory retrieval-induced AMPAR internalization. Regardless, synaptic weakening and re-silencing may reset synapses and allow them to be modified through altering their AMPAR content and distribution, and when this is done across the entire population of memory-encoding synapses it allows for memory content to be updated.

2.5.2 Complexities of Cocaine-Associated Memories and Behaviors

Cocaine-associated memories are complex and contain information related to unconditioned responses, discrete and contextual conditioned stimuli, motivation, value, action, and outcome. These different aspects of cocaine-associated memories are not reactivated in isolation in our experimental setup as rats are exposed to the cues and context, and allowed to respond operantly. This contrasts with previous studies examining the reconsolidation of cocaine-associated memories, which typically will extinguish specific aspects, such as the context and/or operant response (Fuchs et al., 2009; Rich et al., 2019b). Therefore, our results do not specify which specific components of cocaine memories are controlled by cocaine- generated synapses. However, since our experiments were primarily confined to the NAc, cocaine-generated synapses within this area may contribute to the encoding of values associated with conditioned stimuli, which may include both discrete and contextual cues (Sugam et al., 2014; West and Carelli, 2016). Given the role of the NAc shell in encoding context (Fuchs et al., 2008; Ito et al., 2008), it might be expected cocaine-generated synapses within the shell may preferentially encode contextual associations. In contrast, cocaine-generated synapses within the NAc shell, as well as those in the NAc core, may contribute to the encoding of multiple aspects of cocaine-associated memories. Our present study randomly sampled silent synapses, presumably from all main NAc excitatory inputs that likely encompass many different aspects of cocaine memories, however, our previous studies have found that cocaine experience generates silent synapses in all NAc afferents examined thus far, including the mPFC, BLA, and PVT (Lee et al., 2013; Ma et al., 2014; Neumann et al., 2016a). Therefore, cocaine-generated synapses within individual projections may encode specific aspects of cocaine memories, while collectively these synapses encode broader, multifaceted

cocaine memories. Future studies will be needed, however, to delineate how cocaine-generated synapses contribute to cocaine-associated memories and behavior.

When evaluating the translational potential of our current findings, boundary effects should be considered. While the training procedures used in the current study produce robust and persistent memories and 'incubated' drug seeking typically seen after extensive exposure to drugs (Conrad et al., 2008; Grimm et al., 2001), they do not adequately model the overtraining that occurs in human subjects with years of drug taking (Taylor et al., 2008). Overtraining can produce memories that are resistant to destabilization on traditional memory reactivation, although such boundary conditions may be transient (Wang et al., 2009). It will be important for future studies to determine whether such boundary conditions result from impaired re-silencing of cocaine-generated synapses, or if these synapses may no longer be critical for the memory. In addition, this issue is further complicated in the case of addiction, where long periods of drug use that promote compulsive behaviors that trigger the engagement and dominance of other neural circuits, such as the dorsal striatum, to govern behavior (Bender and Torregrossa, 2021; Lüscher et al., 2020). It remains to be determined if cocaine-generated synapses contribute to this process or not.

2.5.3 Concluding Remarks

Cocaine-generated silent synapses are sparsely distributed across several NAc afferents, but collectively form a unique synaptic population, whose dynamic changes control the encoding, destabilization, and reconsolidation of cocaine memories. These synapses may represent a discrete synaptic ensemble, through which cocaine memories are stored, retrieved and reconsolidated, and can be potentially targeted for clinical benefits.

3.0 Rac1 Activity Regulates the Functional State of Cocaine-Generated Synapses

This Chapter is adapted from portions of the published manuscript:

Wright, W.J., Graziane, N.M., Neumann, P.A., Hamilton, P.J., Cates, H.M., Fuerst, L., Spenceley, A., Mackinnon-Booth, N., Iyer, K., Huang, Y.H., Shaham, Y., Schlüter, O.M., Nestler, E.J., & Dong, Y. (2020) Silent synapses dictate cocaine memory destabilization and reconsolidation. ***Nature Neuroscience,*** 23(1); 32-46.

3.1 Overview

Cocaine-associated memories are persistent and long-lasting, however, upon retrieval they can be transiently destabilized and rendered susceptible to disruptions, before they are reconsolidated. These dynamics of cocaine-associated memories are, in part, mediated by dynamic changes in the functional state of cocaine-generated synapses within the NAc, such that synapses are rapidly re-silenced following memory retrieval, before they functionally re-mature. Thus, targeting these synapses may have therapeutic potential. However, the mechanisms regulating these dynamic changes in synaptic state remain unknown. Here, we show that the activity of the small GTPase, Rac1, is also dynamically altered following the retrieval of cocaine-associated memories, displaying a decrease in activity before returning back to normal activity levels. This decrease in Rac1 activity is sufficient and necessary for the re-silencing of cocaine-generated synapses following memory retrieval. Furthermore, artificially increasing the activity of Rac1 serves to stabilize synapses in their current state, irrespective if this is a weakened or strengthened state. Targeting Rac1 activity allows for the manipulation of synaptic states, such that they can be driven to or maintained in a weakened and silent state, and ultimately regulated the expression of

cocaine-associated memories. Together, these findings highlight Rac1 as a molecular switch regulating synaptic stability, which can be directly targeted for memory disruption.

3.2 Introduction

Memories associated with drugs are persistent and last long after drug use has ceased, the reactivation of which can trigger cravings and relapse (Hyman et al., 2006b). As such, there is great interest in identifying mechanisms that can disrupt such drug-associated memories for the development of effective therapeutics. One potential avenue that has garnered much attention is by utilizing the natural dynamics of memories. Specifically, upon retrieval memories become transiently destabilized and made susceptible to disruption, before they are reconsolidated and stabilized once again (Dudai, 2012; Nader and Hardt, 2009; Torregrossa and Taylor, 2013). Indeed, disrupting reconsolidation following retrieval-induced destabilization of drug-associated memories has been effective in suppressing subsequent drug seeking behavior in rodent models (Fuchs et al., 2009; Lee et al., 2005; Lee et al., 2006; Miller and Marshall, 2005; Torregrossa and Taylor, 2013). However, there has been less success in human patients (Dunbar and Taylor, 2017; Jobes et al., 2015; Lonergan et al., 2016). Identifying the neural mechanisms that underlie memory destabilization and reconsolidation may allow for more precise and robust disruption of drug-associated memories by directly manipulating these processes.

Cocaine experience triggers synaptic remodeling within the NAc, a key node within the reward circuitry, that contributes to drug seeking behavior after withdrawal (Wolf, 2016a; Wright and Dong, 2020). This synaptic remodeling is mediated in part by the generation of new synapses, which are initially immature AMPAR-silent synapses. These cocaine-generated synapses then

functionally mature through the recruitment of CP-AMPARs during withdrawal, and critically contribute to subsequent cocaine seeking (Huang et al., 2009; Lee et al., 2013; Ma et al., 2014). Furthermore, we recently demonstrated that dynamic changes in the functional state of cocaine-generated synapses, namely their re-silencing and re-maturation, contributes to the destabilization and reconsolidation of cocaine-associated memories. Therefore, these cocaine-generated synapses may represent a discrete synaptic ensemble, through which aspects of cocaine-associated memories are encoded, and targeting the mechanisms regulating their functional state may allow for more effective disruption of cocaine-associated memories.

Synaptic state is governed by a plethora of different processes that regulate the structure and function of the synapse. One component of the synapse that may play a particularly important role conferring stability to the synapse is the actin cytoskeleton (Cingolani and Goda, 2008). The actin cytoskeleton plays a critical role in regulating the trafficking and anchoring of AMPARs within the PSD (Allison et al., 1998; Zhou et al., 2001), as well as being essential for maintaining synaptic structure (Fukazawa et al., 2003; Honkura et al., 2008; Okamoto et al., 2004; Okamoto et al., 2007). Furthermore, there is evidence that the actin cytoskeleton also contributes to maintenance and stability of memories (Kim et al., 2019; Lunardi et al., 2018; Medina et al., 2020; Rex et al., 2010). Therefore, dynamic restructuring of the actin cytoskeleton may underlie the changes in synaptic state observed following memory reactivation.

The actin cytoskeleton within dendritic spines is highly complex and regulated by a large number of factors and signaling pathways (Cingolani and Goda, 2008). However, one class of signaling molecules that play a critical role in the activity-dependent remodeling of the actin cytoskeleton are the Rho class of small GTPases, which play a role in the regulation of actin depolymerization and polymerization (Hedrick and Yasuda, 2017; Nishiyama and Yasuda, 2015;

Yasuda, 2017). The most studied Rho-GTPases include RhoA, which generally is thought to promote actin depolymerization and spine shrinkage (Li et al., 2000; Nakayama et al., 2000; Tashiro et al., 2000), and Cdc42 and Rac1, which promote actin polymerization and spine enlargement (Hedrick et al., 2016; Murakoshi et al., 2011; Tashiro et al., 2000). Rac1 activity, however, may preferentially serve to stabilize the actin cytoskeleton, rather than drive its enlargement (Nakayama et al., 2000; Tashiro and Yuste, 2004), and this effect may occur regardless of synaptic state (Hayashi-Takagi et al., 2015). Thus, Rac1 may play a critical role in regulating the stability of synapses and ultimately the memories they encode. This prompted us to examine if changes in the activity of Rac1 underlie the dynamic changes in the functional state of cocaine-generated synapses during the destabilization and reconsolidation of cocaine-associated memories.

3.3 Methods

3.3.1 Subjects

Male Sprauge-Dawley rats (postnatal day 35-40 with 130-150g body weight on arrival) (Charles River) were used in all experiments. Rats were singly housed on a 12hr light/dark cycle (light on/off at 7:00/19:00) with food and water available *ad libitum*. Rats were allowed to habituate their housing cages for approximately 1-2 week before catheter surgery. All rats were used in accordance with protocols approved by the Institutional Care and Use Committee at the University of Pittsburgh.

3.3.2 Catheter Implantation

Catheter implantation surgery for self-administration was performed as described previously (Lee et al., 2013; Mu et al., 2010a). Briefly, a silastic catheter was inserted into the right jugular vein by 2.5 cm, and the distal end was led subcutaneously to the back between the scapulae. Catheters were constructed of silastic tubing (length, 10 cm; inner diameter, 0.0508 cm; outer diameter, 0.09398 cm) and attached to a commercially available Vascular Access Button (Instech). Rats were allowed to recover for approximately 5 days following surgery, during which their wellbeing and weight were monitored. During the recovery period, the catheter was flushed daily with 1 ml kg^{-1} heparin (10 U ml^{-1}) and gentamicin antibiotics (5 mg ml^{-1}) in sterile saline to minimize potential infection and catheter occlusion.

3.3.3 Self-Administration Apparatus

All behavioral experiments were conducted in operant conditioning chambers enclosed within sound attenuating cabinets (Med Associates). Each chamber (29.53 x 24.84 x 18.67 cm^3) contains an active and an inactive nose poke hole, a food dispenser, a conditioned stimulus light within each nose poke hole and a house light. No food or water was provided in the chamber during the training or testing session.

3.3.4 Intravenous Cocaine Self-Administration Training

Cocaine self-administration training began approximately 5 days after catheter implantation. On day 1, rats were placed in the self-administration chamber for an overnight

training session on a fixed ratio 1 reinforcement schedule. Nose poking in the active hole resulted in a cocaine infusion (0.75 mg kg^{-1} over 3-6 secs) and illumination of the conditioned stimulus light inside the nose poke hole as well as the house light. The conditioned stimulus light remained on for 6 secs, whereas the house light was illuminated for 20 secs, during which any additional nose pokes were counted but resulted in no cocaine infusions. After the 20 sec timeout period, the house light was turned off, and the next nose poke in the active hole resulted in a cocaine infusion. Nose pokes in the inactive hole had no reinforced consequences, but were recorded.

Rats first underwent one overnight training session, approximately 12 hrs long, to facilitate acquisition. Only rats that received at least 80 cocaine infusions during the overnight session were allowed to proceed to the 5 day cocaine self-administration training regimen (< 2% of rats failed to meet criteria). The same, or similar, self-administration procedures/standards were used in our previous studies (Lee et al., 2013; Ma et al., 2014; Ma et al., 2016). Rats then underwent 5 days cocaine self-administration training, where they underwent the same cocaine self-administration procedure described above for 2hrs daily. After the fifth day of training, rats were placed back in their home cages and remained there during the subsequent withdrawal days. Cocaine-trained rats that failed to meet the self-administration criteria (≥ 15 infusions per session, 70% active-to-inactive nose poke response ratio) were excluded from further experimentation and analysis.

3.3.5 Withdrawal Phase

Rats were returned to their home cage after each self-administration training session. After the 5 day procedure, the rats were singly housed in their home cage for drug withdrawal, with food and water available *ad libitum*. Withdrawal day 1 was operationally defined as 20-26 hours after

the last session of cocaine self-administration training. Withdrawal day 45 was operationally defined as 40-48 days after the last session of cocaine self-administration training.

3.3.6 Memory Retrieval

Memory retrieval sessions were performed in the same manner as the cocaine seeking test procedure as detailed below, except that the retrieval session lasted 10-15 min.

3.3.7 Cocaine Seeking Test

Cocaine seeking was assessed in an extinction test (1 hr) conducted after 1 day or 45 days of withdrawal from cocaine self-administration. During the extinction test session, rats were placed back in the operant chamber, where active nose pokes resulted in contingent delivery of the conditioned stimulus light cues, but not cocaine. The number of nose pokes to the active hole was used to quantify cocaine seeking. Nose pokes to the inactive hole were also recorded.

3.3.8 Viral Vectors and Delivery

We used the bicistronic p1005 HSV vector to express dnRac1, caRac1, Rac1-C450M (control), pa-dnRac1, and paRac1 combined with green fluorescent protein (GFP) or mCherry, as described previously (Dietz et al., 2012b; Wu et al., 2009). These HSVs were prepared using the same methods described previously (Dietz et al., 2012b; LaPlant et al., 2010; Maze et al., 2010). Earlier work shows that HSVs infect neurons only, and in the NAc, the vast majority of HSV-

infected neurons are MSNs (Barrot et al., 2002). In our recordings, we came across very few transduced inhibitory interneurons (~10 throughout the entire study) and no transduced cholinergic interneurons. Thus, effects mediated by HSV-mediated transduction are most attributable to MSNs.

Due to the rapid and transient HSV-mediated expression, rats were bilaterally implanted with guide cannulae (Plastics One) on withdrawal day 35 targeting the NAc shell (in mm: anterior-posterior (AP), +1.60; medial-lateral (ML), ±1.00; dorsal-ventral (DV), -6.80), which were secured to the skull using dental cement. Rats were injected with HSVs 12–16 hrs before electrophysiological or behavioral experiments on withdrawal day 45. During injection, rats were lightly anesthetized and HSV (1 μl per side) was bilaterally infused (100 nl min^{-1}) through 32-gauge needles extending 1 mm below the cannulae into the NAc shell (in mm: AP, +1.60; ML, ±1.00; DV, −7.80). Infusing needles were left in place for 10 min following injection to prevent backflow and allow for sufficient diffusion of HSV vectors away from the injection site. This approach minimized potential behavioral disturbance following acute intracranial surgeries and allowed for the insertion of optic fibers for the photoactivation experiments (see section "Photostimulation of paRac1").

For electrophysiology experiments, viral injections and expression were visually verified in brain slices prepared for recording, while for behavioral experiments, immunohistochemistry and confocal microscopy (see section "Immunohistochemistry and confocal microscopy") were used for verification. Rats with inaccurate injections or weak viral expression were excluded from data analysis.

3.3.9 LIMKi Injections

To manipulate the PAK-LIMK-cofilin pathway in vivo, we infused CRT0105950 (Tocris), a highly selective LIMK1/2 inhibitor (LIMKi) (Mardilovich et al., 2015), through the cannulae previously installed in rats for the delivery of virus and optical fibers (see previous section). LIMKi was dissolved in 1% dimethylsulfoxide and 0.1 M Dulbecco's sterile PBS. We used 1% dimethylsulfoxide and 0.1 M Dulbecco's sterile PBS as the vehicle control. Infusion of the LIMKi to the NAc shell was performed as described for the peptide infusions (Chapter 2). Briefly, LIMKi at 10 μM (1 μl per side), a dose shown to sufficiently inhibit LIMK with minimal negative effects on cell viability (Mardilovich et al., 2015), was infused into the NAc shell through a preinstalled cannula at a rate of 200 nl min^{-1}. All, electrophysiology recordings were performed within the 200-mm radius of the injection center.

3.3.10 Photoactivation of Rac1

The activity of paRac1 is sharply increased following photostimulation, and then decays exponentially with a half-life (T1/2) ≈ 10 secs at room temperature (Wu et al., 2009). The decay kinetics are likely faster in vivo. We used a stimulation protocol composed of 473-nm laser pulses at frequency of 10 Hz, pulse duration of 0.5 ms and laser intensity of 10 mW mm^{-2}. Laser was generated and controlled by a 473-nm blue laser diode (IkeCool), and the pulse patterns were generated through a waveform isolator (A.M.P.I.). The photostimulation protocol was delivered for 10 min to match the duration of cue re-exposure. Stimulation parameters in this protocol have been verified to introduce minimal tissue damage in behaving rats in our previous studies (Yu et al., 2017), and were used in all photoactivation experiments presented here.

For in vivo photostimulation experiments, rats were bilaterally implanted with guide cannulae (Plastics One) targeting the NAc shell (in mm: AP, +1.60; ML, ±1.00; DV, −6.00) on withdrawal day 35. For rats receiving photostimulation on withdrawal day 45, the rats were slightly restrained and two 200-μm-core optical fibers were bilaterally inserted through the cannulae. The length of the optical fiber was adjusted such that the tip would rest ~300 μm dorsal to the viral injection site (in mm: AP, +1.60; ML, ±1.00; DV, −7.50). Immediately after the optical fiber was secured, the rat was placed back into its home cage or in the operant chamber, depending on the experiment being performed, with the fiber attached to a tether system to allow rats free movement during photostimulation. After the stimulation session, the optical fibers were removed and the rat was placed back into its home cage. For behavioral experiments testing the effects of paRac1 activation 24 h after cue re-exposure, a second photostimulation session 5 h after cue re-exposure was performed to extend the duration of Rac1 activation within the destabilization window.

3.3.11 Rac1 Activity Assay

At specified time points, the rats were killed by decapitation, and the brain was quickly removed and snap-frozen in 2-methylbutane (Sigma Aldrich) for 1 min. Using a brain matrix, 2-mm-thick brain slices were prepared and tissue punches containing the NAc were extracted. The punched tissue was homogenized in lysis buffer (4 °C) and then centrifuged at 14,000g for 2 min at 4 °C. The supernatant was collected and snap-frozen. Lysate was stored at −80 °C. Rac1- GTP was quantified with the Rac1 G-LISA Activation Assay (Absorbance Based; Cytoskeleton) according to the manufacture instructions. Rac1-GTP levels were then assessed by the absorbance of each sample at 490 nm.

3.3.12 Preparation of Acute Brain Slices

Rats were decapitated following isoflurane anesthesia. For NAc-containing slices, coronal slices (250 μm thick) containing the NAc were prepared on a VT1200S vibratome (Leica) in 4 °C cutting solution containing (in mM): 135 N-methyl-d-glutamine, 1 KCl, 1.2 KH_2PO_4, 0.5 $CaCl_2$, 1.5 $MgCl_2$, 20 choline-HCO_3 and 11 glucose, saturated with 95%O_2/5%CO_2 and pH adjusted to 7.4 with HCl. Osmolality was adjusted to 305 mmol kg^{-1}. Immediately after cutting, slices were transferred and incubated in the artificial cerebrospinal fluid (aCSF) containing (in mM): 119 NaCl, 2.5 KCl, 2.5 $CaCl_2$, 1.3 $MgCl_2$, 1 NaH_2PO_4, 26.2 $NaHCO_3$ and 11 glucose, with the osmolality adjusted to 280–290 mmol kg^{-1}. Slices were placed in the aCSF saturated with 95% O_2/5% CO_2 at 37 °C for 30 min and then held at 20–22 °C for at least 30 min before experimentation.

3.3.13 Electrophysiological Recordings

3.3.13.1 Whole-Cell Recordings

All recordings were made from MSNs located in the medial NAcSh. During recordings, slices were superfused with aCSF, heated to 30–32 °C by passing the solution through a feedback-controlled in-line heater (Warner) before entering the recording chamber. To measure excitatory postsynaptic current (EPSC) responses, electrodes (2–5 MΩ) were filled with a cesium-based internal solution (in mM: 135 $CsMeSO_3$, 5 CsCl, 5 TEA-Cl, 0.4 EGTA (Cs), 20 HEPES, 2.5 Mg-ATP, 0.25 Na-GTP, 1 QX-314 (Br), pH 7.3). Picrotoxin (0.1 mM) was included in the aCSF during all recordings to inhibit $GABA_A$ receptor-mediated currents. Presynaptic afferents were stimulated by a constant-current isolated stimulator (Digitimer), using a monopolar electrode (glass pipette

filled with aCSF). Series resistance was typically 7–20 MΩ, uncompensated and monitored continuously during recording. Cells with a change in series resistance >20% were excluded from data analysis. Synaptic currents were recorded with a MultiClamp 700B amplifier, filtered at 2.6–3 kHz, amplified five times and digitized at 20 kHz.

3.3.13.2 Silent Synapse Recording and Analysis

NAc shell MSNs were randomly selected for recording. The minimal stimulation assay was performed as previously described (Brown et al., 2011a; Graziane et al., 2016; Huang et al., 2009; Isaac et al., 1995; Lee et al., 2013; Liao et al., 1995; Ma et al., 2014; Ma et al., 2016; Neumann et al., 2016b). After obtaining small (~50 pA) EPSCs at −70 mV, the stimulation intensity was reduced in small increments to the point that failures versus successes of synaptically evoked events (EPSCs) could be clearly distinguished. The stimulation intensity and frequency were then kept constant for the rest of the experiment. The amplitudes of both AMPAR and NMDAR ESPCs resulting from single vesicular release are relatively large in NAcSh MSNs (for example, ~15 pA for AMPAR mEPSCs at −70 mV), which facilitates the judgment of successes versus failures. For each cell, 50–100 traces were recorded at −70 mV, and 50–100 traces were recorded at +50 mV. Recordings were then repeated at −70 mV and +50 mV for another round or two. Only cells with relatively constant failure rates (changes <15%) between rounds were used to assess percentage of silent synapses. We visually detected failures versus successes at each holding potential over 50–100 trials to calculate the failure rate, as described previously (Brown et al., 2011a; Graziane et al., 2016; Huang et al., 2009; Lee et al., 2013; Ma et al., 2014; Ma et al., 2016; Neumann et al., 2016b). We performed this analysis in a blind manner such that a small number of ambiguous responses were categorized in a fully unbiased way.

To quantify percentage of silent synapses, we made two theoretical assumptions: (1) the presynaptic release sites are independent, and (2) release probability across all synapses, including silent synapses, is identical. Thus, the percentage of silent synapses was calculated using the equation: $1 - \ln(F_{-70})/ \ln(F_{+50})$, in which F_{-70} was the failure rate at −70 mV and F_{+50} was the failure rate at +50 mV, as rationalized previously (Liao et al., 1995). Note that in this equation, the failure rate is the only variable that determines the percentage of silent synapses. The amplitudes of EPSCs are used to present failures or successes, but do not have analytical value. In the cases in which these two theoretical assumptions are not true, the above equation was still used, as the results were still valid in predicting the changes of silent synapses qualitatively as previously rationalized (Huang et al., 2015b; Ma et al., 2014). he amplitude of an EPSC was determined as the mean value of the EPSC over a 1-ms time window around the peak, which was typically 3–4 ms after the stimulation artifact. To assess the percentage of silent synapses, only the rates of failures versus successes, not the absolute values of the amplitudes, were used. At +50 mV, successful synaptic responses were conceivably mediated by both AMPARs and NMDARs, and inhibiting AMPARs by NBQX (5 μM) modestly reduces the amplitudes of EPSCs (Graziane et al., 2016). Despite the effects of NBQX on the amplitudes, the failure rate of synaptic responses at +50 mV was not altered during AMPAR inhibition (Graziane et al., 2016). Thus, in the minimal stimulation assay assessing the percentage of silent synapses, the results will not be affected, whether the synaptic responses at +50 mV are mediated by NMDARs alone or by both AMPARs and NMDARs.

3.3.14 Immunohistochemistry and Confocal Microscopy

At 1–4 d after behavioral testing, when HSV expression remained readily detectable, rats were transcardially perfused with 0.1 M sodium phosphate buffer, followed by 4% paraformaldehyde (PFA, wt/wt) in 0.1 M phosphate buffer. Brains were removed and postfixed in 4% PFA overnight at 4 °C. Following postfix, whole brains were stored in 30% sucrose in phosphate buffer with 0.1% sodium azide at 4 °C until sectioning. Coronal sections (100 μm thick) containing the NAc were then prepared on a VT1200S vibratome (Leica) in 0.1 M PBS and then stored in cryoprotectant (30% sucrose, 30% ethelyne glycol, in phosphate buffer) at −20 °C until staining.

Immunohistochemistry was performed as previously described (Winters et al., 2012). Briefly, floating sections were washed in PBS 3 × 5 min and then permeabilized with 0.1% Triton X-100 in PBS for 15 min. Sections were then washed 3 × 5 min in PBS and blocked with 5% normal donkey serum in PBS for 2 h. Sections were next incubated overnight at 4 °C with a primary antibody against GFP (1:1,000, monoclonal mouse anti-GFP; Abcam). Sections were subsequently washed 3 × 5 min in PBS and incubated for 2 h at room temperature with a secondary antibody (1:500, ALEXA 488 donkey anti-mouse; Abcam). Sections were washed again 3 × 5 min in PBS before they were mounted in ProLong Gold Antifade with DAPI (Molecular Probes).

Sections were imaged and captured with a Leica TCS SP5 confocal microscope equipped with Leica Application Suite software (Leica). Slices were imaged with a 5x or 10x air objective and the entire slice was captured using automated tile scanning and image stitching functions. From these images, viral expression and localization could be determined. All representative images were captured with a 10x air objective. In addition, high-magnification images of

transduced neurons were captured using a 40x oil immersion objective to verify viral expression in intact neurons.

3.3.15 Dendritic Spine Labeling and Imaging

To visualize dendritic spines, MSNs were filled with Alexa 594 dye using single-cell microinjections, and the labeled dendritic spines were quantified as described previously (Dumitriu et al., 2012; Dumitriu et al., 2011). Briefly, the rats were transcardially perfused with ice-cold 1% PFA in 0.1 M phosphate buffer, followed by 4% PFA and 0.125% glutaraldehyde in 0.1 M phosphate buffer. Brains were removed and postfixed in 4% PFA and 0.125% glutaraldehyde in 0.1 M phosphate buffer for 12–14 hrs at 4 °C. Following postfix, the brains were transferred into 0.1 M PBS and sectioned into 250-μm-thick slices using a VT1200S vibratome (Leica). Cells were filled shortly after slicing (within 4 hrs). Cells within the NAc shell were impaled with a fine micropipette containing 5 mM Alexa 594 hydrazide (Invitrogen) and injected with 1–10 nA of negative current until dendrites and spines were filled. Based on the presence of GFP signals, transduced and nontransduced cells were visually targeted and filled in the same rat. After filling, the slices were mounted in ProLong Gold Antifade (Molecular Probes) on slides for imaging. Spacers (240 μm thick) were placed along the edge of the slide before mounting to avoid compression of the slices by the overlying coverslip and to prevent deformation of spine morphologies.

Images were captured with a Leica TCS SP5 confocal microscope equipped with Leica Application Suite software (Leica). Individually filled neurons were visualized with a 63x oil immersion objective for final verification of their neuronal types (for example, MSNs versus interneurons). Individual dendritic segments were focused on and scanned at 0.69-μm intervals

along the z axis to obtain a z-stack. After capture, all images were deconvolved within the Leica Application Suite software. Analyses were performed on two-dimensional projection images using ImageJ (NIH). Secondary dendrites were sampled and analyzed due to their significant cellular and behavioral correlates (Graziane et al., 2016; Robinson and Kolb, 1999). For each neuron, 1–4 (2.1 average) dendritic segments of ~20 μm in length were analyzed. For each group, 4–8 transduced cells and 4-8 non-transduced cells per rat were analyzed. Similar to our previous studies (Brown et al., 2011a; Graziane et al., 2016; Wang et al., 2020), we operationally divided spines into three categories: (1) mushroom-like spines were dendritic protrusions with a head diameter >0.5 μm or >2x the spine neck diameter; (2) stubby spines were dendritic protrusions with no discernable head and a length of ≤0.5 μm; and (3) thin/filopodia-like spines were dendritic protrusions with a length of >0.5 μm and head diameter <0.5 μm or no discernable head. During counting of dendritic spines, spine head diameters were also measured for analysis.

3.3.16 Statistics

All results are shown as mean ± s.e.m. All experiments were replicated in 3–16 rats. All data collection was randomized. All data were assumed to be normally distributed, but this was not formally tested. No statistical methods were used to predetermine sample sizes, but our sample sizes are similar to those reported in previous publications (Graziane et al., 2016; Lee et al., 2013; Ma et al., 2014; Ma et al., 2016; Neumann et al., 2016b; Wang et al., 2020). All data were analyzed offline and investigators were blinded to experimental conditions during the analyses.

Repeated experiments for the same group were pooled together for statistical analysis. For electrophysiology and dendritic spine experiments, the sample sizes are presented as *n/m*, where n is the number of cells and m is the number of rats. For behavioral experiments, the sample sizes

are presented as *n*, which is the number of rats. Animal-based statistics were used for all data analyses. For electrophysiological experiments, we averaged the values of all the cells from each rat to obtain an animal-based mean value for statistical analysis (Graziane et al., 2016; Lee et al., 2013; Ma et al., 2016). For dendritic spine experiments, we averaged individual dendritic segment values from each cell to obtain a cell-based value, and then averaged cell-based values from each rat to obtain animal-based values for statistical analysis (Dumitriu et al., 2012; Dumitriu et al., 2011). Statistical significance was assessed using unpaired t-tests, one-way analysis of variance (ANOVA) or repeated-measures two-way ANOVA, as specified in the related text. Two-tailed tests were performed for analyses. Statistical significance was set at $P < 0.05$ for all experiments. Statistical analyses were performed in GraphPad Prism (v.8).

3.4 Results

3.4.1 Decreased Rac1 Triggers the Re-Silencing of Cocaine-generated Synapses

To explore the role of Rac1 in the dynamic changes in the functional state of cocaine-generated synapses during memory destabilization and reconsolidation, we first trained rats to self-administer cocaine, during which each intravenous infusion was paired with a light cue to form cocaine-cue associations. Then, after a period of prolonged withdrawal (45 days), we briefly (10 min) re-exposed the rats to the cocaine-associated cues through an extinction session in the same operant chambers to reactivate and destabilize the cocaine-associated memories (Lee et al., 2005), before assessing Rac1 activity levels. Using enzyme-linked immunosorbent assay (ELISA) to

measure the levels of Rac1-GTP, the active form of Rac1, we observed that after cue re-exposure

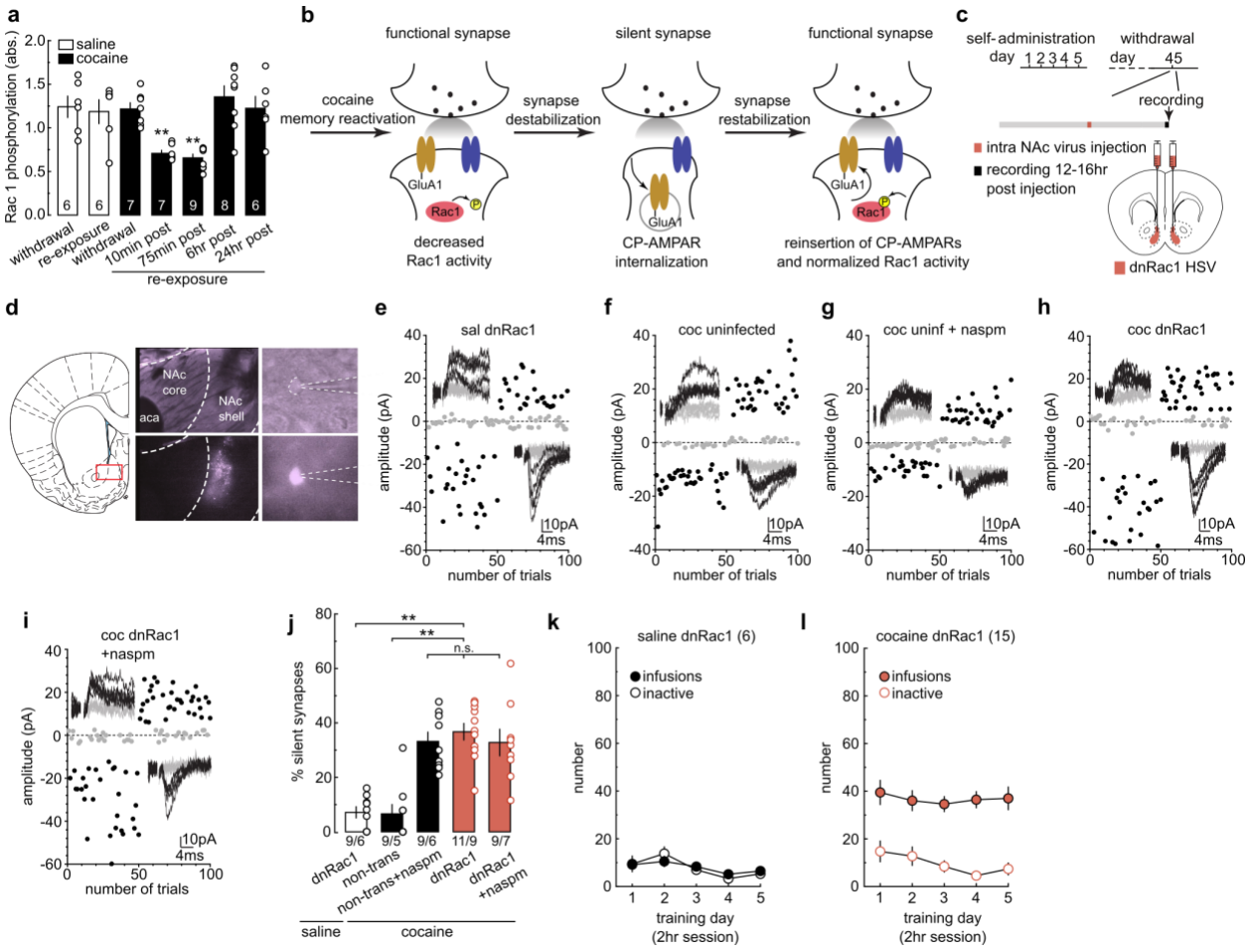

Figure 18. Decreased Rac1 Activity Triggers the Re-Silencing of Cocaine-Generated Synapses

(**a**) Summarized ELISA results showing transiently decreased levels of active Rac1 in NAcSh on cue re-exposure in cocaine-trained but not saline-trained rats (saline withdrawal = 1.24 ± 0.122, n = 6 animals; saline re-exp = 1.19 ± 0.136, n = 6 animals; cocaine withdrawal = 1.23 ± 0.071, n = 7 animals; cocaine 10 min = 0.708 ± 0.033, n = 7 animals; cocaine 75 min = 0.658 ± 0.041, n = 9 animals; cocaine 6 h = 1.36 ± 0.125, n = 8 animals; cocaine 24 h = 1.23 ± 0.136, n = 6 animals; $F_{6,42} = 9.133$, $p < 0.0001$, one-way ANOVA; *P < 0.05, Bonferroni post-test). (**b**) Diagram illustrating the hypothesis that the transient downregulation of active Rac1 triggers re-silencing of the already matured silent synapses in cocaine-trained rats. (**c**) Diagram showing the timeline for experiments involving intra-NAc Shell expression of dnRac1. (**d**) Example images showing dnRac1-expressing NAc Shell MSNs during recordings. (**e-i**) EPSCs evoked at -70mV and +50mV (insets) over 100 trials from example recordings for each group (**e**, saline dnRac1; **f**, cocaine uninfected; **g**, cocaine uninfected + naspm; **h,** cocaine dnRac1; **i**, cocaine dnRac1 + naspm. (**j**)

Summary showing that expressing dnRac1 in NAcSh MSNs increased the percentage of silent synapses selectively in cocaine-trained rats on withdrawal day 45 and that CP- AMPAR inhibition did not further increase this percentage (saline dnRac1 = 7.32 ± 2.73, n = 6 animals; cocaine nontrans = 6.32 ± 2.59, n = 5 animals; cocaine nontrans NASPM = 33.97 ± 4.14, n = 6 animals; cocaine dnRac1 = 36.47 ± 3.46, n = 9 animals; cocaine dnRac1 NASPM = 31.67 ± 4.83, n = 7 animals; $F_{2,28}$ = 14.46, p < 0.0001, one-way ANOVA; **P < 0.01, Bonferroni post-test). (**k,l**) Self-administration training data of all rats used in electrophysiology recordings.

on withdrawal day 45, levels of active Rac1 in the NAc shell were decreased transiently in cocaine-trained rats, and then returned to normal levels 6 hrs later, when the memory has reconsolidated (**Figure 18 a**). In contrast, cue re-exposure did not alter the levels of active Rac1 in saline-trained control rats (**Figure 18 a**). This result suggests that memory reactivation triggers a decrease in Rac1 activity, which follows the time course of memory destabilization.

This observation prompted us to test whether the decrease in active Rac1 plays a causal role in destabilizing cocaine-generated synapses to allow their re-silencing after cue re-exposure (**Figure 18 b**). To manipulate the levels of active Rac1 in the NAc shell, we utilized a herpes simplex virus (HSV) vector to express a dominant negative form of Rac1 (dnRac1), which interferes with the activity of endogenously active Rac1, in the NAc shell 45 days after cocaine self-administration. We then assessed the level of silent synapses in HSV-infected MSNs ~12–16 hrs after viral injection using the minimal stimulation assay (**Figure 18 c,d**). dnRac1 expression had no effect on the basal percentage of silent synapses in saline-trained rats (**Figure 18 e,j**), indicating dnRac1 expression alone does not generate silent synapses in the NAc shell of rats without prior cocaine experience. In contrast, the percentage of silent synapses was significantly increased in dnRac1-expresing NAc shell MSNs in cocaine-trained rats, compared to nontransduced MSNs (**Figure 18 f,h,j**). The increased percentage of silent synapses induced by

dnRac1 expression was similar to the levels observed in nontransduced MSNs when CP-AMPARs

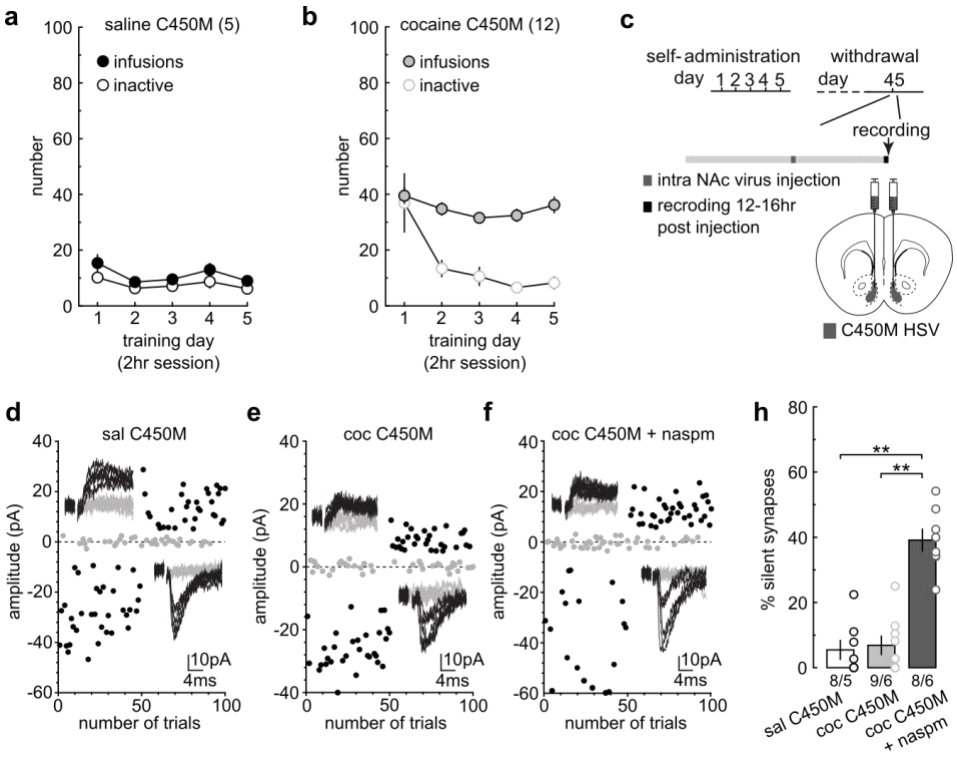

Figure 19. Expression of C450M, an Inactive Control for caRac1, Does Not Affect Silent Synapse Levels

(**a,b**) Self-administration training data of rats used in the following electrophysiology experiments. (**c**). Diagram showing the experimental timeline for self-administration, withdrawal, HSV-mediated expression of C450M, and electrophysiology. (**d-f**) Example EPSCs (inset) over trials in the minimal stimulation assay of C450M-expressing NAcSh MSNs in saline (**d**)- and cocaine-trained rats (**e**), and the effects of CP-AMPAR inhibition (**f**). (**h**) Summary showing that C450M expression did not affect the % silent synapses in saline- or cocaine-trained rats, and the low % silent synapses in cocaine-trained rats was restored to high levels by naspm inhibition of CP-AMPARs (saline = 6.64 ± 4.15, n = 5 animals; cocaine = 6.04 ± 2.27, n = 6 animals; cocaine naspm = 36.76 ± 3.48, n = 6 animals, $F_{2,14}$=29.20, p<0.0001, one-way ANOVA; **p<0.01, Bonferroni posttest).

were blocked with NASPM (200μM) (**Figure 18 g,j**), suggesting the dnRac1-induced silent synapses may be the cocaine-generated synapses enriched in CP-AMPARs. Indeed, the application of NASPM did not further increase the percentage of silent synapses in dnRac1-expressing MSNs

(**Figure 18i,j**), supporting the notion that the silent synapses observed after

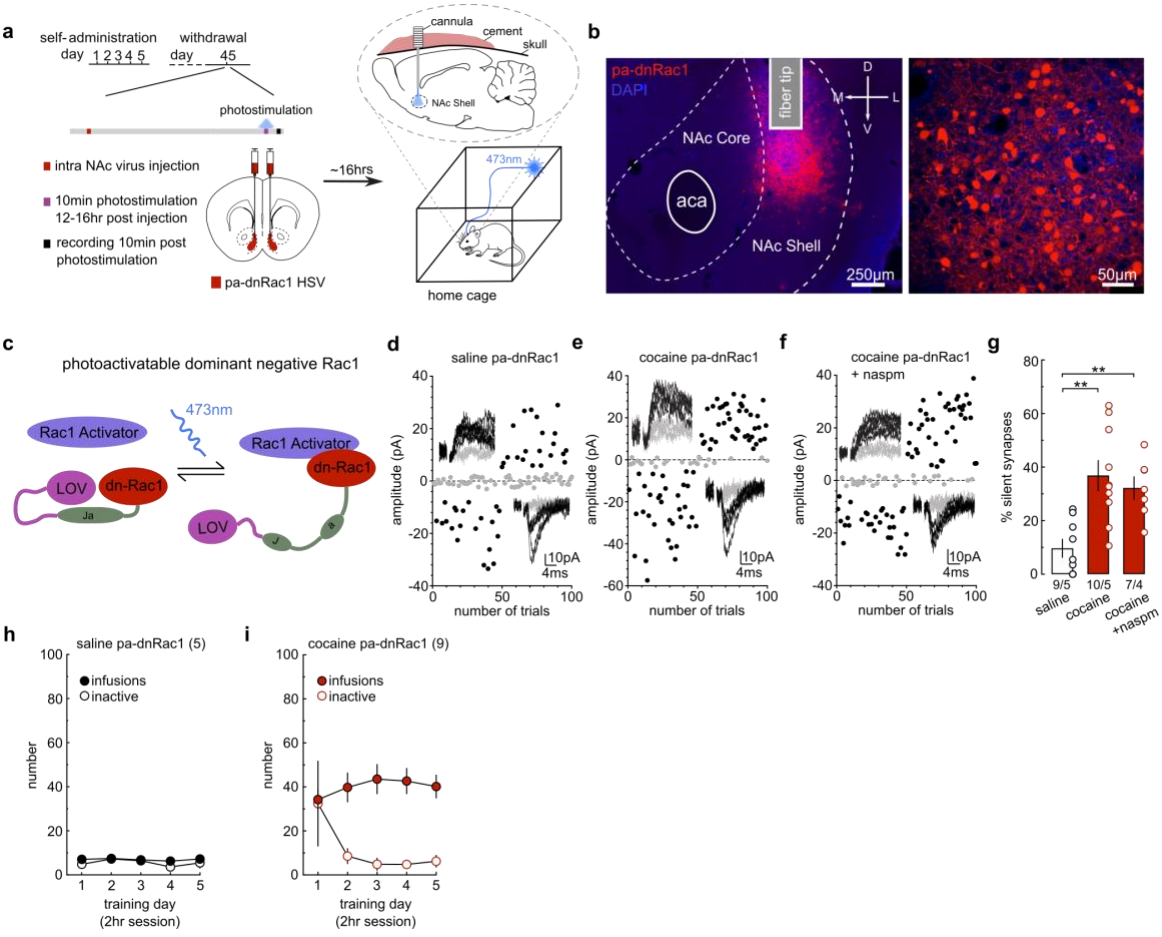

Figure 20. Transient Reduction in Rac1 Activity is Sufficient for Synaptic Re-Silencing

(**a**) Diagrams showing the experimental design, in which NAc Shell pa-dnRac1 was photoactivated for 10 min while rats remained in their home cage. (**b**) Example images of an NAcSh slice (left) and MSNs (right) showing HSV-mediated expression of pa-dnRac1. All animals used in **g** had pa-dnRac1 expression localized within the NAc Shell. (**c**) Diagram illustrating the design concept of pa-dnRac1. The binding of pa-dnRac1 to Rac1 activators prevents them from activating endogenous Rac1, leading to reduced Rac1 activity levels. (**d-f**) EPSCs evoked at −70 mV and +50 mV during the minimal stimulation assay (insets) over 100 trials from example pa-dnRac1-expressing MSNs in saline- (**d**) and cocaine-trained rats (**e**), and the effects of NASPM (**f**). (**g**) Summary showing that stimulating pa-dnRac1 on withdrawal day 45 did not affect the percentage of silent synapses in saline-trained rats, but increased the percentage of silent synapses in cocaine-trained rats, and this increase was not affected by NASPM (saline = 9.08 ± 1.70, n = 5 animals; cocaine = 35.91 ± 4.89, n = 5 animals; cocaine NASPM = 33.07 ± 4.21, n = 4 animals; $F_{2,11}$ = 15.56, p =

0.0006, one-way ANOVA; **P < 0.01, Bonferroni post-test). (**h,i**) Self-administration training data of all rats used in electrophysiology recordings.

dnRac1 were the same set of cocaine-generated silent synapses. These effects of dnRac1 are not likely due to nonspecific effects of HSV transduction or protein overexpression given that a control HSV (HSV-C450M), which expresses a mutant, nonfunctional form of Rac1, exerted no effect on silent synapses (**Figure 19**). These findings indicate that a decrease in Rac1 activity is sufficient to trigger the re-silencing of cocaine-generated synapses in the NAc shell.

While HSV-mediated expression of dnRac1 ensures sufficient Rac1 inhibition, it does not effectively capture the rapid temporal dynamics of synaptic re-silencing that naturally occur following cue re-expo- sure. To manipulate dnRac1 in a temporally controlled manner, we expressed a photoactivatable form of dnRac1 (pa-dnRac1), in which dnRac1 is fused with a photoreactive light oxygen voltage (LOV) domain, which prevents dnRac1 from interacting with its effectors (Wang et al., 2010; Wu et al., 2009). Upon exposure to 473-nm laser, the LOV domain dissociates from dnRac1, allowing dnRac1 to interfere with the activity of endogenous Rac1 in a temporally controlled manner (**Figure 20 a-c**).

On withdrawal day 45, we injected HSV-pa-dnRac1 bilaterally into the rat NAc shell, and 12–16 hrs later, inserted optical fibers into NAcSh through preinstalled guide cannulae (**Figure 20 a**). We photostimulated NAc shell pa-dnRac1 for 10 min while rats were in their home cages, and assessed the level of silent synapses in transduced neurons immediately after. This manipulation did not affect the percentage of silent synapses in saline-trained rats (**Figure 20 d,g**), but increased the percentage of silent synapses in cocaine- trained rats (**Figure 20 e,g**). Furthermore, application of NASPM did not additionally change this percentage of silent synapses (**Figure 20 f,g**), again suggesting that silent synapses observed after dnRac1 stimulation were the same, cocaine-

generated synapses. Taken together, these findings demonstrate a transient decrease in active Rac1 levels is sufficient to destabilize cocaine-generated synapses from their matured state and trigger re-silencing.

3.4.2 High Levels of Active Rac1 Stabilize Synaptic State

We next tested whether maintaining high levels of active Rac1 prevents the re- silencing of cocaine-generated synapses in response to cue re- exposure. We expressed a constitutively active mutant (ca) of Rac1, which is locked within its active conformation (Dietz et al., 2012a). At 12–16h after intra-NAcSh injection of HSV-caRac1, saline- or cocaine-trained rats received cue re-exposure (on withdrawal day 45) and were assessed for silent synapses 10 min later, a time point when cocaine-generated synapses have normally been re-silenced (**Figure 21 a**). Expression of caRac1 did not affect the percentage of silent synapses in saline- trained rats with cue re-exposure (**Figure 21 b,g**), indicating high levels of active Rac1 alone does not alter the level of silent synapses. In contrast, caRac1 expression prevented the re-emergence of silent synapses in cocaine-trained rats following cue re-exposure, which was still observed in nontransduced neurons (**Figure 21 c-g**). Importantly, application of NASPM restored the high percentage of silent synapses in caRac1-expressing MSNs (**Figure 21 f,g**), indicating that cocaine-generated silent synapses were still present and stabilized in their unsilenced, mature state. Thus, maintaining high levels of active Rac1 prevents the re-silencing of cocaine-generated synapses after memory retrieval.

To characterize Rac1's temporally dynamic regulation, we employed a photoactivatable form of caRac1 (HSV-paRac1) (Wu et al., 2009), which operates mechanistically the same as the

pa-dnRac1 used earlier (**Figure 22 a-c**). On withdrawal day 45, we injected HSV-paRac1

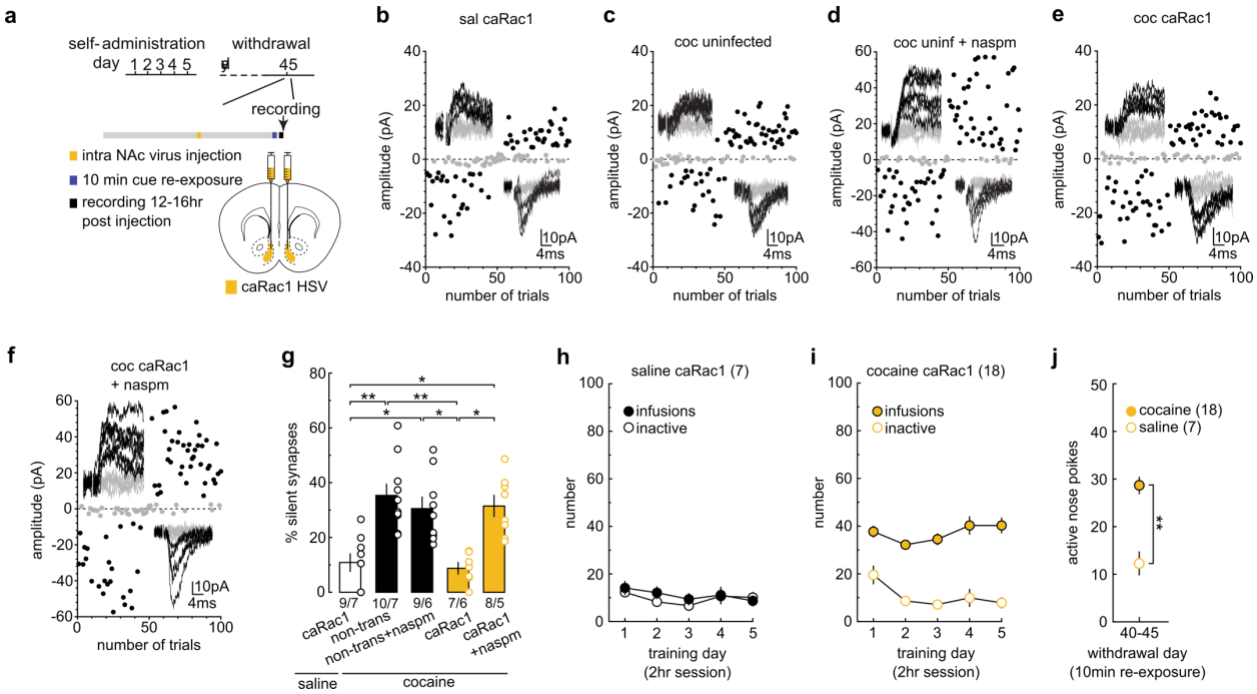

Figure 21. Increasing Rac1 Activity Prevents Cue-Induced Synaptic Re-Silencing

(**a**) Diagram showing the experimental timeline. (**b-f**) EPSCs evoked at −70 mV and +50 mV during the minimal stimulation assay (insets) over 100 trials from example recordings for all groups (**b**, saline caRac1; **c**, cocaine uninfected; **d**, cocaine uninfected + naspm; **e**, cocaine caRac1; **f**, cocaine caRac1 + naspm). (**g**) Summary showing that caRac1 expression prevented the cue re-exposure-induced increase in the percentage of silent synapses in cocaine-trained rats after 45 d of withdrawal from self-administration, while perfusion of NASPM restored this percentage to high levels (saline caRac1 = 10.34 ± 2.90, n = 7 animals; cocaine nontrans = 37.22 ± 5.40, n = 7 animals; cocaine nontrans NASPM = 27.94 ± 4.94, n = 6 animals; cocaine caRac1 = 8.49 ± 2.10, n = 6 animals; cocaine caRac1 NASPM = 30.76 ± 3.17, n = 5 animals; $F_{4,26} = 10.44$, $p < 0.0001$, one-way ANOVA; *P < 0.05, **P < 0.01, Bonferroni post-test). (**h,i**) Self-administration training data of all rats used in electrophysiology experiments. (**j**) Summary of nose poke responding during the 10-min cue re-exposure session showing cocaine-trained rats exhibited higher levels of cue-induced nose poke responding compared to saline trained rats (saline = 12.29 ± 2.39, n = 7 animals; cocaine = 28.67 ± 1.69, n = 18 animals, $t_{23}=5.29$, $p<0.0001$, two- tail, unpaired t-test).

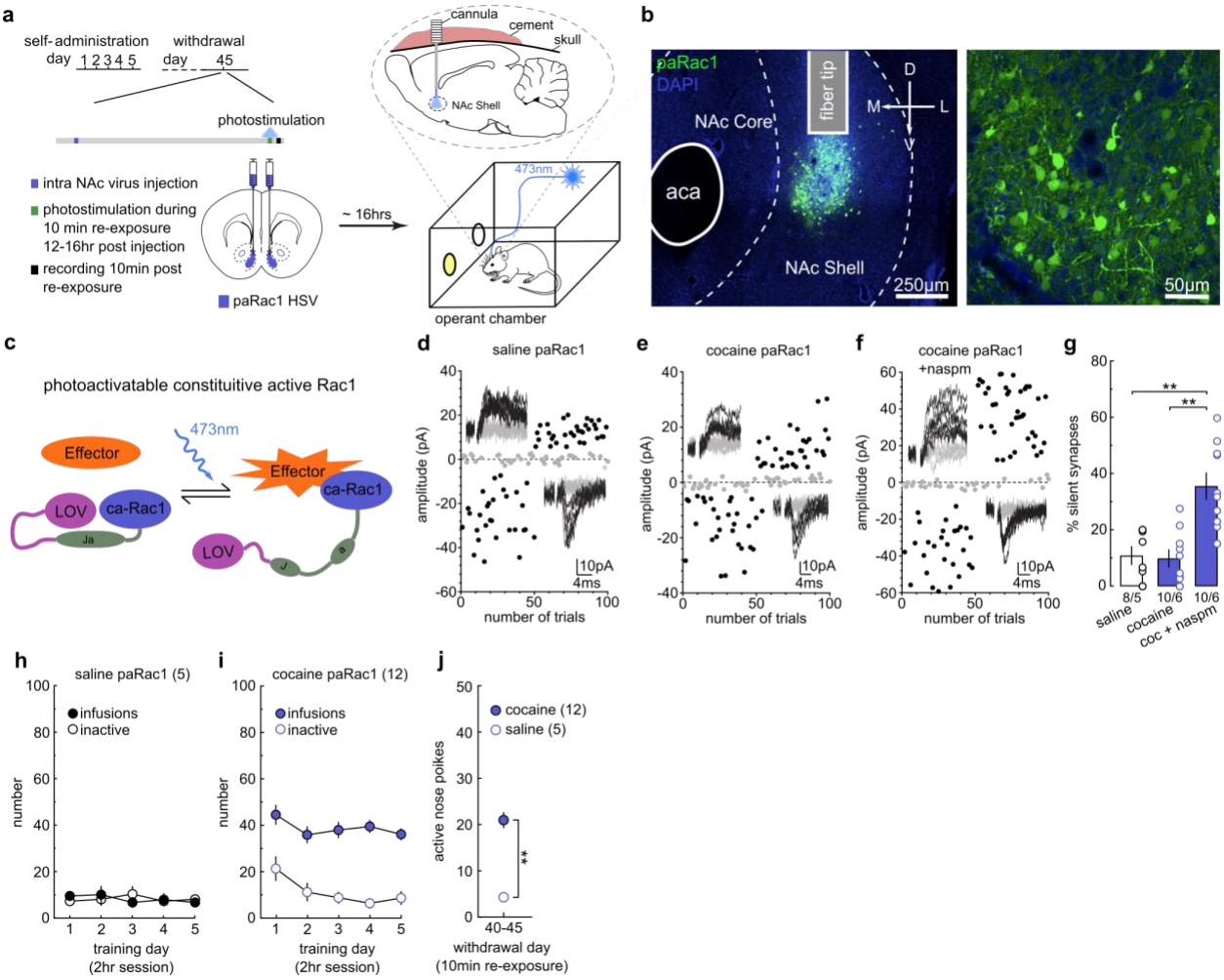

Figure 22. Transiently Increasing Rac1 Activity is Sufficient to Prevent Synaptic Re-Silencing

(**a**) Diagrams showing the experimental design, in which NAc Shell pa-Rac1 was photoactivated during the 10 min cue re-exposure in rats on withdrawal day 45. (**b**) Example images of an NAc Shell slice (left) and MSNs (right) showing HSV-mediated expression of paRac1. All animals used had paRac1 expression localized within the NAc Shell. (**c**) Diagram illustrating the design concept of paRac1. (**d-f**) EPSCs evoked at −70 mV and +50 mV during the minimal stimulation assay (insets) over 100 trials from example paRac1-expressing MSNs in saline- (**d**) and cocaine-trained rats (**e**), and the effects of NASPM (**f**). (**g**) Summary showing that stimulating paRac1 during cue re-exposure prevented cue re-exposure-induced re-silencing of the matured silent synapses in cocaine-trained rats, which was revealed by perfusion of NASPM; paRac1 stimulation did not affect the percentage of silent synapses in saline-trained rats (saline = 12.32 ± 2.74, n = 5 animals; cocaine = 9.39 ± 2.81, n = 6 animals; cocaine NASPM = 34.83 ± 5.09, n = 6 animals; $F_{2,14}$ = 13.74, p = 0.0005, one-way ANOVA; **P < 0.01, Bonferroni post-test). (**h,i**) Self-administration

training data of all rats used in electrophysiology recordings. (**j**) Summary of nose poke responding during the 10-min cue re-exposure session showing cocaine-trained rats exhibited higher levels of cue-induced nose poke responding compared to saline trained rats (saline = 4.60 ± 0.51, n= 5 animals; cocaine = 21.08 ± 1.62, n = 12 animals, t15=6.41, $p<0.0001$, two-tail, unpaired t-test).

bilaterally in the NAc shell, and 12–16 h later, inserted optical fibers through preinstalled guide cannulae. Stimulation of NAc shell paRac1 during cue re-exposure did not affect the percentage of silent synapses in saline-trained rats (**Figure 22 d,g**), but prevented the cue re-exposure-induced increase in the percentage of silent synapses in cocaine-trained rats (**Figure 22 e,g**). The low percentage of silent synapses in these paRac1 MSNs was restored to high levels by application of NASPM (**Figure 19 f,g**), indicating that the cocaine- generated synapses were not eliminated but stabilized in the unsilenced state with CP-AMPARs when high levels of active Rac1 were maintained.

To verify these findings with an alternative and independent approach, we next examined the morphology of dendritic spines, which is correlated with the maturational state of glutamatergic synapses (Holtmaat and Svoboda, 2009). In NAc shell slices, we filled MSNs with Alexa 594 dye and imaged dendritic spines along their secondary dendrites. NAc shell dendritic spines can be categorized into at least four subtypes: (1) mushroom- like spines, (2) long-thin spines, (3) filopodia-like spines and (4) stubby spines (Graziane et al., 2016) (see Methods). Larger, mushroom-like spines are thought to represent stronger, more mature synapses, while long-thin and filopodia-like spines are weaker, more immature synapses with few or no AMPARs (Holtmaat and Svoboda, 2009), which is supported by our previous studies examining cocaine-induced silent synapses in the NAc shell (Graziane et al., 2016; Wang et al., 2020).

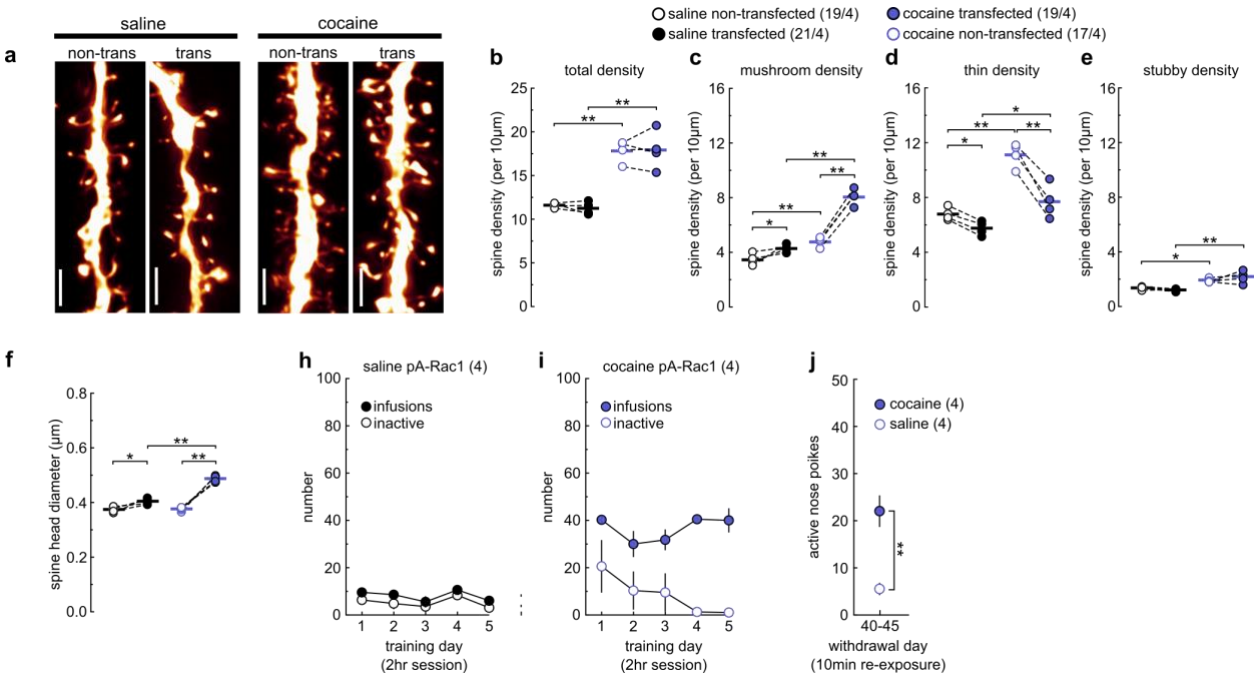

Figure 23. Transient Increase in Rac1 Activity Prevents Retrieval-Induced Changes in Spine Morphology

(**a**) Example NAcSh dendrites of MSNs with and without paRac1 expression from saline-trained rats and cocaine-trained rats with photostimulation during cue re-exposure. Scale bar, 2.5 μm. (**b**) Summary showing that the total spine density was increased in cocaine-trained rats after cue re-exposure for both nontransduced and transduced MSNs compared with saline-trained rats (saline nontrans = 11.62 ± 0.138, n = 4 animals; saline trans = 11.23 ± 0.363, n = 4 animals; cocaine nontrans = 17.83 ± 0.631, n = 4 animals; cocaine trans = 17.94 ± 1.11, n = 4 animals; $F_{1,6}$ = 55.47, p = 0.0003, RM two-way ANOVA, drug main effect; **P < 0.01, Bonferroni post-test). (**c**) Summary showing that the increased density of mushroom-like spines was preserved in pcRac1-expressing MSNs from cocaine-trained rats after cue re-exposure, while the density in nontransduced MSNs decreased. paRac1 stimulation also led to a small, but significant, increase in mushroom-like spine density in saline-trained rats (saline nontrans = 3.46 ± 0.216, n = 4 animals; saline trans = 4.28 ± 0.140, n = 4 animals; cocaine nontrans = 4.77 ± 0.175, n = 4 animals; cocaine trans = 8.04 ± 0.295, n = 4 animals; $F_{1,6}$ = 57.03, p = 0.0003, RM two-way ANOVA, drug × transduced interaction; *P < 0.05, **P < 0.01, Bonferroni post-test). (**d**) Summary showing that the decreased density of thin spines was preserved in paRac1-expressing MSNs from cocaine-trained rats after cue re-exposure, while the density in nontransduced MSNs increased. paRac1 stimulation also led to a small, but significant, decrease in thin spine density in saline-trained rats (saline nontrans = 6.80 ± 0.230, n = 4 animals; saline trans = 5.76 ± 0.253, n = 4 animals; cocaine nontrans = 11.12 ± 0.439, n = 4 animals; cocaine trans = 7.70 ± 0.618, n = 4 animals; $F_{1,6}$ = 30.88, p = 0.0014, RM two-way ANOVA,

drug × transduced interaction; *P < 0.05, **P < 0.01, Bonferroni post-test). (**e**) Summary showing that the density of stubby spines is increased in cocaine- trained rats after cue re-exposure for both nontransduced and transduced MSNs compared with saline-trained rats (saline nontrans = 1.37 ± 0.060, n = 4 animals; saline trans = 1.22 ± 0.050, n = 4 animals; cocaine nontrans = 1.95 ± 0.070, n = 4 animals; cocaine trans = 2.20 ± 0.225, n = 4 animals; $F_{1,6}$ = 35.71, p = 0.0010, RM two-way ANOVA, drug main effect; *P < 0.05, **P < 0.01, Bonferroni post-test). (**f**) Summary showing that the increased mean spine head diameter was preserved in paRac1-expressing MSNs from cocaine-trained rats after cue re-exposure, while the density in nontransduced MSNs normalized back to saline control levels. paRac1 stimulation also led to a small, but significant, increase in spine head diameter in saline-trained rats (saline nontrans = 0.375 ± 0.005, n = 4 animals; saline trans = 0.405 ± 0.006, n = 4 animals; cocaine nontrans = 0.377 ± 0.004, n = 4 animals; cocaine trans = 0.488 ± 0.006, n = 4 animals; $F_{1,6}$ = 37.43, p = 0.0009, RM two-way ANOVA, drug × transduced interaction; *P < 0.05, **P < 0.01, Bonferroni post- test). (**h,i**) Self-administration training data of all rats used in electrophysiology recordings. (**j**) Summary of nose poke responding during the 10-min cue re-exposure session showing cocaine-trained rats exhibited higher levels of cue-induced nose poke responding compared to saline trained rats (saline = 5.50 ± 1.19, n = 4 animals; cocaine = 22.00 ± 3.24, n = 4 animals, t6=4.78, p=0.0031, two-tail, unpaired t-test).

The spine morphology of NAc shell MSNs mirrored our electrophysiology findings. Specifically, stimulation of paRac1 did not change the density of total spines in either saline- or cocaine- trained rats compared with nontransduced MSNs within the same rats (**Figure 23 a,b**). However, cue re-exposure-contingent paRac1 stimulation maintained the high density of mushroom-like spines and low density of thin spines in cocaine-trained rats during the subsequent destabilization window, thus preventing the spine-weakening process induced by cue re-exposure as seen in the nontransduced MSNs (**Figure 23 c-e**). Consistent with this, photostimulation also maintained the high mean spine head diameter of dendritic spines in paRac1-expressing MSNs, compared with nontransduced MSNs in the same cocaine-trained rats with cue re-exposure

(**Figure 23 f**). Note that paRac1 stimulation also slightly affected the spine densities and spine

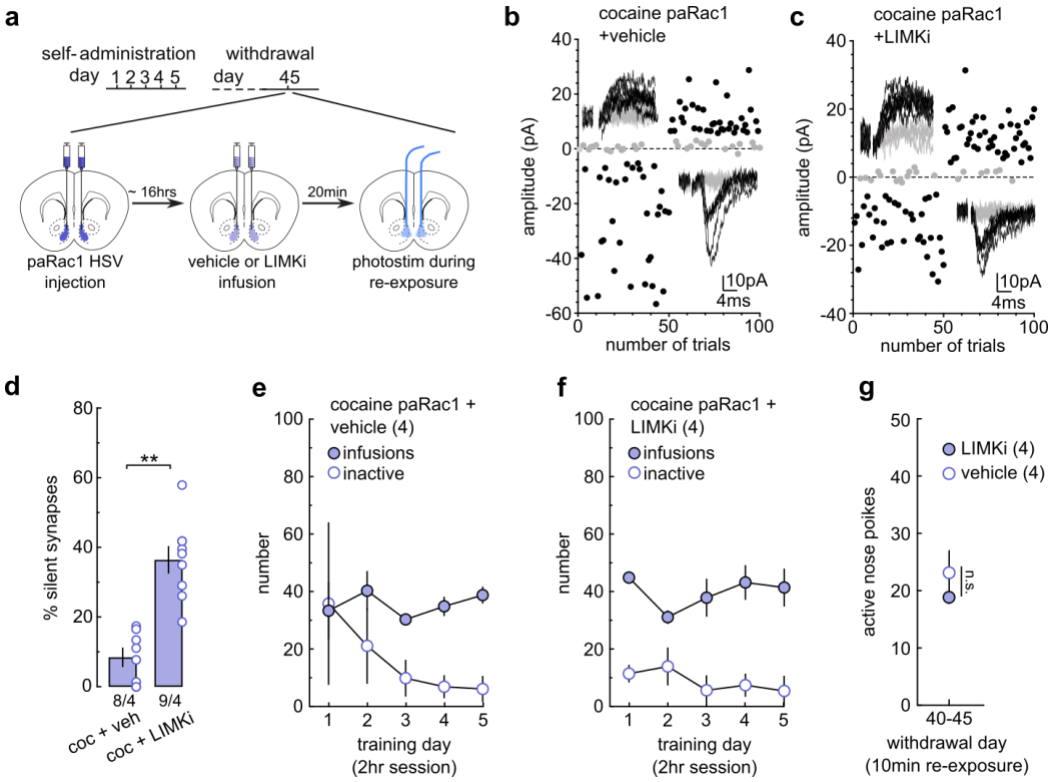

Figure 24. Rac1 Prevents Synaptic Re-Silencing through the PAK-LIMK-Cofilin Pathway

(**a**) Diagram showing the experimental timeline for LIMKi experiments. (**b, c**) EPSCs evoked at −70 mV and +50 mV during the minimal stimulation assay (insets) over 100 trials from example paRac1-expressing MSNs from cocaine-trained rats with photostimulation during cue re-exposure with pretreatment of vehicle (**b**) or LIMKi (**c**). (**d**) Summary showing that pretreatment of LIMKi blocked the effect of paRac1 stimulation on preventing cocaine- generated synapses from re-silencing, such that the percentage of silent synapses was increased compared with vehicle-treated rats (cocaine vehicle (veh) = 8.55 ± 1.59, n = 4 animals; cocaine LIMKi = 41.73 ± 6.34, n = 4 animals; t6 = 5.08, P = 0.0023, two-sided unpaired t-test). (**e,f**) Self-administration training data of all rats used in electrophysiology recordings. (**g**) Summary of nose poke responding during the 10-min cue re-exposure session showing nose poke responding was not different in animals treated with vehicle or LIMKi (vehicle = 23.50 ± 3.80, n = 4 animals; LIMKi = 19.25 ± 1.03, n = 4 animals, t6=1.08, p=0.3215, two-tail, unpaired t-test).

head diameter in saline-trained rats (**Figure 23 a-f**), but these effects are rather minimal (~5%), and in our view, do not confound the interpretation that increases levels of active Rac1 stabilizes synapses in their mature state.

Rac1 activity can regulate a variety of different processes in addition to its regulation of the cytoskeketon, including protein translation (Hedrick and Yasuda, 2017; Tolias et al., 2005). Rac1 primarily mediates its effects on the actin cytoskeleton through the PAK-LIMK-cofilin signaling pathway, the activation of which inhibits cofilin activity to prevent actin severing (Cingolani and Goda, 2008). Therefore, to determine if active Rac1 stabilizes synaptic state through the regulation of the actin cytoskeleton we inhibited the PAK-LIMK-cofilin pathway with a LIMK inhibitor (LIMKi). We infused the LIMKi into the NAc shell ~20 min before photostimulating paRac1 during the 10 min cue re-exposure session to disconnect the link between LIMK and Rac1 (**Figure 24 a**). In cocaine-trained rats with vehicle infusion, paRac1 stimulation prevented the re-emergence of silent synapses after cue re-exposure (**Figure 24 b,d**), replicating our previous results. However, paRac1 stimulation could no longer pre- vent cue re-exposure-induced re-emergence of silent synapses in cocaine-trained rats given intra-NAc shell LIMKi infusion (**Figure 24 c,d**). These results suggest that active Rac1 stabilizes cocaine-generated synapses through the PAK-LIMK-cofilin pathway-mediated regulation of actin cytoskeleton.

3.4.3 Stabilizing Cocaine-Generated Synapses in a Weakened State

The above results show that, while a decrease in active Rac1 triggers dynamic changes (silencing) in the synaptic state of cocaine-trained rats, maintaining high levels of active Rac1 locks synapses in their current mature state despite cue re-exposure. We thus asked whether active

Rac1 can also lock cocaine-generated synapses within the weakened state once they are re-silenced

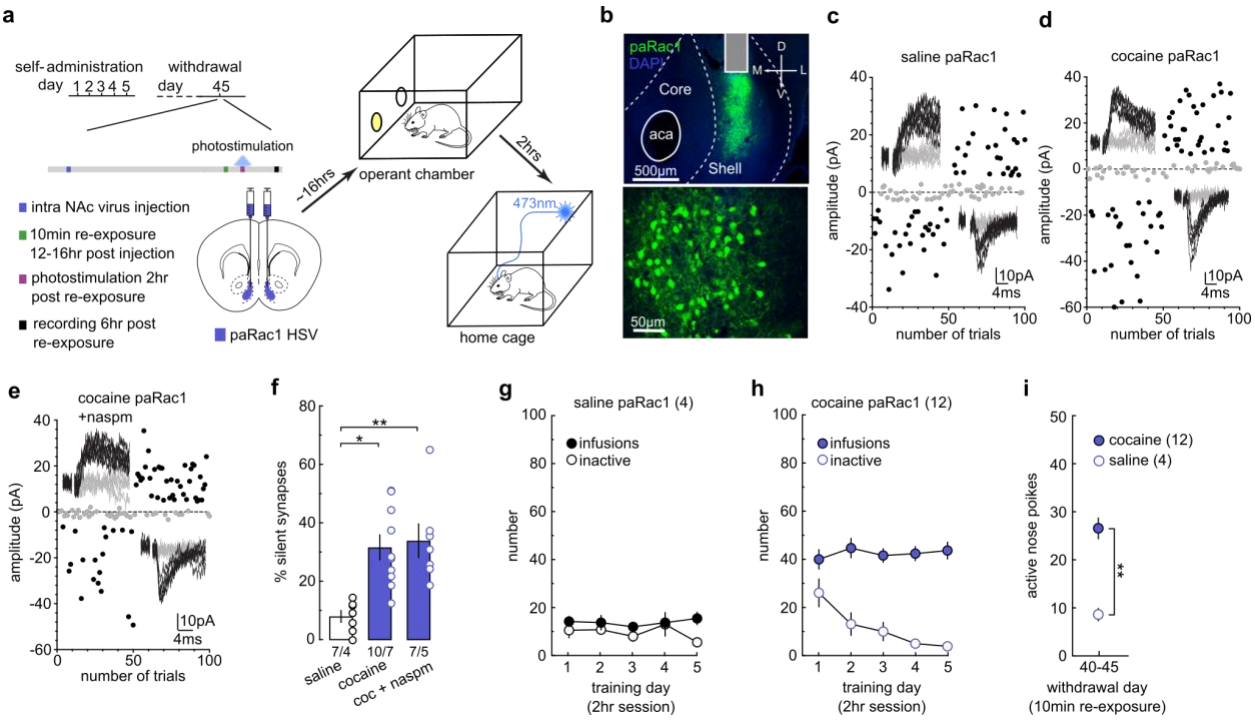

Figure 25. Increasing Rac1 Activity is Capable of Maintaining a Silent Synaptic State

(**a**) Diagrams showing the experimental design in which paRac1 is photoactivated 2 h after cue re-exposure in cocaine-trained rats on withdrawal day 45. (**b**) Example images of NAc Shell slices (top) and MSNs (bottom) showing HSV-mediated expression of paRac1. All animals used in experiments had paRac1 expression localized to the NAc shell. (**c**) EPSCs evoked at −70 mV and +50 mV during the minimal stimulation assay (insets) over 100 trials from example NAc Shell MSNs with paRac1 photoactivation after cue re-exposure in saline- (**c**) and cocaine-trained rats (**d**), and the effects of NASPM (**e**). (**f**) Summary showing that stimulating paRac1 after cue re-exposure did not affect the percentage of silent synapses in saline-trained rats, but locked cocaine-generated silent synapses within their silent state in cocaine-trained rats beyond the presumable 6-h destabilization window, and CP-AMPAR inhibition by NASPM did not further increase the percentage of silent synapses (saline = 8.30 ± 2.46, n = 4 animals; cocaine = 32.82 ± 3.48, n = 7 animals; cocaine NASPM = 36.32 ± 7.65, n = 5 animals; $F_{2,13} = 7.64$, $p = 0.0064$, one-way ANOVA; *P < 0.05, **P < 0.01, Bonferroni post-test). (**g,h**) Self-administration training data of all rats used in electrophysiology recordings. (**i**) Summary of nose poke responding during the 10-min cue re-exposure session showing cocaine-trained rats exhibited higher levels of cue-induced nose poke responding compared to saline trained

rats (saline = 8.50 ± 1.26, n = 4 animals; cocaine = 26.50 ± 2.13, n = 12 animals, t_{14}=4.69, p=0.0003, two-tail, unpaired t-test).

after cue re-exposure. We again used HSV-paRac1 to stimulate Rac1 activity in cocaine- trained rats but 2 h after cue re-exposure, when cocaine-generated synapses have been re-silenced (**Figure 25 a,b**), and assessed silent synapses 6h later, when cocaine-generated synapses normally return to a mature state. We observed that the percentage of silent synapses was not affected in saline-trained rats (**Figure 25 c,f**), but strikingly were maintained at high levels in cocaine-trained rats (**Figure 25 d,f**). In addition, the percentage of silent synapses was not further increased by the application of NASPM (**Figure 25 e,f**), indicating these silent synapses are the cocaine-generated synapses that are enriched in CP-AMPARs. Thus, after cocaine-generated synapses are re-silenced by cue re-exposure, elevated Rac1 activity is capable of maintaining them in the silent state.

We further confirmed these results by examining spine morphology. Following the same paRac1 stimulation and re-exposure procedures as above, MSNs with paRac1 activation exhibited similar density of total spines (**Figure 26 a,b**), but lower densities of mushroom-like spines and higher densities of thin spines compared with nontransduced MSNs from the same rats (**Figure 26 c,d**). The concurrent downshift of mushroom-like and upshift of thin spines suggest that cocaine-generated synapses weakened by cue re-exposure were stabilized in the weakened state. This conclusion is further sup- ported by observations of decreased mean spine head diameter in MSNs with paRac1 stimulation (**Figure 26 f**). Meanwhile, paRac1 stimulation did not affect any dendritic spine subtypes in saline-trained rats (**Figure 26 a-f**).

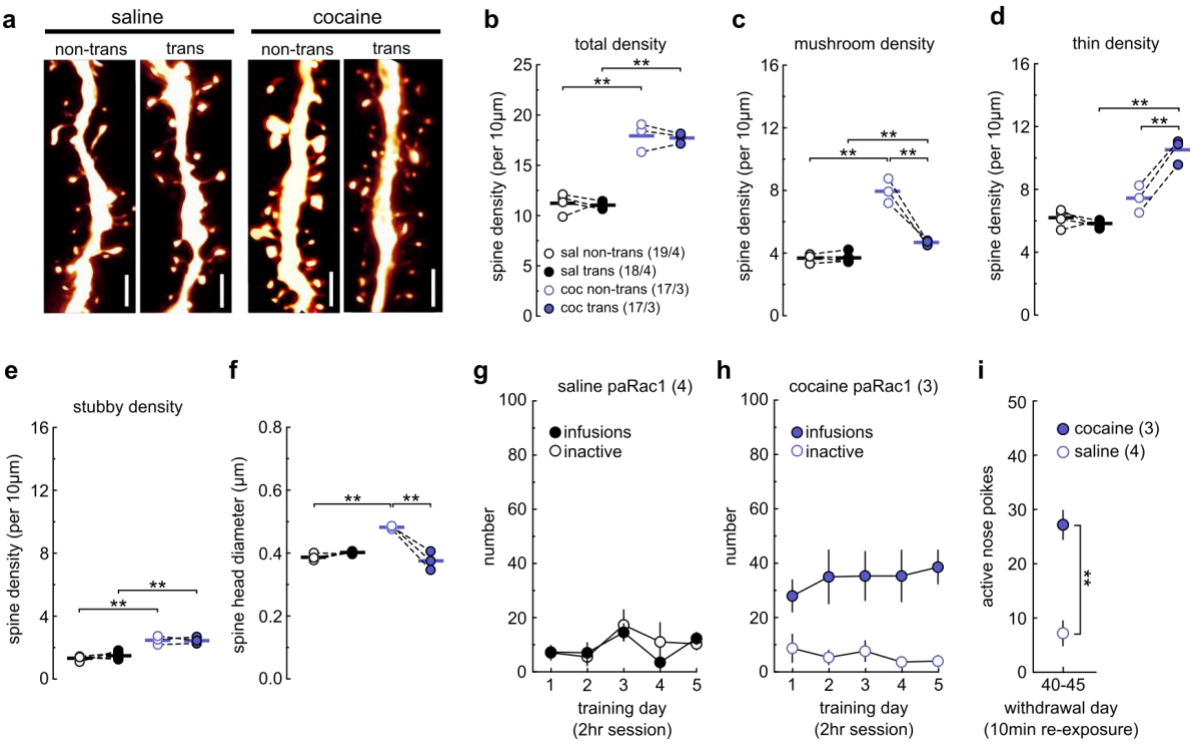

Figure 26. Increasing Rac1 Activity is Capable of Maintaining Thin Spine Morphology

(**a**) Example NAc Shell dendrites of MSNs nontransduced and transduced with paRac1 from saline- and cocaine-trained rats that received photostimulation 2 h after cue re- exposure. Scale bar, 2.5 µm. (**b**) Summary showing that the total spine density was increased in cocaine-trained rats 6 h after cue re-exposure for both nontransduced and transduced MSNs compared with saline-trained rats (saline nontrans = 11.22 ± 0.484, n = 4 animals; saline trans = 11.03 ± 0.199, n = 4 animals; cocaine nontrans = 17.88 ± 0.827, n = 3 animals; cocaine trans = 17.67 ± 0.298, n = 3 animals; $F_{1,5}$ = 148.0, p < 0.0001, RM two-way ANOVA, drug main effect; **P < 0.01, Bonferroni post-test). (**c**) Summary showing that the density of mushroom-like spines was decreased in transduced MSNs from cocaine-trained rats 6 h after cue re-exposure, while the density in nontransduced MSNs remained high (saline nontrans = 3.69 ± 0.130, n = 4 animals; saline trans = 3.71 ± 0.175, n = 4 animals; cocaine nontrans = 7.96 ± 0.451, n = 3 animals; cocaine trans = 4.69 ± 0.091, n = 3 animals; $F_{1,5}$ = 58.92, p = 0.0006, RM two-way ANOVA, drug × transduction interaction; **P < 0.01, Bonferroni post-test). (**d**) Summary showing that the density of thin spines was increased in transduced MSNs from cocaine-trained rats 6 h after cue re-exposure, while the density in nontransduced MSNs returned to the saline control level (saline nontrans = 6.20 ± 0.280, n = 4 animals; saline trans = 5.83 ± 0.128, n = 4 animals; cocaine nontrans = 7.45 ± 0.498, n = 3 animals; cocaine trans = 10.53 ± 0.461, n = 3 animals; $F_{1,5}$ = 55.71, p = 0.0007, RM two-way ANOVA, drug × transduction interaction; **P < 0.01, Bonferroni post- test). (**e**) Summary

showing that the density of stubby spines was increased in cocaine-trained rats 6 h after cue re-exposure for both nontransduced and transduced MSNs compared with saline controls (saline nontrans = 1.32 ± 0.080, n = 4 animals; saline trans = 1.49 ± 0.135, n = 4 animals; cocaine nontrans = 2.47 ± 0.159, n = 3 animals; cocaine trans = 2.45 ± 0.120, n = 3 animals; $F_{1,5} = 79.42$, $p = 0.0003$, RM two-way ANOVA, drug main effect; **P < 0.01, Bonferroni post-test). (**f**) Summary showing that the mean spine head diameter was decreased in transduced MSNs from cocaine-trained rats 6 h after cue re-exposure, while the spine head diameter in nontransduced MSNs remained high (saline nontrans = 0.387 ± 0.005, n = 4 animals; saline trans = 0.402 ± 0.002, n = 4 animals; cocaine nontrans = 0.482 ± 0.003, n = 3 animals; cocaine trans = 0.375 ± 0.017, n = 3 animals; $F_{1,5} = 65.19$, $p = 0.0005$, RM two-way ANOVA, drug × transduction interaction; **P < 0.01, Bonferroni post-test). (**g,h**) Self-administration training data of all rats used in electrophysiology recordings. (**i**) Summary of nose poke responding during the 10-min cue re-exposure session showing cocaine-trained rats exhibited higher levels of cue-induced nose poke responding compared to saline trained rats (saline = 7.00 ± 2.27, n = 4 animals; cocaine = 27.00 ± 2.65, n = 3 animals, t_5=5.74, p =0.0022, two-tail, unpaired t-test).

Similar to the stabilization of mature synapses, the PAK-LIMK-cofilin pathway is also essential for active Rac1 to stabilize cocaine-generated synapses in a silent, weakened state (**Figure 27 a**). In cocaine-trained rats, intra-NAc shell infusion of LIMKi, but not vehicle, ~20min before photostimulation prevented paRac1 from maintaining high levels of silent synapses beyond the 6 hr destabilization window (**Figure 27 b-d**). Thus, the same actin cytoskeleton-regulating pathway is employed by active Rac1 to lock cocaine-generated synapses in their current state, regardless of whether they are in a silent or unsilenced state. It is worth noting that the PAK-LIMK- cofilin pathway in vivo likely responds to the fluctuations of active Rac1 levels in a highly

dynamic and complicated manner depending on the activity state of other GTPases regulating this

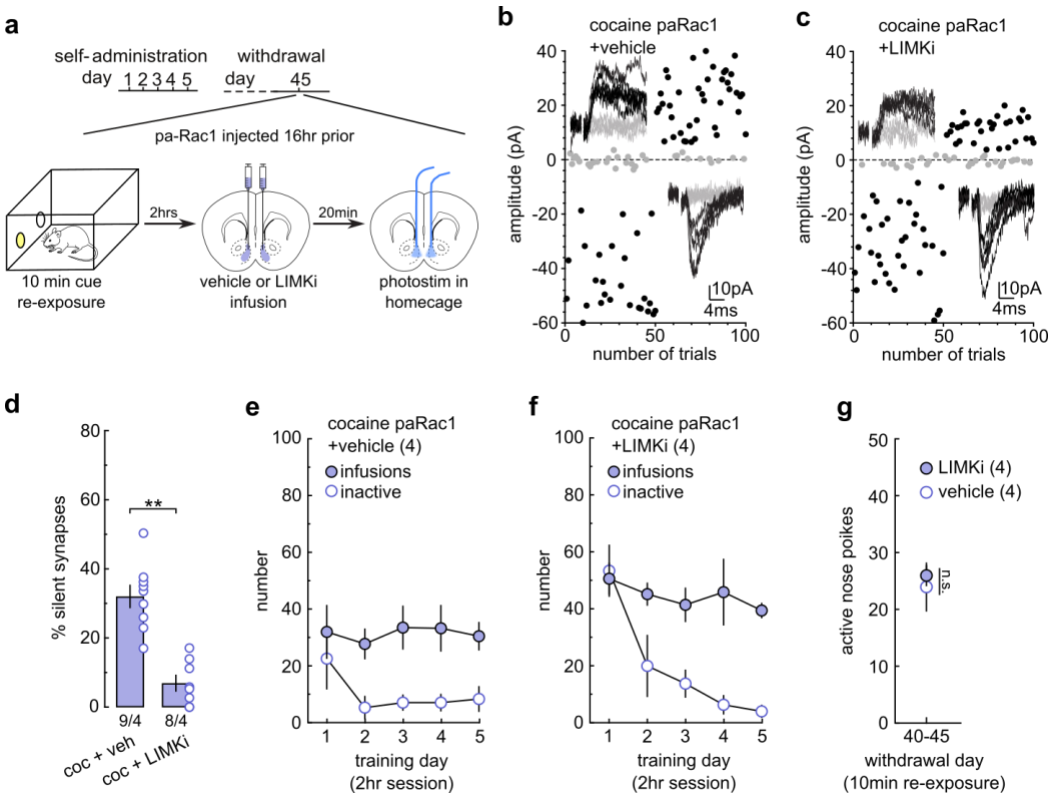

Figure 27. Rac1 Activity Maintains a Silent Synaptic State through the PAK-LIMK-Cofilin Pathway

(**a**) Diagram showing the experimental timeline for LIMKi experiments. (**b,c**) EPSCs evoked at −70 mV and +50 mV during the minimal stimulation assay (insets) over 100 trials from example paRac1-expressing MSNs from cocaine-trained rats receiving photostimulation 2 h after cue re-exposure with pretreatment of vehicle (**b**) or LIMKi (**c**). (**d**) Summary showing that pretreatment with LIMKi blocked the effect of paRac1 stimulation on keeping cocaine-generated synapses in a silent state, such that the percentage of silent synapses was decreased compared with vehicle-treated rats (cocaine vehicle = 32.52 ± 1.45, n = 4 animals; cocaine LIMKi = 7.02 ± 2.11, n = 4 animals; $t_6 = 9.95$, $p < 0.0001$, two-sided, unpaired t-test). (**e,f**) Self-administration training data of all rats used in electrophysiology recordings. (**g**) Summary of nose poke responding during the 10-min cue re-exposure session showing nose poke responding was not different in animals treated with vehicle or LIMKi (vehicle = 24.00 ± 4.18, n = 4 animals; LIMKi = 26.00 ± 1.73, n = 4 animals, t_6=0.44, p=0.6742, two-tail, unpaired t-test).

pathway. As such, the manipulation of this pathway with different timing may result in different synaptic consequences.

3.4.4 Regulating Synaptic State Regulates Cocaine-Associated Memory Reactivation

If the functional state of cocaine-generated synapses in the NAc shell dictates the strength or reactivation of cocaine memories as hypothesized and supported by our previous findings, stabilizing synapses in their mature and silent states should preserve and compromise the behavioral outputs of cocaine-associated memories, respectively. To test this idea, we first stabilized cocaine- generated synapses in their mature state by stimulating paRac1 in cocaine-trained rats during cue re-exposure, and then measured cue-induced cocaine seeking 6 hrs later (**Figure 28 a**). Cocaine-trained rats that received this paRac1 stimulation exhibited high cocaine seeking, comparable to control rats (with the same cocaine and photostimulation procedures, but expressing the control HSV-C450M) (**Figure 28 b,c**). As an additional control, paRac1 stimulation also did not affect operant responding in saline-trained rats (**Figure 28 d,e**). Thus, stabilizing cocaine-generated synapses via paRac1 stimulation does not alter subsequent memory reactivation or seeking behaviors. In contrast, when we stabilized cocaine-generated synapses in their silent state by stimulating paRac1 2h after cue re-exposure, cue-induced cocaine seeking was decreased, compared with C450M control rats when measured 6 h after cue re- exposure (**Figure 29 a-c**). This manipulation did not affect operant responding in saline-trained rats (**Figure 29 d,e**).

To examine if paRac1 photostimulation could result in long-term memory effects, we tested another set of cocaine-trained rats with two paRac1 stimulations within the destabilization window (2 and 5h after cue re-exposure). These rats exhibited lower levels of cue-induced cocaine

seeking compared with C450 control rats when measured >24 h after cue re-exposure (**Figure 29**

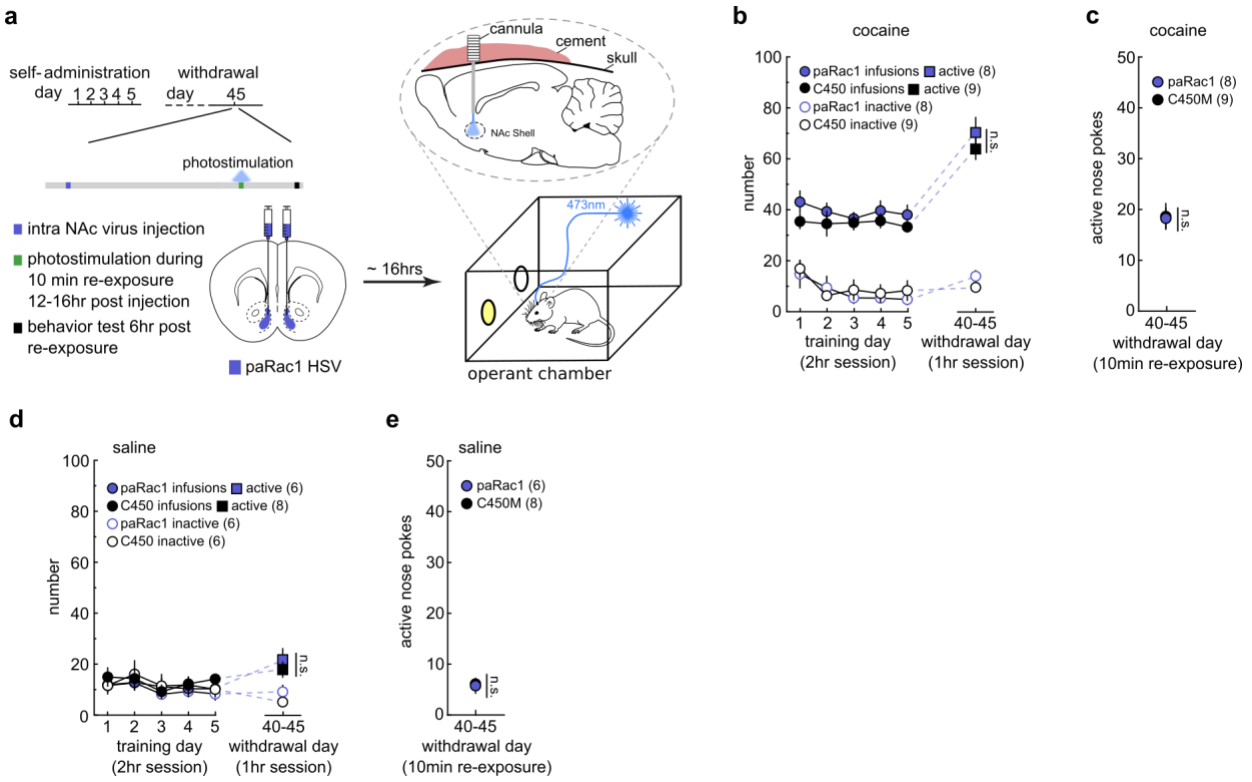

Figure 28. Maintaining Cocaine-Generated Synapses in a Mature State Does Not Affect Seeking Behavior a) **(a)** Diagrams showing the experimental design, in which NAc Shell pa-Rac1 was photoactivated during the 10 min cue re-exposure in rats on withdrawal day 45 before undergoing behavioral testing 6hrs later. **(b)** Summary showing that cocaine-trained rats with photostimulation of paRac1 during cue re-exposure exhibited comparable levels of cue-induced cocaine seeking as in C450M control rats, measured 6 h after cue re-exposure (C450 active = 63.89 ± 4.15, n = 9 animals; pa-Rac1 active = 70.38 ± 6.00, n = 8 animals; C450 inactive = 9.33 ± 1.53, n = 9 animals; pa-Rac1 inactive 13.75 ± 2.20, n = 8 animals; $F_{1,15} = 0.07$, $p = 0.79$, RM two-way ANOVA, withdrawal day 45 lever × virus interaction, NS > 0.05). **(c)** Nose poke responding during the 10-min cue re- exposure session in cocaine-trained rats showing rats with intra-NAc Shell stimulation of paRac1 and intra-NAc Shell stimulation of C450M exhibited similar nose poke responding during the cue re-exposure session (C450M = 18.78 ± 2.52, n = 9 animals; paRac1 = 18.38 ± 1.97, n = 8 animals, t_{15}=0.12, p=0.9033, two-tail, unpaired t-test, n.s. > 0.05). **(d)** Summary showing that saline-trained rats with photostimulation of intra- NAc Shell paRac1 and photostimulation of intra-NAc Shell C450M (control) during cue re-exposure exhibited similar cue-induced seeking, measured 6 hr after cue re-exposure (C450 active = 17.88 ± 2.95, n = 8 animals; paRac1 active = 21.83 ± 4.31, n = 6 animals; C450 inactive

= 5.13 ± 0.915, n = 8 animals; paRac1 inactive = 9.17 ± 2.60, n = 6 animals, $F_{1,12}$=0.0002, *p*=0.9878, two-way RM ANOVA, withdrawal day 45 hole x virus interaction, n.s. > 0.05). **(e)** Nose poke responding during the 10-min cue re-exposure session in saline- trained rats showing rats with intra-NAcSh stimulation of paRac1 and intra-NAcSh stimulation of C450M exhibited similar nose poke responding during the cue re-exposure session (C450M = 6.00 ± 0.707, n = 8 animals; paRac1 = 5.67 ± 1.48, n = 6 animals, t_{12}=0.22, *p*=0.8286, two-tail, unpaired t-test, n.s. > 0.05).

f,g). Thus, stabilizing cocaine-generated synapses in a silent state through paRac1 undermines the intensity or reactivation of cocaine memories, leading to decreased cocaine seeking.

We further explored the relationship between the functional state of cocaine-generated synapses and cocaine-associated memories by examining cocaine seeking while the memory is still destabilized after an initial retrieval event. Previous studies have found that following the reactivation of fear memories, fear-related freezing behavior remains persistent even when the memory is destabilized (Monfils et al., 2009). We similarly found that cocaine-trained rats maintained elevated cocaine seeking behaviors when tested 2 hrs after an initial cue re-exposure session, when the memory is destabilized (**Figure 30 a,b**). This result dissociates the dynamics of cocaine-generated synapses from the ongoing expression of cocaine seeking during the destabilization window. Therefore, the functional state of cocaine-generated synapses in the NAc shell does not determine the expression of cocaine seeking once the memories have been reactivated. However, when using pa-dnRac1 to manipulate the functional state of cocaine-generated synapses, we observed that re-silencing these synapses before, but not after, cue re-exposure-induced memory reactivation led to a significant reduction in cocaine seeking behavior (**Figure 30 b-e**). Thus, the functional state of cocaine-generated NAc shell synapses may preferentially control the reactivation of cocaine-associated memories, while once activated, the behavioral expression of these memories during the destabilization window is driven by other processes (**Figure 30 f**).

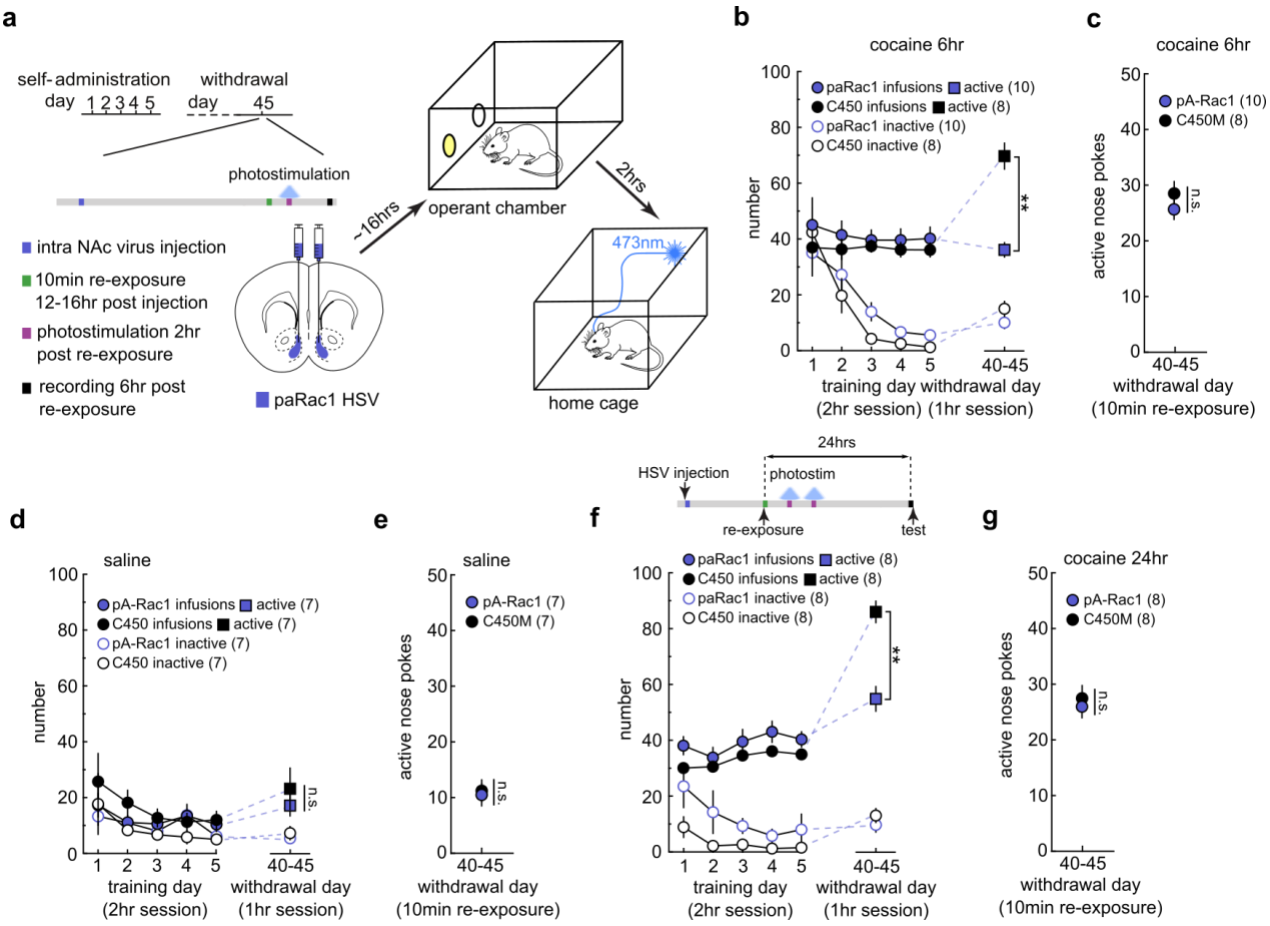

Figure 29. Maintaining Cocaine-Generated Synapses in a Silent State Impairs Cocaine Seeking Behavior

(**a**) Diagrams showing the experimental design in which paRac1 is photoactivated 2 h after cue re-exposure in cocaine-trained rats on withdrawal day 45 before undergoing behavioral testing either 6hr or 24hr later. (**b**) Summary showing that cocaine-trained rats with photostimulation of paRac1 2 h after cue re-exposure exhibited decreased cue-induced cocaine seeking compared with C450M control rats when measured 6 h after re-exposure (C450 active = 69.88 ± 4.69, n = 8 animals; pa-Rac1 active = 36.20 ± 2.59, n = 10 animals; C450 inactive = 15.13 ± 2.66, n = 8 animals; pa-Rac1 inactive = 10.10 ± 2.15, n = 10 animals; $F_{1,16} = 31.89$, $p < 0.0001$, RM two-way ANOVA, withdrawal day 45 lever × virus interaction; **P < 0.01, Bonferroni post-test). (**c**) Nose poke responding during the 10-min cue re- exposure session in cocaine-trained rats showing rats with intra-NAc Shell stimulation of paRac1 and intra-NAc Shell stimulation of C450M exhibited similar nose poke responding during the cue re-exposure session (C450M = 28.63 ± 2.16, n = 8 animals; paRac1 = 25.80 ± 1.79, n = 10 animals, t_{16}=1.02, p=0.3246, two-tail, unpaired t-test, n.s. > 0.05). (**d**) Summary showing that rats with NAc Shell paRac1 and rats with NAc Shell C450M (control) receiving intra-NAcSh photostimulation 2 hr after cue re-exposure exhibited similar cue-induced nose poke responding, measured 6

hr after cue re-exposure (C450 active = 23.43 ± 7.57, n = 7 animals; paRac1 active = 17.43 ± 3.72, n = 7 animals; C450 inactive = 7.57 ± 2.31, n = 7 animals; paRac1 inactive = 5.71 ± 1.96, n = 7 animals, $F_{1,12}$=0.23, *p*=0.6370, two-way RM ANOVA, withdrawal day 45 hole x virus interaction, n.s. > 0.05). (**e**) Nose poke responding during the 10-min cue re-exposure session in saline- trained rats showing rats with intra-NAcSh stimulation of paRac1 and intra-NAcSh stimulation of C450M exhibited similar nose poke responding during the cue re-exposure session (C450M = 11.29 ± 1.92, n = 7 animals; paRac1 = 10.57 ± 1.96, n =7 animals, t_{12}=0.26, *p*=0.7993, two-tail, unpaired t-test, n.s. > 0.05). (**f**) Summary showing that cocaine-trained rats with photostimulation of paRac1 2 h after cue re-exposure exhibited decreased cue-induced cocaine seeking compared with C450M control rats when measured 24 h after re-exposure (C450 active = 86.13 ± 3.82, n = 8 animals; pa-Rac1 active = 55.88 ± 4.40, n = 8 animals; C450 inactive = 13.00 ± 2.47, n = 8 animals; pa-Rac1 = 9.63 ± 2.61, n = 8 animals; $F_{1,14}$ = 15.55, *p*= 0.0015, RM two-way ANOVA, withdrawal day 45 lever × virus interaction; **P < 0.01, Bonferroni post-test). (**g**) Nose poke responding during the 10-min cue re- exposure session in cocaine-trained rats showing rats with intra-NAc Shell stimulation of paRac1 and intra-NAc Shell stimulation of C450M exhibited similar nose poke responding during the cue re-exposure session (C450M = 27.50 ± 2.31, n = 8 animals; paRac1 = 26.00 ± 2.00, n = 8 animals, t14=0.42, p=0.6308, two-tail, unpaired t-test, n.s. > 0.05).

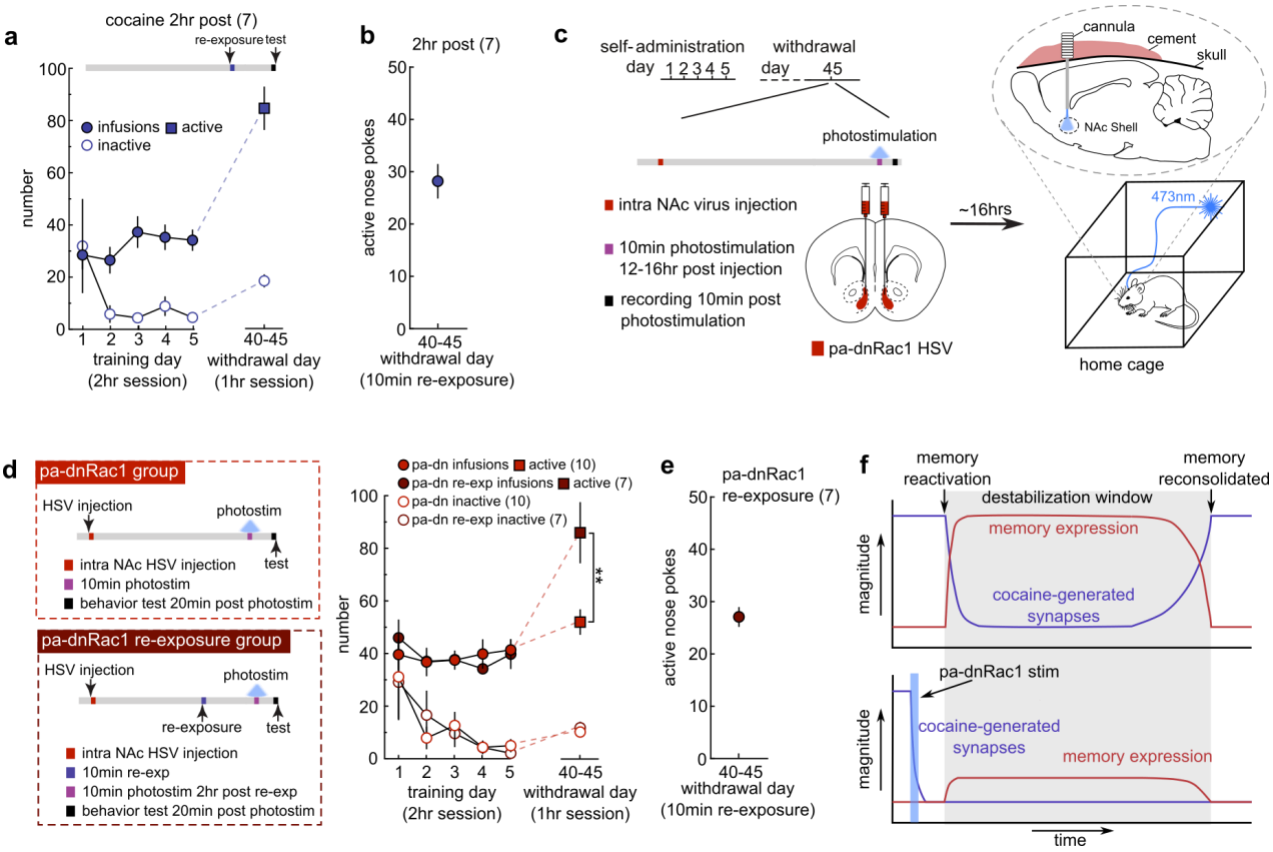

Figure 30. Dissociation Between Cocaine-Generated Synapses and Seeking During Memory Destabilizatoin

(**a**) Summary showing that the nose poke responding remained at high levels in cocaine-trained rats when tested 2 h after cue re-exposure (cocaine 2 h post = 84.86 ± 8.08, n = 7 animals). (**b**) Nose poke responding during the cue re-exposure session of rats who underwent cue-induced seeking test 2hrs later (28.00 ± 3.20, n = 7 animals). (**c**) Diagrams showing the experimental design, in which NAc Shell pa-dnRac1 was photoactivated for 10 min while rats remained in their home cage. (**d**) (left) Diagrams showing the experimental timeline for cocaine-trained rats that received stimulation of pa-dnRac1 without (top) and with (bottom) previous cue re-exposure. (right) Summary showing that rats that received pa-dnRac1 stimulation without previous cue re-exposure exhibited decreased cue-induced cocaine seeking compared with rats with previous (2 h before) cue re-exposure (pa-dnRac1 active = 52.00 ± 4.54, n = 10 animals; pa-dnRac1 re-exp active = 85.71 ± 11.23, n = 7 animals; pa-dnRac1 inactive = 10.50 ± 1.17, n = 10 animals; pa-dnRac1 re-exp inactive = 12.14 ± 2.01, n = 7 animals; $F_{1,15} = 9.17$, $p = 0.0085$, RM two-way ANOVA, withdrawal day 45 lever × group interaction; **P < 0.01, Bonferroni post-test). (**e**) Nose poke responding during the cue re-exposure session of rats who underwent cue re-exposure before pa-dnRac1 stimulation (pa-dnRac1 re-exp = 26.00 ± 1.84, n = 7 animals). (**f**) Hypothetical diagrams illustrating the dissociation between the functional state of cocaine-

generated synapses and the behavioral expression (seeking) following reactivation of cocaine memories. Top: after cue re-exposure-induced memory reactivation, cocaine-generated synapses are re-silenced, while cocaine seeking remains at high levels for a few hours. Bottom: when cocaine-generated synapses are re-silenced and weakened beforehand, cue re-exposure does not induce high-level cocaine seeking. Thus, cocaine-generated silent synapses are involved in the storage or reactivation of cocaine memories, while cocaine seeking expressed during the memory destabilization window is driven by an independent mechanism.

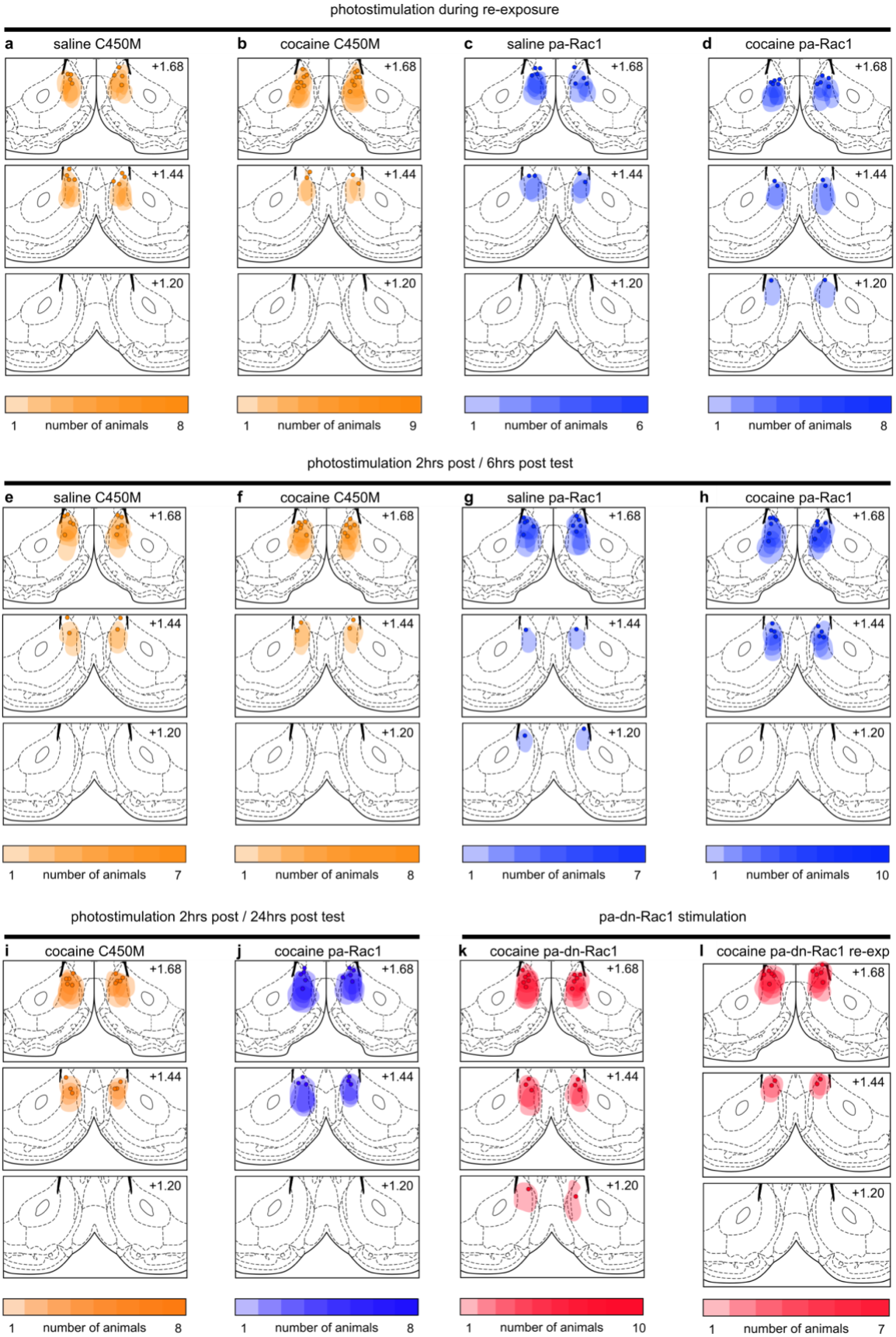
photostimulation during re-exposure
a saline C450M
b cocaine C450M
c saline pa-Rac1
d cocaine pa-Rac1
+1.68
+1.44
+1.20
1 number of animals 8
1 number of animals 9
1 number of animals 6
1 number of animals 8
photostimulation 2hrs post / 6hrs post test
e saline C450M
f cocaine C450M
g saline pa-Rac1
h cocaine pa-Rac1
1 number of animals 7
1 number of animals 8
1 number of animals 7
1 number of animals 10
photostimulation 2hrs post / 24hrs post test
pa-dn-Rac1 stimulation
i cocaine C450M
j cocaine pa-Rac1
k cocaine pa-dn-Rac1
l cocaine pa-dn-Rac1 re-exp
1 number of animals 8
1 number of animals 8
1 number of animals 10
1 number of animals 7

Figure 31. Verification of Viral and Optic Fiber Localization for all Behavioral Experiments

(**a-d**) Schematics mapping the viral expression and optical fiber tip (dots) localization for all rats included in data analysis for behavioral experiments presented in Figure 25. (**e-j**) Schematics mapping the viral expression and optic fiber tip localization for all rats included in data analysis for behavioral experiments presented in Figure 26. (**k,l**) Schematics mapping the viral expression and optic fiber tip localization for all rats included in data analysis for behavioral experiments presented in Figure 27.

3.5 Discussion

Recent work has highlighted the importance of dynamic changes in the functional state of synapses in the destabilization and reconsolidation of memories, although, the mechanisms that underlie these dynamics remain unknown. Our current findings identify the small GTPase Rac1 as a key signaling molecule in the regulation of the functional state of cocaine-generated synapses and underlies their dynamic changes during the destabilization and reconsolidation of cocaine-associated memories. These results highlight Rac1 as a potential molecular target to modify the content of cocaine-associated memories for potential therapeutic benefit.

3.5.1 Signaling Substrates Governing Synaptic State

Once formed, synapses can be stably maintained in a functionally mature state for a lifetime, or destabilized and eliminated during memory retrieval and reconsolidation (Yang et al., 2009). The stability of synapses are finely controlled by several processes and signaling molecules, among which Rho family GTPases, including Rac1, control focal changes in activated synapses (Hedrick et al., 2016; Murakoshi et al., 2011; Nishiyama and Yasuda, 2015; Yasuda, 2017).

Following cocaine memory retrieval, we found that the level of active Rac1 transiently decreases, and mimicking this decrease destabilizes cocaine-generated synapses. In contrast, increasing active Rac1 levels prevents the natural re-silencing of cocaine-generated synapses after memory retrieval. These findings suggest that active Rac1 stabilizes synapses, while dynamic decreases in active Rac1 levels destabilize synapses for modification. Importantly, restoring high levels of active Rac1 during the destabilization window is also capable of stabilizing cocaine-generated synapses in their silent state, indicating that active Rac1 stabilizes synapses in their current state, irrespective of whether they are in a weakened or strengthened state. In this case, Rac1-based manipulations might be developed to dynamically control the functional state of cocaine-generated synapses independent of their natural retrieval-induced dynamics, or alternatively extended/modulate these natural dynamics.

Our findings that Rac1 stabilizes the synaptic state are consistent with the general role of Rac1 in regulating the synaptic actin cytoskeleton. Specifically, Rac1 activates the PAK-LIMK signaling pathway, which phosphorylates and inhibits cofilin (Cingolani and Goda, 2008). Cofilin regulates the actin cytoskeleton by two main mechanisms: actin severing, and increasing the off-rate of actin monomers, both favoring actin depolymerization (Cingolani and Goda, 2008). However, actin severing also generates free barbed ends for elaboration and polymerization of actin, favoring actin polymerization (Ghosh et al., 2004). Thus, the dynamic balance between these two processes determines how a change in Rac1-cofilin signaling affects the stability of the actin cytoskeleton. In mature and stably functioning synapses, the level of active Rac1 is often relatively high (Yasuda, 2017), resulting in a persistent inhibition of cofilin that prevents both actin depolymerization-mediated structural shrinkage and actin polymerization- mediated enlargement. Such a high stability of actin scaffolding and synaptic structure favors AMPARs to be maintained

within the postsynaptic density (Allison et al., 1998; Zhou et al., 2001), and molecular trafficking to be confined within the synapse (Obashi et al., 2019), promoting the functional stability of the synapse. In contrast, a decrease in Rac1 will allow for the depolymerization and/or polymerization of the actin cytoskeleton, which in turn allows for the functional and structural modification of synapses (Cingolani and Goda, 2008; Fukazawa et al., 2003; Honkura et al., 2008; Okamoto et al., 2004; Okamoto et al., 2007; Zhou et al., 2001). Based on these results and analyses, we interpret the role of Rac1 after cocaine withdrawal such that a decrease in active Rac1 levels is a permissive step for CP-AMPAR internalization, while the CP-AMPAR internalization is likely driven by Rac1-independent mechanisms.

3.5.2 Synapse-Specific Effects

One of our most striking findings was the specificity of which manipulating Rac1 activity had on the functional state of different populations of synapses. Specifically, we found that inhibiting Rac1 appeared to selectively re-silence cocaine-generated synapses that are enriched with CP-AMPARs. This finding is quite striking given that Rac1 is distributed across dendrites and spines (Hedrick et al., 2016; Murakoshi et al., 2011), and its basal activity doesn't appear to be significantly altered by cocaine experience. Therefore, it is somewhat unexpected that globally inhibiting Rac1 activity would have such synapse specific effects. While it still is not clear what underlies this specificity, there are several unique features of cocaine-generated synapses that may explain this phenomenon.

One of the defining characteristics of the cocaine-generated synapses we examined in this study is the enrichment of CP-AMPARs. In many brain regions, early-stage expression of NMDAR-dependent LTP is partially mediated by synaptic insertion of CP-AMPARs, which are

replaced by CI-AMPARs during the late stage (Guire et al., 2008; Morita et al., 2013; Plant et al., 2006; Shi et al., 2001), which has led to the suggestion that CP-AMPARs are not as synaptically stable as CI-AMPARs (Isaac et al., 2007). Therefore, the decrease in Rac1 activity alone may be sufficient to trigger the internalization of CP-AMPARs, while CI-AMPARs may need additional signals (e.g. NMDAR activity) to trigger their internalization during memory destabilization (Shehata et al., 2018). Alternatively, the synaptic selectively may arise due to differences in the basal dynamics of the actin cytoskeleton at different synapses. It has previously been found that cocaine self-administration leads to an increase in actin cycling (increased depolymerization and polymerization) (Toda et al., 2006), and this may occur within specific synaptic populations, such as cocaine-generated synapses. This increased actin cycling may make the cytoskeleton more susceptible to Rac1 inhibition, while normal synapses may require complementary changes in the activity of other GTPases such as RhoA or cdc42 to trigger significant changes in the actin cytoskeleton and ultimately synaptic state. Future studies will be needed to understand the mechanisms underlying these synapse-specific effects of Rac1 manipulation. However, this synaptic specificity may be beneficial for the development of therapeutics as it may allow for more precise targeting of cocaine-encoding synapses.

3.5.3 Synaptic State and Memory Reactivation and Expression

Previous studies have demonstrated that functionally mature cocaine-generated synapses contribute to cocaine seeking, a behavioral readout of cocaine-associated memories, after prolonged withdrawal (Lee et al., 2013; Ma et al., 2014; Ma et al., 2016) (Chapter 2). Our current findings continue to support this relationship between mature cocaine-generated synapses and cocaine seeking, such that driving or holding these synapses into a silent state attenuates

subsequent seeking behavior. However, a dissociation between synaptic state and cocaine seeking emerges after memory reactivation, when cocaine-generated synapses are re-silenced but cocaine seeking behavior persists during the destabilization window. This suggests that memory reactivation may engage other processes to drive seeking behavior, independent of cocaine-generated synapses. This is supported by our findings that inhibiting Rac1 activity, and thus re-silencing cocaine-generated synapses, before memory reactivation decreased cocaine seeking, however, when the same manipulation was done after memory reactivation cocaine seeking was not affected. We hypothesize that cocaine-generated synapses are key substrates for the storage or reactivation of cocaine memories; once the memories are reactivated, the behavioral expression is maintained by an independent set of mechanisms. This is supported by previous studies that have implied that the substrates underlying the initial encoding, storage, and expression of memories may be dissociable (Caffaro et al., 2012; Mamou et al., 2006; Otis et al., 2013; Roy et al., 2017a). This scenario explains high levels of cocaine seeking during the memory destabilization window in our current studies of cocaine memories, as well as in studies of fear memories (Monfils et al., 2009). This mechanistic dissociation may also be physiologically beneficial, as it allows for the memory-encoding substrates to be destabilized for modification without sacrificing the ongoing behavioral output.

It remains unknown what mechanisms may be engaged to drive the behavioral expression of cocaine-associated memories, but one possibility is that once the memory-encoding neural substrates within the NAc are activated, this may trigger the engagement of downstream circuits to mediate seeking behavior, and the activity of these downstream areas is either self-sustaining or controlled by other inputs. Alternatively, other transient adaptations may compensate for the weakening of encoding neural substrates to support the ongoing behavior. One such

'compensatory' adaptation may be the transient potentiation of other populations of synapses within the NAc. Indeed this is well documented to occur during the reinstatement of cocaine seeking after extinction, and this plasticity contributes to the expression of seeking behaviors (Gipson et al., 2013a; Roberts-Wolfe et al., 2018; Smith et al., 2014; Smith et al., 2016; Spencer et al., 2016). It has also been documented within the hippocampus, that memory reactivation triggers a transient increase in the intrinsic membrane excitability of neurons and that subsequent memory reactivation shortly afterwards depends on this enhanced excitability (Pignatelli et al., 2018). Preliminary findings suggest that a similar enhancement in membrane excitability may also occur following the reactivation of cocaine-associated memories (**Appendix B**). However, future studies are needed to determine if this change in excitability has any behavioral relevance.

3.5.4 Concluding Remarks

Cocaine-generated synapses contribute to the dynamics of cocaine-associated memories, and here we have identified Rac1 as a critical regulator of the functional state of these synapses. These findings reveal a novel role for Rac1 in regulating synaptic function and position it as a molecular switch in the control of synaptic state. These findings also pinpoint Rac1 as a potential molecular substrate to be targeted for the development of therapeutic interventions in the treatment of addiction.

4.0 Cocaine-Generated Synapses Contribute to Cocaine-Associative Neural Activity

4.1 Overview

The expression of cocaine-associated memories and the persistence of cocaine seeking behavior are thought to be driven by changes in neural activity within the brain's reward circuits, including the nucleus accumbens (NAc). However, the underlying cellular mechanisms that govern these cocaine-associated activity dynamics remain undetermined. To explore the synaptic underpinnings governing cocaine-associated activity within the NAc, we assessed the role of silent synapses, which are generated in the NAc by cocaine self-administration and then functionally mature during withdrawal to contribute to cocaine seeking behavior. We show that during withdrawal from cocaine self-administration there is an enhanced recruitment and activation of neurons with the NAc associated with cues and behaviors. Critically, we demonstrate that blocking cocaine-induced synaptogenesis prevents this enhancement in NAc activity during withdrawal, as well as attenuates cocaine seeking behavior, causally linking cocaine-generated synapses with changes in neural activity and cocaine seeking. Furthermore, these effects were selective for neural activity associated with cues and behavior, as there was little to no effect on spontaneous activity or the encoding of spatial information within the NAc, suggesting cocaine-generated synapses may preferentially encode cocaine-associated cues and/or behaviors. These results provide some of the first evidence of the role synaptogenesis has in regulating neural activity *in vivo*, as well as provide more evidence that cocaine-generated synapses may represent a discrete synaptic ensemble contributing to the encoding of cocaine-associated memories and behaviors.

4.2 Introduction

Consuming drugs of abuse leads to the formation of drug-associated memories, and the reactivation of these memories promotes subsequent relapse and drug seeking behavior (Hyman et al., 2006b). Memories and the behaviors they drive are ultimately represented by specific neural activity patterns within the brain (Ju and Bassett, 2020; Ruff et al., 2018; Sussillo, 2014; Yuste, 2015). Thus, it is important to delineate the neural activity dynamics, as well as the mechanisms governing these dynamics, in order to understand how drug-associated memories are encoded and expressed.

Previous studies have identified several brain regions that display dynamic neural activity associated with cocaine taking and seeking, including the NAc. Neurons in the NAc display dynamic changes (increases and/or decreases) in firing rates during the behavioral responding (e.g. lever press) for cocaine, as well as in response to cocaine-associated stimuli, which are thought to represent the encoding of cocaine-associated memories and/or behaviors (Carelli and Ijames, 2000; Carelli et al., 2000; Chang et al., 1994; Ghitza et al., 2003; Peoples and West, 1996). These activity profiles emerge only during the acquisition and withdrawal from cocaine self-administration (Carelli and Wondolowski, 2003; Ghitza et al., 2003; Saddoris et al., 2011), suggesting a role in the learning and encoding of cocaine-associated memories and/or behavior. Interestingly, this neural encoding not only persists during abstinence, but is also enhanced (Guillem et al., 2014; Hollander and Carelli, 2005, 2007), which may contribute to the increases in cocaine craving and seeking observed following prolonged withdrawal (Grimm et al., 2001). While these findings have begun to parse out the neural activity dynamics that may encode cocaine-associated memories and behavior, the underlying mechanisms that shape these dynamics remain unknown.

Cocaine experience triggers significant synaptic remodeling within the NAc (Wright and Dong, 2020), and it is generally thought that such synaptic plasticity reshapes neural activity patterns to encode new memories and behaviors (Asok et al., 2019; Chaudhuri and Fiete, 2016; Magee and Grienberger, 2020). Alternatively, learning-induced changes in the activity dynamics may be mediated by other neural processes, such as adaptations in intrinsic membrane excitability, or may simply be driven by changes in input signals being transmitted from upstream brain areas. While there is some indirect evidence supporting the role of synaptic plasticity (Peters et al., 2014; Tye et al., 2008; Vega-Villar et al., 2019; Wu et al., 2020), there is still little direct evidence demonstrating a causal link between synaptic remodeling and learning-induced changes in neural activity dynamics.

In the present study, we have sought to directly link cocaine-induced synaptic remodeling to cocaine-associated neural activity within the NAc. Specifically, we have assessed the role of cocaine-generated synapses. These synapses are nascent, immature silent synapses that are generated *de novo* in the NAc during cocaine self-administration training, and then functionally mature via the recruitment of AMPARs during withdrawal (Lee et al., 2013; Ma et al., 2014; Neumann et al., 2016a; Wright et al., 2020). Furthermore, these cocaine-generated synapses have been demonstrated to contribute to cocaine seeking behaviors as well as the dynamics of cocaine-associated memories (Lee et al., 2013; Ma et al., 2014; Wright et al., 2020). These findings have prompted us to investigate if the generation and maturation of these cocaine-generated silent synapses contributes to the emergence of cocaine-associated neural activity dynamics within the NAc.

4.3 Methods

4.3.1 Subjects

Male wild-type C57BL/6 mice (7 weeks old at the start of experimentation) (Jackson Laboratory) were used in all experiments. Mice were singly housed on a 12hr light/dark cycle (light on/off at 7:00/19:00) with food and water available *ad libitum*. Mice were allowed to habituate in their housing cages for approximately 1 week before surgery. All mice were used in accordance with protocols approved by the Institutional Care and Use Committee at the University of Pittsburgh.

4.3.2 Virus Injection and GRIN Lens Implantation

To visualize neural activity within the NAc we expressed the calcium indicator GCaMP6m with the use of an AAV9 viral vector (pAAV.hsyn.GCaMP6m.WPRE.SV40, at titer $\geq 1\times10^{13}$ vg/mL; Addgene)(Chen et al., 2013). Delivery of the virus to the NAc *in vivo* was performed through standard stereotaxic microinjection, as previously reported (Wang et al., 2018; Wang et al., 2020; Wang et al., 2021; Yu et al., 2017). Briefly, mice were anesthetized with a xylazine-ketamine mixture (5-10/50-100 mg/kg; i.p.), and Carprofen (5mg/kg; s.c.) also given as an additional analgesic agent. The skull was then exposed and a hole (~ 1mm diameter) was drilled above the NAc (in mm: anterior-posterior (AP), +1.50; medial-lateral (ML), +0.73). A 32-gauge microinjection needle was then lowered down into the brain to the NAc (in mm: AP, +1.50; ML, +0.73; DV, -4.25) and 0.5µl of virus was injected at a rate of 200nl min^{-1}. The microinjection

needle was left in place for at least 5 min following injection to prevent backflow and allow for sufficient diffusion of the virus away from the injection site.

During the same surgery procedure, a Gradient-Index (GRIN) Lens (0.5mm diameter; Grintech) was implanted directly above the NAc following viral infusion, using procedures to those previously described (Resendez et al., 2016). Briefly, following removal of the microinjections needle, the surfaced of the brain was inspected and any remaining dura was gently removed, with care to minimize any bleeding. If bleeding occurred, the surgical site was thoroughly irrigated with sterile saline until all blood was washed away. Following removal of the dura, approximately 1mm of the cortex directly above the NAc was gently aspirated in order to reduce the buildup of intracranial pressure by the insertion of the GRIN lens. After aspiration, the surface of the brain was irrigated with sterile saline to remove any potential blood. The GRIN lens was then inserted into the brain using a custom 3D printed lens holder and slowly lowered down to the NAc ((in mm: AP, +1.50; ML, +0.73; DV, -4.25). The lens was then affixed to the skull using a small amount of superglue followed by dental cement. After the hardening of the dental cement, the grip on the lens holder was loosened and the lens was observed to assure it was securely affixed with no movement. A small plastic protective covering was then placed over the lens to protect it until baseplate attachment (see below), where it was secured with superglue and dental cement.

After at least 4 weeks following the implantation of the GRIN lens, viral expression was assessed and the MiniScope baseplate was attached. Briefly, mice were anesthetized as described above and placed in a stereotax. The protective covering was then removed and the lens surface was visually inspected to ensure there was no damage. A MiniScope with an attached baseplate was then stereotaxically lowered above the lens, where the orientation of the Miniscope was

adjusted such that the entire surface of the lens was in focus. The vertical placement of the MiniScope was then adjusted until a focal plane with a blood vessel and/or visible cells was found, at which point the baseplate was affixed to the skull using dental cement. Following fixation, the focal plane was imaged once again to ensure there was no significant deviation during the fixation process. After the dental cement was hardened, the MiniScope was removed and a protective cap was secured within the baseplate to protect the lens.

4.3.3 Wire-Free MiniScope

To image the neural activity of MSNs within the NAc during cocaine self-administration and seeking, we used the open-source UCLA MiniScope (v3) (miniscope.org) (Cai et al., 2016). In order to prevent tangling between the MiniScope cable and self-administration tethers, we chose to use a recently developed modified version of the v3 MiniScope that is wire-free (Shuman et al., 2019). This wire-free MiniScope is largely the same as the original wired version, however, with the additional features of being battery powered and logging the imaging data onto onboard removable memory. A limiting factor for the imaging duration of the wire-free MiniScope is the size and efficiency of the battery used. We utilized a single-cell lithium-polymer battery (Power Stream, GM041215, 45 mAH, 1.1 g), which allowed a maximum recording time of approximately 30min. Including the battery, the wire-free MiniScope weighs ~4g. The wire-free MiniScope utilizes an adjustable LED (470nm) to allow for the excitation of GCaMP6 and collects images at a frame rate of 20Hz. For detailed description of the design and construction of the wire-free MiniScope please see (Shuman et al., 2019) (http://miniscope.org/index.php/Wire-free_Miniscope).

4.3.4 Catheter Implantation

Catheter implantation surgery for self-administration was performed as described previously (Lee et al., 2013; Yu et al., 2017). Briefly, a silastic catheter was inserted into the right jugular vein by ~1 cm, and then the distal end was led subcutaneously to the back between the scapulae. Catheters were constructed of silastic tubing (length, 7cm; 0.30mm inner diameter x 0.64mm outer diameter) and attached to a commercially available Vascular Access Button (Instech). Mice were allowed to recover for at least 5 days following surgery, during which their wellbeing and weight were monitored. During the recovery period, the catheter was flushed daily with sterile saline containing cefazolin (3 mg mL^{-1}) and heparin (3 U mL^{-1}) to minimize potential infection and catheter occlusion.

4.3.5 Self-Administration Apparatus

All behavioral experiments were conducted in operant conditioning chambers enclosed within sound attenuating cabinets (Med Associates). Each chamber (15.24 x 13.34 x 12.7 cm^3) contains an active and an inactive lever press, a food dispenser, a conditioned stimulus light above each lever, a house light, and speaker for auditory tone delivery. No food or water was provided in the chamber during the training or testing session.

4.3.6 Intravenous Cocaine Self-Administration Training

Cocaine self-administration training began at least 5 days after catheter implantation. On day 1, mice were placed in the self-administration chamber for an overnight training session on a

fixed ratio 1 reinforcement schedule. Pressing on the active lever resulted in a cocaine infusion (0.75 mg kg^{-1} over 3-6 secs) and illumination of the conditioned stimulus light above the lever and the house light as well as the delivery of an auditory cue. Both the stimulus light and the house light remained illuminated for 20 secs, during which any additional lever presses were counted but resulted in no cocaine infusions. The auditory cue (1000Hz, 80db, 20 pulses at 1Hz) was also presented over the same 20 sec period. After the 20 sec timeout period, the lights were turned off and the auditory cue ceased, and the next press on the active lever resulted in a cocaine infusion. Presses on the inactive lever had no reinforced consequences, but were recorded.

Mice first underwent one overnight training session, approximately 12 hrs long to facilitate acquisition. Only mice that received at least 80 cocaine infusions during the overnight session were allowed to proceed to the 11 day cocaine self-administration training regimen. Similar self-administration procedures/standards were used in our previous studies (Lee et al., 2013; Ma et al., 2014; Wright et al., 2020; Yu et al., 2017). Mice then underwent 11 days of cocaine self-administration training, where they underwent the same cocaine self-administration procedure described above in 2 hr daily training sessions. Every other day, beginning on training day 1 (d1, d3, d5, d7, d9, d11), mice underwent calcium imaging during the training session, while on the others they underwent training while wearing a dummy scope with similar weight and dimensions to the wire-free MiniScope. After the 11^{th} day of training, mice were placed back in their home cages and remained there during withdrawal. Cocaine-training mice that failed to meet the self-administration criteria (≥ 15 infusions per session, 70% active-to-inactive nose poke response ratio) were excluded from further experimentation and analysis.

4.3.7 Withdrawal Phase

Mice were returned to their home cage after each self-administration training session. After the 11 day procedure, the mice were singly housed in their home cage during withdrawal, with food and water available *ad libitum*. Early withdrawal was operationally defined as 40-50 hours after the last session of cocaine self-administration training. This time point was chosen over an earlier time to avoid any potential photobleaching that may occur due to multiple imaging session in close proximity between training day 11 and early withdrawal. Late withdrawal was operationally defined as 20-22 days after the last session of cocaine self-administration training.

4.3.8 Cocaine Seeking Test

Cocaine seeking was assessed in an extinction test (30 min) conducted during both early and late withdrawal from cocaine self-administration. During the extinction test session, mice were placed back in the operant chamber, where presses on the active lever resulted in contingent delivery of the stimulus light and tone cues, but not cocaine. The number of active lever presses was used to quantify cocaine seeking. Presses on the inactive lever were also recorded, but had no consequence.

4.3.9 Gabapentin Treatment

To prevent the generation of silent synapses, we administered gabapentin daily during cocaine self-administration. Gabapentin solution (100 mg ml^{-1}) was prepared freshly each day before it was administered via i.p. injection (100 mg kg^{-1}) 1 hr to 30 min before the start of each

training session. A second daily injection was also given 8-12 hrs after the first injection. This administration protocol has previously been demonstrated to block cocaine-induced generation of silent synapses (Wang et al., 2020). Saline injections were used as control.

4.3.10 Preparation of Acute Brain Slices

Mice were decapitated following isoflurane anesthesia. For NAc-containing slices, coronal slices (250 μm thick) containing the NAc were prepared on a VT1200S vibratome (Leica) in 4 °C cutting solution containing (in mM): 135 N-methyl-d-glutamine, 1 KCl, 1.2 KH_2PO_4, 0.5 $CaCl_2$, 1.5 $MgCl_2$, 20 choline-HCO_3 and 11 glucose, saturated with 95%O_2/5%CO_2 and pH adjusted to 7.4 with HCl. Osmolality was adjusted to 305 mmol kg^{-1}. Immediately after cutting, slices were transferred and incubated in artificial cerebrospinal fluid (aCSF) containing (in mM): 119 NaCl, 2.5 KCl, 2.5 $CaCl_2$, 1.3 $MgCl_2$, 1 NaH_2PO_4, 26.2 $NaHCO_3$ and 11 glucose, with the osmolality adjusted to 280–290 mmol kg^{-1}. Slices were placed in the aCSF saturated with 95% O_2/5% CO_2 at 37 °C for 30 min and then held at 20–22 °C for at least 30 min before experimentation.

4.3.11 Slice Electrophysiology

All recordings were made from MSNs located in the medial NAcSh. During recordings, slices were superfused with aCSF, heated to 30–32 °C by passing the solution through a feedback-controlled in-line heater (Warner) before entering the recording chamber. To measure excitatory postsynaptic current (EPSC) responses, electrodes (2–5 MΩ) were filled with a cesium-based internal solution (in mM: 135 $CsMeSO_3$, 5 CsCl, 5 TEA-Cl, 0.4 EGTA (Cs), 20 HEPES, 2.5 Mg-ATP, 0.25 Na-GTP, 1 QX-314 (Br), pH 7.3). Picrotoxin (0.1 mM) was included in the aCSF during

all recordings to inhibit $GABA_A$ receptor-mediated currents. Presynaptic afferents were stimulated by a constant-current isolated stimulator (Digitimer), using a monopolar electrode (glass pipette filled with aCSF). Series resistance was typically 7–20 MΩ, uncompensated and monitored continuously during recording. Cells with a change in series resistance >20% were excluded from data analysis. Synaptic currents were recorded with a MultiClamp 700B amplifier, filtered at 2.6–3 kHz, amplified five times and digitized at 20 kHz.

NAc shell MSNs were randomly selected for recording. The minimal stimulation assay was performed as previously described (Brown et al., 2011a; Graziane et al., 2016; Huang et al., 2009; Isaac et al., 1995; Lee et al., 2013; Liao et al., 1995; Ma et al., 2014; Ma et al., 2016; Neumann et al., 2016b). After obtaining small (~50 pA) EPSCs at −70 mV, the stimulation intensity was reduced in small increments to the point that failures versus successes of synaptically evoked events (EPSCs) could be clearly distinguished. The stimulation intensity and frequency were then kept constant for the rest of the experiment. The amplitudes of both AMPAR and NMDAR ESPCs resulting from single vesicular release are relatively large in NAcSh MSNs (for example, ~15 pA for AMPAR mEPSCs at −70 mV), which facilitates the judgment of successes versus failures. For each cell, 50–100 traces were recorded at −70 mV, and 50–100 traces were recorded at +50 mV. Recordings were then repeated at −70 mV and +50 mV for another round or two. Only cells with relatively constant failure rates (changes <15%) between rounds were used to assess percentage of silent synapses. We visually detected failures versus successes at each holding potential over 50–100 trials to calculate the failure rate, as described previously (Brown et al., 2011a; Graziane et al., 2016; Huang et al., 2009; Lee et al., 2013; Ma et al., 2014; Ma et al., 2016; Neumann et al., 2016b). We performed this analysis in a blind manner such that a small number of ambiguous responses were categorized in a fully unbiased way.

To quantify percentage of silent synapses, we made two theoretical assumptions: (1) the presynaptic release sites are independent, and (2) release probability across all synapses, including silent synapses, is identical. Thus, the percentage of silent synapses was calculated using the equation: $1 - \ln(F_{-70})/ \ln(F_{+50})$, in which F_{-70} was the failure rate at −70 mV and F_{+50} was the failure rate at +50 mV, as rationalized previously (Liao et al., 1995). Note that in this equation, the failure rate is the only variable that determines the percentage of silent synapses. The amplitudes of EPSCs are used to present failures or successes, but do not have analytical value. In the cases in which these two theoretical assumptions are not true, the above equation was still used, as the results were still valid in predicting the changes of silent synapses qualitatively as previously rationalized (Huang et al., 2015b; Ma et al., 2014). he amplitude of an EPSC was determined as the mean value of the EPSC over a 1-ms time window around the peak, which was typically 3–4 ms after the stimulation artifact. To assess the percentage of silent synapses, only the rates of failures versus successes, not the absolute values of the amplitudes, were used. At +50 mV, successful synaptic responses were conceivably mediated by both AMPARs and NMDARs, and inhibiting AMPARs by NBQX (5 μM) modestly reduces the amplitudes of EPSCs (Graziane et al., 2016). Despite the effects of NBQX on the amplitudes, the failure rate of synaptic responses at +50 mV was not altered during AMPAR inhibition (Graziane et al., 2016). Thus, in the minimal stimulation assay assessing the percentage of silent synapses, the results will not be affected, whether the synaptic responses at +50 mV are mediated by NMDARs alone or by both AMPARs and NMDARs.

4.3.12 *In Vivo* Calcium Imaging Procedure

In vivo calcium imaging was performed both during self-administration training and the cocaine seeking tests during withdrawal with the wire-free MiniScope. To minimize the potential of photobleaching, each imaging session was separated by at least 1 day, and as such imaging was performed only every other day during the self-administration training, starting on day 1. On non-imaging days, mice underwent the same procedure, but the wire-free MiniScope was replaced with a dummy scope, which had the same weight and dimensions as the wire-free MiniScope.

Before each imaging session, mice were head-fixed using a small metal bar attached to the MiniScope baseplate, where we then attached the wire-free MiniScope to the baseplate. We then recorded a short video through the MiniScope to check imaging focal plane. Using this imaging video, we made any necessary adjustments to try to match the same imaging focal plane across days as well as adjust the LED intensity. LED intensity was always kept below 1mW to minimize photobleaching. Note that due to the onboard memory storage setup of the wire-free MiniScope, this prevented adjustments of the focal plane to be made with direct video feedback and instead required adjustments to be made blind before rechecking the imaging video. In some instances, this resulted in poor alignment of the focal plane across days.

Once the wire-free MiniScope was attached and adjusted to the correct focal plane and LED intensity, the battery was attached and secured to the wire-free MiniScope and the mouse was placed into the operant self-administration training. Behavior was captured with an infrared video camera EPL IR Wide Angle camera (Ailipu Technology Co. LTd) mounted directly above the operant chamber at 30fps and was also used to determine the onset of the wire-free MiniScope, which was later used to temporally align imaging and behavioral data. After the wire-free MiniScope was on, the self-administration training session was initiated. To minimize

photobleaching from extended imaging sessions, imaging was performed only during the first 20 min of the behavioral session, at which point the wire-free MiniScope automatically turned off. The mouse would then complete the remainder of the session undisturbed with the inactive MiniScope still attached. After the session, mice were removed from the operant chamber, briefly head-fixed to detach the wire-free MiniScope, and then returned to their home cage.

4.3.13 Immunohistochemistry and Confocal Microscopy

Following the completion of all *in vivo* calcium imaging experimentation, we verified the localization of the GRIN lens and imaging plane. Mice were deeply anesthetized and then transcardially perfused with 0.1 M sodium phosphate buffer, followed by 4% paraformaldehyde (PFA, wt/wt) in 0.1 M phosphate buffer. Brains were removed and postfixed in 4% PFA overnight at 4 °C. Following postfix. Whole brains were then stored in 30% sucrose in phosphate buffer with 0.1% sodium azide at 4 °C until sectioning. Coronal sections (50-100 μm thick) containing the NAc were then prepared on a VT1200S vibratome (Leica) in 0.1 M PBS and then stored in cryoprotectant (30% sucrose, 30% ethelyne glycol, in phosphate buffer) at −20 °C until staining.

Immunohistochemistry was performed as previously described (Winters et al., 2012). Briefly, floating sections were washed in PBS 3 × 5 min and then permeabilized with 0.1% Triton X-100 in PBS for 15 min. Sections were then washed 3 × 5 min in PBS and blocked with 5% normal donkey serum in PBS for 2 h. To amplify GCaMP6m signal, sections were next incubated overnight at 4 °C with a primary antibody against GFP (1:1,000, monoclonal mouse anti-GFP; Abcam). Sections were subsequently washed 3 × 5 min in PBS and incubated for 2 h at room temperature with a secondary antibody (1:500, ALEXA 488 donkey anti-mouse; Abcam). Sections

were washed again 3 × 5 min in PBS before they were mounted in ProLong Gold Antifade with DAPI (Molecular Probes).

Sections were imaged and captured with a Leica TCS SP5 confocal microscope equipped with Leica Application Suite software (Leica). Slices were imaged with a 5x or 10x air objective and the entire slice was captured using automated tile scanning and image stitching functions. From these images, viral expression and localization could be determined. All representative images were captured with a 10x air objective.

4.3.14 Quantification and Statistical Analysis

4.3.14.1 Calcium Image Video Processing

Raw calcium image videos were processed using the open-source CaImAn analysis pipeline optimized for one-photon calcium imaging using python (v3.7) (https://github.com/flatironinstitute/CaImAn). For detailed description of CaImAn see (Giovannucci et al., 2019). Briefly, images are first corrected for any motion artifacts using the NoRMCorre algorithm, which corrects non-rigid motion artifacts by estimating motion vectors over a set of overlapping field of views (FOVs) (Pnevmatikakis and Giovannucci, 2017). This process is modified for one-photon micro-endoscopic images, where the motion is estimated on a high pass spatially filtered dataset, which removes the smooth background signal of one-photon images and creates enhanced spatial landmarks. The inferred motion fields are then applied to the original video frames to correct for motion.

Source extraction is then performed using a modified version of non-negative matrix factorization (CNMF) framework that has been optimized to handle the more complex background contamination associated with the larger integration volume of one photon images (CNMF-E)

(Giovannucci et al., 2019; Pnevmatikakis et al., 2016; Zhou et al., 2018). CNMF-E is initialized using an extension of the GreedyROI method (Giovannucci et al., 2019; Pnevmatikakis et al., 2016) and then extracts component spatial footprints (shape and localization) and component activity traces. Component quality is evaluated and classified using unsupervised and supervised learning methods based on the localized spatio-temporal signature of each FOV (Giovannucci et al., 2019). The correlation of the spatial footprint across time is used to evaluate the spatial footprint consistency, and the component is rejected if below a specified threshold θ_{sp}, which we set to $\theta_{sp} = 0.8$. The peak signal to noise ratio (SNR) is also computed for each component and the component is rejected if below a specified threshold θ_{SNR}, which we set to $\theta_{SNR} = 8$. In addition, a 4-layer convolutional neural network (CNN) is used to classify spatial footprints into true and false components, with true components corresponding to footprints resembling a soma (Giovannucci et al., 2019). The activity traces of each extracted component are then denoised producing a smoothed calcium trace (Friedrich et al., 2017). Lastly, each accepted extracted component was manually inspected by the experimenter to ensure the quality of all components included in the final dataset.

All extracted calcium fluorescence traces were then downsampled to 100ms bins and then z-scored for all subsequent analyses, except for the estimation of spatial fields (see below).

4.3.14.2 Behavioral Video Processing

Mouse position was extracted from behavioral videos using DeepLabCut, an open-source deep learning pipeline for markerless estimation of body position (Mathis et al., 2018). The DeepLabCut network was trained to detect the self-administration button, the midbody, and base of the tail of mice throughout self-administration sessions. These three points were used to estimate

the position of the mouse within the chamber. Positional data was subsequently binned to 100ms for further analyses.

4.3.14.3 Identification of Calcium Transients

To assess overall neural activity levels, we calculated the frequency and amplitude of calcium transients. We defined calcium transients as peaks in the activity traces with a peak prominence of at least 2 times the standard deviation of the entire trace. This was performed using the signal.find_peaks module from the SciPy library in python (v3.7). These peaks were then used to calculate the frequency of transients and the average transient amplitude throughout an entire behavioral session.

4.3.14.4 Identification of Spatially Tuned Neurons

To identify spatially tuned neurons and estimate their spatial fields, we adopted a Gaussian Process (GP) regression model-based Bayesian approach developed for the estimation of tuning curves from calcium fluorescence imaging data (Park et al., 2014). This GP regression approach has previously been used to estimate neural spatial fields from calcium imaging data, including during cocaine seeking behaviors (Cameron et al., 2019; Murugan et al., 2017).

We chose to adopt this approach over others more traditionally used because of several advantages, which have previously been detailed (Murugan et al., 2017). Briefly, this approach takes into account the relatively slow dynamics of the calcium indicator to avoid the misattribution of neural activity to incorrect locations. In our case, we set GCaMP6m $\tau = 1.25$ based on previous findings optimizing the inference of spikes from GCaMP6m (Pachitariu et al., 2018). In addition, it also automatically estimates the smoothness of spatial receptive fields by using a maximum likelihood approach known as ‘maximum marginal likelihood’ (Bishop, 2006). This is important

given the limited *priori* knowledge about the smoothness of spatial fields of NAc neurons during cocaine self-administration behaviors. Lastly, a Bayesian approach allows for the quantification of the uncertainty about the influence of behavioral variables on neural activity in the form of a posterior distribution over model parameters.

The fitting of this model to neural data has previously been described in detail (Murugan et al., 2017; Park et al., 2014). We first discretized the behavioral chamber into bins of ~1 cm, resulting in a discrete place field map of 16 x 15 bins. The Gaussian process places a multivariate non-zero Gaussian prior distribution over the field $P(\mathbf{f}) = \mathcal{N}(0,\mathbf{K})$, where the i, j'th element of the covariance matrix $\mathbf{K}$ is given by the Gaussian covariance matrix $\mathbf{K}(i,j) = \rho \exp(-||\mathbf{x}_i - \mathbf{x}_j||^2 / (2\delta^2))$, $\mathbf{x}_i$ and $\mathbf{x}_j$ are the spatial location of the i'th and j'th bins of the spatial field, respectively. The prior is governed the hyperparameters marginal variance, ρ, which defines the marginal prior variance of the field elements, and length scale, δ, which determines the degree of smoothness. The neural activity in each time bin given the mouse's location is assumed to follow a Gaussian distribution, $P(y(t)|(x(t)) = \mathcal{N}(f(x(t)), \sigma^2)$, where $y(t)$ is the neural activity, which is deconvolved from the raw calcium fluorescence data, at time t, $x(t)$ is the mouse's spatial location at time t, and the distribution has mean $f(x(t))$ and variance σ^2. The hyperparametrs ρ and δ, as well as σ^2 are set by maximizing marginal likelihood, or the conditional probability of the data given these hyperparameters. This allows for the identification of the optimal smoothing for spatial fields directly from the data without prior assumptions. The maximum *a posteriori* (MAP) estimate is then used to determine the spatial field with the use of standard formulas for the posterior under Gaussian prior and likelihood $f= \mathbf{X}^T \mathbf{X} + \sigma^2 \mathbf{K}^{-1})^{-1} \mathbf{X}^T \mathbf{Y}$, where $\mathbf{X}$ is the design matrix (spatial bin x temporal bin), in which each row carries a 1 in the corresponding column representing the spatial

bin the mouse was located in during that time bin, and **Y** is the corresponding neural activity. This results in an estimated spatial field for each neuron.

To determine if the estimated spatial field for each neuron was significant we used a 10-fold cross-validation approach. We estimated the spatial field for each neuron using 90% of the data and then compared the predicted fluorescence (based solely on this spatial field) to the actual fluorescence of the held-out data (10%). This process was repeated 10 times, and neurons were considered to be significantly spatially tuned only when the predicted and actual fluorescence were found to be significantly correlated (Pearson's correlation coefficient, $p < 0$ .01) for each fold.

4.3.14.5 Identification of Lever Press Responsive Neurons

To determine if neurons displayed significant changes in activity following a lever press and during cue presentation, we adopted an approach similar to those previously used (Corder et al., 2019; Grewe et al., 2017; Gründemann et al., 2019; Liang et al., 2018; McHenry et al., 2017; Otis et al., 2017; Otis et al., 2019). We took the neural activity from a 5 sec post lever press interval for each lever press and took the mean of the activity throughout the interval, obtaining the averaged post lever press activity for each lever press for each neuron. For each neuron, we also took the averaged neural activity from a 5 sec pre lever press interval for each lever press. We pooled the averaged activity across all the lever presses and calculated a p-value for each neuron by using a two-tailed Wilcoxon rank-sum test to compare the pre- and post-lever press activity. We designated any neurons for which $p < 0.05$ as being significantly responsive to the lever press. Significantly responsive neurons were subsequently divided into excited and inhibited neurons if they displayed an increase or decrease in activity, respectively.

4.3.14.6 Statistics

All analyses were carried out using Python v3.7 (calcium activity analysis), MATLAB R2019a (spatial field estimation), and Prism v8 (behavioral analysis). All results are presented as mean ± s.em., unless otherwise stated. No statistical methods were used to predetermine sample sizes, but sample sizes are similar to previously published reports of similar experiments (Cameron et al., 2019; Grewe et al., 2017; Wright et al., 2020; Yu et al., 2017).

Analyses were performed on either the number of animals (behavioral) or the number of cells (electrophysiology and calcium imaging) pooled together for each group. Sample sizes are presented as *n*/*m*, where *n* is the number of cells and *m* is the number of mice, unless otherwise stated. For the comparison of mean differences, statistical significance was assessed using unpaired t-tests, paired t-tests, two-way analysis of variance (ANOVA), or repeated-measures two-way ANOVA as specified in the text. For all significant ANOVA results, post-hoc comparisons were made using Bonferroni multiple comparisons corrections. For comparing the percentages of neurons, statistical significance was assessed with Fisher's exact test. Correlations were performed by calculating Pearson's correlation coefficients. Significance was set at $p < 0.05$.

4.4 Results

In order to assess the influence of cocaine-generated silent synapses over neural activity dynamics within the NAc, we chose to prevent their generation during the acquisition of cocaine self-administration. To prevent the generation of silent synapses within the NAc, we blocked the signaling of the α2δ-1 auxiliary calcium channel subunit with gabapentin (GBP, 100mg/kg;

Figure 32 a) (**see Methods**), which is the neuronal receptor for the syanptogeneic protein

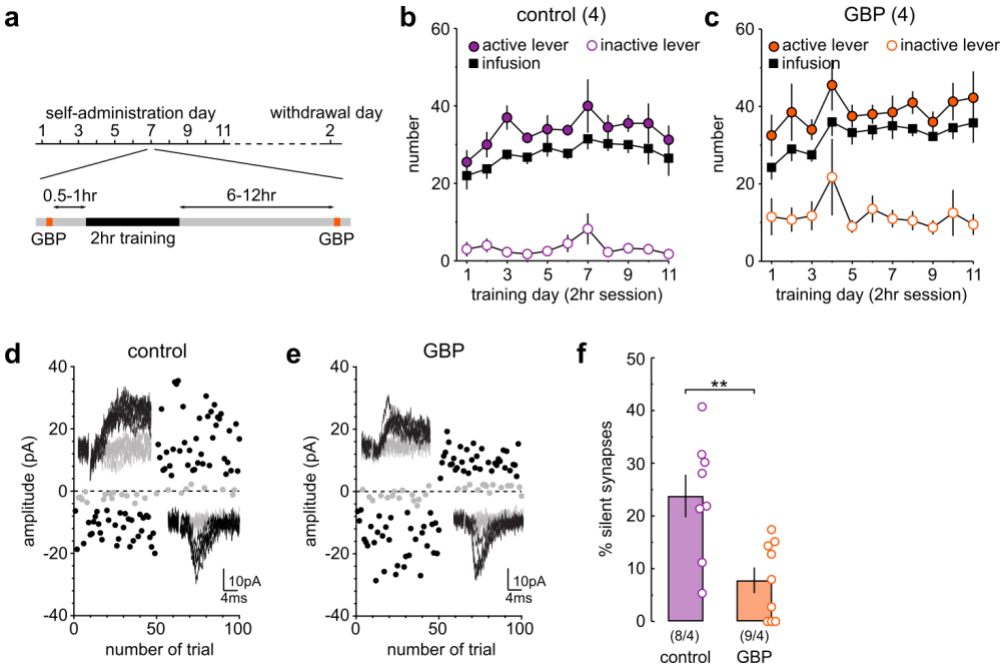

Figure 32. Gabapentin Prevents the Cocaine-Induced Generation of Silent Synapses in Mice

(a) Diagram showing experimental timeline of self-administration training and GBP treatment. **(b,c)** Self-administration training data of control **(b)** and GBP **(c)** mice used in the following electrophysiology experiments. **(d,e**) EPSCs evoked at -70mV and +50mV (insets) over 100 trials from example recordings for control **(d)** and GBP **(e)** mice. **(f)** Summary showing the percentage of silent synapses lower following GBP treatment compared to controls (control = 23.81±4.05, n = 8 cells/4 mice; GBP = 7.83±2.42, n = 9 cells/4 mice; $t_{15} = 3.48$, $p = 0.0034$, two-tail unpaired t-test). Data presented as mean ± s.e.m. ** $p < 0.01$.

thromobospondin and is critical for synaptogenesis (Eroglu et al., 2009; Eroglu and Barres, 2010; Risher et al., 2018). GBP administration was recently demonstrated to prevent cocaine-induced generation of silent synapses within the NAc of rats undergoing 5-day cocaine self-administration (Wang et al., 2020). We further confirmed the effectiveness of GBP treatment in blocking cocaine-induced generation of silent synapse in mice undergoing 11 days of cocaine self-administration training, which was used for subsequent *in vivo* calcium imaging (**Figure 32 a**). Both control and

GBP treated mice acquired and maintained cocaine self-administration behavior throughout the 11 day training period (**Figure 32 b,c**), consistent with previous reports that GBP does not affect acquisition (Wang et al., 2020). Two days after the completion of cocaine self-administration training (withdrawal day 2; WD2), we performed minimal stimulation electrophysiology recordings to estimate the percentage of silent synapses in NAc MSNs (**see Methods**). Consistent with previous studies (Brown et al., 2011b; Huang et al., 2009; Lee et al., 2013), we found the percentage of silent synapses was significantly increased in control mice (**Figure 32 d,f**), indicative of cocaine-induced synaptogenesis. In contrast, mice treated with GBP displayed low levels of silent synapse (**Figure 32 e,f**), suggesting a lack of cocaine-induced generation of silent synapses. These results further demonstrate effectiveness of GBP in preventing cocaine-induced synaptogenesis within the NAc.

We next examined how preventing cocaine-induced synaptogenesis affected neural activity dynamics within the NAc. To record neural activity dynamics within the NAc during freely moving cocaine self-administration and cocaine seeking behaviors in mice, we employed *in vivo* calcium imaging in combination with microendoscopy and head-mounted wire-free miniScopes (**Figure 33 a**). To image calcium dynamics in the NAc, which serve as a proxy for neural activity, we injected an AAV viral vector expressing the fluorescent genetically-encoded calcium indicator (GECI) GCaMP6m into the NAc, which led to robust expression in NAc neurons (**Figure 33 b**). To visualize calcium activity *in vivo* within the deep lying NAc, we gained optical access through a GRIN lens implanted to the NAc and imaged GCaMP6m fluorescence with an open-source head-mounted wire-free miniScope while mice freely moved within the cocaine self-administration chamber (**Figure 33 a-c**). From imaging videos individual neurons were identified using CNMF-

E (Giovannucci et al., 2019; Pnevmatikakis et al., 2016) (**see Methods**), from which calcium

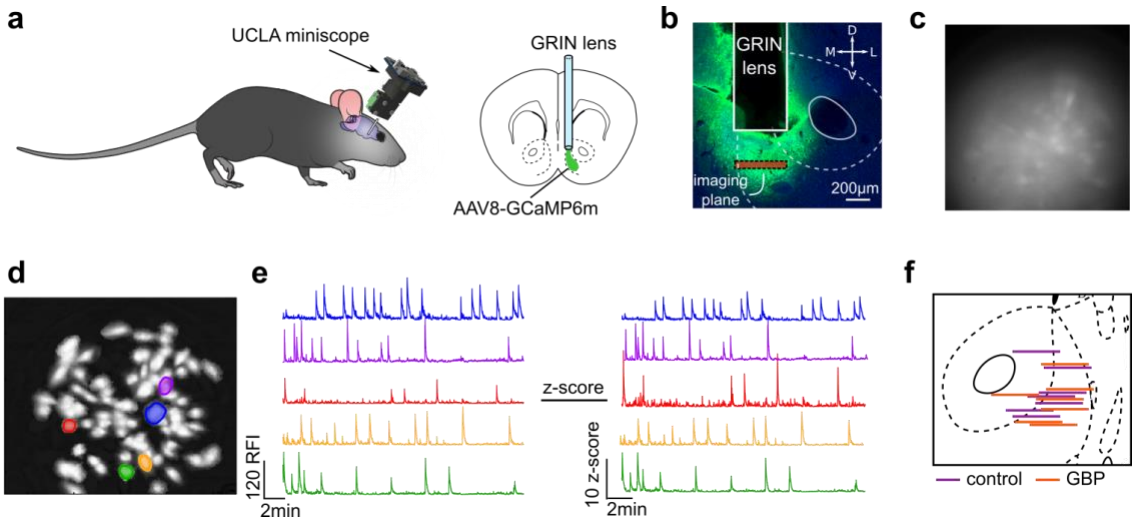

Figure 33. *In Vivo* Calcium Imaging in Freely Moving Mice during Cocaine Seeking

(a) Schematic showing wire-free miniScope and GRIN lens implanted to the NAc to allow for *in vivo* calcium imaging of the NAc. **(b)** Example image of a NAc slice showing GCaMP6m expression, GRIN lens localization, and imaging focal plane within the NAc. **(c)** Example image of raw, unprocessed calcium imaging video obtain from the wire-free miniScope during cocaine self-administration training. **(d)** Example cell map showing individual neurons identified and extracted by CNMF-e during a single imaging session. **(e)** Denoised (left) and z-scored (right) calcium traces of neurons shown in **(d)** (RFI = relative fluorescence). **(f)** Schematic mapping the localization of imaging focal plane for all animals used in subsequent analyses.

activity dynamics were extracted (**Figure 33 d-e**). While GCaMP6m was expressed within all neuron types within the NAc, we assumed recorded neurons were MSNs given these neurons represent the vast majority (~95%) of neurons in the NAc (Kawaguchi, 1993; Kreitzer, 2009). Furthermore, we were able to rule out the contribution of FSIs within our dataset based on the relatively fast rise and decay kinetics of the calcium transients we observed (**Figure 33 e**), which are inconsistent with the very slow and prolonged transients previously reported in striatal FSIs (Gritton et al., 2019). We confirmed that neurons imaged were within the NAc in all mice included

for subsequent analyses. The majority of imaged neurons belonged within the shell subdivision

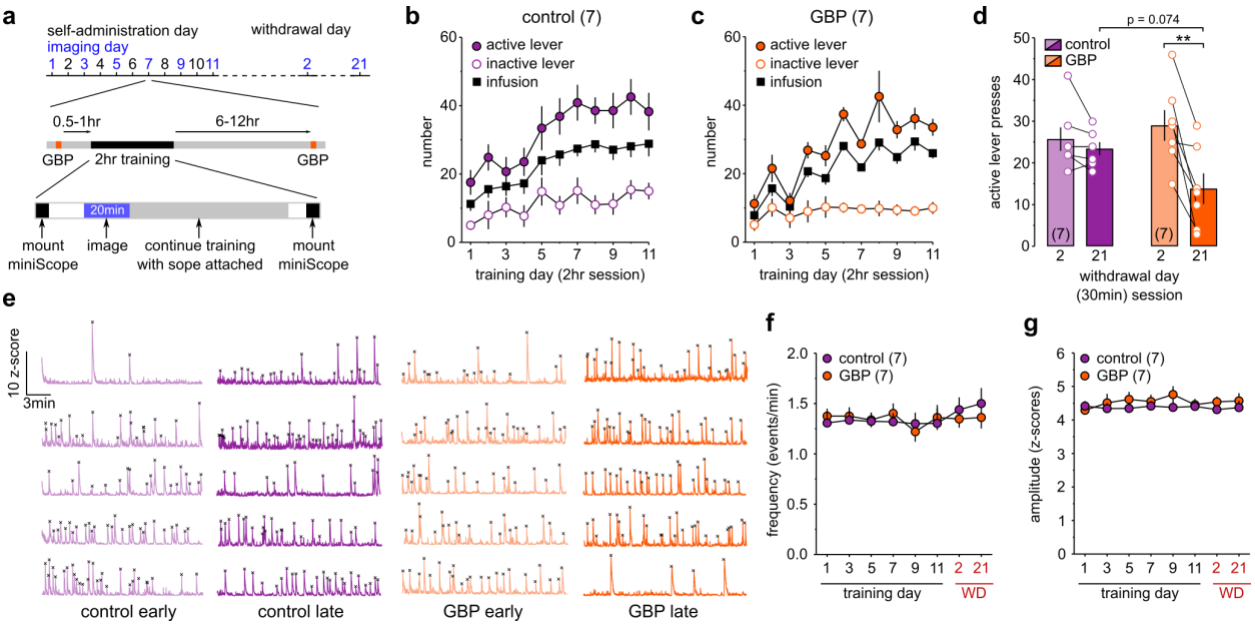

Figure 34. Effects of Blocking Cocaine-Induced Synaptogenesis on Behavior and Spontaneous Activity

(a) Diagram showing experimental timeline of cocaine self-administration, calcium imaging, and GBP treatment. **(b,c)** Self-administration training data of control **(b)** and GBP **(c)** mice used in calcium imaging experiments. **(d)** Summary showing GBP treated mice exhibited lower levels of cocaine seeking on withdrawal day 21 compared to withdrawal day 2, while cocaine seeking was maintained in control mice (control WD2 = 25.74±2.83; control WD21 = 23.43±1.57, n = 7 mice; GBP WD2 = 29.00±3.70; GBP WD21 = 13.86±3.66, n = 7 mice; $F_{(1,12)} = 11.68$, $p = 0.0051$, RM two-way ANOVA, day x treatment interaction; ** $p < 0.01$ Bonferroni post-test). **(e)** Example z-scored calcium traces from the same control mouse (purple) and GBP mouse (orange) imaged during early and late withdrawal. 'x' marks the peak location of identified calcium transients. **(f)** Summary showing the frequency of calcium transients during entire imaging sessions does not change during self-administration training or during cocaine seeking during withdrawal in both control and GBP mice ($F_{(7,80)} = 1.26$, $p = 0.2809$, RM two-way ANOVA, main effect of day) **(g)** Summary showing the amplitude of calcium transients during entire imaging sessions does not change during self-administration training or during cocaine seeking during withdrawal in both control and GBP mice ($F_{(1,80)} = 0.89$, $p = 0.5211$, RM two-way ANOVA, main effect of day). Data are presented at mean ± s.e.m.

within the NAc, however some neurons were also imaged within the NAc core (**Figure 33 f**). For all results reported below we have not attempted to distinguish between neurons within the NAc core and shell. Importantly, GRIN lens placements were similar across different groups (**Figure 33 f**), indicating neurons were sampled from similar sub regions of the NAc and are unlikely to underlie any detected differences.

Mice underwent 11 days of self-administration training, during which *in vivo* calcium imaging was performed (**Figure 34 a**) (**see Methods**). To minimize potential photobleaching effects, *in vivo* calcium imaging was performed every other day, beginning on day 1, and for only the first 20min of each session. On days when imaging was not performed, mice underwent the same procedures except a dummy scope, with similar weight and dimensions to the miniScope, was attached to the mouse's head (**see Methods**). *In vivo* calcium imaging procedures had minimal effects on the acquisition of cocaine self-administration behavior, with both control and GBP mice displaying cocaine self-administration behavior, with clear discrimination between active and inactive levers, throughout the 11 day training period (**Figure 34 b,c**). Furthermore, both groups also displayed cue-induced cocaine seeking behavior during early withdrawal (WD2) from cocaine self-administration (**Figure 34 d**). Cocaine seeking behavior was maintained at a similar level throughout withdrawal (WD21) in control mice (**Figure 34 d**), but did not further increase, or 'incubate', as is seen under certain conditions in rats (Grimm et al., 2001; Lee et al., 2013; Wright et al., 2020). In contrast, cocaine seeking behavior significantly decreased in GBP treated mice during late withdrawal (WD21) compared to early withdrawal (**Figure 34 d**). These results are consistent with previous findings demonstrating that cocaine-generated synapses contribute to cocaine seeking behavior after a period of prolonged withdrawal (Lee et al., 2013; Wang et al., 2020; Wright et al., 2020). Furthermore, they provide additional evidence that cocaine-generated

synapses do not uniquely contribute to incubation effects (Wang et al., 2020). We first assessed overall activity levels within the NAc by measuring the frequency and amplitude of identified calcium transients (**see Methods**) (**Figure 34 e**).

We found that for both control and GBP mice the frequency of calcium transients remained consistent throughout cocaine self-administration training and cue-induced cocaine seeking during early and late withdrawal (**Figure 34 f**). Furthermore, there was no difference in the frequency of calcium transients between control and GBP mice (**Figure 34 f**). Similar results were also found for the amplitude of calcium transients (**Figure 34 g**). Together, these results indicate there are no changes in the overall activity levels within the NAc during the acquisition of cocaine self-administration, nor during cue-induced seeking. Furthermore, blocking the generation of silent synapses has no effect on the overall neural activity level within the NAc.

Next, we examined neural activity within the NAc associated with cocaine seeking behavior. We limited our analyses to cocaine seeking sessions during withdrawal as this period is when behavioral differences between control and GBP mice became apparent. Previous studies have demonstrated that neurons in the NAc encode spatial information (Lansink et al., 2008; Lansink et al., 2009; McGinty et al., 2013; Sjulson et al., 2018; Trouche et al., 2019), and such information may contribute to cocaine seeking behavior (Cruz et al., 2014; Fuchs et al., 2008; Ito et al., 2008). Therefore, we examined if the activity of neurons in the NAc displayed spatial selectivity within the cocaine self-administration chamber (**see Methods**). To assess spatial selectivity, we tracked the positional location of the mice from behavioral videos using DeepLabCut (Mathis et al., 2018) (**Figure 35 a,b**). The positional location was used to estimate spatial fields for each imaged neuron from a given mouse, which were then assessed for

significance (**see Methods**). In control mice, we found a relatively large percentage of neurons to

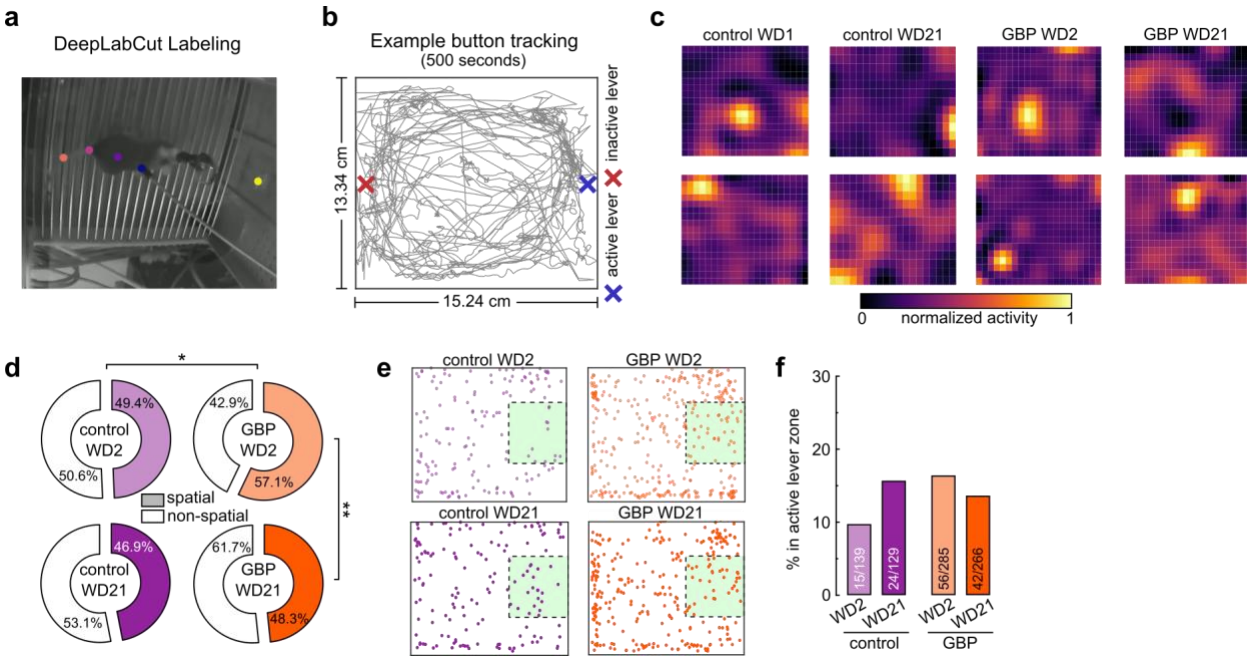

Figure 35. Spatial Coding in the NAc during Cocaine Seeking

(a) Example image of behavioral video labeled with DeepLabCut. Colored dots represent labeled body parts and lever position. **(b)** Example path tracking from a single mouse (500 sec of data) during cocaine seeking. Colored 'X' indicate the location of the active (blue) and inactive (red) levers in the chamber. **(c)** Example estimated spatial fields for single neurons determined to have significant spatial coding (**see Methods**) from control and GBP mice on withdrawal day 2 and 21. **(d)** Summary showing GBP treatment increased the percentage of neurons with significant spatial coding on withdrawal day 2, which then returned back to control levels on withdrawal day 21 (control WD2 = 49.4%, n = 154/312 neurons / 6 mice; control WD21 = 46.9%, n = 153/326 neurons / 6 mice; GBP WD2 = 57.1%, n = 341/597 neurons / 7 mice; GBP WD21 = 48.3%, n = 308/637 neurons/ 7 mice; $^{**}p < 0.01$, $^{*}p < 0.05$ Fisher's exact test). **(e)** Schematic showing peak activity locations of all significant spatial coding neurons are distributed throughout the self-administration chamber. Green square represents the area defined to be concentrated around the active lever. **(f)** Summary showing there is no change in the percentage of spatial coding neurons around the active lever (control WD1 = 9.74%, n = 15/154 neurons / 6 mice; control WD21 = 15.69%, n = 24/153 neurons / 6 mice; GBP WD1 = 16.42%, n = 56/341 neurons / 7 mice; GBP WD21 = 13.64%, n = 42/308 neurons / 7 mice).

display significant spatial selectivity (49.4%) during cocaine seeking on WD2, which did not change throughout withdrawal (**Figure 35 c,d**). Interestingly, we found there to be a significantly greater percentage of neurons with spatial selectivity (57.1%) in GBP treated mice on WD2, which subsequently decreased back to control levels later in withdrawal (**Figure 35 c,d**). As spatial encoding in the NAc is often biased towards reward locations (Lansink et al., 2008; Lansink et al., 2009), we also examined the peak location of spatial fields for all neurons displaying spatial selectivity. We found the peak location of spatial fields to be distributed throughout the operant chamber in both control and GBP mice in both early and late withdrawal (**Figure 35 e**). We also found no difference in the percentage of spatial neurons with spatial field concentrated around the active lever (**Figure 35 f**). Together, these findings demonstrate that neurons within the NAc encode spatial information, which is not altered during withdrawal. Furthermore, NAc neurons in GBP treated mice may display enhanced spatial coding during early withdrawal, which is not maintained at later time points.

We next examined neural activity associated with active lever pressing, the primary readout of cocaine seeking behavior in our paradigm. Neurons within the NAc displayed clear changes in activity time locked to active lever pressing (**Figure 36 a,b**), consistent with previous electrophysiology studies (Carelli and Ijames, 2000; Carelli et al., 2000; Ghitza et al., 2003; Hollander and Carelli, 2005, 2007). Neurons were classified as responsive if their peak activity in the 5s after active lever pressing was significantly greater than a baseline period 5s before active lever pressing (**see Methods**). In control mice, we found a relatively small percentage (16.22%) of neurons within the NAc were responsive to active lever pressing during early withdrawal (**Figure 36 c**), similar to what has been previously reported from electrophysiology studies (Carelli

and Ijames, 2000; Carelli et al., 2000; Hollander and Carelli, 2005, 2007). We found a relatively

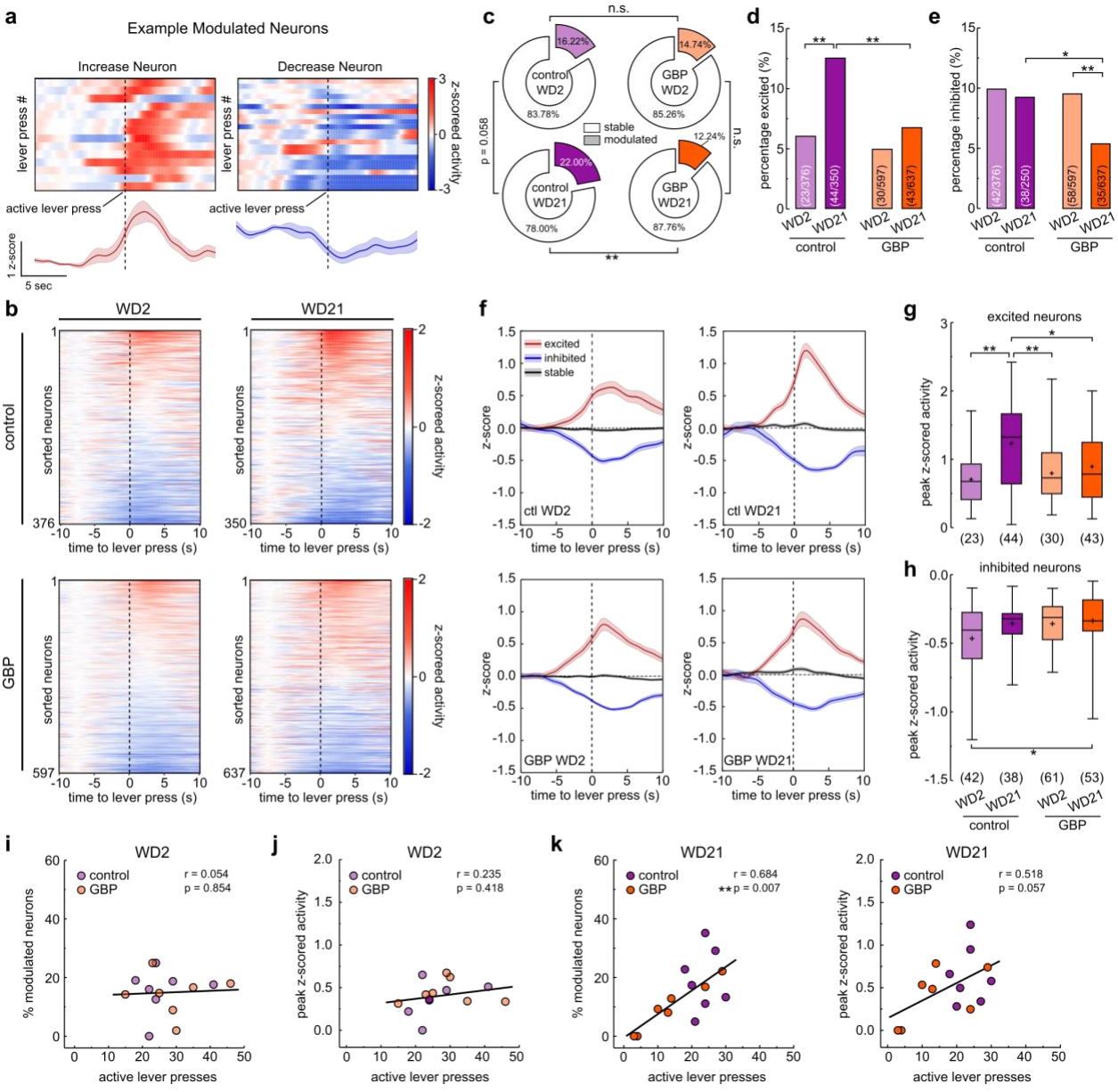

Figure 36. Blocking Cocaine-Induced Synaptogesis Prevents Increase in Excitatory Responses in Late Withdrawal

(a) Example neurons displaying significant phasic responses to active lever pressing. Heatmaps represent z-scored activity for each active lever press. Traces below represent the mean ± s.e.m. activity for all active lever press trials. **(b)** Heatmaps showing mean z-scored activity around active lever pressing for all imaged neurons for each group and withdrawal day. **(c)** Summary showing the percentage of significantly responsive neurons is greater in control mice compared to GBP mice on withdrawal day 21 (control WD1 = 16.27%, n = 61/376 neurons / 7 mice; control WD21

= 22.00%, n = 77/350 neurons / 7 mice; GBP WD1 = 14.74%, n = 88/597 neurons / 7 mice; GBP WD21 = 12.24%, n = 78/637 neurons / 7 mice; ** $p < 0.01$ Fisher's exact test). **(d)** Summary showing the percentage of significantly excited neurons increases in control mice during withdrawal, which does not occur when synaptogenesis is blocked (control WD1 = 6.1%, n = 23/376 neurons / 7 mice; control WD21= 12.6%, n = 44/350 / 7 mice; GBP WD1 = 5.0%, n = 30/597 neurons / 7 mice; GBP WD21 = 6.8%, n = 43/637 neurons / 7 mice; ** $p < 0$ .01 Fisher's exact test). **(e)** Summary showing the percentage of significantly inhibited neurons decreased during late withdrawal when synaptogenesis is blocked ((control WD1 = 10.1%, n = 42/376 neurons / 7 mice; control WD21= 9.4%, n = 38/350 / 7 mice; GBP WD1 = 9.7%, n = 58/597 neurons / 7 mice; GBP WD21 = 5.5%, n = 35/637 neurons / 7 mice; * $p < 0.05$, ** $p < 0$ .01 Fisher's exact test). **(f)** Mean ± s.e.m. activity traces of all excited (red), inhibited (blue), and stable (black) neurons for each group and withdrawal day. **(g)** Summary showing peak activity of excited neurons is increased during late withdrawal in control mice, which does not occur when synaptogenesis is blocked (control WD1 = 0.705±0.08, n = 23 neurons; control WD21 = 1.231±0.09, n = 44 neurons; GBP WD1 = 0.794 ± 0.08, n = 30 neurons; GBP WD21 = 0.892 ± 0.08; $F_{(1,136)} = 5.49$, $p = 0.0206$, two-way ANOVA, day x treatment interaction, *$p < 0.05$, **$p < 0.01$ Bonferroni post-test). **(h)** Summary showing peak activity of inhibited neurons is decreased during early withdrawal in control mice compared to during late withdrawal in GBP mice ((control WD1 = -0.465±0.05, n = 42 neurons; control WD21 = -0.355±0.03, n = 38 neurons; GBP WD1 = -0.356 ± 0.02, n = 361neurons; GBP WD21 = -0.335 ± 0.03; $F_{(1,160)} = 4.403$, $p = 0.0374$, two-way ANOVA, main effect of day, *$p < 0.05$ Bonferroni post-test). **(i-l)** Scatter plots of the percentage of responsive neurons **(i,k)** or peak activity of responsive neurons **(j,l)** versus number of active lever presses on withdrawal day 2 **(i,j)** and withdrawal day 21 **(k,l).** Percentage of responsive neurons was correlated with number of active lever presses on withdrawal day 21. Data are presented as mean ± s.e.m. Bar graphs show max to min (whiskers), 75th and 25th percentiles (boxes), median (line) and mean (+).

similar percentage (14.74%) of responsive neurons in GBP treated mice on WD2 compared to controls (**Figure 36 c**). Interestingly, we found that the percentage (22.00%) of responsive neurons in control mice trended towards an increase during late withdrawal (**Figure 36 c**). In contrast, no such increase was observed in GBP treated mice after late withdrawal and the percentage (12.24%)

of responsive neurons was significantly lower when compared to controls at this time point (**Figure 36 c**).

When we separated neurons based on their response type (excitation vs. inhibition), we found a significant increase in the percentage of neurons displaying excitations during withdrawal in control mice (WD2: 6.1%, WD21: 12.6%) (**Figure 36 d**). There was no change in the percentage of neurons displaying excitations during withdrawal in GBP treated mice (WD2: 5.0%, WD21: 6.8%) (**Figure 36 d**). Importantly, there was a significantly smaller percentage of excited neurons in the GBP treated mice during late withdrawal compared to the control mice at this time point (**Figure 36 d**). On the other hand, we found there was no change in the percentage of neurons displaying inhibitions during withdrawal in control mice (WD2: 10.1%, WD21: 9.4%) (**Figure 36 e**). In contrast, there was significant decrease in the percentage of inhibited neurons during withdrawal in GBP treated mice (WD2: 9.7%, WD21: 5.5%) (**Figure 36 e**). Furthermore, the percentage of inhibited neurons during late withdrawal in GBP treated mice was significantly smaller compared to control mice at this time point (**Figure 36 e**).

Beyond changes in the percentages of responsive neurons, we also found changes in the response magnitudes of neurons during withdrawal (**Figure 36 f**). Specifically, we found there to be a significant increase in the magnitude of excitations during late withdrawal in control mice (**Figure 36 g**). This increase was not observed in mice treated with GBP (**Figure 36 g**). Furthermore, the magnitude of excitations in GBP mice were significantly smaller when compared to control mice during late withdrawal (**Figure 36 g**). In contrast, we did not observe any changes in the magnitude of inhibitions during late withdrawal in either control mice or GBP treated mice (**Figure 36 h**). However, there was a significant decrease in the magnitude of inhibitions when comparing control mice during early withdrawal to GBP treated mice during late withdrawal

(**Figure 36 h**). Together, these results demonstrate that during withdrawal from cocaine self-administration there is an increase in the percentage and responsiveness of neurons excited by lever pressing with minimal changes in the inhibited neurons, and blocking cocaine-induced generation of synapses prevents this enhanced activation of NAc neurons while also reducing inhibitory responses.

The above results prompted us to examine the relationship between the responsiveness of NAc neurons and cocaine seeking behavior during early and late withdrawal. During early withdrawal, we found there to be no relationship between either the percentage of responsive neurons nor the neural response magnitude and cocaine seeking behavior (**Figure 36 i,j**). In contrast, during late withdrawal there was a significant correlation between the percentage of responsive neurons and cocaine seeking behavior (**Figure 36 k**). There was also a trend towards a correlation between the magnitude of neural responses and cocaine seeking behavior at this time point (**Figure 36 l**). These findings suggest that the neural activity within the NAc may regulate cocaine seeking behaviors during late withdrawal, while having less influence over seeking behaviors during early withdrawal.

4.5 Discussion

The development of cocaine seeking behaviors is associated with the emergence of phasic activity patterns within the NAc during acquisition and withdrawal, which are thought to contribute to the encoding of cocaine-associated memories and/or behavior (Carelli and Ijames, 2000; Ghitza et al., 2003; Hollander and Carelli, 2007; Peoples and West, 1996). However, the mechanisms that shape these neural dynamics remain unclear. Our current results provide evidence

that cocaine-induced synaptogenesis contributes to the enhanced neural representation of cocaine seeking behaviors within the NAc that emerges during withdrawal. To our knowledge, this is one of the first demonstrations of a causal link between synaptogenesis and changes in neural activity *in vivo*, and provide further evidence that cocaine-generated synapses may represent a discrete synaptic ensemble contributing to the encoding of cocaine-associated memories and behaviors.

4.5.1 Synaptic Contribution to Cocaine-Associated Neural Activity During Late Withdrawal

Previous *in vivo* electrophysiology studies in rats have found that neurons in the NAc display phasic changes in activity associated with cocaine seeking behaviors and that these phasic responses continue to evolve during prolonged withdrawal. Specifically, several studies have demonstrated that a greater percentage of NAc neurons are excited, and more strongly excited, by cocaine-associated behaviors and cues following an extended period of withdrawal from cocaine self-administration, which correlate with the enhanced seeking seen at this time (Guillem and Ahmed, 2018; Guillem et al., 2014; Hollander and Carelli, 2005, 2007). These findings suggest that more neurons are recruited into neural ensembles encoding cocaine-associated information during withdrawal.

Our results replicate these findings in mice, where we observed an increase in the percentage of neurons excited during lever pressing, as well as an increase in the magnitude of these excitations, after a period of prolonged withdrawal (**Figure 36**). In contrast, we found no change in the percentage or responsiveness of inhibited neurons. We subsequently found that blocking the generation of new silent synapses during cocaine self-administration prevented both the increased in the percentage of excited neurons as well as the magnitude of their excitatory

responses during prolonged withdrawal (**Figure 36**), indicating that the generation of new synapses contributes to the subsequent activation of neurons within the NAc during withdrawal. Interestingly, we also found a decrease in the percentage of neurons inhibited during lever pressing during late withdrawal when synaptogenesis was blocked. Given the primary effects of gabapentin on excitatory synapses, this effect may reflect changes in local disynaptic inhibition.

The selective influence of cocaine-generated synapses over neural activity during late withdrawal versus early withdrawal is consistent with the relatively delayed functional maturation of these synapses, which typically begins after approximately 7 days of withdrawal (Huang et al., 2009; Lee et al., 2013). Furthermore, this effect was not due to a general reduction in NAc activity, as blocking cocaine-induced synaptogenesis did not alter the basal and spontaneous activity of neurons within the NAc (**Figure 34**). In addition, we also found that blocking synaptogenesis during self-administration training selectively attenuated cocaine seeking behavior following withdrawal. Together, these findings suggest that the generation, and subsequent maturation, of new synapses leads to the recruitment of new neurons into cocaine-associated neural ensembles within the NAc during withdrawal, which ultimately contributes cocaine seeking behavior.

Activity within the NAc has been found to contribute to the encoding of information related to spatial information associated with rewards, in addition to that related to discrete cues as discussed above (Lansink et al., 2008; Lansink et al., 2009; Trouche et al., 2019). We also found that the activity of a relatively large percentage of neurons within the NAc displayed spatial selectivity during cocaine seeking during withdrawal (**Figure 35**). However, in contrast to activity associated with lever pressing, we did not observe any significant changes in this spatial encoding between early and late withdrawal. This contrasts to previous findings that that cocaine experience enhanced the encoding of spatial information related to cocaine-associated contexts (Sjulson et al.,

2018). However, this discrepancy is likely explained by the fact we have examined only periods during withdrawal, and suggests that changes in spatial encoding within the NAc may occur earlier during acquisition. In addition, we did not observe preferential spatial coding around the active lever, which one might expect given NAc neurons have previously been shown to encode spatial information relevant to reward locations (Lansink et al., 2008; Lansink et al., 2009). However, mice may form a spatial association with the entirety of the operant chamber with cocaine reward, resulting in diffuse spatial coding throughout the chamber as observed. This is consistent with a previous CPP study that found enhanced spatial encoding in the entire cocaine-paired chamber (Sjulson et al., 2018).

Interestingly, we found that blocking cocaine-induced synaptogenesis resulted in an increase in the percentage of neurons within the NAc displaying spatial selectivity during early withdrawal, which then returned back to normal levels during late withdrawal (**Figure 35**). This is difficult to reconcile with the fact that cocaine-generated synapses are initially silent during early withdrawal and then functionally mature during withdrawal, and thus it is unclear how blocking synaptogenesis leads to increased spatial coding within the NAc during early withdrawal. One explanation is through the blockage of $\alpha 2\delta$-1 receptors on presynaptic terminals by gabapentin, which may result in a temporary decrease in presynaptic P/Q-type voltage-gated calcium channel expression and changes in release probability (Hoppa et al., 2012) and then alter activity within the NAc. This possibility will need to be explored in future studies. Regardless, however, the lack of an effect of blocking cocaine-induced synaptogenesis on spatial coding during late withdrawal suggests that these synapses, at least in their functionally mature state, do not contribute substantially to the encoding of spatial information within the NAc. Together, with our previous findings, this suggests that cocaine-generated synapses within the NAc primarily contributes to the

encoding of cocaine-associated cues and/or behavior. This is consistent with previous findings demonstrating blocking cocaine-induced synaptogenesis does not affect cocaine seeking behavior in the absence of discrete cues (Wang et al., 2020).

4.5.2 Relationship with Previous Electrophysiology Studies

As discussed above, our results are largely consistent with previous electrophysiology studies conducted in rats that have found an increase in the responsiveness of NAc neurons to cocaine-associated cues and behavior during withdrawal (Guillem and Ahmed, 2018; Guillem et al., 2014; Hollander and Carelli, 2005, 2007). However, unlike these previous studies, we did not observe a concurrent increase in cocaine seeking behavior at this time compared to earlier withdrawal (**Figure 34**). This difference may be explained by the use of mice in the current study, which often display decreases in seeking during withdrawal (Terrier et al., 2016), and as such an increase in NAc activity may be necessary to maintain cocaine seeking levels specifically in mice. Alternatively, our results may suggest that an increase in NAc activity may also be important for the maintenance of cocaine seeking behavior more generally. Previous evidence indicates that the NAc is not critical for cocaine seeking before an extended period of withdrawal (Cornish et al., 1999; Ito et al., 2004; Rossi et al., 2020), and thus NAc activity may only regulate cocaine seeking behavior during later withdrawal. Our findings support this idea, where we found a correlation between NAc activity and cocaine seeking behavior only following prolonged withdrawal but not earlier (**Figure 36**). This scenario is somewhat reminiscent of systems consolidation that occurs for fear memory, where other brain areas, such as the mPFC, are recruited in order to maintain fear memories (DeNardo et al., 2019; Kitamura et al., 2017). However, this remains speculation and future studies will be needed to determine if such a process does indeed occur.

Previous electrophysiology studies have also found that increases in the responsiveness of neurons within the NAc to cocaine-associated cues and behavior occur primarily within the core subdivision rather than the shell (Hollander and Carelli, 2005, 2007). While our dataset likely consisted of neurons within both the core and shell subdivisions, the majority were within the NAc shell (**Figure 33**). It is possible our results may have been driven by neurons within the NAc core, however, we believe this is somewhat unlikely given mice with high percentages of responsive neurons had GRIN lenses localized solely within the NAc shell. Thus, our results suggest that neurons within the NAc shell may also increase their responsiveness to NAc cocaine-associated cues and stimuli. This finding is supported by other previous electrophysiology studies that have found robust cue encoding within the shell (Ghitza et al., 2003) and increases in responsive neurons throughout the NAc, including the shell, during withdrawal (Guillem and Ahmed, 2018). Differences in the recruitment of NAc shell neurons between these studies may be due to differences in behavioral paradigms. It is also possibly due to recordings made in different areas of the shell, such as the ventral shell (Hollander and Carelli, 2007) versus the more dorsal medial shell in the current study. This may be particularly relevant given the ventral shell may negatively regulate reward seeking behaviors while the dorsal shell promotes (Al-Hasani et al., 2015), however, this will need to be explored in greater detail.

4.5.3 Limitations and Additional Considerations

There are several limitations that should be considered when interpreting the current findings. First, the current findings rely on *in vivo* calcium imaging, which serves only as a proxy for neural activity and may preferentially reflect higher firing rates or burst firing. Given the relatively low firing rates typically observed in the NAc (Carelli et al., 2000; Carelli and

Wondolowski, 2003; Chang et al., 1994; Peoples and West, 1996; Roitman et al., 2005), calcium imaging likely under detects changes in activity, especially decreases in activity. Thus, our results may underrepresent the actual changes in excitatory and inhibitory responses within the NAc. Second, in the behavioral paradigm used in the current study the cocaine-associated cue is contingently presented with lever pressing action. As such, it is difficult to distinguish if neural responses associated with lever pressing are related to the encoding of information related to cocaine-associated cues or behavioral action. Our findings are consistent with previous studies examining cue presentations in isolation (Guillem and Ahmed, 2018; Hollander and Carelli, 2007), however, future studies will need to temporally dissociate cue presentations and behavioral actions with the use of discriminative stimulus self-administration protocols to more clearly determine if neural responses are encoding cocaine-associated cues or behavioral actions (Madangopal et al., 2019). Third, the data presented here do not track the same neurons across days, and thus do not capture how the activity of individual neurons may evolve during withdrawal.

4.5.4 Concluding Remarks

Cocaine experience generates new synapses within the NAc that subsequently functionally mature during withdrawal to contribute to cocaine seeking behavior. Our current findings demonstrate that cocaine-generated synapses contribute to activity patterns within the NAc associated with cocaine seeking, providing further evidence that synapses may represent a synaptic ensemble contributing to the encoding of cocaine-associated memories and/or behaviors.

5.0 General Discussion

The formation of maladaptive memories associated with drug use is a critical component in driving relapse after periods of abstinence. As such, there has been intense investigation to identify the neural substrates underlying drug-associated memory and the persistence of drug seeking behavior, with particular focus on drug-induced synaptic adaptations within the brain's reward circuity. However, most studies to date have been constrained to the interrogation of relatively broad and functionally heterogeneous neuronal and synaptic populations, such as entire cell-types or major afferent projections, that are broadly implicated in other behaviors. Therefore, it has been difficult to ascertain specific and discrete synaptic substrates underlying drug-associated memories and drug seeking behaviors. Through the work presented in this dissertation I have attempted to provide additional evidence for the existence of such a discrete synaptic population contributing to the encoding of cocaine-associated memories and behaviors.

Previous studies have identified a population of immature, AMPAR-silent synapses that are generated within the NAc by cocaine experience through synaptogenesis (Huang et al., 2009; Lee et al., 2013; Ma et al., 2014; Wang et al., 2020). These synapses functionally mature during subsequent withdrawal and contribute to cocaine seeking, positioning them as possible candidates for discrete synaptic substrates underlying cocaine-associated memories. I have further shown that changes in the functional state of these cocaine-generated synapses contribute to the natural dynamics of cocaine-associated memories, namely destabilization and reconsolidation (Chapter 2). Specifically, I demonstrated that the reactivation of cocaine-associated memories triggers a transient re-silencing of cocaine generated synapses within the NAc, followed by their functional re-maturation, which contributes to the reconsolidation of cocaine-associated memories and

subsequent cocaine seeking behavior. In addition, I have identified the small GTPase Rac1 as a molecular switch that regulates the stability of cocaine-generated synapses to control their functional state (Chapter 3). Specifically, I demonstrated that a decrease in Rac1 activity is necessary for the natural re-silencing of cocaine-generated synapses, while increased Rac1 activity serves to stabilized these synapses, irrespective of their current synaptic state (silent vs. mature). Lastly, I provide evidence that cocaine-generated synapses contribute to the neural activity dynamics within the NAc associated with the encoding of cocaine seeking behaviors during withdrawal (Chapter 4).

Together, this evidence supports the hypothesis that cocaine-generated synapses may represent a specific population of synapses, or a synaptic ensemble, that selectively encodes aspects of cocaine-associated memories and behaviors. In the following sections I will discuss how these findings may contribute to our understanding of the encoding of memories in general and in the specific context of addiction, as well as the limitations and shortcomings that should be considered in the interpretation of these results.

5.1 Discrete Synaptic Substrates Underlying Memory

Understanding the neural basis of memory has been one of the fundamental goals of neuroscience throughout the history of the field, and has been the subject of considerable research and debate. One of the most prominent theories posits that synaptic plasticity underlies memory, wherein memorable experiences trigger the remodeling of synaptic connections between neurons that allows for activity patterns representing the experience to be readily reactivated at a later time (Hebb, 1949; Magee and Grienberger, 2020). Given the vast amounts of information and

experiences typically stored in the adult brain, a natural extension of this theory is that memories are encoded by sparse populations, or ensembles, of synapses (Chklovskii et al., 2004; Josselyn et al., 2015; Poo et al., 2016; Rogerson et al., 2014). While there is now substantial evidence that synaptic plasticity contributes to learning and memory formation (LeGates et al., 2018; Ma et al., 2018; Nabavi et al., 2014; Penn et al., 2017; Rogan et al., 1997; Stuber et al., 2008; Takahashi et al., 2003; Tye et al., 2008; Whitlock et al., 2006), there has been little evidence that specific memories are indeed encoded in a sparse, discrete synaptic population, with most evidence coming from correlative studies tracking the generation and stabilization of synapses *in vivo* (Fu et al., 2012; Hofer et al., 2008; Holtmaat et al., 2006; Lai et al., 2012; Parkhurst et al., 2013; Xu et al., 2009; Yang et al., 2014; Yang et al., 2009). In recent years, however, a few studies have begun to provide more direct evidence for the existence of memory-specific synaptic ensembles. Perhaps the most striking evidence comes from a study that utilized a novel approach to label and eliminate/weaken synapses that were generated and potentiated during motor learning. Strikingly, selectively eliminating and weakening these synapses only impaired the associated motor skill, but not other similar motor tasks, demonstrating this select population of synapses encoded the learned motor skill (Hayashi-Takagi et al., 2015). A subsequent study provided additional evidence that different memories encoded in the same population of neurons are encoded in separable, discrete synapses on these neurons (Abdou et al., 2018), further demonstrating the existence of memory-specific synaptic ensembles, even in single neurons.

We believe the findings on cocaine-generated synapses presented in this dissertation, in conjunction with previous studies from our lab, provide additional evidence in supporting discrete synaptic ensembles as the synaptic substrates underlying memory. Firstly, given that cocaine-generated synapses are generated by the cocaine-associated experience itself (Huang et al., 2009;

Lee et al., 2013)(Chapters 2-4), they are highly likely to encode information specifically about cocaine. However, it is important to note that this has not been directly tested and should be the subject of future studies to confirm that these synapses do not contribute to other NAc-dependent memories. Secondly, impairing the functionality of these synapses through a variety of different methods (e.g. optical depotentiation, prevention of generation, Rac1-dependent silencing, etc.) attenuates cocaine seeking behavior (Lee et al., 2013; Ma et al., 2014; Ma et al., 2016; Wang et al., 2020)(Chapters 2-4), implying they contribute to the recall and/or expression of cocaine-associated memories. Thirdly, the changes in the functional state of cocaine-generated synapses regulates memory destabilization and reconsolidation (Chapters 2,3), indicating these synapses regulate the natural dynamics and state of cocaine-associated memories. Lastly, these synapses are important for the recruitment and activation of neurons within the NAc whose activity is associated with cocaine seeking during withdrawal (Chapter 4), suggesting cocaine-generated synapses contribute, at least in part, the encoding of cocaine-associated behaviors at the circuit level. Collectively, these findings argue that cocaine-generated synapses represent a discrete synaptic ensemble contributing to the encoding of cocaine-associated memories, adding to previous evidence for the existence of such discrete synaptic memory substrates. In addition, they also extend previous findings by emphasizing the importance of synaptogenesis in the encoding of memory.

Perhaps one of the most novel findings presented here is that the seemingly same population of synapses appears to regulate the recall, destabilization, and reconsolidation of a memory. This is perhaps an expected result. Yet, evidence demonstrating a discrete synaptic population regulates the dynamics of multiple memory states has been lacking. Previous studies have shown that memory destabilization is triggered by synaptic weakening in circuits that have

also been shown to undergo synaptic strengthening during learning (Doyère et al., 2007; Lopez et al., 2015; Rao-Ruiz et al., 2011; Shehata et al., 2018). However, the weakened synapses are not necessarily the same ones strengthened during learning that contribute to memory encoding. The results presented in Chapters 2 and 3 extend these previous findings and provide evidence that the same cocaine-generated synapses that contribute to cocaine seeking also undergo dynamic changes in their functional state to regulate memory destabilization and reconsolidation. Preliminary findings have also found that memory-specific synapses within the lateral amygdala undergo similar dynamic changes corresponding with the state of fear memories (Choi, 2020). These findings indicate that multiple states of a single memory are controlled by the same synaptic population and understanding the natural processes that govern the functionality of these synapses may provide insights into strategies for disrupting the encoding of maladaptive memories, such as those associated with addiction (discussed below).

It is important, however, to acknowledge that one of significant limitations of the work presented here is that as synapses were examined in *in vitro* preparations at different time points in separate animals, we cannot definitively conclude the synapses enriched with CP-AMPARs we observe after withdrawal are indeed the exact same ones generated during cocaine self-administration, even if our lab's findings fit with such a scenario. To overcome this limitation, future studies will need to be able to visualize individual synapses within the NAc *in vivo* and track them throughout self-administration training and withdrawal. This is particularly relevant given synaptic turnover is well documented in the cortex (Chen et al., 2015; Yang et al., 2014; Yang et al., 2009), and it will be important to determine if such turnover is prevalent within the NAc as well, as different brain regions display different turnover rates (Attardo et al., 2015). However, even if the CP-AMPAR-enriched synapses are not the same silent synapses generated during self-

administration, our findings still indicate the same population of synapses, in this case those enriched with CP-AMPARs, that encode cocaine seeking also regulate the destabilization and reconsolidation of cocaine-associated memories at this given point in time.

Another quite striking finding presented here is the emergence of a dissociation between cocaine-generated synapses and cocaine seeking behavior that emerges only after memory reactivation, where synapses are silent but seeking remains elevated (Chapter 3). Given that cocaine-generated synapses are critical for cocaine seeking prior to memory reactivation, but not after, we hypothesize that cocaine-generated synapses are key substrates for the storage and/or reactivation of cocaine-associated memories, however, once the memories are reactivated other mechanisms are engaged to maintain behavioral expression over a certain period of time. To our knowledge, this is one of the first demonstrations that separable neural substrates may underlie the reactivation and behavioral expression of a memory. However, we speculate this phenomenon may be generalizable to other types of memories, not just cocaine-associated, as it is documented that expression of fear memories remains elevated throughout memory destabilization despite the synaptic depotentiation mentioned earlier (Monfils et al., 2009; Rao-Ruiz et al., 2011). Furthermore, previous studies have demonstrated that memory reactivation and behavioral expression can be pharmacologically dissociated (Mamou et al., 2006), which may suggest dissociable neural substrates underlie these processes. From a behavioral viewpoint, such a mechanistic dissociation may be advantageous as it would allow for the memory-encoding substrates to be destabilized for modification to update memory content without sacrificing the ongoing behavioral output in that moment. Future studies will be needed to determine if separable neural substrates do indeed underlie memory reactivation versus behavioral expression, or if other processes explain our current findings. To aid in this determination, these studies will also need to

determine what other mechanisms are engaged by memory reactivation that drive the continued behavioral expression of cocaine-associated memories as has been discussed elsewhere in this dissertation (see Chapter 3 Discussion and Appendix B).

While the findings presented here provide some insights into the synaptic encoding of memory, there remain many important unanswered questions. One of the outstanding questions within the field is how synapses generated and/or potentiated during learning are selected for stabilization during consolidation. *In vivo* imaging studies have demonstrated that only a portion of synapses generated during learning are stabilized and retained long term (Chen et al., 2015; Li et al., 2017; Peters et al., 2014; Yang et al., 2014; Yang et al., 2009). Thus, mechanisms must exist that allow for the selection of useful synapses for stabilization. One widely held theory that has emerged in part from studies during early development is that only those synapses that are frequently activated, and thus likely the most useful, are selected for maturation and are integrated within the circuity (Cohen-Cory, 2002; Holtmaat and Caroni, 2016; Katz and Shatz, 1996; Stephan et al., 2012; Waites et al., 2005). In this scenario, synapse generation has a degree of randomness to create sufficient connection opportunities, while maturation refines and specifies the connections that are useful. Thus, understanding this step is critical to fully understand the synaptic encoding of memories. This may be particularly important in the context of addiction, where a dysfunctional selection process may lead to aberrant information encoding that contributes to the persistence of maladaptive behavior (see below).

Memories are typically consolidated in the absence of direct exposure to the related experience (Dudai, 2004, 2012; Dudai et al., 2015; Klinzing et al., 2019), which begs the question what activities may drive synaptic maturation and stabilization during periods of such quiescence? One possibility is the replay of patterned neural activity within the circuits that represent an

experience. In the hippocampus, it is well documented that neural ensembles are activated during learning are often reactivated and replay their temporal dynamics at later times (Ólafsdóttir et al., 2018), and that this replay contributes to long-term memory consolidation (Girardeau et al., 2009; Jadhav et al., 2012). Such replays may provide essential activity signals to select the most useful synapses for maturation. In line with this viewpoint, it has been shown in the cortex that neural reactivation is associated with the stabilization of nascent synapses (Cichon and Gan, 2015), and the reactivation of a neural ensemble strengthens the functional connectivity between neurons within the ensemble (Sugden et al., 2020). However, these studies still fail to directly link activity replay to synaptic stabilization.

In the context of addiction, neural ensembles within the NAc related to the encoding of rewarding experiences display reactivation dynamics during periods of quiescence (Lansink et al., 2008; Pennartz et al., 2004). This suggests that replay mechanisms exist within reward circuits, and may contribute to the maturation of cocaine-generated synapses during withdrawal, and should be examined in future studies. However, there are some hints that synaptic selection mechanisms may go awry following cocaine experience. For example, there is quite a robust and persistent increase in the density of synapses (Dumitriu et al., 2012; Robinson et al., 2001; Robinson and Kolb, 1997, 1999), which is driven by synaptogenesis (Wang et al., 2020). Such persistent increases in spine density are typically not seen under normal learning conditions (Chen et al., 2015; Peters et al., 2014; Yang et al., 2009), which suggests there may be a deficit in the selection of which synapses will be eliminated. One scenario is that most, if not all, synapses generated by cocaine experience subsequently mature and stabilize during withdrawal, possibly driven by dysregulated homeostatic plasticity processes driving the upregulation of CP-AMPARs (Wang et al., 2018). It is unclear how aberrant synaptic selection affects the encoding of drug-associated

memories within the NAc, but could possibly contribute to their maladaptive features. As such, it may be fruitful for future studies to examine synaptic selection is indeed altered following cocaine self-administration and what mechanisms may underlie it.

5.2 Molecular Mechanisms Regulating Synaptic and Memory State

In essence, memory is the storage of information, which can later be accessed and utilized. In order for information to be maintained over time, there must be a persistence of the substrates or states representing this information. The maintenance of such states is extremely challenging in dynamic systems, such as the nervous system where neural activity rapidly evolves and biological materials (e.g. proteins) constantly turn over. Such volatility can drive drift or decay of the state overtime. Therefore, mechanisms must exist that resist these forces and maintain the representation of the information. Such processes can be conceptualized as having attractor-like dynamics, where forces naturally drive a system to a set point or state and resist any deviations away from it. Attractor dynamics have long been hypothesized to underlie memories (Chaudhuri and Fiete, 2016; Hopfield and Tank, 1986; Knierim and Zhang, 2012; Marr, 1971), and indeed there is growing evidence that activity within neural circuits display attractor-like dynamics that may contribute to memory (Carrillo-Reid et al., 2008; Chaudhuri et al., 2019; Domnisoru et al., 2013; Finkelstein et al., 2021; Inagaki et al., 2019; Pennartz et al., 1994; Wills et al., 2005; Wimmer et al., 2014; Yoon et al., 2013; Zagha et al., 2015). Theoretically, synapses may also display attractor-like dynamics whereby active molecular signaling drive processes (e.g. receptor trafficking) to maintain a set synaptic state, ultimately serving to stabilize the synapse and its information content.

There are several ways through which attractor-like dynamics may be achieved at the synapses, the most notable one however is through positive feedback mechanisms (Chaudhuri and Fiete, 2016). Identifying such positive feedback mechanisms has been at the center of attempts to identify 'memory molecules', whose activity is self-sustaining in order to overcome molecular turnover. An early proposal for such a 'memory molecule' was that of a phosphorylation-dependent kinase that was capable of autophosphorylation (Lisman, 1985). A major synaptic protein that possesses these traits is CaMKII, which plays an important role in learning and memory (for review see (Lisman et al., 2012). CaMKII is thought to have two general modes of function; stimulated activity that is dependent on calcium and calmodulin signals, and autonomous activity that is dependent on autophosphorylation. It has been clearly established that stimulated CaMKII activity is critical for the induction of functional and structural LTP, as well as learning (Buard et al., 2010; Hayashi et al., 2000; Lee et al., 2009; Malinow et al., 1989; Murakoshi et al., 2017; Poncer et al., 2002), while there is some evidence suggesting that autonomous activity is involved in the maintenance of synaptic potentiation and memory retention (Rossetti et al., 2017; Sanhueza et al., 2011). This has led to the hypothesis that following learning, CaMKII sustains a level of activity within the synapse via autophosphorylation, which is critical for the maintenance of the memory encoding. This hypothesis has been cast in doubt though, with a recent study demonstrating that CaMKII autophosphorylation is not necessary for the maintenance of LTP, but rather contributes to the integration of calcium signals (Chang et al., 2017).

Autophosphorylation, however, is not the only positive feedback mechanism that allows for sustained molecular signals. Mutual activation between two molecules also allows for the formation of a positive feedback loop, where each molecule sustains the activity of the other. Interestingly, CaMKII has recently been found to participate in such a positive feedback loop with

Tiam1, a Rac1-GEF (Saneyoshi et al., 2019). Specifically, following LTP induction, Tiam1 directly binds to the autophosphorylation site of CaMKII, resulting in the constitutive activation of CaMKII, which in turn phosphorylates and activates Tiam1, producing a self-sustaining signaling complex. Furthermore, Tiam1-dependent activation of its downstream effector, Rac1, was necessary for the maintenance of structural LTP (Saneyoshi et al., 2019). This self-sustaining activity signal that serves to stabilize synaptic state is consistent with the notion of attractor-like dynamics at the level of the synapse.

The findings described above are of particular interest in light of the findings presented in Chapter 3, where we found Rac1 acted as a molecular switch to regulate the stability of cocaine-generated synapses. Specifically, we found that inhibiting Rac1 activity triggered the re-silencing of cocaine-generated synapses, while increasing its activity prevented the natural re-silencing of these synapses induced by memory reactivation. This is consistent with a scenario where persistent Rac1 activity serves to stabilize synaptic state and prevents any deviations away. This is further supported by our findings that increasing Rac1 activity is also capable of stabilizing synapses in a silenced state, which suggests that Rac1 activity is indeed a stabilizing force, regardless of current synaptic state, rather than simply driving synaptic potentiation that may counteract synaptic weakening. To our knowledge, this is one of the first demonstrations of a postsynaptic signaling pathway that performs such a function, and highlight a novel role for Rac1 as a synaptic stabilizer.

While our findings indicate Rac1 is indeed a synaptic stabilizer there are several points that need consideration and warrant future investigation. First, our demonstration that Rac1 activity is capable of stabilizing silent synapses was limited to the period of memory reconsolidation. Thus, it still remains to be determined if Rac1 is capable of stabilizing against more powerful events, such as interference from new learning. However, previous findings that increasing Rac1 activity

prevents the acquisition of cocaine CPP and associated plasticity suggest capability (Dietz et al., 2012b), although this needs to be more thoroughly tested.

In our current study, we have not determined the upstream signals triggering the natural decrease in Rac1 activity following memory reactivation. As discussed above, one mechanism that may lead to persistent Rac1 activity is the sustained activation of the CaMKII-Tiam1 positive feedback loop (Saneyoshi et al., 2019). It is unclear how such a mechanism may be disengaged by external stimuli (e.g. memory reactivation). However, one mechanism may involve the competitive binding of an alternate binding partner to the autophosphorylation site of CaMKII, which may occlude Tiam1 binding. Interestingly, it has previously been demonstrated that CaMKII directly binds with GluN2B-containing NMDARs at the autophosphorylation site (Bayer et al., 2001), and this binding is dependent on NMDAR activation (Bayer et al., 2006; Thalhammer et al., 2006). Therefore, during memory reactivation GluN2B-containing NMDARs may be activated and trigger an increase with CaMKII binding that produces a decrease in Tiam1 phosphorylation and ultimately Rac1 activity. This is supported by previous studies demonstrating a critical role of NMDARs, and specifically GluN2B-containing NMDARs, in memory destabilization following memory reactivation (Mamou et al., 2006; Milton et al., 2013). However, the role of CaMKII and NMDARs activation needs to be directly tested. This is particularly important as Rac1 activity is also regulated by other signaling pathways, such as BDNF and PKC (Harward et al., 2016; Hedrick et al., 2016; Tu et al., 2020), which have been implicated in cocaine-associated memories (Famous et al., 2008; Graham et al., 2007; Grimm et al., 2003; Li et al., 2013a; McCutcheon et al., 2011a; Ortinski et al., 2015; Schmidt et al., 2013).

Lastly, the synapse-specific effects we observed, specifically that decreasing Rac1 selectively triggered the re-silencing of cocaine-generated synapses, but not others, needs to be

considered to fully understand the functional role of Rac1. If Rac1 is indeed critical in the stabilization of synaptic state, it might be expected that decreasing Rac1 activity should affect synapses more uniformly than we observed. However, there may be redundancy in the mechanisms that regulate synaptic stability, such that disrupting one in isolation (e.g. Rac1) may not result in synaptic destabilization. If this is the case, then our results may indicate that other synaptic stabilization mechanisms are impaired or absent at cocaine-generated synapses. For example, most proteins that are thought regulate the stabilization of AMPARs in the synapse interact primarily with the GluA2 subunit, which is absent from CP-AMPARs (Derkach et al., 2007; Diering and Huganir, 2018). As cocaine-generated synapses are highly enriched in CP-AMPARs, these other stabilization mechanisms that depend on GluA2 subunit may be absent and unable to compensate for decreases in Rac1. It is also possible that additional signaling pathways must also be engaged to trigger synaptic destabilization under normal conditions, which may not be necessary in cocaine-generated synapses due to the altered properties of this synapse (see Chapter 3 Discussion for previous discussion of this topic). Alternatively, decreasing Rac1 may have indeed destabilized synapses more uniformly in the current study, but signals/forces driving changes in synaptic state were absent, and thus most synapses remained unaltered. In contrast, altered properties of cocaine-generated synapses (e.g. enhanced AMPAR recycling and actin cycling) may naturally drive synaptic changes and Rac1 activity normally stabilizes against this. Understanding the true mechanisms underlying the synapse specific effects we observed in the current study will help clarify the precise function of Rac1 in synaptic stabilization while also potentially revealing additional mechanisms critical for this process.

5.3 Implications for Memory Encoding at the Circuit Level

Within the brain, information is ultimately represented in the activity patterns of neural circuits, and as such learning must modify neural activity dynamics. There has been extensive work in delineating how memories are encoded in neural activity patterns and how such patterns emerge during learning (Ahmed et al., 2020; Gonzalez et al., 2019; Grewe et al., 2017; Inagaki et al., 2019; Park et al., 2021; Peters et al., 2014; Reinert et al., 2021; Zhou et al., 2020). However, there has been little investigation into the underlying cellular processes that drive the remodeling of activity dynamics during learning. Synaptic plasticity has long been hypothesized to underlie learning and memory by shaping the coordinated activity neural ensembles (Hebb, 1949), yet this fundamental theory has not been thoroughly tested directly, as most studies have relied on broad pharmacological inhibition of ion channels in the context of place cell activity (Bittner et al., 2017; Kentros et al., 1998; Nakazawa et al., 2002), whose role in memory encoding remains uncertain (Goode et al., 2020; Tanaka et al., 2018) (but see (Robinson et al., 2020)). This is particularly true for the potential role of synaptogenesis, which may be particularly important for the generation of novel activity patterns given circuit dynamics are constrained by neural connectivity (McKenzie et al., 2021; Oby et al., 2019; Sadtler et al., 2014).

In Chapter 4 we sought to directly assess the role of synaptogenesis on the neural encoding of cocaine seeking behaviors within the NAc. We found that during cocaine seeking, there was a relatively small percentage of neurons that displayed phasic activity associated with seeking behavior. This was consistent with previous electrophysiology studies (Carelli et al., 2000; Ghitza et al., 2003; Hollander and Carelli, 2007) as well as with the general theory that memories and behaviors are encoded in sparse neural ensembles, or so called engram cells (discussed below) (Josselyn and Tonegawa, 2020). Furthermore, we found that during withdrawal the percentage of

neurons with phasic activity increased, suggesting the additional recruitment of neurons into the cocaine-associated ensemble. Critically, we found that blocking cocaine-induced synaptogenesis prevented this additional recruitment of NAc neurons, indicating that the formation of new synaptic connections may play an important role in the formation of functional neural ensembles. This finding is consistent with previous studies utilizing IEG-based strategies to statically label engram cells where it has been found that engram cells display significant increases in both the number and efficacy of synapses, which is important for the reactivation of cells during recall (Choi et al., 2018; Kitamura et al., 2017; Roy et al., 2017b; Ryan et al., 2015; Zhou et al., 2019). Taken together, these findings suggest that the formation of new connections between neurons is a key mechanistic step in forming and maintaining functional neural ensembles that may encode specific behaviors or memories.

One inconsistency, however, with our findings and the engram cell theory is that we have consistently found cocaine-generated synapses in a majority of neurons recorded from *in vitro* (Brown et al., 2011a; Huang et al., 2009; Lee et al., 2013; Ma et al., 2014; Neumann et al., 2016b) (Chapter 2-4). If cocaine-generated synapses are key to the formation of neural ensembles, it might be expected for them to be generated selectively within these neurons. There is some evidence that cocaine-generated synapses are enriched in engram cells. Previous studies, using an IEG-based labeling strategy, found silent synapses preferentially in labeled engram cells within the NAc following cocaine experience (Koya et al., 2012; Whitaker et al., 2016). Initially, these silent synapses were interpreted as being different than those reported by our lab as they lacked GluN2B-containing NMDARs and were observed 10-14 days after cocaine exposure. However, when interpreting these studies it is important to consider key design elements of these experiments, namely that to label the engram cells animals underwent memory reactivation before recordings

were made 90min later (Koya et al., 2012; Whitaker et al., 2016). Given our findings presented in Chapter 2 and 3, it is very likely that the silent synapses detected in these studies are cocaine-generated synapses that had matured during the 10-14 days of withdrawal, but were then re-silenced following memory reactivation. This interpretation could indicate that cocaine-generated synapses are preferentially generated in engram cells. However, our studies have still reported a significantly higher prevalence of cocaine-induced synaptogenesis than was reported in those studies. This could be due to several factors. First, these previous studies used non-contingent cocaine exposure, and thus may not recruit as many neurons in the NAc versus self-administration. This explanation, however, seems insufficient to explain the degree of differences observed between the two lines of research. Second, as the silent synapses observed were likely ones re-silenced by memory reactivation, cocaine experience may have generated synapses in other neurons, but if those neurons weren't reactivated strongly enough then the synapses may not have been re-silenced and thus detected.

The scenario described above could be interpreted in two ways; 1) cocaine-generated synapses are wide spread and not specific for cocaine encoding neurons, or 2) the population of cocaine encoding neurons is significantly larger than implicated by IEG-based labeling studies. Several lines of evidence lend their support to the second interpretation. First, the use of IEG-based methods significantly limits labeling to very strongly activated neurons that are undergoing plasticity and transcriptional modification (Kovács, 2008). In addition to this, most studies utilize only one IEG, but there are several activity-dependent IEGs that have been shown to be induced in separate neural ensembles that all contribute to a memory (Sun et al., 2020b) As such, neurons labeled with these methods do not accurately reflect the neurons activated during an event, especially under conditions, such as recall, when significant plasticity may not be occurring. This

is supported by significant incongruities between IEG-based labeling methods and studies that directly record neural activity in vivo during a variety of memory-based tasks (Ahmed et al., 2020; Cruz et al., 2014; Grewe et al., 2017; Hollander and Carelli, 2007; Koya et al., 2009; Liu et al., 2012; Ramirez et al., 2015; Sjulson et al., 2018). Thus, methods using IEG-dependent labeling likely fail to fully capture memory encoding ensembles.

Secondly, a key tenet of the engram cell theory, is that the same, sparse neural ensemble is stable across time in order to encode the memory (Josselyn et al., 2015; Josselyn and Tonegawa, 2020). However, there is substantial evidence from *in vivo* recording studies that the activity of individual neurons is unstable over days, with information only being reliably represented at the level of the population, if at all (Attardo et al., 2018; Deitch, 2020; Driscoll et al., 2017; Gonzalez et al., 2019; Grewe et al., 2017; Hainmueller and Bartos, 2018; Huber et al., 2012; Levy et al., 2021; Liberti et al., 2016; Montijn et al., 2016; Rule et al., 2019; Schoonover et al., 2021; Sweis et al., 2021; Ziv et al., 2013). In addition, recent studies have also suggested that information is represented broadly across a neural population, rather than in a select few neurons (Kyriazi et al., 2020; Stefanini et al., 2020). Together, these findings challenge the theory that memories are encoded in a sparse and stable ensemble of engram cells, and rather suggest the activity of larger, more dynamic neural populations may underlie memory encoding. Indeed, there is growing support for the later scenario, where the activity of large neural ensembles can be conceptualized as neural representational spaces, where the dynamics within this space underlies cognitive processes, including memory (Barack and Krakauer, 2021; Vyas et al., 2020). One observation from IEG-based studies that may be seemingly hard to reconcile with is the demonstration that inhibiting or activating sparse engram cells is capable of suppressing or promoting memory recall, respectively (Cruz et al., 2014; Kitamura et al., 2017; Koya et al., 2009; Liu et al., 2012; Ramirez

et al., 2013; Ramirez et al., 2015). These findings, however, can be explained if IEG-labeled neurons represent ‘hub’ neurons, whose activity may regulate larger ensembles through processes such as pattern completion, a scenario supported by several recent studies (Carrillo-Reid et al., 2019; Carrillo-Reid et al., 2016; Daie et al., 2021; Marshel et al., 2019; Peron et al., 2020).

If memories are indeed encoded in more distributed and dynamic neural ensembles, it remains unclear what synaptic mechanisms would underlie it. It is reasonable to suspect more wide spread synaptic remodeling may contribute to shaping the neural representational space, as well as the dynamics within this space, of such a population. The distributed of generation synapses by cocaine experience would be consistent with such a model. It is difficult to determine from our data if cocaine-generated synapses may support broader population dynamics contributing to cocaine-associated behaviors. This is due to the limited scope of our analyses, which focused primarily on activity at the moment of lever pressing. However, cocaine seeking behavior is complex and does not reduce down simply to the action, with other ongoing cognitive process that influence seeking behavior (e.g. decision making) likely occurring throughout other times during a behavioral session. Furthermore, we have not tracked neurons across days, and thus we cannot know if the neurons with cocaine-associated activity are stable across time. It will be important for future studies to assess how cocaine-generated synapses may contribute to behaviorally relevant neural activity in the NAc more broadly to fully determine how these synapses contribute to the encoding of cocaine-associated behaviors.

5.4 Implications for the Treatment of Addiction

Drug addiction is an acquired behavioral state that develops progressively through repeated drug experience, and this behavioral state is perpetuated by persistent drug cravings that drive the relapse of drug use. Cravings and relapse are often precipitated by the reactivation of memories associated with drug use, and as such drug addiction is often conceptualized as a pathological form of memory that drives maladaptive behavior. Therefore, targeting the neural substrates that encode drug-associated memories, as well as the mechanisms that regulate these substrates, may allow for the successful treatment of addiction. The findings presented in this dissertation have provided some insights into the neural underpinnings of cocaine-associated memories and behaviors that may inform the development of therapeutic strategies for the treatment of addiction.

The findings throughout this dissertation provide additional evidence that cocaine-generated synapses may represent a selective substrate that encodes aspects of cocaine-associated memories (see earlier discussions). The identification of a discrete synaptic population that contributes to cocaine seeking behavior may allow for much more precise therapeutic targeting of cocaine-associated memories, which may mitigate addiction-related behaviors with minimal side effects. While selectively targeting a discrete population of synapses in human patients still possesses significant challenges, our findings have highlighted some unique features of cocaine-generated synapses that may aid in selectively targeting them. Most notably, the findings presented in Chapter 3 demonstrated that inhibition of Rac1 activity preferentially re-silenced cocaine-generated synapses and suppressed cocaine seeking behavior, suggesting that targeting Rac1 activity may be a viable strategy to selectively target cocaine-associated memories. However, future studies will need to more fully understand the mechanisms underlying this apparent selectivity to determine if this is indeed a viable strategy (see earlier discussion). These studies

will also need to be accompanied by the development of selective pharmacological Rac1 inhibitors and activators, as current Rac1 inhibitors (e.g. NSC23766) have wide spread off target effects (e.g. direct NMDAR and mAChR inhibition), in order to safely target Rac1 in human patients (Hou et al., 2014; Levay et al., 2013).

Previous studies have attempted to utilize the natural destabilization of memories following reactivation in order to disrupt maladaptive memories. Preclinical studies in rodents have implemented both the use of pharmacological methods to disrupt reconsolidation as well as behavioral strategies, such as extinction or counter conditioning, that may allow for the updating of the memory (Goltseker et al., 2017; Haubrich et al., 2015; Luo et al., 2015; Monfils et al., 2009; Otis et al., 2013; Quirk et al., 2010; Rich et al., 2016; Sanchez et al., 2010; Sartor and Aston-Jones, 2014; Xue et al., 2012). These approaches, particularly behavioral strategies, have shown some promise in human patients, but they are still not fully effective (Jobes et al., 2015; Lonergan et al., 2016; Schiller et al., 2010; Sevenster et al., 2012, 2013; Xue et al., 2012). Understanding the precise neural mechanisms that regulate memory destabilization and reconsolidation may improve the efficacy of memory destabilization strategies.

In this dissertation, we demonstrate that the destabilization and reconsolidation of cocaine-associated memories is, at least in part, driven by the dynamic re-silencing and re-maturation of cocaine-generated synapses. Directly targeting the cellular mechanisms driving synaptic re-maturation (e.g. CP-AMPAR exocytosis) may improve the disruption of cocaine-associated memories following their retrieval-induced destabilization. Alternatively, directly targeting the cellular mechanisms triggering re-silencing (e.g. Rac1) may enhance, or even prolong, memory destabilization and may improve the efficacy of behavioral interventions. Our findings also suggest the potential efficacy of alternative strategies. For example, re-silencing cocaine-generated

synapses may render them more susceptible to modification (Ma et al., 2016), therefore, methods that may trigger synaptic plasticity paired with memory destabilization may degrade the synaptic encoding of cocaine-associated memories. Theoretically this could potentially be achieved through deep-brain stimulation (DBS) or repetitive transcranial magnetic stimulation (rTMS), which can alter neural activity in human patients (Ashkan et al., 2017; Chervyakov et al., 2015). While the mechanisms underlying effects of DBS and rTMS are uncertain (Ashkan et al., 2017; Chervyakov et al., 2015), both methods can be tuned to induce synaptic plasticity under the appropriate conditions (Creed et al., 2015; Soundara Rajan et al., 2017). These methods have shown some promise in human patients to date, however, results have been inconsistent (Gorelick et al., 2014; Müller et al., 2013). The clinical efficacy of these methods may be improved if paired with conditions that may favor synaptic remodeling, such as following memory reactivation, and warrant future investigation.

While our findings provide some insights into potential therapeutic strategies for addiction, there remain many areas that require further clarification and investigation. As discussed earlier (see Chapter 2 Discussion), all of our studies have been conducted under relatively limited training conditions, which may not adequately model the extensive exposure and re-exposure that occurs in humans with years of drug taking (Taylor et al., 2008). Extensive training and robust memories may limit memory destabilization of memories when reactivated, at least transiently (Wang et al., 2009), although it is unclear if this occurs for cocaine-associated memories. If such boundary conditions do develop, it will be important to determine the underlying mechanisms as this will greatly influence the appropriate therapeutic strategy necessary. For example, failure of memories to destabilize after extensive experience may be due to a lack of engagement of cellular processes triggering memory destabilization (e.g. synaptic re-silencing), or it could indicate that the memory

representation may have changed and no longer dependent on the same neural substrates. Indeed, there is already some evidence that the underlying substrates encoding cocaine-associated memories and behaviors may evolve over time. Specifically, studies have shown that extensive cocaine experience can lead to the transition of 'habit-like' compulsive behaviors, which are encoded in the dorsal striatum (for reviews see (Everitt and Robbins, 2005, 2013, 2016; Lüscher et al., 2020). Furthermore, as discussed earlier, the NAc may be preferentially involved in the encoding of cocaine seeking behaviors after some period of withdrawal, which may indicate some sort of systems consolidation, as occurs for hippocampal-dependent and fear memories. It is possible that if the substrates underlying cocaine-associated memories do evolve over time, different therapeutic strategies may be effective only at specific times. Thus, understanding these potential changes of the neural representation of cocaine-associated memories will help inform what therapeutic strategies may be effective depending on the patient's drug use and abstinence history.

5.5 Conclusions

In summary, this dissertation has provided insights into the synaptic mechanism underlying cocaine-associated memories and behaviors. Specifically, we have further highlighted a critical role of cocaine-generated synapses by demonstrating the function of these synapses in regulating cocaine-associated memory dynamics as well as their contributions in shaping neural activity associated with cocaine seeking behaviors. These findings lend support to the hypothesis that cocaine-generated synapses represent discrete synaptic substrates encoding aspects of cocaine-associated memories and behaviors. Despite the advances these findings make, they also highlight

the significant gaps remaining in our understanding of how cocaine-associated memories are encoded and expressed, both at the cellular and systems levels, which will need to be further explored in future studies.

Appendix A A Feedforward Inhibitory Circuit Mediated by CB1-Expressing Fast-Spiking Interneurons in the Nucleus Accumbens

This Chapter is adapted from the published manuscript:

Wright, W.J., Schlüter, O.M., & Dong, Y., (2017) A feedforward inhibitory circuit mediated by CB1-expressing fast-spiking interneurons in the nucleus accumbens. ***Neuropsychopharmacology***, 42(5); 1146-1156.

Appendix A.1 Overview

The nucleus accumbens (NAc) gates motivated behaviors through the functional output of principle medium spiny neurons (MSNs), while dysfunctional output of NAc MSNs contributes to a variety of psychiatric disorders. Fast-spiking interneurons (FSIs) are sparsely distributed throughout the NAc, forming local feedforward inhibitory circuits. It remains elusive how FSI-based feedforward circuits regulate the output of NAc MSNs. Here, we investigated a distinct subpopulation of NAc FSIs that express the cannabinoid receptor type-1 (CB1). Using a combination of paired electrophysiological recording and pharmacological approaches, we characterized and compared feedforward inhibition of NAc MSNs from CB1+ FSIs and lateral inhibition from recurrent MSN collaterals. We observed that $CB1^+$ FSIs exerted robust inhibitory control over a large percentage of nearby MSNs, in contrast to local MSN collaterals, which provided only sparse and weak inhibitory input to their neighboring MSNs. Furthermore, $CB1^+$ FSI-mediated feedforward inhibition was preferentially suppressed by endocannabinoid (eCB) signaling, while MSN-mediated lateral inhibition was unaffected. Lastly, we demonstrated that

$CB1^+$ FSI synapses onto MSNs are capable of undergoing experience-dependent long-term depression in a voltage- and eCB-dependent. These findings demonstrated that $CB1^+$ FSIs are a major source of local inhibitory control of MSNs and a critical component of the feedforward inhibition circuitry regulating the output of the NAc.

Appendix A.2 Introduction

The nucleus accumbens (NAc) has been conceptualized as a limbic-motor interface gating motivated behaviors, while deviated functional output of the NAc contributes to a variety of psychiatric states, including addiction and depression (Hyman et al., 2006b; Mogenson et al., 1980; Nestler et al., 2002; Wise, 1987). The functional output of the NAc is mediated by medium spiny neurons (MSNs), whose activation is driven by the integration of excitatory inputs (Brog et al., 1993; Meredith et al., 1992; Wilson and Kawaguchi, 1996). An essential component regulating the activation and output of MSNs are local feedforward inhibitory circuits. In the dorsal striatum, the output of MSNs is grossly regulated by fast-spiking interneurons (FSIs) (Koos and Tepper, 1999; Tepper et al., 2008). Although greatly outnumbered by MSNs, FSIs are distributed throughout the ventral and dorsal striatum, with each FSI innervating hundreds of MSNs (Luk and Sadikot, 2001; Tepper et al., 2008). These FSIs provide tonic inhibition as well as timing-dependent feedforward inhibition to MSNs upon excitation (Koos and Tepper, 1999; Mallet et al., 2005). The function of FSIs has primarily been characterized in the dorsal striatum. While sharing many features, the NAc also exhibits distinct circuitry differences with the dorsal striatum (Kupchik et al., 2015; Zhou et al., 2003). It remains elusive how FSI-mediated feedforward circuits function in the NAc to orchestrate the output of MSNs.

We recently identified a subpopulation of neurons in the NAc that uniquely express the cannabinoid receptor type-1 (CB1) (Winters et al., 2012). Unlike the dorsal striatum, CB1-expressing ($CB1^+$) neurons in the NAc are exclusively FSIs, with indistinguishable biophysical properties from parvalbumin (PV)-expressing FSIs (Winters et al., 2012). However, these $CB1^+$ FSIs represent a unique subpopulation of FSIs; they do not completely overlap with PV^+ FSIs, and are highly sensitive to endocannabinoids (eCBs) (Winters et al., 2012). Because eCBs are release by activated MSNs, $CB1^+$ FSI-mediated feedforward inhibition is regulated by MSN activity. Our present study targeted this unique, yet underexplored, population of NAc FSIs, and demonstrated that $CB1^+$ FSIs exerted robust inhibitory control over MSNs, in contrast to local MSN collaterals, which provided only sparse and weak inhibition to neighboring MSNs. Furthermore, the $CB1^+$ FSI-mediated feedforward inhibition was also preferentially suppressed by eCB signaling, which is capable of inducing long-term depression (LTD) at these synapses. These results suggest $CB1^+$ FSIs as a unique source of local inhibitory control of MSNs and a critical component of the circuits governing the output of the NAc.

Appendix A.3 Methods

Appendix A.3.1 Animals

Animals used were CB1-tdTomato knock-in mice (~25g; 50-90d old). These mice express the soluble fluorophore tdTomato (tdT) under the endogenous CB1 promoter as previously described (Winters et al., 2012), allowing for the visualization of $CB1^+$ neurons in brain slices. Male and female mice were used. We examined potential sex differences for the basic functional

properties of $CB1^+$ FSI-to-MSN and MSN-to-MSN synapses and found no differences between sexes (CB1-to-MSN or MSN-to-MSN, $p>0.05$ for all measures, t-test; **Figure 37**). Therefore, for all subsequent experiments, data from both sexes were combined for final data analysis. All mice used were single housed on a 12h light/dark cycle (light on/off 7:00/19:00) with food and water available *ad libitum*. Animals were sacrificed for electrophysiology at the beginning of the light cycle. All animals were used in accordance with protocols approved by the Institutional Animal Care and Use Committee at the University of Pittsburgh.

Appendix A.3.2 Preparation of NAc Acute Slices

Mice were decapitated after isofluorane anesthesia. Coronal slices (250μm) were prepared on a VT1200S vibratome (Leica, Germany) in 4ºC cutting solution containing (in mM) 135 N-methyl-D-glutamine, 1 KCl, 1.2 KH_2PO_4, 0.5 $CaCl_2$, 1.5 $MgCl_2$, 20 choline-HCO_3, and 11 glucose, saturated with 95% O_2/5% CO_2, pH 7.4 (305-310mM mOsm). Slices were incubated in artificial cerebrospinal fluid (aCSF) containing (in mM) 119 NaCl, 2.5 KCl, 2.5 $CaCl_2$, 1.3 $MgCl_2$, 1 NaH_2PO_4, 26.2 $NaHCO_3$, and 11 glucose, saturated with 95% O_2/5% CO_2 (285-290mM mOsm), for 30min at 37ºC. Slices in aCSF were then allowed to recover for 30min at room temperature before electrophysiological recordings.

Appendix A.3.3 Electrophysiology Recordings

All recordings were made in the medial NAc shell. During recordings, slices were superfused with aCSF, heated to 29-31ºC by passing solution through a feedback controlled in-line heater (Warner, CT). Cells were visually targeted using DIC/fluorescence microscopy

(Olympus, BX-51). $CB1^+$ cells were identified by tdTomato fluorescence (**Figure 37 a,b**). Whole-cell patch clamp recordings were made using a Multiclamp 700B amplifier and Digidata 1440A digitizer (Molecular Devices) through boroscilicate glass electrodes (2-5MΩ). Recordings were filtered at 3kHz, amplified 5 times, and digitized at 20kHz using Clampfit 10.2 (Molecular Devices). Series resistance was 8-23MΩ, uncompensated, and monitored throughout the recordings. Cells with a change in series resistance >15% were excluded for analysis.

Paired recordings were used to assess the properties of unitary inhibitory postsynaptic currents (uIPSCs) from $CB1^+$ FSI to MSN synapses and synapses between MSNs. To record connected pairs, postsynaptic MSNs were randomly sampled within a ~100µm radius from the presynaptic cell, within the approximate axonal arbor of FSIs and MSNs (~200-300µm) (Kawaguchi, 1993; Koos et al., 2004). The presynaptic patch pipette was filled with potassium-based internal solution (in mM: 130 K-methanesulfate, 10 KCl, 10 Hepes, 0.4 EGTA, 2 $MgCl_2$, 3 Mg-ATP, 0.25 Na-GTP; pH 7.3, 290mM mOsm), while postsynaptic pipettes were filled with high chloride, cesium-based internal solution (in mM: 15 $CsMeSO^4$, 140 CsCl, 4 TEA-Cl, 0.4 EGTA (Cs), 20 Hepes, 3 Mg-ATP, 0.25 Na-GTP, 5 QX-314(Br), pH 7.3, 290mM mOsm) to enhance IPSCs. This arrangement allowed for connectivity to be tested in one direction.

To evoke uIPSCs, presynaptic cells were held in current-clamp mode with membrane potential adjusted to -60mV, to ensure reliable action potential generation. The postsynaptic cell was held at -70mV in voltage-clamp mode. Brief current injections (1ms, 1300pA) into the presynaptic cell were used to evoke single action potentials. When paired pulses were used, the inter-pulse interval was 50ms. For non-stationary multiple probability fluctuation analysis (MPFA) recordings, a train of 6 action potentials were evoked in the presynaptic cell at 20Hz. Given that the rate of connectivity is heavily dependent on whether connections are preserved, we

always 1) recorded from pairs deep within the slice where local fibers are better preserved; and 2) recorded pairs with similar distance, to avoid bias and normalize recording conditions. NBQX (5μM) was included in the bath to isolate uIPSCs, except during LTD experiments.

Simultaneous dual voltage-clamp recordings were used to compare excitatory postsynaptic currents (EPSCs) in $CB1^+$ FSIs and MSNs. Cells were held at -70 mV unless otherwise stated. For all EPSC recordings, electrodes were filled with cesium-based internal solution (in mM: 135 $CsMeSO_4$, 5 CsCl, 5 TEA-Cl, 0.4 EGTA (Cs), 20 Hepes, 3 Mg-ATP, 0.25 Na-GTP, 1 QX-314(Br), pH7.3, 290mM mOsm). Picrotoxin (100 μM) was included in aCSF to inhibit $GABA_A$-mediated currents. Presynaptic afferents were electrically stimulated with a constant isolated stimulator (Digitimer, UK), using a monopolar electrode (glass pipette filled with aCSF). When paired pulses were used, the inter-pulse interval was 50 ms. To assess depolarization-induced suppression of excitation (DSE) in $CB1^+$ FSIs, voltage-clamp recordings were used to record EPSCs. These recordings were made in the same manner as dual recordings. All chemicals used were purchased from Sigma-Aldrich (St. Louis, MO, USA) or Tocris (UK).

Appendix A.3.4 Data Acquisition, Analysis, and Statistics

Connection probability was calculated as the percentage of functionally connected pairs from the total number of pairs sampled. Pairs were determined to be functionally connected if presynaptically evoked action potentials elicited uIPSCs in the postsynaptic cell (**Figure 37 A,B**). uIPSC amplitudes were determined by averaging the current amplitudes over a 1-ms segment around the uIPSC peak relative to its baseline. Synaptic delay of uIPSC was determined by measuring the time from the peak of the evoked action potential to the deflection of the postsynaptic uIPSC. The decay kinetics of uIPSCs was assessed by fitting the decaying segment

of uIPSCs with a single exponential function to obtain the decay time constant, τ. The activation kinetics of uIPSCs was assessed by the time to peak, which was measured as the time interval between the downward deflection of the uIPSC to the peak amplitude. Paired pulse ratio (PPR) was measured by dividing the amplitude of the second uIPSC by that of the first. The coefficient of variance (CV) analysis was done as previously described (Kullmann, 1994). Briefly, CV was estimated from 30-50 consecutive trials. Sample variances (SVs) were calculated for uIPSC amplitudes and sweep noises. CV was calculated as the square root of the difference for the sample variances (SVuIPSC –SVnoise), divided by the mean uIPSC amplitude.

For MPFA, ~50 uIPSCs were used from each cell at 6 different release probability conditions achieved by a 6-pulse train of presynaptic action potentials at 20Hz(Clements and Silver, 2000; Neumann et al., 2016b; Scheuss and Neher, 2001; Scheuss et al., 2002; Silver, 2003). The mean amplitude of uIPSCs at each time point of the train (I) was calculate by averaging the peak amplitudes of all uIPSCs at this time point. Variance of uIPSCs at each time point in the train was calculated and plotted against their mean. With the assumptions that presynaptic release sites operate independently and that the release probability of synapses is uniform, the amplitudes of uIPSCs can be expressed as:

$$I = NPrQ \qquad [Eq1]$$

where N is the number of release sites, Pr is the presynaptic release probability, and Q is the quantal size. For a binomial model, the variance (σ^2) of uIPSC amplitudes can be expressed as:

$$\sigma^2 = NQ^2Pr(1 - Pr) \qquad [Eq2]$$

Based on the above equations, the following equation can be derived:

$$\sigma^2 = IQ - (I/N)^2 \qquad [Eq3]$$

This equation predicts the parabolic relationship between σ^2 and I. As such, the variance-mean relationship was fit with Eq 3 to estimate N and Q. Pr was then calculated with Eq 1.

Results are shown as mean±SEM. Statistical significance was assessed with Fisher's exact test, paired or unpaired two-tail t-tests, one-way ANOVA, or two-way ANOVA with repeated measures, as specified. Cell-based statistics were performed for electrophysiology data. Significance was set at α=0.05.

Appendix A.4 Results

Appendix A.4.1 CB1+ FSIs Provide More Robust Inhibition to MSNs than Recurrent MSN Collaterals

In addition to FSIs-mediated feedforward inhibition, MSNs also receive lateral feedback inhibition from recurrent MSN collaterals (Tepper et al., 2008). As such, we compared inhibitory inputs to MSNs from $CB1^+$ FSIs versus MSN collaterals, to determine the relative weight of control these two inhibitory circuits have over MSNs. To isolate synaptic transmission between these distinct circuits, we performed paired recordings between either $CB1^+$ FSIs and MSNs (CB1-to-MSN) or between neighboring MSNs (MSN-to-MSN) to evoke uIPSCs in a mouse line in which $CB1^+$ neurons are genetically labeled with tdT (CB1-tdT mice) (**Figure 37 a,b**).

We observed that 60.0% (87/145) of CB1-to-MSN pairs recorded were functionally connected, in contrast to 10.3% (24/233) of the connectivity rate between MSN-to-MSN pairs (Fisher's exact test; p<0.0001; **Figure 37 c**). These different connectivity rates suggest that $CB1^+$

FSIs exerts more global influence over the activity of local MSNs than neighboring MSNs. For

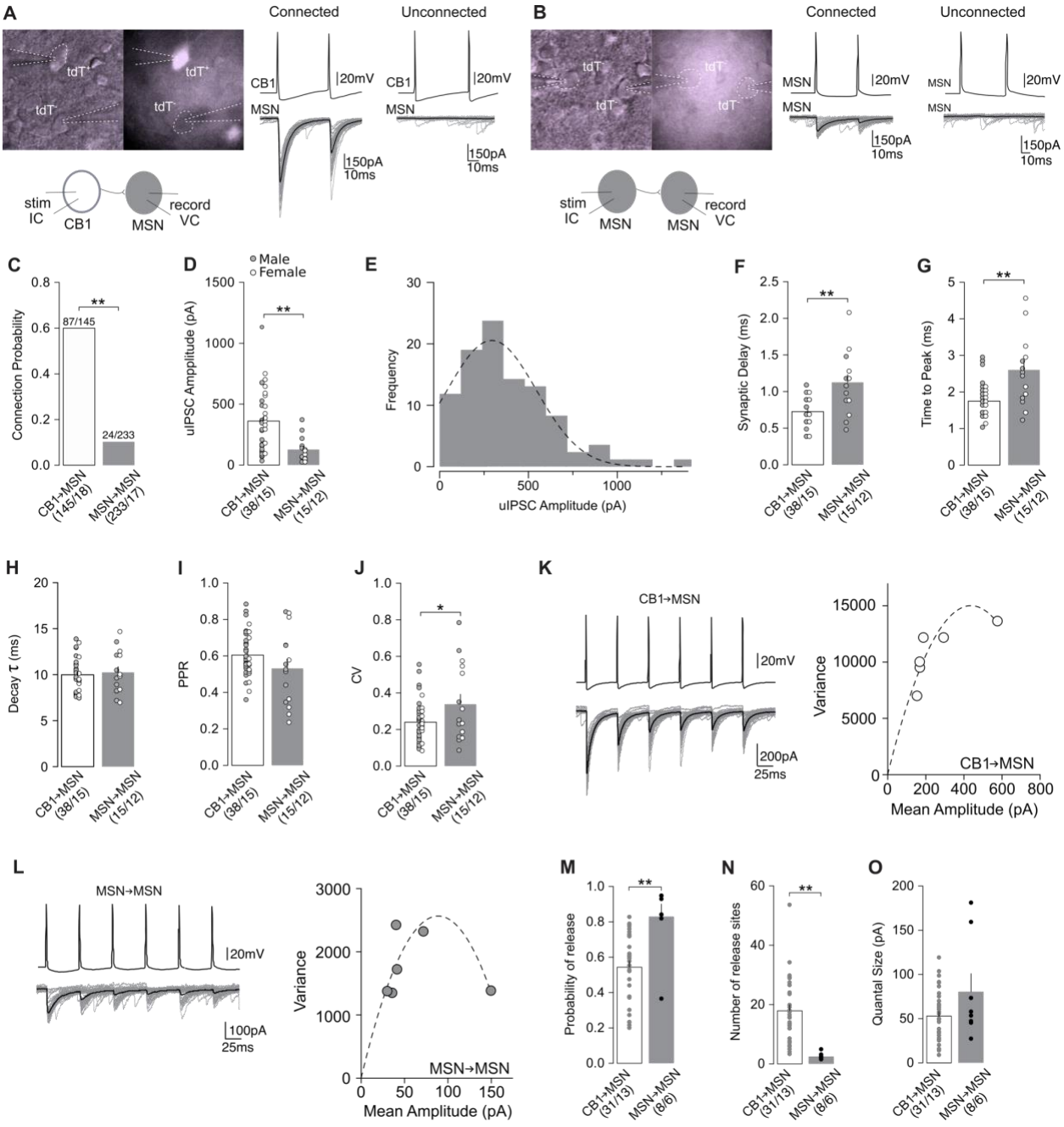

Figure 37. Comparison of CB1-to-MSN and MSN-to-MSN Inhibitory Synaptic Transmissions

(A) Representative images and schematic diagram (left) of paired recordings between CB1^{+} FSI (tdT^{+}) and MSN (tdT^{-}), and representative uIPSC traces from functionally connected (middle) and unconnected (right) CB1-to-MSN pairs. **(B)** Representative images and schematic diagram (left) of paired recordings between MSN (tdT^{-}) and MSN (tdT^{-}), and representative uIPSC traces from functionally connected (middle) and unconnected (right) MSN-to-MSN pairs.

(C) Summary showing CB1-to-MSN pairs exhibited a greater probability of connectivity of MSN-to-MSN pairs. **(D)** Summary showing amplitude of uIPSCs was greater at CB1-to-MSN synapses than MSN-to-MSN synapses**. (E)** Distribution of uIPSCs with a Gaussian fit showing a monomodal distribution. **(F)** Summary showing uIPSCs evoked at CB1-to-MSN synapses had a shorter synaptic delay than uIPSCs at MSN-to-MSN synapses. **(G)** Summary showing uIPSCs evoked at CB1-to-MSN synapses had shorter time to peak than uIPSCs MSN-to-MSN synapses. **(H)** Summary showing uIPSCs evoked at CB1-to-MSN and MSN-to-MSN synapses have similar decay kinetics. **(I)** Summary showing similar PPR of uIPSC responses at CB1-to-MSN and MSN-to-MSN synapses. **(J)** Summary showing uIPSC responses at MSN-to-MSN synapses had a greater CV than uIPSC responses at CB1-to-MSN synapses. **(K)** Example uIPSC traces (left) and their hyperbolic variance-mean fitted plot (right) at CB1-to-MSN synapses upon 6-pulse 20 Hz stimulation. **(L)** Example uIPSC traces (left) and their hyperbolic variance-mean fitted plot (right) at MSN-to-MSN synapses upon 6-pulse 20 Hz stimulation. **(M)** Summary showing MSN-to-MSN synapses had a higher presynaptic release probability than CB1-to-MSN synapses. **(N)** Summary showing CB1-to-MSN pairs had a greater number of release sites than MSN-to-MSN pairs. **(O)** Summary showing similar quantal size at CB1-to-MSN and MSN-to-MSN synapses. n/m represents number of cells/number of animals. * $p < 0.05$, ** $p < 0.01$. Error bars represent SEM.

connected pairs, the amplitude of uIPSCs was ~2.8 fold greater at CB1-to-MSN synapses (361.6 ± 38.15pA) than MSN-to-MSN synapses (128.2±26.01pA) (unpaired two-tail t-test: t_{51}=3.69, p=0.0005; **Figure 37 d**), further demonstrating that $CB1^+$ FSIs provide stronger inhibitory input to MSNs than MSNs. Our previous results suggest that $CB1^+$ FSIs can be divided into two subpopulations, PV^+ and PV^- FSIs (Winters et al., 2012). A distribution analysis indicates a monomodal pseudonormal distribution of CB1-to-MSN uIPSCs, implying a similar synaptic connectivity of these two subpopulations of $CB1^+$ FSIs to MSNs (**Figure 37 e**). Our further analyses indicate that CB1-to-MSN uIPSCs displayed a shorter synaptic delay (CB1-to-MSN, 0.73 ± 0.03 ms; MSN-to-MSN, 1.13 ± 0.11 ms; unpaired two-tail t-test: t_{51}=4.86, p<0.0001; **Figure 37 f**) and faster time to peak (CB1-to-MSN, 1.75±0.08ms; MSN-to-MSN, 2.61±0.25ms; unpaired

two-tail t-test: t_{51}=4.37, p<0.0001; **Figure 37 g**) than MSN-to-MSN uIPSCs, while there was no difference in the decay kinetics (CB1-to-MSN, 29.71±1.15ms; MSN-to-MSN, 30.79±2.55ms; unpaired two-tail t-test: t_{51}=0.44, p=0.66; **Figure 37 h**). The faster activation kinetics suggest that synapses from CB1$^+$ FSIs may be located on more proximal somatodendritic sites of MSNs than synapses form MSN collaterals, and therefore more effective in transmitting synaptic signals.

Further analyses indicate that CB1-to-MSN and MSN-to-MSN synapses exhibit different synaptic properties. We first measured the PPR and CV, differences in which may reflect differences in presynaptic release probability. No difference was detected in the PPR between CB1-to-MSN pairs (0.61±0.02) and MSN-to-MSN pairs (0.53±0.05)(unpaired two-tail t-test: t_{51}=1.64, p=0.11; **Figure 37 i**). In contrast, the CV of MSN-to-MSN pairs (0.34±0.05) was significantly greater than CB1-to-MSN pairs (0.24±0.02) (unpaired two-tail t-test: t_{51}=2.22, p=0.0311; **Figure 37 j**). Similar PPRs suggest that CB1-to-MSN and MSN-to-MSN synapses have similar presynaptic release probabilities, while a greater CV suggests that MSN-to-MSN synapses have lower release probability. However, CV is also influenced by the number of release sites (Kullmann, 1994). To clarify this, we performed the MPFA (see **Methods**) to determine the quantal properties of CB1-to-MSN and MSN-to-MSN synapses. The MPFA involves evoking 5-7 consecutive uIPSCs at 20Hz between functionally connected pairs, causing each uIPSC to stabilize at different a release probability (Pr) (**Figure 37 k,l**). The mean amplitudes and variance of each Pr condition are then plotted and fitted with a parabolic curve (**Figure 37 k,l**), which is then used to calculate the Pr, number of release sites (N), and quantal size (Q) (see **Methods**). The MPFA revealed that MSN-to-MSN synapses had a greater Pr (CB1-to-MSN, 0.54 ± 0.04; MSN-to-MSN, 0.83 ± 0.07; unpaired two-tail t-test: t_{37}=3.67, p=0.0008; **Figure 37 m**). However, CB1-to-MSN pairs had a substantially greater N (CB1-to-MSN, 17.93±1.99; MSN-to-MSN, 2.51±0.38;

unpaired two-tail t-test: t_{37}=3.89, p=0.0004, **Figure 37 n**), indicating intensive synaptic innervation. No difference in Q was identified, indicating similar postsynaptic responsiveness to transmitter release at CB1-to-MSN and MSN-to-MSN synapses (CB1-to-MSN, 52.98 ± 5.35; MSN-to-MSN, 80.58 ± 20.3; unpaired two-tail t-test: t_{37}=1.899, p=0.0654; **Figure 37 o**). Collectively, these results demonstrate that feedforward inhibition from $CB1^+$ FSIs exerts stronger inhibition over MSNs than lateral inhibition from MSN collaterals, partially due to more release sites.

Appendix A.4.2 CB1 Signaling Selectively Suppresses Inhibitory Input from $CB1^+$ FSIs

MSNs in the NAc do not express CB1, while $CB1^+$ FSIs do (Winters et al., 2012), predicting that eCBs released upon activation of MSNs may selectively modulate inhibitory transmission from $CB1^+$ FSIs. To determine this, we compared the sensitivity of uIPSCs between CB1-to-MSN synapses versus MSN-to-MSN synapses to the synthetic CB1 agonist WIN 5512-2 (5μM) during paired recordings. Application of WIN 55212-2 depressed the amplitude of CB1-to-MSN uIPSCs (0.33±0.07 relative to baseline), while MSN-to-MSN uIPSC amplitude was minimally affected (0.98±0.13 relative to baseline), indicating eCB signaling selectively suppresses CB1-to-MNS inhibitory transmission (RM two-way ANOVA, Cell-type x Time interaction: $F_{1,13}$=22.01, p=0.0004; CB1-to-MSN baseline vs. CB1-MSN WIN, p<0.0001; MSN-

to-MSN baseline vs. MSN-to-MSN WIN, p=1.0; CB1-to-MSN WIN vs. MSN-to-MSN WIN,

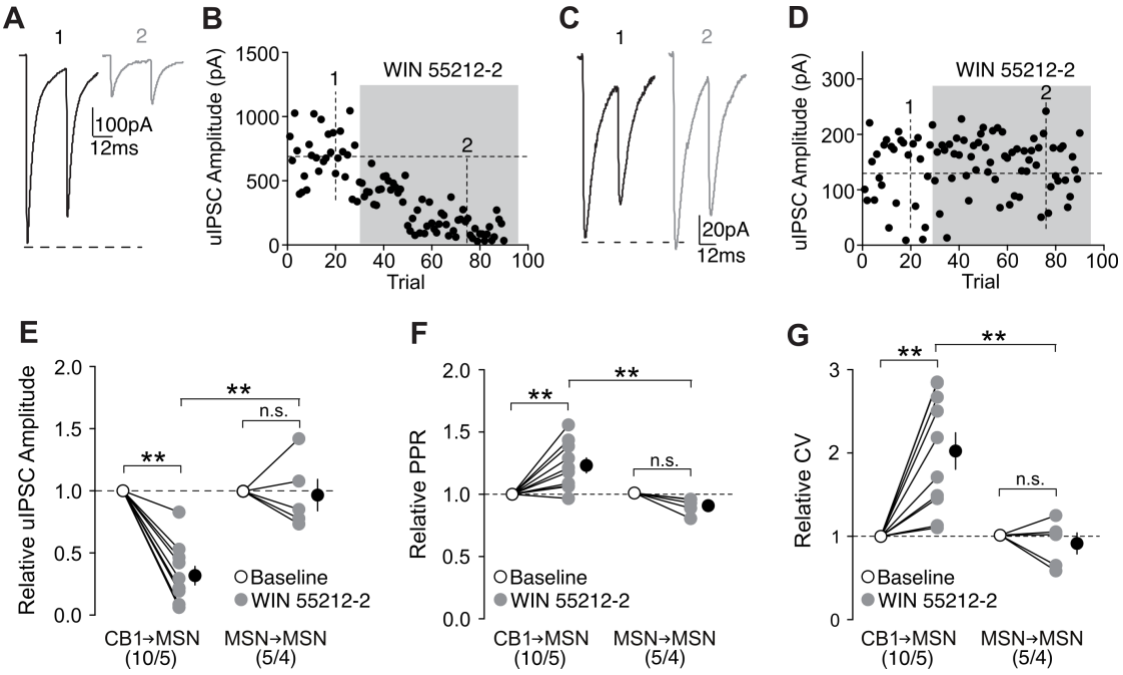

Figure 38. CB1 Signaling Preferentially Suppresses Inhibitory Input from CB1$^+$ FSIs

(A,B) uIPSC traces **(A)** and time course of uIPSC amplitude **(B)** from an example functionally connected CB1-to-MSN pair before (1) and during (2) perfusion of WIN 55212-2 (5 µM). **(C,D)** uIPSC traces **(C)** and time course of uIPSC amplitude **(D)** from an example functionally connected MSN-to-MSN pair before (1) and during (2) perfusion of WIN 55212-2 (5µM). **(E)** Summary showing perfusion of WIN 55212-2 decreased the amplitude of uIPSCs at CB1-to-MSN synapses, while uIPSCs at MSN-to-MSN synapses were insensitive to WIN 55212-2. **(F)** Summary showing that perfusion of WIN 55212-2 increased the PPR of uIPSCs at CB1-to-MSN synapses, while uIPSCs at MSN-to-MSN synapses were unaffected. **(G)** Summary showing that perfusion of WIN 55212-2 increased the CV of uIPSC responses at CB1-to-MSN synapses, while uIPSCs at MSN-to-MSN synapses were unaffected. n/m represents number of cells/number of animals. * $p < 0.05$, ** $p < 0.01$. Error bars represent SEM.

p<0.0001, Bonferroni posttest; **Figure 38 a-e**). The reduction in uIPSC amplitudes at CB1-to-MSN synapses by WIN 55212-2 was associated with an increase in the PPR (CB1-to-MSN, 1.23±0.06 relative to baseline; MSN-to-MSN, 0.89±0.029; RM two-way ANOVA, Cell-type x Time interaction: $F_{1,13}$=13.52, p=0.0028; CB1-to-MSN baseline vs. CB1-to-MSN WIN, p=0.0014;

MSN-to-MSN baseline vs. MSN-to-MSN WIN, p=0.3727; CB1-to-MSN WIN vs. MSN-to-MSN WIN, p<0.0001, Bonferroni posttest; **Figure 38 f**) and CV (CB1-to-MSN, 1.99±0.22 relative to baseline; MSN-to-MSN, 0.89±0.12; RM two-way ANOVA, Cell-type x Time interaction: $F_{1,13}$=11.07, p=0.0055; CB1-to-MSN baseline vs. CB1-MSN WIN, p=0.0003; MSN-to-MSN baseline vs. MSN-to-MSN WIN, p=1.0; CB1-to-MSN WIN vs. MSN-to-MSN WIN, p=0.0001, Bonferroni posttest; **Figure 38 g**), consistent with the typical CB1-mediated inhibition of presynaptic release observed throughout the brain (Castillo et al., 2012).

Tonic eCB signaling, which can be triggered by spontaneous release or neuronal activities, modulates basal synaptic transmission in the hippocampus, cerebellum, and dorsal striatum (Adermark and Lovinger, 2009; Kreitzer and Regehr, 2001; Lee et al., 2015). We examined this possibility at CB1-to-MSN synapses by testing the sensitivity of these synapses to the CB1 selective inverse agonist AM251 (2μM) at a dose that effectively prevents CB1 activation (Chevaleyre and Castillo, 2003; Kreitzer and Malenka, 2005; Lee et al., 2015; Yin and Lovinger, 2006). Application of AM251 slightly increased the amplitude of uIPSCs at CB1-to-MSN synapses (relative to baseline during AM251, 1.16±0.06), indicating tonic eCB-mediated suppression of CB1-to-MSN transmission (paired two-tail t-test: t_9=2.62, p=0.03; **Figure 39 a-c**). This increase in amplitude was associated with a decrease in PPR (relative to baseline: 0.88±0.05; paired two-tail t-test: t_9=2.50, p=0.34; **Figure 35 d**), but no change in CV (relative to baseline: 0.95±0.05; paired two-tail t-test: t_9=1.01, p=0.34; **Figure 39 e**).

Appendix A.4.3 Comparison of Excitatory Inputs to CB1$^+$ FSIs and MSNs

Excitatory inputs are likely the primary driving force for CB1$^+$ FSI-mediated feedforward inhibition of NAc MSNs. We simultaneously recorded CB1$^+$ FSI and MSN in the NAc, and

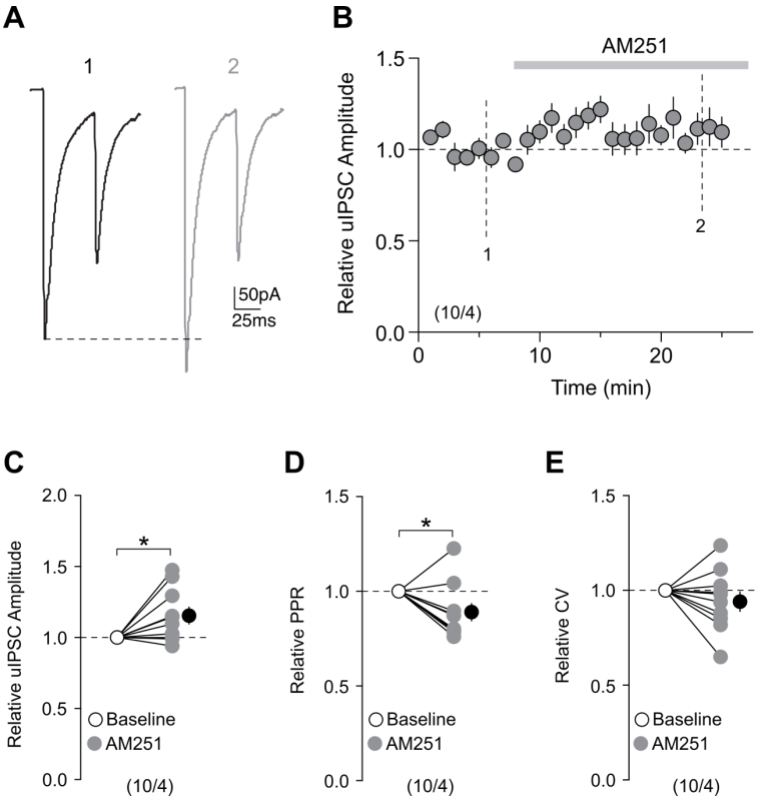

Figure 39. Tonic eCB Signaling Suppresses Basal CB1-to-MSN Inhibitory Transmission

(A) Example uIPSC traces before (1) and after (2) the application of AM251 (2µM). **(B)** Summary time course showing AM251 (2µM) application increases the amplitude of uIPSCs at CB1-to-MSN synapses. **(C)** Summary showing application of AM251 increased the amplitude of uIPSCs at CB1-to-MSN synapses. **(D)** Summary showing application of AM251 decreased the PPR at CB1-to-MSN synapses. **(E)** Summary showing application of AM251 does not alter the CV at CB1-to-MSN synapses. n/m represents number of cells/number of animals. * $p < 0.05$. Error bars represent SEM.

measured EPSCs of these two cells evoked by the same electrical stimulation of presynaptic fibers (**Figure 40 a**). Stimulation consistently evoked EPSCs with much larger amplitudes in CB1$^+$ FSIs

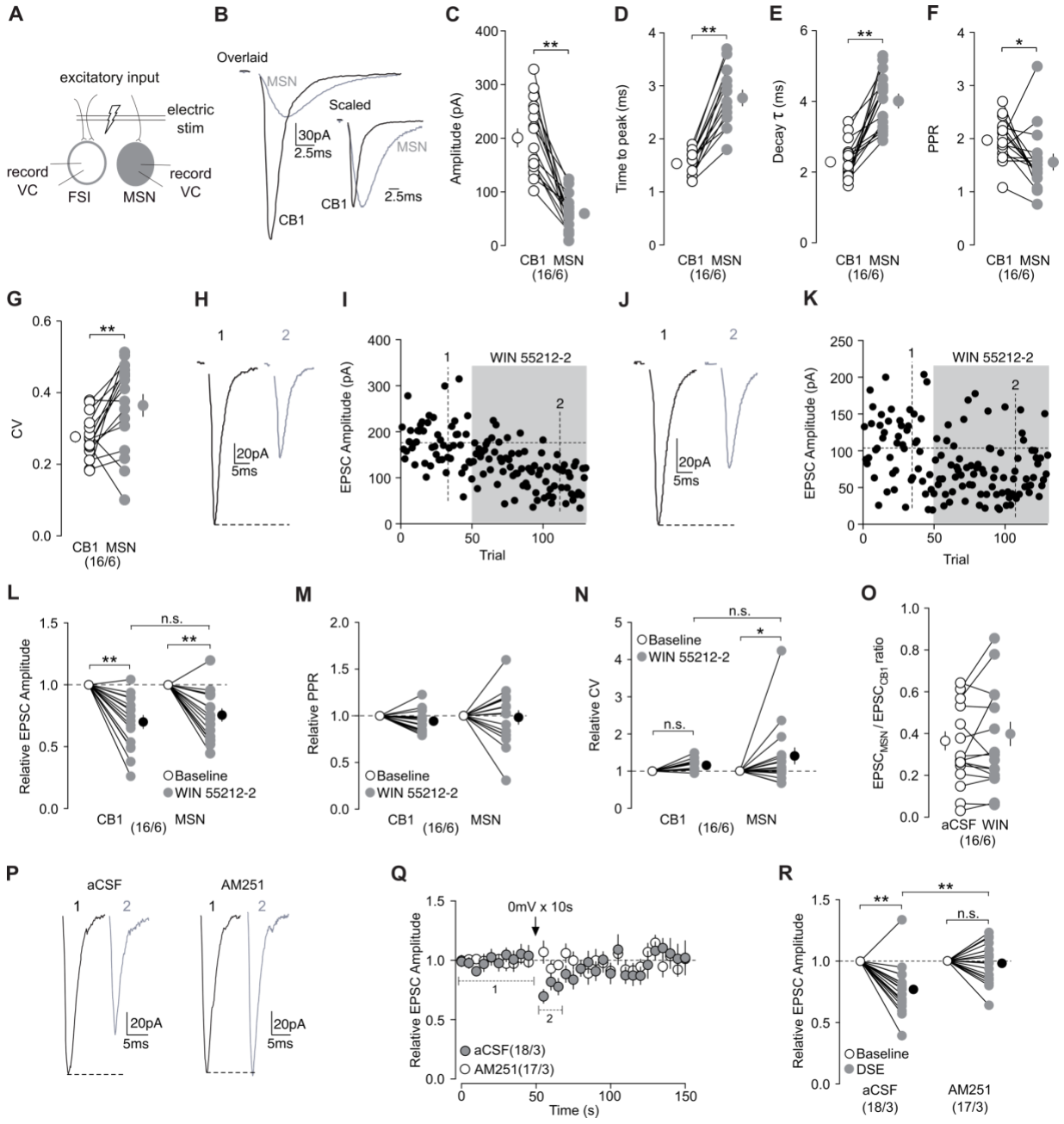

Figure 40. Comparison of Excitatory Inputs to CB1$^+$ FSIs and MSNs and their Modulation by CB1

(A) Schematic diagram showing simultaneous dual recordings of a CB1$^+$ FSI and an MSN upon the same electrical stimulation of presynaptic excitatory inputs. **(B)** Example traces from evoked EPSCs in the simultaneously recorded CB1$^+$ FSI (black) and MSN (gray). Overlaid traces (left) showing different activation and decay kinetics. **(C)** Summary

showing the amplitudes of EPSCs were larger in $CB1^+$ FSIs than MSNs. **(D,E)** Summary showing EPSCs evoked in $CB1^+$ FSIs exhibited a shorter time to peak **(D)** and decay kinetics **(E)** than EPSCs in MSNs. **(F)** Summary showing the PPR of EPSCs evoked in $CB1^+$ FSIs was greater than EPSCs in MSNs. **(G)** Summary showing the CV of EPSCs evoked in MSNs was greater than $CB1^+$ FSIs. **(H,I)** EPSCs evoked in an example CB1+ FSI **(H)** and the time course of the EPSC amplitudes before (1) and during (2) perfusion of WIN 55212-2 (5 μM). **(J,K**) EPSCs evoked in an example MSN **(J)** and the time course of EPSC amplitudes **(K)** before (1) and during (2) perfusion of WIN 55212-2 (5 μM). Examples shown in **H-K** are from a $CB1^+$ FSI and a MSN recorded simultaneously. **(L)** Summary showing that perfusion of WIN 55212-2 decreased amplitude of EPSCs evoked in $CB1^+$ FSIs and MSNs to a similar degree. **(M)** Summary showing that perfusion of WIN 55212-2 did not affect the PPR of EPSCs evoked in $CB1^+$ FSIs and MSNs. **(N)** Summary showing that perfusion of WIN 55212-2 increased the CV of EPSCs evoked in MSNs but no in $CB1^+$ FSIs **(O)** Summary showing that perfusion of WIN 55212-2 did not alter the $EPSC_{MSN}/EPSC_{CB1}$ ratio of simultaneously recorded pairs. **(P)** EPSCs evoked in an example $CB1^+$ FSI before (1) and after (2) a brief depolarization (0mV for 10s) in the absence (left) and presence (right) of AM251 (2 μM). **(Q)** Summarized time course showing that DSE was readily induced in $CB1^+$ FSIs and was prevented by AM251 (2 μM). **(R)** Summary showing that DSE decreased the amplitude of EPSCs in $CB1^+$ FSIs, which was blocked by AM251. n/m represents number of cells/number of animals. * $p < 0.05$, ** $p < 0.01$. Error bars represent SEM.

(203.20±16.97 pA) compared to EPSCs in MSNs (60.33±8.27 pA) for all pairs recorded (paired two-tail t-test: t_{15}=7.38, p<0.0001; **Figure 40 b,c**). The time to the peak amplitude of EPSCs was consistently faster in $CB1^+$ FSIs (1.54±0.06ms) than MSNs (2.78±0.15ms) (paired two-tail t-test: t_{15}=10.05, p<0.0001; **Figure 40 b,d**). Furthermore, the decay kinetics of evoked EPSCs were also faster in $CB1^+$ FSIs (CB1, 6.81±0.60 ms; MSN, 10.65±0.65 ms; paired two-tail t-test: t_{15}=6.33, p<0.0001; **Figure 40 b,e**). To determine if the different magnitudes of evoked EPSCs were due to presynaptic or postsynaptic differences, we assessed the PPR and CV. Both $CB1^+$ FSIs and MSNs had relatively large PPRs ($CB1^+$ FSI, 1.99±0.10; MSN, 1.58±0.15), suggesting glutamatergic afferents within the NAc have a low probability of presynaptic release relative to inhibitory inputs

(**Figure 40 h**). The PPR in MSNs was significantly lower than $CB1^+$ FSIs, suggesting excitatory inputs to MSNs have a higher release probability (paired two-tail t-test: t_{15}=2.33, p=0.0344; **Figure 40 f**). In contrast, MSNs displayed a greater CV (0.36±0.03) compared to $CB1^+$ FSIs (0.27±0.01) (paired two-tail t-test: t_{15}=2.981, p=0.0093; **Figure 40 g**). As mentioned above, CV is also indicative of the number of release sites in addition to release probability, and the greater CV observed here could be due to a fewer number of release sites to MSNs. These presynaptic differences, however, do not fully explain the differences in the EPSC amplitudes at these two synapse types, suggesting additional postsynaptic differences being involved. Collectively, our results suggest that $CB1^+$ FSIs receive more functional excitatory inputs than MSNs in the NAc.

Given the differences in basal excitatory input to $CB1^+$ FSIs and MSNs, we decided to explore possible differences in eCB-mediated modulation of excitatory inputs to these two cell types. We assessed the sensitivity of glutamatergic inputs to $CB1^+$ FSIs and MSNs to WIN 55212-2 (5μM) during simultaneous recordings of $CB1^+$ FSIs and MSNs. Application of WIN 55212-2 depressed the amplitude of evoked EPSCs in both $CB1^+$ FSIs and MSNs to a similar degree (relative to baseline: CB1, 0.70±0.05; MSN, 0.75±0.05; RM two-way ANOVA, Time main effect: $F_{1,30}$=55.98, p<0.0001; CB1 baseline vs CB1 WIN, p<0.0001; MSN baseline vs MSN WIN, p<0.0001; CB1 WIN vs MSN WIN, p=0.5977, Bonferroni posttest; **Figure 40 h-l**). Reduction in EPSC amplitude was not accompanied by a change in PPR (relative to baseline: CB1, 0.94±0.03; MSN, 0.98±0.07; RM two-way ANOVA, Time main effect: $F_{1,30}$=1.03, p=0.3189; **Figure 40 m**), while only MSNs displayed an increase in CV during perfusion of WIN 55212-2 (CB1, 1.16±0.04 relative to baseline; MSN, 1.39±0.22 relative to baseline; RM two-way ANOVA, Time main effect: $F_{1,30}$=5.99, p=0.0205; CB1 baseline vs CB1 WIN, p=0.6363; MSN baseline vs MSN WIN, p=0.0410; CB1 WIN vs MSN WIN, p=0.3145, Bonferroni posttest; **Figure 40 n**). The lack of

effects on PPR and CV suggest that there is negligible effect on presynaptic release by WIN 55212-2, which is inconsistent with the predominant presynaptic effects of CB1 (Castillo et al., 2012). However, due to the relatively low release probabilities under basal conditions, a potential reduction in release probability may be difficult to detect with PPR and CV measurements. Nonetheless, our results show that CB1 activation similarly suppresses excitatory inputs to $CB1^+$ FSIs and MSNs in the NAc. Importantly, CB1 activation does not alter the relative weight of excitatory inputs to $CB1^+$ FSIs versus MSNs, as there was no change in the $EPSC_{MSN}/EPSC_{CB1}$ ratio during WIN 55221-2 application (aCSF, 0.33 ± 0.05; WIN ,0.36±0.06; paired two-tail t-test: t_{15}=1.13, p=0.278; **Figure 40 o**).

The above results suggest that eCBs are capable of modulating excitatory inputs to $CB1^+$ FSIs. However, it is unclear whether this occurs under normal physiological conditions as it is unknown whether $CB1^+$ FSIs are capable of producing and releasing eCBs. One way to determine it is to test for depolarization-induced suppression of inhibition (DSI) or excitation (DSE). Previously, it was shown that DSI is not induced at CB1-to-CB1 inhibitory synapses, despite the presence of CB1 at these synapses (Winters et al., 2012). Here, we tested for DSE at excitatory inputs to $CB1^+$ FSIs. A brief (10 sec) depolarization to 0 mv reliably induced DSE in $CB1^+$ FSIs, which was prevented by the CB1-selective antagonist AM251 (2 μM) (relative to baseline: aCSF, 0.77±0.05; AM251, 0.99±0.04; RM two-way ANOVA, Time x aCSF/AM251 interaction: $F_{1,33}$=12.59, p=0.0012; aCSF baseline vs aCSF DSE, p<0.0001; AM251 baseline vs AM251 DSE, p=1.0; aCSF DSE vs AM251 DSE, p<0.0001, Bonferroni posttest; **Figure 40 p-r**), indicating that the $CB1^+$ FSIs are capable of releasing eCBs to modulate excitatory inputs.

Results above (**Figure 37**) show that excitation of CB1+ FSIs resulted in subsequent inhibition of MSNs. To determine if excitatory inputs drive disynaptic inhibition of MSNs through

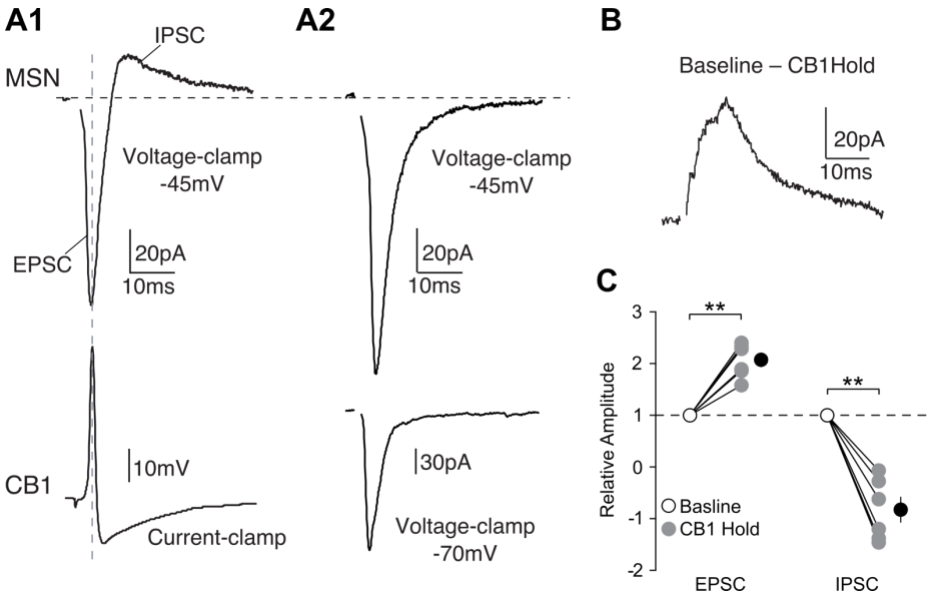

Figure 41. Disynaptic IPSC Events in NAc MSNs

(A1) Representative traces showing a fast inward current EPSC following by a delayed outward current IPSC when MSN is held at -45mV. Note the end of the EPSC coincides with the action potential firing in the simultaneous recorded $CB1^+$ FSIs. **(A2)** When the $CB1^+$ FSI was held at -70mV in voltage clamp to prevent action potential firing, the amplitude of the EPSC increased while the IPSC disappeared. **(B)** Trace generated by subtracting the MSN responses when the $CB1^+$ FSI was held at -70 (A2) from the MSN responses when the $CB1^+$ FSI was allowed to fire (A1), displaying an isolated outward IPSC. **(C)** Summary showing the amplitude of the inward EPSC increased while the outward IPSC disappeared after $CB1^+$ FSI was held. n/m represents number of cells/number of animals. ** $p <$ 0.01. Error bars represent SEM.

CB1+ FSIs, a hallmark of feedforward inhibition, we simultaneously recorded an MSN and a CB1+ FSI. We recorded the MSN in the voltage-clamp mode and held it at -45mV to allow for the detection of IPSCs, while recording CB1+ FSIs in the current clamp mode to monitor action potential firing. Activation of excitatory inputs evoked a fast inward current (EPSC) in the MSN,

followed by a short-delayed outward current (IPSC), indicative of disynaptic inhibition (**Figure**

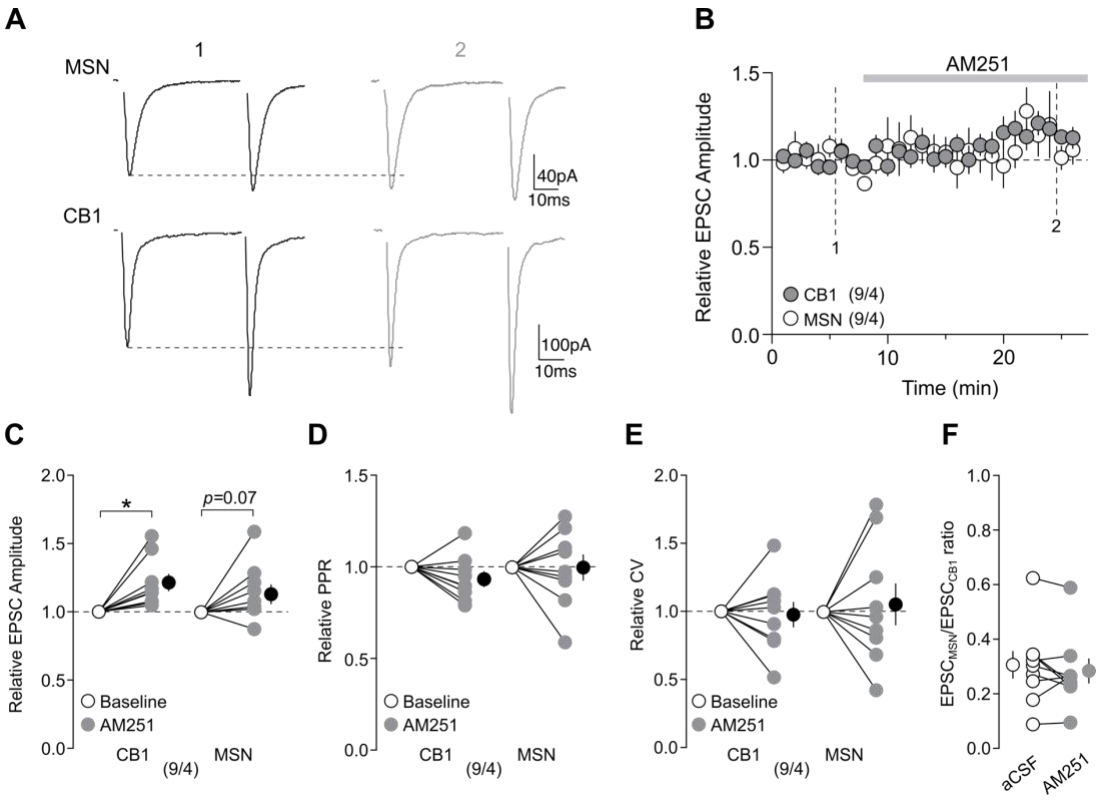

Figure 42. Tonic eCB Signaling at Excitatory Synapses in the NAc

(A) Example EPSC traces from simultaneously recorded MSN (top) and CB1$^+$ FSI (bottom) before (1) and after (2) the application of AM251 (2μM). **(B)** Summary time course showing AM251 application gradually increases the amplitude of EPSCs evoked in CB1$^+$ FSIs (gray) and MSNs (white). **(C)** Summary showing application of AM251 increased the amplitude of EPSCs in CB1$^+$ FSIs and trended to increase EPSCs in MSNs. **(D)** Summary showing AM251 had no effect on PPR of EPSCs in either CB1$^+$ FSIs or MSNs. **(E)** Summary showing AM251 had no effect on the CV of EPSCs in either CB1$^+$ FSIs or MSNs. **(F)** Summary showing that application of AM251 did not alter the $EPSC_{MSN}/EPSC_{CB1}$ ratio of simultaneously recorded pairs. n/m represents number of cells/number of animals. * $p <$ 0.05. Error bars represent SEM.

41 a). When the CB1+ FSI was switched to voltage clamp mode and held at -70mV to prevent action potential generation, the same excitatory input elicited inward current with increased amplitudes (2.06 %baseline; paired two-tail t-test: t5=7.90, p<0.0001), while the outward current

disappeared (-0.83 %baseline; paired two-tail t-test: t5=7.56, p<0.0001), demonstrating CB1+ FSIs as the source of the disynaptic inhibition of MSNs (**Figure 41 a-c**).

Lastly, we assessed if tonic eCB signaling modulates excitatory inputs to $CB1^+$ FSIs and MSNs as was determined for CB1-to-MSN synapses. During perfusion of AM251 (2μM), the amplitudes of evoked EPSCs in $CB1^+$ FSIs were increased (relative to baseline: 1.21±=0.06), and the amplitudes of evoked EPSCs in MSNs exhibited a trend toward increase (relative to baseline: 1.14±0.07; RM two-way ANOVA: time main effect, $F_{1,16}$=15.09, p=0.00; CB1 baseline vs. CB1 AM251, p=0.01; MSN baseline vs. MSN WIN, p=0.08; CB1 WIN vs. MSN WIN, p=0.64, Bonferroni posttest; **Figure 42 a-c**). The increase in amplitudes was not accompanied by significant changes in PPR (relative to baseline: CB1, 0.93±0.04; MSN, 0.99±0.07; RM two-way ANOVA: time main effect, $F_{1,16}$=0.78, p=0.39; **Figure 42 d**) nor CV (relative to baseline: CB1, 0.98±0.09; MSN, 1.07±0.15; RM two-way ANOVA: time main effect, $F_{1,16}$=0.06, p=0.82; **Figure 42 e**). The lack of significant effects on PPR and CV may be due to the small effects of AM251 that were subthreshold for PPR and CV detection. Furthermore, the $EPSC_{MSN}/EPSC_{CB1}$ ratio was not altered by AM251 (aCSF, 0.30±0.05; AM251, 0.28±0.04; paired two-tail t-test: t_8=1.08, p=0.31; **Figure 42 f**), indicating a similar modulation intensity by tonic eCBs at excitatory inputs to $CB1^+$ FSIs and MSNs.

Appendix A.4.4 eCB-Dependent Long-Term Depression of CB1-to-MSN Synapses

In addition to short-term plasticity, eCBs have been implicated in NAc LTD (Robbe et al., 2002). We performed paired recordings to examine unitary synaptic transmission from a $CB1^+$ FSI to an MSN. After a stable baseline period, we applied LFS (2Hz for 80sec), 3 times with 2-min

intervals through an electrical stimulator placed in the recording area, which presumably activated

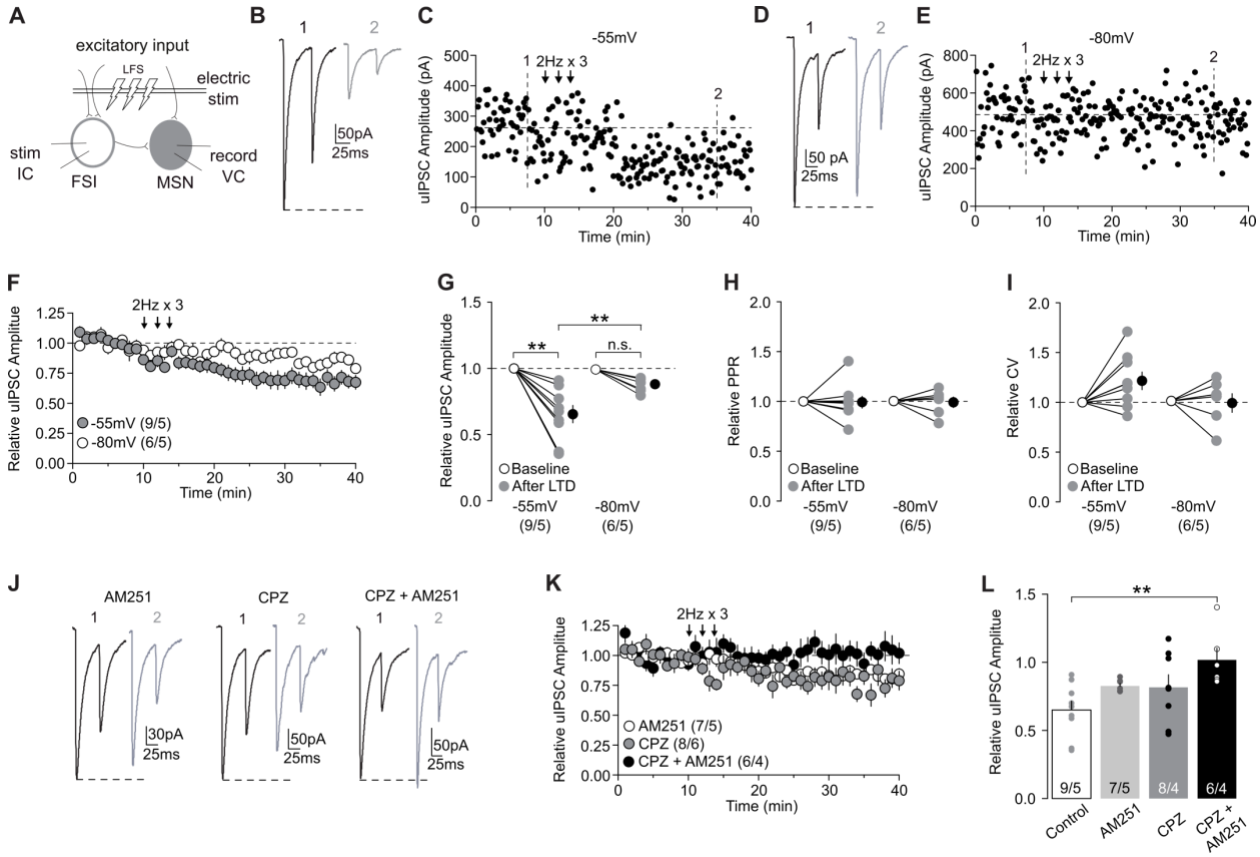

Figure 43. eCB-Mediated LTD of CB1-to-MSN Inhibitory Transmission

(A) Schematic diagram showing paired recordings of a CB1+ FSI and its connected MSN upon a LFS (2 Hz x 80 sec, repeated 3 times) of synaptic inputs. (B,C) uIPSCs (B) and the time course of uIPSC amplitudes (C) from an example CB1-to-MSN pair before (1) and following (2) LFS when MSNs were held at -55mV during delivery of LFS. (D,E) uIPSCs (D) and the time course of uIPSC amplitudes (E) from an example CB1-to-MSN pair before (1) and following (2) LFS when MSNs were held at -80mV during delivery of LFS. (F) Summary showing that LFS induced LTD at CB1-to-MSN synapses when MSNs were held at -55mV, while the magnitude of LTD was reduced when MSNs were held at -80mV during LFS. (G) Summary showing that the uIPSC amplitudes at CB1-to-MSN synapses were decreased after LFS when MSNs were held at -55mV but not -80mV during LFS. (H) Summary showing that the PPR of uIPSCs was not significantly affected following LFS. (I) Summary showing that the CV of uIPSCs was not significantly affected following LFS. (J) Example uIPSC traces from CB1-to-MSN pairs before (1) and following (2) LFS when MSNs were held at -55mV during LFS delivery in the presence of AM251 (2 μM; left), CPZ (10 μM; middle), and AM251 (2 μM) + CPZ (10 μM). (K) Summary showing that LTD was abolished by AM251 + CPZ, but

not by AM251 or CPZ alone. (L) Summary showing that the decrease in uIPSC amplitudes following LFS (control) was partially prevented by AM251 or CPZ alone, but completely prevented by AM251 + CPZ. n/m represents number of cells/number of animals. * $p < 0.05$, ** $p < 0.01$. Error bars represent SEM.

synaptic inputs to both recorded FSIs and MSNs (**Figure 43 a**). This LTD induction protocol was adapted from a similar LFS protocol (1Hz x 80sec) that has been shown to reliably induced eCB-mediated LTD at CB1-to-MSN synapses in the dorsal striatum (Mathur et al., 2013). MSNs in the NAc transition between a hyperpolarized down-state and a depolarized up-state *in vivo* (Wilson and Kawaguchi, 1996), which has been shown to gate the induction of eCB-dependent LTD at inhibitory synapses in the dorsal striatum (Mathur et al., 2013). Therefore, we held the postsynaptic MSN at either -80mV or -55mV, mimicking the down- and upstate respectively, during the delivery of LFS.

When MSNs were held at -55mV, LFS to FSI-to-MSN synapses reliably induced pronounced LTD of uIPSCs, while uIPSCs were only marginally depressed following LFS when MSNs were held at -80mV (relative to baseline: -55mV, 0.65±0.07; -80mV, 0.88±0.02; RM two-way ANOVA, Time vs Holding interaction: $F_{1,13}$=7.56, p=0.0165; -55 mV baseline vs -55mV LTD, p<0.0001; -80mV baseline vs. -80mV LTD, p=0.1579; -55mV LTD vs. -80mV LTD, p=0.0012, Bonferroni posttest; **Figure 43 b-g**). Decreased uIPSCs from either induction condition was not associated with a change in PPR (relative to baseline: -55 mV, 1.0±0.06; -80mV, 0.99±0.05; RM two-way ANOVA, Time main effect: $F_{1,13}$=0.03, p=0.8735; **Figure 43 h**), nor a change in the CV (relative to baseline: -55 mV, 1.23±0.09; -80mV, 1.0±0.09; RM two-way ANOVA, Time main effect: $F_{1,13}$=2.532, p=0.1356; **Figure 43 i**). These findings suggest that CB1-to-MSN synapses in the NAc are capable of undergoing activity-dependent LTD, but it is sensitive to the functional state (down- vs. upstate) of MSNs.

We next sought to determine the mechanisms mediating this voltage-sensitive LTD. Since LFS only induced pronounced LTD when MSNs were depolarized to -55mV, we focused our mechanistic investigation under this condition. Our PPR and CV measurements suggest LTD at CB1-to-MSN synapses following LFS is not mediated by a decrease in presynaptic release probability, arguing against a CB1-dependent mechanism. However, we also failed to see changes in PPR and CV of evoked EPSCs following CB1 activation (**Figure 40 m,n**), and therefore a potential CB1-mediated mechanism cannot be ruled out based solely on PPR and CV measurements. Furthermore, although not statistically significant, there was a ~20% increase in CV following LFS at -55 mV on average (**Figure 43 i**), which may suggest a subtle change in release probability but subthreshold for PPR and CV detection. This is supported by previous reports that PPR and CV measurements are not always capable of detecting the presynaptic effects of eCB-mediated LTD (Pan et al., 2008). Therefore, we tested the role of CB1 activation in the induction of LTD at CB1-to-MSN synapses. Blocking CB1 activation with AM251 (2μM) partially reduced the magnitude of LTD induced at CB1-to-MSN synapses (0.83±0.02 relative to baseline; **Figure 43 j-l**). The incomplete prevention suggests the involvement of other mechanisms in addition to CB1 activation.

Presynaptic CB1 is not the only target for eCBs within the brain; transient receptor potential vanilloid 1 (TRPV1) channels are postsynaptic targets for certain eCBs, such as anandamide (AEA) (Castillo *et al*, 2012). TRPV1 activation has recently been shown to contribute to the induction of eCB-mediated LTD at both excitatory and inhibitory synapses (Chávez et al., 2010; Chávez et al., 2014), and TRPV1-dependent LTD at NAc excitatory synapses (Grueter et al., 2010). We therefore examined the potential contribution of TRPV1 to LTD at CB1-to-MSN synapses. The magnitude of LTD was reduced (0.82±0.09 relative to baseline) when TRPV1

channels were blocked with capsazepine (CPZ; 10μM), a TRPV1-selective antagonist, but was not abolished, suggesting TRPV1 activation also contributes to the induction of LTD at CB1-to-MSN synapses (**Figure 43 j-l**). Since blocking either CB1 or TRPV1 activation partially reduced the magnitude of LTD, we next tested if their concurrent activation is the key for the full-magnitude expression of LTD. Co-application of AM251 (2μM) and CPZ (10μM) completely abolished the induction of LTD (CPZ + AM251, 1.02±0.09 relative to baseline; one-way ANOVA: $F_{3,26}$=4.22, p = 0.0147; Control vs CPZ + AM251, p=0.0092; all other comparisons, p>0.05, Bonferroni posttest; **Figure 43 j-l**). These results demonstrate that activity-dependent eCB signaling, through activation of both CB1 and TRPV1, mediates LTD at CB1-to-MSN synapses.

Appendix A.5 Discussion

Our current study characterizes several basic properties of the $CB1^+$ FSI circuits within the NAc that mediate feedforward inhibition of MSNs. These results may provide essential knowledge in understanding how the output of the NAc is regulated by complex circuit mechanisms under physiological and pathophysiological conditions

Appendix A.5.1 Feedforward and Feedback Inhibitory Control in the NAc

The local inhibition of NAc MSNs can be mediated by both feedforward and lateral feedback circuits, arising from local GABAergic interneurons and MSN axon collaterals, respectively (Tepper et al., 2008). Feedforward and lateral feedback inhibition both influence neural activity patterns, however, in fundamentally different ways. For example, feedforward

circuits may act to gate the activation of specific neural ensembles, while lateral feedback may confer winner-take-all properties to competing neural ensembles (Kepecs and Fishell, 2014).

We observed that $CB1^+$ FSIs provide a large percentage of neighboring MSNs with powerful inhibitory input, allowing $CB1^+$ FSIs to exert strong and global influence over the output of nearby MSNs to potentially control ensembles rather than individual MSNs. In contrast, MSNs have very sparse connectivity rates and deliver relatively weak inhibition to connected MSNs, thus providing limited influence over a select subset of MSNs. These differential effects are consistent with the circuit roles of FSIs and MSN collaterals in the dorsal striatum (Gittis et al., 2010; Koos and Tepper, 1999; Koos et al., 2004; Taverna et al., 2004). It should also be noted that connectivity rates measured in brain slices are likely underestimated as some local connections may be severed during the slice preparation. Furthermore, it is also possible the connectivity between MSNs could have been underestimated if responses between pairs were too small to be distinguished from noise. Regardless, this does not change the conclusion that $CB1^+$ FSIs serve as the predominating source of local inhibition to MSNs.

uIPSCs at CB1-to-MSN synapses exhibited shorter synaptic delays and faster activation kinetics than those at MSN-to-MSN synapses, suggesting that $CB1^+$ FSIs synapse on proximal or perisomatic locations, while MSN collaterals synapse on more distal regions of the dendritic tree, similar to the anatomical setups in the dorsal striatum (Bolam et al., 1983; Kubota and Kawaguchi, 2000; Wilson and Groves, 1980). This differential connectivity confers distinct functional roles to these two inhibitory circuits, as perisomatic inhibition is positioned to control the spiking output of principle cells (Kepecs and Fishell, 2014), while distal inhibition is positioned to gate excitatory inputs (Lovett-Barron et al., 2012; Milstein et al., 2015) and influence synaptic plasticity (Hayama et al., 2013).

Investigation into the quantal properties revealed that CB1-to-MSN unitary transmission has a larger number of synaptic release sites than MSN-to-MSN transmission. Given that one central synapse typically possesses only one release site (Biró et al., 2005), this greater number of release sites predicts more synapses within the CB1-to-MSN unitary transmission. On the other hand, MSN-to-MSN synapses have a greater release probability of transmitter release, while both transmissions exhibit similar quantal size. The relatively large number of synapses of the CB1-to-MSN transmission may spread out over more surface area of the MSN to achieve a better overall inhibition, while the higher release probability combined with fewer number of synapses may lead to reliable MSN-to-MSN inhibition but confined to specific anatomical sites.

The functional activity of feedforward and feedback circuits is critically dependent on their activation by excitatory inputs. In response to the same presynaptic stimulation of glutamatergic afferents, $CB1^+$ FSIs exhibited much larger amplitude of EPSCs, with faster activation kinetics, compared to adjacent MSNs. As mentioned above, faster activation kinetics suggests more proximal synaptic localization. If so, these proximal inputs to $CB1^+$ FSIs has two perceivable implications: 1) with less dendritic filtering, proximal input may produce larger somatic responses to evoke action potentials; and 2) action potentials fire with a shorter delay. Moreover, with higher membrane resistance, FSIs often exhibit a shorter latency for depolarization-induced action potential firing compared to MSNs (Kawaguchi, 1993; Winters et al., 2012). These anatomical and biophysical properties allow $CB1^+$ FSIs to quickly respond to excitatory inputs and fire action potentials to inhibit not only recurrent activation, but likely also the initial activation of MSNs upon a train of excitatory input. In addition, our PPR and CV results suggest that $CB1^+$ FSIs receive a greater number of excitatory inputs compared to MSNs, while inputs to MSNs have a higher probability of release. These notions are consistent with anatomical observations in the dorsal

striatum, in which MSNs receive few and distal innervations from a larger number of individual afferent fibers (Zheng and Wilson, 2002), while FSIs receive many and proximal innervations from a smaller number of individual afferents (Ramanathan et al., 2002). This pattern of innervation has also been demonstrated in the NAc for glutamatergic afferents from the ventral tegmental area (VTA)(Qi et al., 2016).

Appendix A.5.2 Modulation of Feedforward Inhibition

Inhibitory synapses throughout the brain undergo a variety of short- and long-term plasticity (Kullmann, 1994). A prominent form of such plasticity is mediated by eCB signaling (Castillo et al., 2012; Kullmann et al., 2012). Our results suggest that eCB signaling in the NAc preferentially suppresses $CB1^+$ FSI-mediated feedforward inhibition, leaving lateral feedback inhibition intact. Specifically, CB1 activation presynaptically depressed inhibitory transmission at CB1-to-MSN synapses. In contrast, inhibitory transmission at MSN-to-MSN synapses was insensitive to CB1 activation, consistent with the selective expression of CB1 in FSIs within the NAc (Winters et al., 2012). This preferential suppression of $CB1^+$ FSI transmission is in contrast to the dorsal striatum, where CB1 activation has been reported to suppress FSI-to-MSN and MSN-to-MSN inhibitory transmission (Freiman et al., 2006). eCBs also modulate excitatory transmission to MSNs in the NAc (Robbe et al., 2001), and we found that excitatory inputs to $CB1^+$ FSIs and MSNs were suppressed by CB1 activation to a similar degree. Furthermore, we observed that $CB1^+$ FSIs were capable of releasing eCBs to excitatory synapses, which is in contrast to select inhibitory synapses onto $CB1^+$ FSIs (Winters et al., 2012). Moreover, our results show that eCB signaling suppresses the glutamatergic inputs to FSIs and MSNs with similar magnitudes, and this eCB-mediated suppression of excitatory transmission is substantially less

than the suppression of inhibitory transmission to $CB1^+$ FSIs. Collectively, the net effect of CB1 activation in the NAc may result in the preferential suppression of feedforward inhibition arising from $CB1^+$ FSIs.

eCB signaling triggers long-term adaptations in synaptic transmission, most commonly LTD (Castillo et al., 2012). eCB-mediated LTD has previously been demonstrated at FSI-to-MSN synapses in the dorsal striatum, where it has a lower induction threshold compared to LTD at excitatory synapses (Adermark and Lovinger, 2009; Mathur et al., 2013). Our current results demonstrate that activity-dependent eCB signaling triggers LTD of the NAc FSI-to-MSN transmission. This form of eCB-LTD is dependent on both presynaptic activation of CB1 and postsynaptic activation of TRPV1 for a full induction. A similar CB1- and TRPV1-dependent mechanism has also been demonstrated to mediate eCB-dependent LTD at excitatory synapses in the NAc, triggering a reduction in presynaptic release and endocytosis of postsynaptic receptors (Grueter et al., 2010). Since MSNs fluctuate between depolarized up-states and hyperpolarized down-states *in vivo* (Wilson and Kawaguchi, 1996), the voltage-sensitivity identified here may gate the induction of LTD at CB1-to-MSN synapses when MSNs are in the upstate and likely be active, potentially favoring subsequent activation through disinhibition of $CB1^+$ FSIs.

Appendix A.5.3 Concluding Remarks

Our study provides an initial characterization of feedforward and lateral feedback inhibition in the NAc arising from $CB1^+$ FSIs and MSN collaterals, respectively. In addition, we identify disinhibition of MSNs from feedforward inhibition as a major target for eCB signaling in the NAc. While our findings provide a framework for conceptualizing how the microcircuits shapes the NAc output, future studies are needed to fully understand how the circuits behaves

when all components are left intact. A deeper understanding of the NAc microcircuits in motivated behaviors may open new avenues for the development of novel therapeutic strategies for psychiatric and psychological disorders

Appendix B Transient Increase in Membrane Excitability Following Cocaine-Associated Memory Reactivation

Appendix B.1 Overview

Cocaine experience results in the formation of enduring cocaine-associated memories, which contribute to the persistence of cocaine seeking behavior during drug abstinence. Similar to other memories, upon retrieval cocaine-associated memories can become transiently destabilized and made labile, before they are reconsolidated again. It was recently demonstrated that the destabilization and reconsolidation of cocaine-associated memories is, at least in part, regulated by the dynamic re-silencing and re-maturation of these synapses in the NAc. However, despite the silencing of these synapses cocaine seeking behavior remains elevated while the memory is destabilized. Here, we have begun to identify potential mechanisms underlying behavioral maintenance during memory destabilization. Focusing on neurocentric processes within the NAc, we found that memory retrieval triggered an increase in the membrane excitability of MSNs, which re-normalized within 6hrs, mirroring the reconsolidation of the memory. This increase in excitability was associated with a decrease in the amplitude of both the fast and medium afterhyperpolarizatoin potential (AHP). These findings demonstrated that in addition to transient synaptic re-silencing, the reactivation of cocaine-associated memories also triggers a transient enhancement of the membrane excitability of MSNs in the NAc, which may contribute to the maintenance of seeking behavior during memory destabilization.

Appendix B.2 Introduction

Consuming drugs of abuse results in the formation of memories associated with the experience of drug use, and these associative memories contribute to subsequent drug seeking and relapse (Hyman et al., 2006b). Drug-associated memories are often enduring, lasting for extended periods following the cessation of drug use, and this persistence represents a challenge in the prevention of relapse (Davis and Smith, 1976; Gawin and Kleber, 1986; Hyman et al., 2006b). Studies have begun to identify the specific neural substrates underlying the encoding of cocaine-associated memories, which can be targeted to disrupt these memories and ameliorate relapse (Lüscher et al., 2020; Nestler and Lüscher, 2019; Wolf, 2016a; Wright and Dong, 2020). One such substrate is a discrete population of silent synapses that are generated within the NAc by cocaine experience (Brown et al., 2011a; Huang et al., 2009), which functionally mature during abstinence to promote subsequent cocaine seeking behavior (Lee et al., 2013; Ma et al., 2014; Ma et al., 2016). Furthermore, we also recently found that the dynamic re-silencing and re-maturation of these cocaine-generated synapses contributes to the natural destabilization and reconsolidation of cocaine-associated memories following their reactivation (Wright et al., 2020). As such, these studies provide compelling evidence that the functional state of cocaine-generated synapses contributes to the encoding of cocaine-associated memories.

However, it was also recently found that a dissociation between synaptic state and cocaine seeking behavior emerges while the memory is destabilized, when cocaine-generated synapses are silent but cocaine seeking persists (Wright et al., 2020). This suggests that memory reactivation may engage other processes to drive seeking behavior, independent of cocaine-generated synapses. This is supported by the observation that re-silencing cocaine-generated synapses before memory reactivation decreased cocaine seeking, however, when the same manipulation was done after

memory reactivation cocaine seeking was not affected. We hypothesize that cocaine-generated synapses are key substrates for the storage or reactivation of cocaine memories; once the memories are reactivated, the behavioral expression is maintained by an independent set of mechanisms. Such a scenario is plausible given previous studies that have implied that the substrates underlying the initial encoding, storage, and expression of memories may be dissociable (Caffaro et al., 2012; Mamou et al., 2006; Otis et al., 2013; Roy et al., 2017a). This would explain the high levels of cocaine seeking during the memory destabilization window, which has also been observed in studies of fear memories (Monfils et al., 2009).

It remains unknown what mechanisms may be engaged to drive the behavioral expression of cocaine-associated memories after their initial reactivation. These mechanisms may involve circuit-level processes, such as the engagement of downstream circuits driving seeking behaviors, which may be self-sustaining or controlled by other inputs. Alternatively, these mechanisms may involve more neurocentric processes within NAc MSNs themselves that compensate for the weakening of the cocaine-generated synapses. Previous studies have identified several possible transient neural adaptations triggered by memory reactivation that may maintain behavioral expression. One well studied adaptation is the transient potentiation of other populations of synapses within the NAc. It has been documented to occur during the reinstatement of cocaine seeking after extinction, and this plasticity contributes to the expression of seeking behaviors (Gipson et al., 2013a; Roberts-Wolfe et al., 2018; Smith et al., 2014; Smith et al., 2016; Spencer et al., 2016). Another possible neural adaptation is the enhancement of the intrinsic membrane excitability of MSNs, which may help maintain neural output despite weaker inputs. This has been documented within the hippocampus, where memory reactivation triggers a transient increase in

the intrinsic membrane excitability of neurons and that subsequent behavioral expression shortly afterwards depends on this enhanced excitability (Pignatelli et al., 2018).

Here we investigated if the reactivation of cocaine-associated memories triggers transient adaptations in the intrinsic membrane excitability of MSNs within the NAc that may compensate for weakened synaptic inputs. We found that memory reactivation via re-exposure to cocaine-associated cues triggered a transient increase in the membrane excitability of MSNs in the NAc, which then renormalized within 6hrs. Furthermore, this increase in excitability was associated with an increase in Rheobase initially, following by a decrease in the amplitude of both the fast and medium afterhyperpolarizatoin potential (AHP) later during the destabilization window. These results demonstrate that the reactivation of cocaine-associated memories triggers a transient increase in the membrane excitability of NAc MSNs, which may serve as a potential mechanism for the maintenance of seeking behavior.

Appendix B.3 Methods

Appendix B.3.1 Subjects

Male Sprauge-Dawley rats (postnatal day 35-40 with 130-150g body weight on arrival) (Charles River) were used in all experiments. Rats were singly housed on a 12hr light/dark cycle (light on/off at 7:00/19:00) with food and water available *ad libitum*. Rats were allowed to habituate their housing cages for approximately 1 week before catheter surgery. All rats were used in accordance with protocols approved by the Institutional Care and Use Committee at the University of Pittsburgh.

Appendix B.3.2 Catheter Implantation

Catheter implantation surgery for self-administration was performed as described previously (Lee et al., 2013; Mu et al., 2010a). Briefly, a silastic catheter was inserted into the right jugular vein by 2.5 cm, and the distal end was led subcutaneously to the back between the scapulae. Catheters were constructed of silastic tubing (length, 10 cm; inner diameter, 0.0508 cm; outer diameter, 0.09398 cm) and attached to a commercially available Vascular Access Button (Instech). Rats were allowed to recover for 3-5 days following surgery, during which their wellbeing and weight were monitored. During the recovery period, the catheter was flushed daily with 1 ml kg^{-1} heparin (10 U ml^{-1}) and gentamicin antibiotics (5 mg ml^{-1}) in sterile saline to minimize potential infection and catheter occlusion.

Appendix B.3.3 Self-Administration Apparatus

All behavioral experiments were conducted in operant conditioning chambers enclosed within sound attenuating cabinets (Med Associates). Each chamber (29.53 x 24.84 x 18.67 cm^3) contains an active and an inactive nose poke hole, a food dispenser, a conditioned stimulus light within each nose poke hole and a house light. No food or water was provided in the chamber during the training or testing session.

Appendix B.3.4 Intravenous Cocaine Self-Administration Training

Cocaine self-administration training began approximately 5 days after catheter implantation. On day 1, rats were placed in the self-administration chamber for an overnight

training session on a fixed ratio 1 reinforcement schedule. Nose poking in the active hole resulted in a cocaine infusion (0.75 mg kg^{-1} over 3-6 secs) and illumination of the conditioned stimulus light inside the nose poke hole as well as the house light. The conditioned stimulus light remained on for 6 secs, whereas the house light was illuminated for 20 secs, during which any additional nose pokes were counted but resulted in no cocaine infusions. After the 20 sec timeout period, the house light was turned off, and the next nose poke in the active hole resulted in a cocaine infusion. Nose pokes in the inactive hole had no reinforced consequences, but were recorded.

Rats first underwent one overnight training session, approximately 12 hrs long, to facilitate acquisition. Only rats that received at least 80 cocaine infusions during the overnight session were allowed to proceed to the 5 day cocaine self-administration training regimen (< 2% of rats failed to meet criteria). The same, or similar, self-administration procedures/standards were used in our previous studies (Lee et al., 2013; Ma et al., 2014; Ma et al., 2016). After the fifth day of training, rats were placed back in their home cages and remained there during the subsequent withdrawal days. Cocaine-trained rats that failed to meet the self-administration criteria (≥ 15 infusions per session, 70% active-to-inactive nose poke response ratio) were excluded from further experimentation and analysis.

Appendix B.3.5 Withdrawal Phase

Rats were returned to their home cage after each self-administration training session. After the 5 day procedure, the rats were singly housed in their home cage for drug withdrawal, with food and water available *ad libitum*. Withdrawal day 1 was operationally defined as 20-26 hours after the last session of cocaine self-administration training. Withdrawal day 45 was operationally defined as 40-48 days after the last session of cocaine self-administration training.

Appendix B.3.6 Memory Retrieval

Memory retrieval sessions were performed in the same manner as the cocaine seeking test procedure as detailed below, except that the retrieval session lasted 10-15 min.

Appendix B.3.7 Cocaine Seeking Test

Cocaine seeking was assessed in an extinction test (1 hr) conducted after 1 day or 45 days of withdrawal from cocaine self-administration. During the extinction test session, rats were placed back in the operant chamber, where active nose pokes resulted in contingent delivery of the conditioned stimulus light cues, but not cocaine. The number of nose pokes to the active hole was used to quantify cocaine seeking. Nose pokes to the inactive hole were also recorded.

Appendix B.3.8 Preparation of Acute Brain Slices

Rats were decapitated following isoflurane anesthesia. For NAc-containing slices, coronal slices (250 μm thick) containing the NAc were prepared on a VT1200S vibratome (Leica) in 4 °C cutting solution containing (in mM): 135 N-methyl-d-glutamine, 1 KCl, 1.2 KH_2PO_4, 0.5 $CaCl_2$, 1.5 $MgCl_2$, 20 choline-HCO_3 and 11 glucose, saturated with 95%O_2/5%CO_2 and pH adjusted to 7.4 with HCl. Osmolality was adjusted to 305 mmol kg^{-1}. Immediately after cutting, slices were transferred and incubated in the artificial cerebrospinal fluid (aCSF) containing (in mM): 119 NaCl, 2.5 KCl, 2.5 $CaCl_2$, 1.3 $MgCl_2$, 1 NaH_2PO_4, 26.2 $NaHCO_3$ and 11 glucose, with the osmolality adjusted to 280–290 mmol kg^{-1}. Slices were placed in the aCSF saturated with 95%

O_2/5% CO_2 at 37 °C for 30 min and then held at 20–22 °C for at least 30 min before experimentation.

Appendix B.3.9 Electrophysiology Recordings

All recordings were made from MSNs located in the medial NAc Shell. Interneurons could be readily distinguished by their relatively depolarized resting membrane potential, higher action potential firing frequency, and or presence of large voltage sag at hyperpolarized potentials (Kawaguchi et al., 1995; Tepper et al., 2008). During recordings, slices were superfused with aCSF, heated to 30–32 °C by passing the solution through a feedback-controlled in-line heater (Warner) before entering the recording chamber. To measure membrane excitability, glass electrodes (2–5 MΩ) were filled with a potassium-based internal solution (in mM: 130 KMeSO3, 10 KCl, 0.4 EGTA, 10 HEPES, 2.5 Mg-ATP, 0.25 Na-GTP, 2 MgCl2-6H2O, pH 7.3). Current clamp recordings were used to measure action potentials evoked by current injection. For all recordings, the resting membrane potential was normalized to -80mV. Series resistance was typically 7–20 MΩ, uncompensated and monitored continuously during recording. Cells with a change in series resistance >20% were excluded from data analysis. All measurements were recorded with a MultiClamp 700B amplifier, filtered at 2.6–3 kHz, amplified five times and digitized at 20 kHz.

Only electrophysiologically stable neurons were included for data analysis. The following procedure was used to measure the membrane excitability of each neuron recorded. Following acquisition of the whole-cell current-clamp configuration, neurons were allowed ~5min to stabilize their resting membrane potentials (< 5mV fluctuations). Recordings were discontinued to membrane stabilization did not occur in this time. After the stabilization period, the resting

membrane potential was adjusted to -80 mV by injecting a small current (usually < 30 pA). A current step protocol (from -200 to +450 pA, with a 50 pA increment; interpulse interval, 15 s) was then repeated at least three times. Neurons that displayed large decreases in action potential amplitude throughout the step protocol were excluded from data analysis. Furthermore, if neurons displayed a run-up or run-down of > 15% in the number of action potentials evoked compared across the three repeats they were also excluded from data analysis. Thus, only MSNs with stable resting membrane potential and stable evoked action potential firing were included in the final analysis.

Additional properties of the action potential were measured following the first action potential elicited by the 300 pA current injection. The threshold of the action potential was defined as the membrane potential at which the dV/dt reached 10 before the spike. The amplitude of the fast afterhyperpolarization potential (fAHP) was defined as the voltage difference between the action potential threshold and the lowest hyperpolarization point after the action potential. The medium afterhyperpolarization potential (mAHP) was defined as the difference of the membrane potentials between the action potential threshold and 10ms after the action potential threshold. Input resistance (Rin) was calculated from the slope of the positive portion of the linear portion of the *I–V* curve around the reversal potential (current steps -100pA to 100pA) in order to avoid confounding from the rectification observed at negative potentials.

Appendix B.3.10 Statistics

All results are shown as mean ± s.e.m. All experiments were replicated in 4–6 rats. All data collection was randomized. All data were assumed to be normally distributed, but this was not formally tested. No statistical methods were used to predetermine sample sizes, but our sample

sizes are similar to those reported in previous publications (Dong et al., 2006; Ishikawa et al., 2009; Mu et al., 2010b; Wang et al., 2018). All data were analyzed offline and investigators were blinded to experimental conditions during the analyses.

Repeated experiments for the same group were pooled together for statistical analysis. For electrophysiology, the sample sizes are presented as *n/m*, where n is the number of cells and m is the number of rats. For behavioral experiments, the sample sizes are presented as *n*, which is the number of rats. Cell-based statistics were used for analyses of electrophysiology data. Statistical significance was assessed using one-way analysis of variance (ANOVA) or repeated-measures two-way ANOVA with Bonferroni posttest, as specified in the related text. Two-tailed tests were performed for analyses. Statistical significance was set at $P < 0.05$ for all experiments. Statistical analyses were performed in GraphPad Prism (v.8).

Appendix B.4 Results

We trained rats to self-administer cocaine, during which each intravenous infusion was paired with a light cue to form cocaine associations. Consistent with our previous studies (Lee et al., 2013; Ma et al., 2014; Ma et al., 2016), rats acquired cocaine-associated memories after 5 days of self-administration training (**Figure 44 a-e**), which could subsequently be reactivated after abstinence by brief re-exposure to the operant chamber and cocaine-associated cues (**Figure 44 f**) (Wright et al., 2020). Following self-administration training, rats underwent prolonged withdrawal (~45 days) before the membrane excitability of NAc MSNs was assessed. In order to determine the effects of memory reactivation on membrane excitability, some rats underwent a brief (10min)

cue re-exposure session on withdrawal day 45 before they were sacrificed at various time points

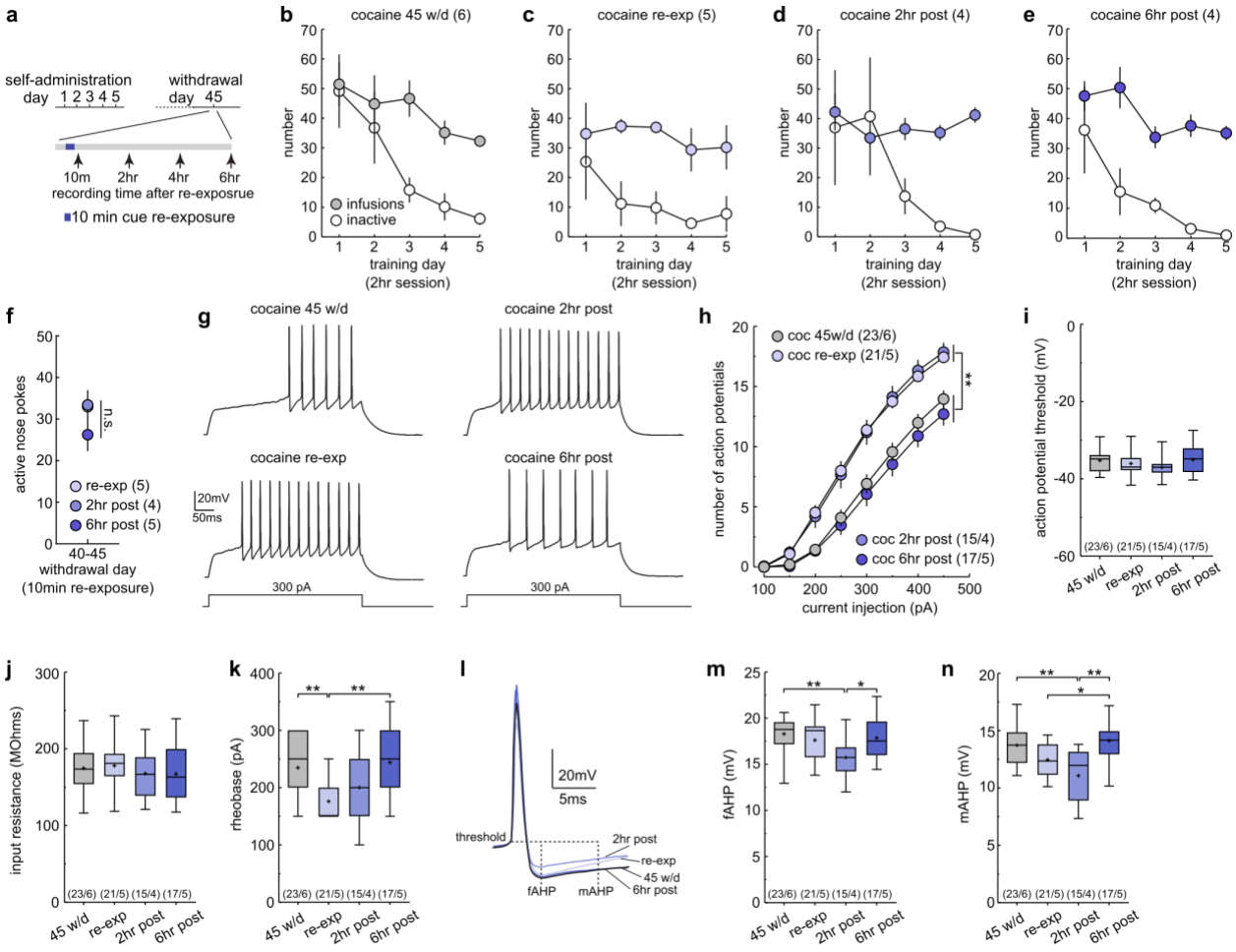

Figure 44. Transient Increase in Intrinsic Excitability following Memory Retrieval

(a) Schematic diagram showing experimental timeline. **(b-e**) Self-administration data of rats used in the following electrophysiology experiments. **(f)** Summary showing no difference in nose poke responding during the 10-min cue re-exposure session between different groups of rats used in the following electrophysiology experiments (re-exp = 33.00±1.41, n =5 rats; 2hr post = 33.00±3.39, n = 4 rats; 6hr post = 26.20±3.81, n = 5 rats; $F_{(2,11)} = 1.74$, $p = 0.22$, one-way ANOVA). **(g)** Example traces excitability traces in response to 300pA current injection. **(h)** Summary showing cue re-exposure increases the intrinsic excitability of NAc MSNs, which persists for at least 2hrs, before returned to pre-re-exposure levels 6hrs later (at 450pA: 45w/d = 13.96±0.729, n = 23 neurons / 6 rats; re-exp = 17.43±0.496, n = 21 neurons / 5 rats; 2hr post = 17.87±0.798, n = 15 neurons / 4 rats; 6hr post = 12.71±0.965; $F_{(21,504)} = 8.44$, $p < 0.001$, RM two-way ANOVA, current x re-exposure interaction, $^{**}p < 0.01$ for 45w/d vs. re-exp 200-450pA, $^{**}p < 0.01$ for 45w/d vs. 2hr post 300-450pA, $^{**}p < 0.01$ for 2hr post vs. 6hr post 300-450pA, $^{**}p < 0.01$ for re-exp vs. 6hr post 200-

450pA, Bonferroni post-test). **(i)** Summary showing there is no change in action potential threshold following cue re-exposure (45w/d = -35.21±0.574, n = 23 neurons / 6 rats; re-exp = -36.01±0.622, n=21 neurons / 5 rats; 2hr post = -37.01±0.639, n = 15 neurons / 4 rats; 6hr post = -35.01±0.857, n =17 neurons / 5 rats; $F_{(3,72)} = 1.61$, $p = 0.195$, one-way ANOVA). **(j)** Summary showing no change in input resistance following cue re-exposure (45w/d = 174.8±6.18, n = 23 neurons / 6 rats; re-exp = 178.1±6.28, n = 21 neurons / 5 rats; 2hrs post = 167.8±7.58, n = 15 neurons / 4 rats; 6hrs post = 167.4±9.01, n=17 neurons / 5 rats; $F_{(3,72)} = 0.5289$, $p = 0.664$, one-way ANOVA). **(k)** Summary showing a decrease in the rheobase immediately after cue re-exposure, but at no other time point (45w/d = 234.8±10.63, n = 23 neurons / 6 rats; re-exp = 176.2±6.56, n = 21 neurons / 5 rats; 2hr post = 200.0±12.91, n = 15 neurons / 4 rats; 6hr post = 244.1±13.48, n = 17 neurons / 5 rats; $F_{(3,72)} = 8.76$, $p < 0.0001$; $^{**}p < 0.01$ Bonferroni post-test). **(l)** Example traces showing AHP after the first action potential elicited after 300pA current injection. **(m**) Summary showing 2hrs following cue re-exposure there is a decrease in fAHP amplitude (45w/d = 18.3±0.38, n = 23 neurons / 6 rats; re-exp = 17.61±0.48; 2hrs post = 15.74±0.54, n = 15 neurons / 4 rats; 6hrs post = 17.86±0.64; $F_{(3,72)} = 4.986$, $p = 0.0034$; $^{**}p < 0.01$ Bonferroni post-test). **(n)** Summary showing there is a decrease in mAHP amplitude 2hrs after cue re-exposure. mAHP amplitude is also decreased immediately after re-exposure compared to 6hrs later (45w/d = 13.72±0.357, n = 23 neurons / 6 rats; re-exp = 12.45±0.318, n = 21 neurons / 5 rats; 2hrs post = 11.07±0.581, n = 15 neurons / 4 rats; 6hrs post = 14.12±0.439, n = 17 neurons / 5 rats; $F_{(3,72)} = 9.89$, $p < 0.001$, one-way ANOVA, $^{*}p < 0.05$, $^{**}p < 0.01$ Bonferroni post-test). Data are presented as mean ± s.e.m. Boxplots show max and min (whiskers), 75th and 25th percentiles (boxes), median (line), and mean (+).

later for electrophysiology recordings. The level of seeking behavior observed during the cue re-exposure session did not differ between the different groups, suggesting similar strength and reactivation of the cocaine-associated memories.

We observed a significant increase in the intrinsic membrane excitability of MSNs in rats that underwent brief cue re-exposure when compared to rats that did not (**Figure 44 g,h**). This increase in membrane excitability was transient, persisting for at least 2 hrs after cue re-exposure before returning to normal levels after 6 hrs (**Figure 44 h**). Thus, the increase in membrane

excitability follows a similar time course as memory destabilization and reconsolidation as well as the dynamic changes in cocaine-generated synapses.

Next, we examined some basic properties of the action potential to begin to identify underlying mechanisms driving the increase in membrane excitability. Brief cue re-exposure had no effect on the action potential threshold, with no difference detected between any of the groups (**Figure 44 i**). We also found there to be no difference in the input resistance between any of the groups (**Figure 44 j**). In contrast, we found that brief cue re-exposure triggered a decreased the rheobase, or the minimal current required to elicit an action potential, which is consistent with an increase in membrane excitability (**Figure 44 k**). Interestingly, this decrease in the rheobase did not persist throughout the destabilization window, increasing again 2hrs after cue re-exposure, despite the membrane excitability still being greater at this time point (**Figure 44 k**). This suggests other mechanisms are likely responsible for the enhanced excitability during the destabilization window.

One notable property of the action potential that regulates overall excitability is the AHP, which defines the relatively refractory periods and functions to suppress the generation of subsequent action potentials. Previous studies have demonstrated that homeostatic changes to membrane excitability in response to changes synaptic input are driven by modulation of the AHP (Ishikawa et al., 2009). To quantify the changes in different components of AHP the peak of AHP was operationally defined as the fast component of AHP (fAHP), and the membrane potential at 10 ms after the onset of action potential was defined as the medium component (mAHP), as has been done in previous studies (Ishikawa et al., 2009; Mu et al., 2010b; Wang et al., 2018) (**Figure 44 l**). We found that immediately following brief cue re-exposure there was no significant change in either fAHP or the mAHP (**Figure 44 m,n**). However, when measured 2hrs after cue re-exposure

the amplitude of both the fAHP and mAHP was decreased compared to rats that did not undergo cue re-exposure (**Figure 44 m,n**), which is consistent with an increase in membrane excitability at this time point.

Appendix B.5 Discussion

Cocaine experience generates new synapses within the NAc, which promote subsequent cocaine seeking behavior after withdrawal (Huang et al., 2009; Lee et al., 2013; Ma et al., 2014). However, recently it was found that following the reactivation and destabilization of cocaine-associated memories a dissociation between the functional state of cocaine-generated synapses and cocaine seeking behavior emerges, where these synapses are re-silenced yet seeking remains elevated (Wright et al., 2020). This dissociation suggests that other mechanisms are engaged by memory reactivation that maintain the expression of cocaine seeking behavior while the memory is destabilized. In this preliminary study, we found that memory reactivation triggers a transient increase in the membrane excitability of MSNs in the NAc, before re-normalizing 6hrs later, mirroring the destabilization and reconsolidation of the memory. This finding is consistent with a recent study that found memory reactivation triggered a transient increase in the membrane excitability of hippocampal engram neurons, which contributed to maintaining appropriate behavior (Pignatelli et al., 2018). Other studies provide further support for enhanced membrane excitability after memory retrieval, where it has been found that the reactivation of reward- and cocaine-associated memories is associated with enhanced excitability of NAc MSNs that were recently activated (Ziminski et al., 2017; Ziminski et al., 2018), however, it wasn't assessed if this enhancement was transient. Therefore, accumulating evidence indicates that memory reactivation

triggers parallel and opposite changes in synaptic input and membrane excitability with a simultaneous weakening of synapses and enhancement of excitability (Pignatelli et al., 2018; Rao-Ruiz et al., 2011; Wright et al., 2020; Ziminski et al., 2017; Ziminski et al., 2018). Such, opposite adaptations may help maintain the relatively spiking output of MSNs, similar to homeostatic mechanisms, and therefore the transient increase in membrane excitability may help maintain cocaine seeking behavior, despite the re-silencing of cocaine-generated synapses.

Our preliminary analyses into the underpinnings of this enhanced excitability, revealed there to be an initial reduction in the rheobase immediately following cue re-exposure, which would contribute to the enhanced excitability observed. The underlying cause for this reduction, however, remains undetermined as it was not associated with a change in either the input resistance nor the action potential threshold. Interestingly, this reduction in rheobase did not persist throughout the destabilization window, and thus likely does not underlie the enhanced excitability observed during this time. Instead, we found there the be a significant decrease in the amplitude of the AHP at the later 2hr time point after cue re-exposure, which is expected to increase excitability. This finding is consistent with a previous study also observing a decrease in the amplitude of the AHP following the reactivation of cocaine-associated memories (Ziminski et al., 2018). It has been demonstrated that homeostatic synaptic-to-membrane plasticity (hSMP) in the NAc, where changes in synaptic input trigger homeostatic adaptations in membrane excitability, is also largely mediated by the modulation of the AHP through the upregulation of SK-type calcium activated potassium channels (Ishikawa et al., 2009). Thus, memory reactivation may trigger mechanisms similar to hSMP, albeit on a different timescale. However, this remains to be determined in subsequent investigations.

While the transient increase in membrane excitability we observed may help maintain the spiking output of MSNs, there still remains no evidence that it contributes to the maintenance of cocaine seeking behavior during memory destabilization. Future studies will need to causally test what role this enhanced excitability has on subsequent cocaine seeking or if it contributes to other processes, such as memory reconsolidation.

Bibliography

Abdou, K., Shehata, M., Choko, K., Nishizono, H., Matsuo, M., Muramatsu, S.-I., and Inokuchi, K. (2018). Synapse-specific representation of the identity of overlapping memory engrams. Science *360*, 1227-1231.

Aceti, M., Vetere, G., Novembre, G., Restivo, L., and Ammassari-Teule, M. (2015). Progression of activity and structural changes in the anterior cingulate cortex during remote memory formation. Neurobiology of Learning and Memory *123*, 67-71.

Adermark, L., and Lovinger, D.M. (2009). Frequency-dependent inversion of net striatal output by endocannabinoid-dependent plasticity at different synaptic inputs. The Journal of neuroscience : the official journal of the Society for Neuroscience *29*, 1375-1380.

Adesnik, H., Li, G., During, M.J., Pleasure, S.J., and Nicoll, R.A. (2008). NMDA receptors inhibit synapse unsilencing during brain development. Proceedings of the National Academy of Sciences of the United States of America *105*, 5597-5602.

Ahmed, M.S., Priestley, J.B., Castro, A., Stefanini, F., Canales, A.S.S., Balough, E.M., Lavoie, E., Mazzucato, L., Fusi, S., and Losonczy, A. (2020). Hippocampal Network Reorganization Underlies the Formation of a Temporal Association Memory. Neuron, 1-16.

Al-Hasani, R., McCall, J.G., Shin, G., Gomez, A.M., Schmitz, G.P., Bernardi, J.M., Pyo, C.-O., Park, S.I., Marcinkiewcz, C.M., Crowley, N.A., *et al.* (2015). Distinct Subpopulations of Nucleus Accumbens Dynorphin Neurons Drive Aversion and Reward. Neuron *87*, 1063-1077.

Alberini, C.M. (2005). Mechanisms of memory stabilization: are consolidation and reconsolidation similar or distinct processes? Trends in neurosciences *28*, 51-56.

Alberini, C.M., and Kandel, E.R. (2014). The regulation of transcription in memory consolidation. Cold Spring Harbor Perspectives in Biology *7*, a021741.

Allen, N.J., and Eroglu, C. (2017). Cell Biology of Astrocyte-Synapse Interactions. Neuron *96*, 697-708.

Allison, D.W., Gelfand, V.I., Spector, I., and Craig, A.M. (1998). Role of actin in anchoring postsynaptic receptors in cultured hippocampal neurons: differential attachment of NMDA versus AMPA receptors. The Journal of neuroscience : the official journal of the Society for Neuroscience *18*, 2423-2436.

Ambroggi, F., Ghazizadeh, A., Nicola, S.M., and Fields, H.L. (2011). Roles of Nucleus Accumbens Core and Shell in Incentive-Cue Responding and Behavioral Inhibition. The Journal of neuroscience : the official journal of the Society for Neuroscience *31*, 6820-6830.

Ambroggi, F., Ishikawa, A., Fields, H.L., and Nicola, S.M. (2008). Basolateral Amygdala Neurons Facilitate Reward-Seeking Behavior by Exciting Nucleus Accumbens Neurons. Neuron *59*, 648-661.

Anderson, S.M., Famous, K.R., Sadri-Vakili, G., Kumaresan, V., Schmidt, H.D., Bass, C.E., Terwilliger, E.F., Cha, J.H.J., and Pierce, R.C. (2008). CaMKII: a biochemical bridge linking accumbens dopamine and glutamate systems in cocaine seeking. Nature Neuroscience *11*, 344-353.

Arendt, K.L., Sarti, F., and Chen, L. (2013). Chronic inactivation of a neural circuit enhances LTP by inducing silent synapse formation. The Journal of neuroscience : the official journal of the Society for Neuroscience *33*, 2087-2096.

Ashkan, K., Rogers, P., Bergman, H., and Ughratdar, I. (2017). Insights into the mechanisms of deep brain stimulation. Nature reviews Neurology *13*, 548-554.

Asok, A., Leroy, F., Rayman, J.B., and Kandel, E.R. (2019). Molecular Mechanisms of the Memory Trace. Trends in neurosciences *42*, 14-22.

Atallah, H.E., McCool, A.D., Howe, M.W., and Graybiel, A.M. (2014). Neurons in the ventral striatum exhibit cell-type-specific representations of outcome during learning. Neuron *82*, 1145-1156.

Attardo, A., Fitzgerald, J.E., and Schnitzer, M.J. (2015). Impermanence of dendritic spines in live adult CA1 hippocampus. Nature *523*, 592-596.

Attardo, A., Lu, J., Kawashima, T., Okuno, H., Fitzgerald, J.E., Bito, H., and Schnitzer, M.J. (2018). Long-Term Consolidation of Ensemble Neural Plasticity Patterns in Hippocampal Area CA1. Cell reports *25*, 640-650.e642.

Augur, I.F., Wyckoff, A.R., Aston-Jones, G., Kalivas, P., and Peters, J. (2016). Chemogenetic Activation of an Extinction Neural Circuit Reduces Cue-Induced Reinstatement of Cocaine Seeking. The Journal of neuroscience : the official journal of the Society for Neuroscience *36*, 10174-10180.

Averbeck, B.B., and Costa, V.D. (2017). Motivational neural circuits underlying reinforcement learning. Nature Neuroscience *20*, 505-512.

Bailey, C.H., Kandel, E.R., and Harris, K.M. (2015). Structural Components of Synaptic Plasticity and Memory Consolidation. Cold Spring Harbor Perspectives in Biology *7*, a021758.

Baimel, C., McGarry, L.M., and Carter, A.G. (2019). The Projection Targets of Medium Spiny Neurons Govern Cocaine-Evoked Synaptic Plasticity in the Nucleus Accumbens. Cell reports *28*, 2256-2263.e2253.

Barack, D.L., and Krakauer, J.W. (2021). Two views on the cognitive brain. Nature Reviews Neuroscience, 1-13.

Barria, A., Muller, D., Derkach, V., Griffith, L.C., and Soderling, T.R. (1997). Regulatory phosphorylation of AMPA-type glutamate receptors by CaM-KII during long-term potentiation. Science *276*, 2042-2045.

Barrot, M., Olivier, J.D.A., Perrotti, L.I., DiLeone, R.J., Berton, O., Eisch, A.J., Impey, S., Storm, D.R., Neve, R.L., Yin, J.C., *et al.* (2002). CREB activity in the nucleus accumbens shell controls gating of behavioral responses to emotional stimuli. Proceedings of the National Academy of Sciences *99*, 11435-11440.

Bastrikova, N., Gardner, G.A., Reece, J.M., Jeromin, A., and Dudek, S.M. (2008). Synapse elimination accompanies functional plasticity in hippocampal neurons. Proceedings of the National Academy of Sciences of the United States of America *105*, 3123-3127.

Bayer, K.U., De Koninck, P., Leonard, A.S., Hell, J.W., and Schulman, H. (2001). Interaction with the NMDA receptor locks CaMKII in an active conformation. Nature *411*, 801-805.

Bayer, K.U., LeBel, E., McDonald, G.L., O'Leary, H., Schulman, H., and De Koninck, P. (2006). Transition from reversible to persistent binding of CaMKII to postsynaptic sites and NR2B. The Journal of neuroscience : the official journal of the Society for Neuroscience *26*, 1164-1174.

Béïque, J.-C., Lin, D.-T., Kang, M.-G., Aizawa, H., Takamiya, K., and Huganir, R.L. (2006). Synapse-specific regulation of AMPA receptor function by PSD-95. Proceedings of the National Academy of Sciences *103*, 19535-19540.

Belin-Rauscent, A., and Belin, D. (2012). Animal Models of Drug Addiction. In, D. Belin, ed., pp. 1-45.

Bender, B.N., and Torregrossa, M.M. (2021). Dorsolateral striatum dopamine-dependent cocaine seeking is resistant to pavlovian cue extinction in male and female rats. Neuropharmacology *182*, 108403-108412.

Berke, J.D. (2018). What does dopamine mean? Nature Neuroscience *21*, 787-793.

Berridge, K.C. (2007). The debate over dopamine's role in reward: the case for incentive salience. Psychopharmacology *191*, 391-431.

Biró, A.A., Holderith, N.B., and Nusser, Z. (2005). Quantal size is independent of the release probability at hippocampal excitatory synapses. The Journal of neuroscience : the official journal of the Society for Neuroscience *25*, 223-232.

Bishop, C.M. (2006). Pattern Recognition and Machine Learning (Springer).

Bittner, K.C., Milstein, A.D., Grienberger, C., Romani, S., and Magee, J.C. (2017). Behavioral time scale synaptic plasticity underlies CA1 place fields. Science *357*, 1033-1036.

Bliss, T.V., and Lomo, T. (1973). Long-lasting potentiation of synaptic transmission in the dentate area of the anaesthetized rabbit following stimulation of the perforant path. The Journal of physiology *232*, 331-356.

Bock, R., Shin, J.H., Kaplan, A.R., Dobi, A., Markey, E., Kramer, P.F., Gremel, C.M., Christensen, C.H., Adrover, M.F., and Alvarez, V.A. (2013). Strengthening the accumbal indirect pathway promotes resilience to compulsive cocaine use. Nature Neuroscience *16*, 632-638.

Bocklisch, C., Pascoli, V., Wong, J.C.Y., House, D.R.C., Yvon, C., De Roo, M., Tan, K.R., and Lüscher, C. (2013). Cocaine disinhibits dopamine neurons by potentiation of GABA transmission in the ventral tegmental area. Science *341*, 1521-1525.

Bolam, J.P., Somogyi, P., Takagi, H., Fodor, I., and Smith, A.D. (1983). Localization of substance P-like immunoreactivity in neurons and nerve terminals in the neostriatum of the rat: a correlated light and electron microscopic study. Journal of neurocytology *12*, 325-344.

Bossert, J.M., Poles, G.C., Wihbey, K.A., Koya, E., and Shaham, Y. (2007). Differential effects of blockade of dopamine D1-family receptors in nucleus accumbens core or shell on reinstatement of heroin seeking induced by contextual and discrete cues. The Journal of neuroscience : the official journal of the Society for Neuroscience *27*, 12655-12663.

Boudreau, A.C., Ferrario, C.R., Glucksman, M.J., and Wolf, M.E. (2009). Signaling pathway adaptations and novel protein kinase A substrates related to behavioral sensitization to cocaine. Journal of Neurochemistry *110*, 363-377.

Boudreau, A.C., Reimers, J.M., Milovanovic, M., and Wolf, M.E. (2007). Cell surface AMPA receptors in the rat nucleus accumbens increase during cocaine withdrawal but internalize after cocaine challenge in association with altered activation of mitogen-activated protein kinases. The Journal of neuroscience : the official journal of the Society for Neuroscience *27*, 10621-10635.

Boudreau, A.C., and Wolf, M.E. (2005). Behavioral sensitization to cocaine is associated with increased AMPA receptor surface expression in the nucleus accumbens. The Journal of neuroscience : the official journal of the Society for Neuroscience *25*, 9144-9151.

Bramham, C.R. (2008). Local protein synthesis, actin dynamics, and LTP consolidation. Current Opinion in Neurobiology *18*, 524-531.

Bramham, C.R., Worley, P.F., Moore, M.J., and Guzowski, J.F. (2008). The immediate early gene arc/arg3.1: regulation, mechanisms, and function. The Journal of neuroscience : the official journal of the Society for Neuroscience *28*, 11760-11767.

Bravo-Rivera, C., Roman-Ortiz, C., Brignoni-Perez, E., Sotres-Bayon, F., and Quirk, G.J. (2014). Neural Structures Mediating Expression and Extinction of Platform-Mediated Avoidance. The Journal of neuroscience : the official journal of the Society for Neuroscience *34*, 9736-9742.

Bravo-Rivera, C., Roman-Ortiz, C., Montesinos-Cartagena, M., and Quirk, G.J. (2015). Persistent active avoidance correlates with activity in prelimbic cortex and ventral striatum. Frontiers in Behavioral Neuroscience *9*, 1-8.

Brebner, K., Wong, T.P., Liu, L., Liu, Y., Campsall, P., Gray, S., Phelps, L., Phillips, A.G., and Wang, Y.T. (2005). Nucleus accumbens long-term depression and the expression of behavioral sensitization. Science *310*, 1340-1343.

Britt, J.P., Benaliouad, F., McDevitt, R.A., Stuber, G.D., Wise, R.A., and Bonci, A. (2012). Synaptic and Behavioral Profile of Multiple Glutamatergic Inputs to the Nucleus Accumbens. Neuron *76*, 790-803.

Brog, J.S., Salyapongse, A., Deutch, A.Y., and Zahm, D.S. (1993). The patterns of afferent innervation of the core and shell in the "accumbens" part of the rat ventral striatum: immunohistochemical detection of retrogradely transported fluoro-gold. The Journal of comparative neurology *338*, 255-278.

Brown, M.T.C., Bellone, C., Mameli, M., Labouèbe, G., Bocklisch, C., Balland, B., Dahan, L., Luján, R., Deisseroth, K., and Lüscher, C. (2010). Drug-driven AMPA receptor redistribution mimicked by selective dopamine neuron stimulation. PLoS ONE *5*, e15870.

Brown, T.E., Lee, B.R., Mu, P., Ferguson, D., Dietz, D., Ohnishi, Y.N., Lin, Y., Suska, A., Ishikawa, M., Huang, Y.H., *et al.* (2011a). A silent synapse-based mechanism for cocaine-induced locomotor sensitization. The Journal of neuroscience : the official journal of the Society for Neuroscience *31*, 8163-8174.

Brown, T.E., Lee, B.R., Mu, P., Ferguson, D., Dietz, D., Ohnishi, Y.N., Lin, Y., Suska, A., Ishikawa, M., Huang, Y.H., *et al.* (2011b). A silent synapse-based mechanism for cocaine-induced locomotor sensitization. J Neurosci *31*, 8163-8174.

Buard, I., Coultrap, S.J., Freund, R.K., Lee, Y.-S., Dell'Acqua, M.L., Silva, A.J., and Bayer, K.U. (2010). CaMKII "autonomy" is required for initiating but not for maintaining neuronal long-term information storage. The Journal of neuroscience : the official journal of the Society for Neuroscience *30*, 8214-8220.

Caffaro, P.A., Suárez, L.D., Blake, M.G., and Delorenzi, A. (2012). Dissociation between memory reactivation and its behavioral expression: scopolamine interferes with memory expression without disrupting long-term storage. Neurobiology of Learning and Memory *98*, 235-245.

Cagniard, B., Beeler, J.A., Britt, J.P., McGehee, D.S., Marinelli, M., and Zhuang, X. (2006). Dopamine scales performance in the absence of new learning. Neuron *51*, 541-547.

Cai, D.J., Aharoni, D., Shuman, T., Shobe, J., Biane, J., Song, W., Wei, B., Veshkini, M., La-Vu, M., Lou, J., *et al.* (2016). A shared neural ensemble links distinct contextual memories encoded close in time. Nature *534*, 115-118.

Caine, S.B., Thomsen, M., Gabriel, K.I., Berkowitz, J.S., Gold, L.H., Koob, G.F., Tonegawa, S., Zhang, J., and Xu, M. (2007). Lack of Self-Administration of Cocaine in Dopamine D1 Receptor Knock-Out Mice. The Journal of neuroscience : the official journal of the Society for Neuroscience *27*, 13140-13150.

Calabrese, B., and Halpain, S. (2005). Essential role for the PKC target MARCKS in maintaining dendritic spine morphology. Neuron *48*, 77-90.

Calipari, E.S., Bagot, R.C., Purushothaman, I., Davidson, T.J., Yorgason, J.T., Peña, C.J., Walker, D.M., Pirpinias, S.T., Guise, K.G., Ramakrishnan, C., *et al.* (2016). In vivo imaging identifies temporal signature of D1 and D2 medium spiny neurons in cocaine reward. Proceedings of the National Academy of Sciences of the United States of America *113*, 2726-2731.

Cameron, C.M., Murugan, M., Choi, J.Y., Engel, E.A., and Witten, I.B. (2019). Increased Cocaine Motivation Is Associated with Degraded Spatial and Temporal Representations in IL-NAc Neurons. Neuron, 1-20.

Cane, M., Maco, B., Knott, G., and Holtmaat, A. (2014). The Relationship between PSD-95 Clustering and Spine Stability In Vivo. The Journal of neuroscience : the official journal of the Society for Neuroscience *34*, 2075-2086.

Carelli, R.M., and Ijames, S.G. (2000). Nucleus accumbens cell firing during maintenance, extinction, and reinstatement of cocaine self-administration behavior in rats. Brain Research *866*, 44-54.

Carelli, R.M., Ijames, S.G., and Crumling, A.J. (2000). Evidence that separate neural circuits in the nucleus accumbens encode cocaine versus "natural" (water and food) reward. The Journal of neuroscience : the official journal of the Society for Neuroscience *20*, 4255-4266.

Carelli, R.M., and Wondolowski, J. (2003). Selective encoding of cocaine versus natural rewards by nucleus accumbens neurons is not related to chronic drug exposure. The Journal of neuroscience : the official journal of the Society for Neuroscience *23*, 11214-11223.

Carlezon, W.A., Duman, R.S., and Nestler, E.J. (2005). The many faces of CREB. Trends in neurosciences *28*, 436-445.

Carrillo-Reid, L., Han, S., Yang, W., Akrouh, A., and Yuste, R. (2019). Controlling Visually Guided Behavior by Holographic Recalling of Cortical Ensembles. Cell, 1-17.

Carrillo-Reid, L., Tecuapetla, F., Tapia, D., Hernández-Cruz, A., Galarraga, E., Drucker-Colin, R., and Bargas, J. (2008). Encoding network states by striatal cell assemblies. Journal of neurophysiology *99*, 1435-1450.

Carrillo-Reid, L., Yang, W., Bando, Y., Peterka, D.S., and Yuste, R. (2016). Imprinting and recalling cortical ensembles. Science *353*, 691-694.

Castillo, P.E., Younts, T.J., Chávez, A.E., and Hashimotodani, Y. (2012). Endocannabinoid Signaling and Synaptic Function. Neuron *76*, 70-81.

Cervo, L., Mukherjee, S., Bertaglia, A., and Samanin, R. (1997). Protein kinases A and C are involved in the mechanisms underlying consolidation of cocaine place conditioning. Brain Research *775*, 30-36.

Chang, H.T., and Kitai, S.T. (1985). Projection neurons of the nucleus accumbens: an intracellular labeling study. Brain Research *347*, 112-116.

Chang, J.-Y., Parra-Bueno, P., Laviv, T., Szatmari, E.M., Lee, S.-J.R., and Yasuda, R. (2017). CaMKII Autophosphorylation Is Necessary for Optimal Integration of Ca2+ Signals during LTP Induction, but Not Maintenance. Neuron *94*, 800-808.e804.

Chang, J.Y., Sawyer, S.F., Lee, R.S., and Woodward, D.J. (1994). Electrophysiological and pharmacological evidence for the role of the nucleus accumbens in cocaine self-administration in freely moving rats. The Journal of neuroscience : the official journal of the Society for Neuroscience *14*, 1224-1244.

Chao, S.Z., Ariano, M.A., Peterson, D.A., and Wolf, M.E. (2002a). D1 dopamine receptor stimulation increases GluR1 surface expression in nucleus accumbens neurons. Journal of Neurochemistry *83*, 704-712.

Chao, S.Z., Lu, W., Lee, H.-K., Huganir, R.L., and Wolf, M.E. (2002b). D(1) dopamine receptor stimulation increases GluR1 phosphorylation in postnatal nucleus accumbens cultures. Journal of Neurochemistry *81*, 984-992.

Chaudhri, N., Sahuque, L.L., Schairer, W.W., and Janak, P.H. (2009). Separable Roles of the Nucleus Accumbens Core and Shell in Context- and Cue-Induced Alcohol-Seeking. Neuropsychopharmacology *35*, 783-791.

Chaudhuri, R., ek, B.G.x.E., Pandey, B., Peyrache, A., and Fiete, I. (2019). The intrinsic attractor manifold and population dynamics of a canonical cognitive circuit across waking and sleep. Nature Neuroscience, 1-13.

Chaudhuri, R., and Fiete, I. (2016). Computational principles of memory. Nature Neuroscience *19*, 394-403.

Chávez, A.E., Chiu, C.Q., and Castillo, P.E. (2010). TRPV1 activation by endogenous anandamide triggers postsynaptic long-term depression in dentate gyrus. Nature Neuroscience *13*, 1511-1518.

Chávez, A.E., Hernández, V.M., Rodenas-Ruano, A., Chan, C.S., and Castillo, P.E. (2014). Compartment-specific modulation of GABAergic synaptic transmission by TRPV1 channels in the dentate gyrus. The Journal of neuroscience : the official journal of the Society for Neuroscience *34*, 16621-16629.

Chavis, P., and Westbrook, G. (2001). Integrins mediate functional pre- and postsynaptic maturation at a hippocampal synapse. Nature *411*, 317-321.

Chen, M.B., Jiang, X., Quake, S.R., and Südhof, T.C. (2020). Persistent transcriptional programmes are associated with remote memory. Nature, 1-21.

Chen, S.X., Kim, A.N., Peters, A.J., and Komiyama, T. (2015). Subtype-specific plasticity of inhibitory circuits in motor cortex during motor learning. Nature Neuroscience *18*, 1109-1115.

Chen, T.-W., Wardill, T.J., Sun, Y., Pulver, S.R., Renninger, S.L., Baohan, A., Schreiter, E.R., Kerr, R.A., Orger, M.B., Jayaraman, V., *et al.* (2013). Ultrasensitive fluorescent proteins for imaging neuronal activity. Nature *499*, 295-300.

Chervyakov, A.V., Chernyavsky, A.Y., Sinitsyn, D.O., and Piradov, M.A. (2015). Possible Mechanisms Underlying the Therapeutic Effects of Transcranial Magnetic Stimulation. Frontiers in human neuroscience *9*, 303.

Chevaleyre, V., and Castillo, P.E. (2003). Heterosynaptic LTD of hippocampal GABAergic synapses: a novel role of endocannabinoids in regulating excitability. Neuron *38*, 461-472.

Chia, C., and Otto, T. (2013). Hippocampal Arc (Arg3.1) expression is induced by memory recall and required for memory reconsolidation in trace fear conditioning. Neurobiology of Learning and Memory *106*, 48-55.

Chklovskii, D.B., Mel, B.W., and Svoboda, K. (2004). Cortical rewiring and information storage. Nature *431*, 782-788.

Choi, D.I.K., Ji-Il; Kim, Jooyoung; Lee, Hoonwon; Choi, Ja Eun; Park, Pojeong; Jung, Hyunsu; Kaang, Bong-Kiun (2020). Synaptic correlates of associative memory in the lateral amygdala. biorxiv.

Choi, J.-H., Sim, S.-E., Kim, J.-I., Choi, D.I., Oh, J., Ye, S., Lee, J., Kim, T., Ko, H.-G., Lim, C.-S., *et al.* (2018). Interregional synaptic maps among engram cells underlie memory formation. Science *360*, 430-435.

Chung, S., Jeong, J.-H., Ko, S., Yu, X., Kim, Y.-H., Isaac, J.T.R., and Koretsky, A.P. (2017). Peripheral Sensory Deprivation Restores Critical- Period-like Plasticity to Adult Somatosensory Thalamocortical Inputs. Cell reports *19*, 2707-2717.

Cichon, J., and Gan, W.-B. (2015). Branch-specific dendritic Ca(2+) spikes cause persistent synaptic plasticity. Nature *520*, 180-185.

Cingolani, L.A., and Goda, Y. (2008). Actin in action: the interplay between the actin cytoskeleton and synaptic efficacy. Nature Reviews Neuroscience *9*, 344-356.

Clem, R.L., and Huganir, R.L. (2010). Calcium-permeable AMPA receptor dynamics mediate fear memory erasure. Science *330*, 1108-1112.

Clements, J.D., and Silver, R.A. (2000). Unveiling synaptic plasticity: a new graphical and analytical approach. Trends in neurosciences *23*, 105-113.

Cohen, J.Y., Haesler, S., Vong, L., Lowell, B.B., and Uchida, N. (2012). Neuron-type-specific signals for reward and punishment in the ventral tegmental area. Nature *482*, 85-88.

Cohen-Cory, S. (2002). The developing synapse: construction and modulation of synaptic structures and circuits. Science *298*, 770-776.

Cole, C.J., Mercaldo, V., Restivo, L., Yiu, A.P., Sekeres, M.J., Han, J.-H., Vetere, G., Pekar, T., Ross, P.J., Neve, R.L., *et al.* (2012). MEF2 negatively regulates learning-induced structural plasticity and memory formation. Nature Neuroscience *15*, 1255-1264.

Conrad, K.L., Tseng, K.Y., Uejima, J.L., Reimers, J.M., Heng, L.-J., Shaham, Y., Marinelli, M., and Wolf, M.E. (2008). Formation of accumbens GluR2-lacking AMPA receptors mediates incubation of cocaine craving. Nature *454*, 118-121.

Corbit, L.H., and Balleine, B.W. (2011). The General and Outcome-Specific Forms of Pavlovian-Instrumental Transfer Are Differentially Mediated by the Nucleus Accumbens Core and Shell. The Journal of neuroscience : the official journal of the Society for Neuroscience *31*, 11786-11794.

Corbit, L.H., Muir, J.L., and Balleine, B.W. (2001). The role of the nucleus accumbens in instrumental conditioning: Evidence of a functional dissociation between accumbens core and shell. The Journal of neuroscience : the official journal of the Society for Neuroscience *21*, 3251-3260.

Corder, G., Ahanonu, B., Grewe, B.F., Wang, D., Schnitzer, M.J., and Scherrer, G. (2019). An amygdalar neural ensemble that encodes the unpleasantness of pain. Science *363*, 276-281.

Cornish, J.L., Duffy, P., and Kalivas, P. (1999). A role for nucleus accumbens glutamate transmission in the relapse to cocaine-seeking behavior. NSC *93*, 1359-1367.

Cornish, J.L., and Kalivas, P. (2000). Glutamate transmission in the nucleus accumbens mediates relapse in cocaine addiction. The Journal of neuroscience : the official journal of the Society for Neuroscience *20*, RC89.

Creed, M., Pascoli, V.J., and Lüscher, C. (2015). Addiction therapy. Refining deep brain stimulation to emulate optogenetic treatment of synaptic pathology. Science *347*, 659-664.

Cruz, F.C., Babin, K.R., Leao, R.M., Goldart, E.M., Bossert, J.M., Shaham, Y., and Hope, B.T. (2014). Role of nucleus accumbens shell neuronal ensembles in context-induced reinstatement of cocaine-seeking. The Journal of neuroscience : the official journal of the Society for Neuroscience *34*, 7437-7446.

Cruz, F.C., Koya, E., Guez-Barber, D.H., Bossert, J.M., Lupica, C.R., Shaham, Y., and Hope, B.T. (2013). New technologies for examining the role of neuronal ensembles in drug addiction and fear. Nature Reviews Neuroscience *14*, 743-754.

Cui, G., Jun, S.B., Jin, X., Pham, M.D., Vogel, S.S., Lovinger, D.M., and Costa, R.M. (2013). Concurrent activation of striatal direct and indirect pathways during action initiation. Nature *494*, 238-242.

Cull-Candy, S., Kelly, L., and Farrant, M. (2006). Regulation of Ca2+-permeable AMPA receptors: synaptic plasticity and beyond. Current Opinion in Neurobiology *16*, 288-297.

Da Silva, W.C., Bonini, J.S., Bevilaqua, L.R.M., Medina, J.H., Izquierdo, I., and Cammarota, M. (2008). Inhibition of mRNA synthesis in the hippocampus impairs consolidation and reconsolidation of spatial memory. Hippocampus *18*, 29-39.

Daie, K., Svoboda, K., and Druckmann, S. (2021). Targeted photostimulation uncovers circuit motifs supporting short-term memory. Nature Neuroscience, 1-25.

Dalton, G.L., Phillips, A.G., and Floresco, S.B. (2014). Preferential involvement by nucleus accumbens shell in mediating probabilistic learning and reversal shifts. The Journal of neuroscience : the official journal of the Society for Neuroscience *34*, 4618-4626.

Davis, G.W. (2013). Homeostatic Signaling and the Stabilization of Neural Function. Neuron *80*, 718-728.

Davis, R.L., and Zhong, Y. (2017). The Biology of Forgetting-A Perspective. Neuron *95*, 490-503.

Davis, W.M., and Smith, S.G. (1976). Role of conditioned reinforcers in the initiation, maintenance and extinction of drug-seeking behavior. The Pavlovian journal of biological science *11*, 222-236.

Day, J.J., Jones, J.L., and Carelli, R.M. (2010). Nucleus accumbens neurons encode predicted and ongoing reward costs in rats. *33*, 308-321.

De Roo, M., Klauser, P., Mendez, P., Poglia, L., and Muller, D. (2008a). Activity-dependent PSD formation and stabilization of newly formed spines in hippocampal slice cultures. Cerebral cortex (New York, NY : 1991) *18*, 151-161.

De Roo, M., Klauser, P., and Muller, D. (2008b). LTP promotes a selective long-term stabilization and clustering of dendritic spines. PLoS Biology *6*, e219.

Deitch, D.R., Alon; Ziv, Yaniv (2020). Representational Drift in the Mouse Visual Cortex. biorxv.

DeNardo, L.A., Liu, C.D., Allen, W.E., Adams, E.L., Friedmann, D., Fu, L., Guenthner, C.J., Tessier-Lavigne, M., and Luo, L. (2019). Temporal evolution of cortical ensembles promoting remote memory retrieval. Nature Neuroscience, 1-15.

Derkach, V.A., Oh, M.C., Guire, E.S., and Soderling, T.R. (2007). Regulatory mechanisms of AMPA receptors in synaptic plasticity. Nature Reviews Neuroscience *8*, 101-113.

Di Chiara, G., and Imperato, A. (1988). Drugs abused by humans preferentially increase synaptic dopamine concentrations in the mesolimbic system of freely moving rats. Proceedings of the National Academy of Sciences *85*, 5274-5278.

Di Ciano, P. (2004). Direct Interactions between the Basolateral Amygdala and Nucleus Accumbens Core Underlie Cocaine-Seeking Behavior by Rats. The Journal of neuroscience : the official journal of the Society for Neuroscience *24*, 7167-7173.

Di Ciano, P., Cardinal, R.N., Cowell, R.A., Little, S.J., and Everitt, B.J. (2001). Differential involvement of NMDA, AMPA/kainate, and dopamine receptors in the nucleus accumbens core in the acquisition and performance of pavlovian approach behavior. The Journal of neuroscience : the official journal of the Society for Neuroscience *21*, 9471-9477.

Diering, G.H., and Huganir, R.L. (2018). The AMPA Receptor Code of Synaptic Plasticity. Neuron *100*, 314-329.

Dietz, D.M., Sun, H., Lobo, M.K., Cahill, M.E., Chadwick, B., Gao, V., Koo, J.W., Mazei-Robison, M.S., Dias, C., Maze, I., *et al.* (2012a). Rac1 is essential in cocaine-induced structural plasticity of nucleus accumbens neurons. Nat Neurosci *15*, 891-896.

Dietz, D.M., Sun, H., Lobo, M.K., Cahill, M.E., Chadwick, B., Gao, V., Koo, J.W., Mazei-Robison, M.S., Dias, C., Maze, I., *et al.* (2012b). Rac1 is essential in cocaine-induced structural plasticity of nucleus accumbens neurons. Nature Neuroscience *15*, 891-896.

Do-Monte, F.H., Quiñones-Laracuente, K., and Quirk, G.J. (2015). A temporal shift in the circuits mediating retrieval of fear memory. Nature *519*, 460-463.

Dobi, A., Seabold, G.K., Christensen, C.H., Bock, R., and Alvarez, V.A. (2011). Cocaine-Induced Plasticity in the Nucleus Accumbens Is Cell Specific and Develops without Prolonged Withdrawal. The Journal of neuroscience : the official journal of the Society for Neuroscience *31*, 1895-1904.

Domnisoru, C., Kinkhabwala, A.A., and Tank, D.W. (2013). Membrane potential dynamics of grid cells. Nature, 1-7.

Dong, Y., Green, T., Saal, D., Marie, H., Neve, R., Nestler, E.J., and Malenka, R.C. (2006). CREB modulates excitability of nucleus accumbens neurons. Nature Neuroscience *9*, 475-477.

Dong, Y., and Nestler, E.J. (2014). The neural rejuvenation hypothesis of cocaine addiction. Trends in pharmacological sciences *35*, 374-383.

Doyère, V., Debiec, J., Monfils, M.-H., Schafe, G.E., and LeDoux, J.E. (2007). Synapse-specific reconsolidation of distinct fear memories in the lateral amygdala. Nature Neuroscience, 1-3.

Driscoll, L.N., Pettit, N.L., Minderer, M., Chettih, S.N., and Harvey, C.D. (2017). Dynamic Reorganization of Neuronal Activity Patterns in Parietal Cortex. Cell, 1-31.

Dudai, Y. (2004). The neurobiology of consolidations, or, how stable is the engram? Annual review of psychology *55*, 51-86.

Dudai, Y. (2012). The Restless Engram: Consolidations Never End. Annual review of neuroscience *35*, 227-247.

Dudai, Y., Karni, A., and Born, J. (2015). The Consolidation and Transformation of Memory. Neuron *88*, 20-32.

Dumitriu, D., LaPlant, Q., Grossman, Y.S., Dias, C., Janssen, W.G., Russo, S.J., Morrison, J.H., and Nestler, E.J. (2012). Subregional, dendritic compartment, and spine subtype specificity in cocaine regulation of dendritic spines in the nucleus accumbens. The Journal of neuroscience : the official journal of the Society for Neuroscience *32*, 6957-6966.

Dumitriu, D., Rodriguez, A., and Morrison, J.H. (2011). High-throughput, detailed, cell-specific neuroanatomy of dendritic spines using microinjection and confocal microscopy. Nature protocols *6*, 1391-1411.

Dunbar, A.B., and Taylor, J.R. (2017). Reconsolidation and psychopathology: Moving towards reconsolidation-based treatments. Neurobiology of Learning and Memory *142*, 162-171.

Dunsmoor, J.E., Niv, Y., Daw, N., and Phelps, E.A. (2015). Rethinking Extinction. Neuron *88*, 47-63.

Durand, G.M., Kovalchuk, Y., and Konnerth, A. (1996). Long-term potentiation and functional synapse induction in developing hippocampus. Nature *381*, 71-75.

Duvarci, S., Nader, K., and LeDoux, J.E. (2005). Activation of extracellular signal-regulated kinase- mitogen-activated protein kinase cascade in the amygdala is required for memory reconsolidation of auditory fear conditioning. The European journal of neuroscience *21*, 283-289.

Ehrlich, I., Klein, M., Rumpel, S., and Malinow, R. (2007). PSD-95 is required for activity-driven synapse stabilization. Proceedings of the National Academy of Sciences *104*, 4176-4181.

El-Husseini, A.E., Schnell, E., Chetkovich, D.M., Nicoll, R.A., and Bredt, D.S. (2000). PSD-95 involvement in maturation of excitatory synapses. Science *290*, 1364-1368.

Elkobi, A., Ehrlich, I., Belelovsky, K., Barki-Harrington, L., and Rosenblum, K. (2008). ERK-dependent PSD-95 induction in the gustatory cortex is necessary for taste learning, but not retrieval. Nature Neuroscience *11*, 1149-1151.

Ellefsen, K.O., Mouret, J.-B., and Clune, J. (2015). Neural modularity helps organisms evolve to learn new skills without forgetting old skills. PLOS Computational Biology *11*, e1004128.

Engert, F., and Bonhoeffer, T. (1999). Dendritic spine changes associated with hippocampal long-term synaptic plasticity. Nature *399*, 66-70.

Epstein, D.H., Preston, K.L., Stewart, J., and Shaham, Y. (2006). Toward a model of drug relapse: an assessment of the validity of the reinstatement procedure. Psychopharmacology *189*, 1-16.

Eroglu, C., Allen, N.J., Susman, M.W., Rourke, N.A.O., Park, C.Y., Ozkan, E., Chakraborty, C., Mulinyawe, S.B., Annis, D.S., Huberman, A.D., *et al.* (2009). Gabapentin Receptor α2δ-1 Is a Neuronal Thrombospondin Receptor Responsible for Excitatory CNS Synaptogenesis. Cell *139*, 380-392.

Eroglu, C., and Barres, B.A. (2010). Regulation of synaptic connectivity by glia. Nature *468*, 223-231.

Eshel, N., Bukwich, M., Rao, V., Hemmelder, V., Tian, J., and Uchida, N. (2015). Arithmetic and local circuitry underlying dopamine prediction errors. Nature *525*, 243-246.

Esteban, J.A., Shi, S.-H., Wilson, C., Nuriya, M., Huganir, R.L., and Malinow, R. (2003). PKA phosphorylation of AMPA receptor subunits controls synaptic trafficking underlying plasticity. Nature Neuroscience *6*, 136-143.

Everitt, B.J., and Robbins, T.W. (2005). Neural systems of reinforcement for drug addiction: from actions to habits to compulsion. Nature Neuroscience *8*, 1481-1489.

Everitt, B.J., and Robbins, T.W. (2013). From the ventral to the dorsal striatum: devolving views of their roles in drug addiction. Neuroscience and biobehavioral reviews *37*, 1946-1954.

Everitt, B.J., and Robbins, T.W. (2016). Drug Addiction: Updating Actions to Habits to Compulsions Ten Years On. Annual review of psychology *67*, 23-50.

Famous, K.R., Kumaresan, V., Sadri-Vakili, G., Schmidt, H.D., Mierke, D.F., Cha, J.H.J., and Pierce, R.C. (2008). Phosphorylation-Dependent Trafficking of GluR2-Containing AMPA Receptors in the Nucleus Accumbens Plays a Critical Role in the Reinstatement of Cocaine Seeking. The Journal of neuroscience : the official journal of the Society for Neuroscience *28*, 11061-11070.

Favaro, P.D., Huang, X., Hosang, L., Stodieck, S., Cui, L., Liu, Y.-z., Engelhardt, K.-A., Schmitz, F., Dong, Y., Löwel, S., *et al.* (2018). An opposing function of paralogs in balancing developmental synapse maturation. PLoS Biology *16*, e2006838.

Feja, M., Hayn, L., and Koch, M. (2014). Nucleus accumbens core and shell inactivation differentially affects impulsive behaviours in rats. Progress in neuro-psychopharmacology & biological psychiatry *54*, 31-42.

Ferrara, N.C., Jarome, T.J., Cullen, P.K., Orsi, S.A., Kwapis, J.L., Trask, S., Pullins, S.E., and Helmstetter, F.J. (2019). GluR2 endocytosis-dependent protein degradation in the amygdala mediates memory updating. Scientific Reports, 1-10.

Ferrario, C.R., Loweth, J.A., Milovanovic, M., Ford, K.A., Galinanes, G.L., Heng, L.J., Tseng, K.Y., and Wolf, M.E. (2011). Alterations in AMPA receptor subunits and TARPs in the rat nucleus accumbens related to the formation of Ca(2)(+)-permeable AMPA receptors during the incubation of cocaine craving. Neuropharmacology *61*, 1141-1151.

Fibiger, H.C., LePiane, F.G., Jakubovic, A., and Phillips, A.G. (1987). The role of dopamine in intracranial self-stimulation of the ventral tegmental area. The Journal of neuroscience : the official journal of the Society for Neuroscience *7*, 3888-3896.

Finkelstein, A., Fontolan, L., Economo, M.N., Li, N., Romani, S., and Svoboda, K. (2021). Attractor dynamics gate cortical information flow during decision-making. Nature Neuroscience, 1-26.

Fitzgerald, P.J., Pinard, C.R., Camp, M.C., Feyder, M., Sah, A., Bergstrom, H.C., Graybeal, C., Liu, Y., ter, O.M.S.u., Grant, S.G., *et al.* (2019). Durable fear memories require PSD-95. 1-12.

Flavell, C.R., Barber, D.J., and Lee, J.L.C. (2011). Behavioural memory reconsolidation of food and fear memories. Nature Communications *2*, 504-509.

Floresco, S.B. (2015). The nucleus accumbens: an interface between cognition, emotion, and action. Annual review of psychology *66*, 25-52.

Floresco, S.B., Montes, D.R., Tse, M.M.T., and van Holstein, M. (2018). Differential Contributions of Nucleus Accumbens Subregions to Cue-Guided Risk/Reward Decision Making and Implementation of Conditional Rules. The Journal of neuroscience : the official journal of the Society for Neuroscience *38*, 1901-1914.

Frankland, P.W., Josselyn, S.A., and Köhler, S. (2019). The neurobiological foundation of memory retrieval. Nature Neuroscience, 1-10.

Freiman, I., Anton, A., Monyer, H., Urbanski, M.J., and Szabo, B. (2006). Analysis of the effects of cannabinoids on identified synaptic connections in the caudate-putamen by paired recordings in transgenic mice. The Journal of physiology *575*, 789-806.

French, R. (1999). Catastrophic forgetting in connectionist networks. Trends in cognitive sciences *3*, 128-135.

French, S.J., and Totterdell, S. (2002). Hippocampal and prefrontal cortical inputs monosynaptically converge with individual projection neurons of the nucleus accumbens. The Journal of comparative neurology *446*, 151-165.

French, S.J., and Totterdell, S. (2003). Individual nucleus accumbens-projection neurons receive both basolateral amygdala and ventral subicular afferents in rats. NSC *119*, 19-31.

Friedrich, J., Zhou, P., and Paninski, L. (2017). Fast online deconvolution of calcium imaging data. PLOS Computational Biology *13*, e1005423.

Fu, M., Yu, X., Lu, J., and Zuo, Y. (2012). Repetitive motor learning induces coordinated formation of clustered dendritic spines in vivo. Nature *482*, 92-95.

Fuchs, R.A., Bell, G.H., Ramirez, D.R., Eaddy, J.L., and Su, Z.I. (2009). Basolateral amygdala involvement in memory reconsolidation processes that facilitate drug context-induced cocaine seeking. The European journal of neuroscience *30*, 889-900.

Fuchs, R.A., Evans, K.A., Parker, M.C., and See, R.E. (2004a). Differential involvement of the core and shell subregions of the nucleus accumbens in conditioned cue-induced reinstatement of cocaine seeking in rats. Psychopharmacology (Berl) *176*, 459-465.

Fuchs, R.A., Evans, K.A., Parker, M.C., and See, R.E. (2004b). Differential involvement of the core and shell subregions of the nucleus accumbens in conditioned cue-induced reinstatement of cocaine seeking in rats. Psychopharmacology *176*, 459-465.

Fuchs, R.A., Ramirez, D.R., and Bell, G.H. (2008). Nucleus accumbens shell and core involvement in drug context-induced reinstatement of cocaine seeking in rats. Psychopharmacology *200*, 545-556.

Fukazawa, Y., Saitoh, Y., Ozawa, F., Ohta, Y., Mizuno, K., and Inokuchi, K. (2003). Hippocampal LTP is accompanied by enhanced F-actin content within the dendritic spine that is essential for late LTP maintenance in vivo. Neuron *38*, 447-460.

Fukushima, H., Zhang, Y., Archbold, G., Ishikawa, R., Nader, K., and Kida, S. (2014). Enhancement of fear memory by retrieval through reconsolidation. eLife *3*, 417-419.

Fusi, S. (2002). Hebbian spike-driven synaptic plasticity for learning patterns of mean firing rates. Biological cybernetics *87*, 459-470.

Fusi, S., and Abbott, L.F. (2007). Limits on the memory storage capacity of bounded synapses. Nature Neuroscience *10*, 485-493.

Gambrill, A.C., and Barria, A. (2011). NMDA receptor subunit composition controls synaptogenesis and synapse stabilization. Proceedings of the National Academy of Sciences of the United States of America *108*, 5855-5860.

Gao, C., Sun, X., and Wolf, M.E. (2006). Activation of D1 dopamine receptors increases surface expression of AMPA receptors and facilitates their synaptic incorporation in cultured hippocampal neurons. Journal of Neurochemistry *98*, 1664-1677.

Gawin, F.H., and Kleber, H.D. (1986). Abstinence symptomatology and psychiatric diagnosis in cocaine abusers. Clinical observations. Archives of general psychiatry *43*, 107-113.

Geddes, C.E., Li, H., and Jin, X. (2018). Optogenetic Editing Reveals the Hierarchical Organization of Learned Action Sequences. Cell *174*, 32-43.e15.

Gerfen, C.R., Engber, T.M., Mahan, L.C., Susel, Z., Chase, T.N., Monsma, F.J., and Sibley, D.R. (1990). D1 and D2 dopamine receptor-regulated gene expression of striatonigral and striatopallidal neurons. Science *250*, 1429-1432.

Ghazizadeh, A., Ambroggi, F., Odean, N., and Fields, H.L. (2012). Prefrontal Cortex Mediates Extinction of Responding by Two Distinct Neural Mechanisms in Accumbens Shell. The Journal of neuroscience : the official journal of the Society for Neuroscience *32*, 726-737.

Ghitza, U.E., Fabbricatore, A.T., Prokopenko, V., Pawlak, A.P., and West, M.O. (2003). Persistent cue-evoked activity of accumbens neurons after prolonged abstinence from self-administered cocaine. The Journal of neuroscience : the official journal of the Society for Neuroscience *23*, 7239-7245.

Ghosh, M., Song, X., Mouneimne, G., Sidani, M., Lawrence, D.S., and Condeelis, J.S. (2004). Cofilin promotes actin polymerization and defines the direction of cell motility. Science *304*, 743-746.

Gibson, G.D., Prasad, A.A., Jean-Richard-Dit-Bressel, P., Yau, J.O.Y., Millan, E.Z., Liu, Y., Campbell, E.J., Lim, J., Marchant, N.J., Power, J.M., *et al.* (2018). Distinct Accumbens Shell Output Pathways Promote versus Prevent Relapse to Alcohol Seeking. Neuron, 1-16.

Giovannucci, A., Friedrich, J., Gunn, P., Kalfon, J., Brown, B.L., Koay, S.A., Taxidis, J., Najafi, F., Gauthier, J.L., Zhou, P., *et al.* (2019). CaImAn an open source tool for scalable calcium imaging data analysis. eLife *8*, 413.

Gipson, C.D., Kupchik, Y.M., and Kalivas, P. (2013a). Rapid, transient synaptic plasticity in addiction. Neuropharmacology, 1-11.

Gipson, C.D., Kupchik, Y.M., Shen, H., Reissner, K.J., Thomas, C.A., and Kalivas, P. (2013b). Relapse Induced by Cues Predicting Cocaine Depends on Rapid, Transient Synaptic Potentiation. Neuron, 1-6.

Girardeau, G., Benchenane, K., Wiener, S.I., Buzsáki, G., and Zugaro, M.B. (2009). Selective suppression of hippocampal ripples impairs spatial memory. Nature Neuroscience, 1-2.

Gittis, A.H., Nelson, A.B., Thwin, M.T., Palop, J.J., and Kreitzer, A.C. (2010). Distinct roles of GABAergic interneurons in the regulation of striatal output pathways. The Journal of neuroscience : the official journal of the Society for Neuroscience *30*, 2223-2234.

Gmaz, J.M., Carmichael, J.E., and van der Meer, M.A. (2018). Persistent coding of outcome-predictive cue features in the rat nucleus accumbens. eLife *7*, 1096.

Goldstein, B.L., Barnett, B.R., Vasquez, G., Tobia, S.C., Kashtelyan, V., Burton, A.C., Bryden, D.W., and Roesch, M.R. (2012). Ventral Striatum Encodes Past and Predicted Value Independent of Motor Contingencies. The Journal of neuroscience : the official journal of the Society for Neuroscience *32*, 2027-2036.

Goltseker, K., Bolotin, L., and Barak, S. (2017). Counterconditioning During Reconsolidation Prevents Relapse of Cocaine Memories. Neuropsychopharmacology *42*, 716-726.

Gonzales, K.K., and Smith, Y. (2015). Cholinergic interneurons in the dorsal and ventral striatum: anatomical and functional considerations in normal and diseased conditions. Annals of the New York Academy of Sciences *1349*, 1-45.

Gonzalez, W.G., Zhang, H., Harutyunyan, A., and Lois, C. (2019). Persistence of neuronal representations through time and damage in the hippocampus. Science *365*, 821-825.

Goode, T.D., Tanaka, K.Z., Sahay, A., and McHugh, T.J. (2020). An Integrated Index: Engrams, Place Cells, and Hippocampal Memory. Neuron, 1-16.

Gorelick, D.A., Zangen, A., and George, M.S. (2014). Transcranial magnetic stimulation in the treatment of substance addiction. Annals of the New York Academy of Sciences *1327*, 79-93.

Graham, D.L., Edwards, S., Bachtell, R.K., DiLeone, R.J., Rios, M., and Self, D.W. (2007). Dynamic BDNF activity in nucleus accumbens with cocaine use increases self-administration and relapse. Nature Neuroscience *10*, 1029-1037.

Gray, J.A., Shi, Y., Usui, H., During, M.J., Sakimura, K., and Nicoll, R.A. (2011). Distinct Modes of AMPA Receptor Suppression at Developing Synapses by GluN2A and GluN2B: Single-Cell NMDA Receptor Subunit Deletion In Vivo. Neuron *71*, 1085-1101.

Graziane, N.M., Sun, S., Wright, W.J., Jang, D., Liu, Z., Huang, Y.H., Nestler, E.J., Wang, Y.T., Schlüter, O.M., and Dong, Y. (2016). Opposing mechanisms mediate morphine- and cocaine-induced generation of silent synapses. Nature Neuroscience *19*, 915-925.

Grewe, B.F., Gründemann, J., Kitch, L.J., Lecoq, J.A., Parker, J.G., Marshall, J.D., Larkin, M.C., Jercog, P.E., Grenier, F., Li, J.Z., *et al.* (2017). Neural ensemble dynamics underlying a long-term associative memory. Nature, 1-23.

Grimm, J.W., Hope, B.T., Wise, R.A., and Shaham, Y. (2001). Neuroadaptation. Incubation of cocaine craving after withdrawal. Nature *412*, 141-142.

Grimm, J.W., Lu, L., Hayashi, T., Hope, B.T., Su, T.-P., and Shaham, Y. (2003). Time-dependent increases in brain-derived neurotrophic factor protein levels within the mesolimbic dopamine system after withdrawal from cocaine: implications for incubation of cocaine craving. The Journal of neuroscience : the official journal of the Society for Neuroscience *23*, 742-747.

Gritton, H.J., Howe, W.M., Romano, M.F., DiFeliceantonio, A.G., Kramer, M.A., Saligrama, V., Bucklin, M.E., Zemel, D., and Han, X. (2019). Unique contributions of parvalbumin and cholinergic interneurons in organizing striatal networks during movement. Nature Neuroscience, 1-20.

Groc, L., Gustafsson, B., and Hanse, E. (2006). AMPA signalling in nascent glutamatergic synapses: there and not there! Trends in neurosciences *29*, 132-139.

Grueter, B.A., Brasnjo, G., and Malenka, R.C. (2010). Postsynaptic TRPV1 triggers cell type-specific long-term depression in the nucleus accumbens. Nature Neuroscience *13*, 1519-1525.

Grueter, B.A., Robison, A.J., Neve, R.L., Nestler, E.J., and Malenka, R.C. (2013). ΔFosB differentially modulates nucleus accumbens direct and indirect pathway function. Proceedings of the National Academy of Sciences of the United States of America *110*, 1923-1928.

Gründemann, J., Bitterman, Y., Lu, T., Krabbe, S., Grewe, B.F., Schnitzer, M.J., and Lüthi, A. (2019). Amygdala ensembles encode behavioral states. Science *364*.

Guillem, K., and Ahmed, S.H. (2018). Incubation of Accumbal Neuronal Reactivity to Cocaine Cues During Abstinence Predicts Individual Vulnerability to Relapse. Nature Neuroscience *43*, 1059-1065.

Guillem, K., Ahmed, S.H., and Peoples, L.L. (2014). Escalation of cocaine intake and incubation of cocaine seeking are correlated with dissociable neuronal processes in different accumbens subregions. Biological Psychiatry *76*, 31-39.

Guire, E.S., Oh, M.C., Soderling, T.R., and Derkach, V.A. (2008). Recruitment of Calcium-Permeable AMPA Receptors during Synaptic Potentiation Is Regulated by CaM-Kinase I. The Journal of neuroscience : the official journal of the Society for Neuroscience *28*, 6000-6009.

Guzowski, J.F., Lyford, G.L., Stevenson, G.D., Houston, F.P., McGaugh, J.L., Worley, P.F., and Barnes, C.A. (2000). Inhibition of activity-dependent arc protein expression in the rat hippocampus impairs the maintenance of long-term potentiation and the consolidation of long-term memory. The Journal of neuroscience : the official journal of the Society for Neuroscience *20*, 3993-4001.

Guzowski, J.F., McNaughton, B.L., Barnes, C.A., and Worley, P.F. (1999). Environment-specific expression of the immediate-early gene Arc in hippocampal neuronal ensembles. Nature Neuroscience *2*, 1120-1124.

Hainmueller, T., and Bartos, M. (2018). Parallel emergence of stable and dynamic memory engrams in the hippocampus. Nature, 1-22.

Hamid, A.A., Pettibone, J.R., Mabrouk, O.S., Hetrick, V.L., Schmidt, R., Vander Weele, C.M., Kennedy, R.T., Aragona, B.J., and Berke, J.D. (2015). Mesolimbic dopamine signals the value of work. Nature Neuroscience *19*, 117-126.

Han, J.-H., Kushner, S.A., Yiu, A.P., Cole, C.J., Matynia, A., Brown, R.A., Neve, R.L., Guzowski, J.F., Silva, A.J., and Josselyn, S.A. (2007). Neuronal competition and selection during memory formation. Science *316*, 457-460.

Han, J.-H., Kushner, S.A., Yiu, A.P., Hsiang, H.-L.L., Buch, T., Waisman, A., Bontempi, B., Neve, R.L., Frankland, P.W., and Josselyn, S.A. (2009). Selective erasure of a fear memory. Science *323*, 1492-1496.

Hartley, N.D., Gaulden, A.D., ldi, R.B.x.E., Winters, N.D., Salimando, G.J., Rosas-Vidal, L.E., Jameson, A., Winder, D.G., and Patel, S. (2019). Dynamic remodeling of a basolateral-to-central amygdala glutamatergic circuit across fear states. Nature Neuroscience, 1-27.

Harward, S.C., Hedrick, N.G., Hall, C.E., Parra-Bueno, P., Milner, T.A., Pan, E., Laviv, T., Hempstead, B.L., Yasuda, R., and McNamara, J.O. (2016). Autocrine BDNF-TrkB signalling within a single dendritic spine. Nature *538*, 99-103.

Hasegawa, S., Sakuragi, S., Tominaga-Yoshino, K., and Ogura, A. (2015). Dendritic spine dynamics leading to spine elimination after repeated inductions of LTD. Scientific Reports *5*, 7707-7706.

Haubrich, J., Crestani, A.P., Cassini, L.F., Santana, F., Sierra, R.O., Alvares, L.d.O., and Quillfeldt, J.A. (2015). Reconsolidation allows fear memory to be updated to a less aversive level through the incorporation of appetitive information. Neuropsychopharmacology *40*, 315-326.

Hayama, T., Noguchi, J., Watanabe, S., Takahashi, N., Hayashi-Takagi, A., Ellis-Davies, G.C.R., Matsuzaki, M., and Kasai, H. (2013). GABA promotes the competitive selection of dendritic spines by controlling local Ca2+ signaling. Nature Neuroscience *16*, 1409-1416.

Hayashi, Y., Shi, S.H., Esteban, J.A., Piccini, A., Poncer, J.C., and Malinow, R. (2000). Driving AMPA receptors into synapses by LTP and CaMKII: requirement for GluR1 and PDZ domain interaction. Science *287*, 2262-2267.

Hayashi-Takagi, A., Yagishita, S., Nakamura, M., Shirai, F., Wu, Y.I., Loshbaugh, A.L., Kuhlman, B., Hahn, K.M., and Kasai, H. (2015). Labelling and optical erasure of synaptic memory traces in the motor cortex. Nature *525*, 333-338.

Hebb, D.O. (1949). The Organization of Behavior; a neuropsychological theory. Wiley, 1-365.

Hedrick, N.G., Harward, S.C., Hall, C.E., Murakoshi, H., McNamara, J.O., and Yasuda, R. (2016). Rho GTPase complementation underlies BDNF-dependent homo- and heterosynaptic plasticity. Nature *538*, 104-108.

Hedrick, N.G., and Yasuda, R. (2017). Regulation of Rho GTPase proteins during spine structural plasticity for the control of local dendritic plasticity. Current Opinion in Neurobiology *45*, 193-201.

Heinsbroek, J.A., Neuhofer, D.N., Griffin, W.C., Siegel, G.S., Bobadilla, A.C., Kupchik, Y.M., and Kalivas, P. (2016). Loss of plasticity in the D2-accumbens pallidal pathway promotes cocaine seeking. The Journal of neuroscience : the official journal of the Society for Neuroscience, 1-37.

Hering, H., and Sheng, M. (2001). Dendritic spines: structure, dynamics and regulation. Nature Reviews Neuroscience *2*, 880-888.

Herry, C., and Garcia, R. (2002). Prefrontal cortex long-term potentiation, but not long-term depression, is associated with the maintenance of extinction of learned fear in mice. The Journal of neuroscience : the official journal of the Society for Neuroscience *22*, 577-583.

Hofer, S.B., Mrsic-Flogel, T.D., Bonhoeffer, T., and Hübener, M. (2008). Experience leaves a lasting structural trace in cortical circuits. Nature *457*, 313-318.

Hollander, J.A., and Carelli, R.M. (2005). Abstinence from cocaine self-administration heightens neural encoding of goal-directed behaviors in the accumbens. Neuropsychopharmacology *30*, 1464-1474.

Hollander, J.A., and Carelli, R.M. (2007). Cocaine-associated stimuli increase cocaine seeking and activate accumbens core neurons after abstinence. The Journal of neuroscience : the official journal of the Society for Neuroscience *27*, 3535-3539.

Holtmaat, A., and Caroni, P. (2016). Functional and structural underpinnings of neuronal assembly formation in learning. Nature Neuroscience, 1-10.

Holtmaat, A., and Svoboda, K. (2009). Experience-dependent structural synaptic plasticity in the mammalian brain. Nature Reviews Neuroscience *10*, 647-658.

Holtmaat, A., Wilbrecht, L., Knott, G.W., Welker, E., and Svoboda, K. (2006). Experience-dependent and cell-type-specific spine growth in the neocortex. Nature *441*, 979-983.

Hong, I., Kim, J., Kim, J., Lee, S., Ko, H.-G., Nader, K., Kaang, B.-K., Tsien, R.W., and Choi, S. (2013). AMPA receptor exchange underlies transient memory destabilization on retrieval. Proceedings of the National Academy of Sciences of the United States of America *110*, 8218-8223.

Honkura, N., Matsuzaki, M., Noguchi, J., Ellis-Davies, G.C.R., and Kasai, H. (2008). The Subspine Organization of Actin Fibers Regulates the Structure and Plasticity of Dendritic Spines. Neuron *57*, 719-729.

Hopfield, J.J., and Tank, D.W. (1986). Computing with neural circuits: a model. Science *233*, 625-633.

Hoppa, M.B., Lana, B., Margas, W., Dolphin, A.C., and Ryan, T.A. (2012). α2δ expression sets presynaptic calcium channel abundance and release probability. Nature *486*, 122-125.

Hou, H., Chavez, A.E., Wang, C.C., Yang, H., Gu, H., Siddoway, B.A., Hall, B.J., Castillo, P.E., and Xia, H. (2014). The Rac1 Inhibitor NSC23766 Suppresses CREB Signaling by Targeting NMDA Receptor Function. The Journal of neuroscience : the official journal of the Society for Neuroscience *34*, 14006-14012.

Howe, M.W., Tierney, P.L., Sandberg, S.G., Phillips, P.E.M., and Graybiel, A.M. (2013). Prolonged dopamine signalling in striatum signals proximity and value of distant rewards. Nature, 1-16.

Huang, F., Chotiner, J.K., and Steward, O. (2007). Actin polymerization and ERK phosphorylation are required for Arc/Arg3.1 mRNA targeting to activated synaptic sites on dendrites. The Journal of neuroscience : the official journal of the Society for Neuroscience *27*, 9054-9067.

Huang, X., Stodieck, S.K., Goetze, B., Cui, L., Wong, M.H., Wenzel, C., Hosang, L., Dong, Y., Löwel, S., and Schlüter, O.M. (2015a). Progressive maturation of silent synapses governs the duration of a critical period. Proceedings of the National Academy of Sciences *112*, E3131-E3140.

Huang, Y.H., Lin, Y., Mu, P., Lee, B.R., Brown, T.E., Wayman, G., Marie, H., Liu, W., Yan, Z., Sorg, B.A., *et al.* (2009). In vivo cocaine experience generates silent synapses. Neuron *63*, 40-47.

Huang, Y.H., Schlüter, O.M., and Dong, Y. (2015b). Silent Synapses Speak Up: Updates of the Neural Rejuvenation Hypothesis of Drug Addiction. The Neuroscientist : a review journal bringing neurobiology, neurology and psychiatry *21*, 451-459.

Huber, D., Gutnisky, D.A., Peron, S., O'Connor, D.H., Wiegert, J.S., Tian, L., Oertner, T.G., Looger, L.L., and Svoboda, K. (2012). Multiple dynamic representations in the motor cortex during sensorimotor learning. Nature *484*, 473-478.

Huganir, R.L., and Nicoll, R.A. (2013). AMPARs and Synaptic Plasticity: The Last 25 Years. Neuron *80*, 704-717.

Huynh, T.N., Santini, E., and Klann, E. (2014). Requirement of Mammalian Target of Rapamycin Complex 1 Downstream Effectors in Cued Fear Memory Reconsolidation and Its Persistence. The Journal of neuroscience : the official journal of the Society for Neuroscience *34*, 9034-9039.

Hyman, S.E. (2005). Addiction: a disease of learning and memory. The American journal of psychiatry *162*, 1414-1422.

Hyman, S.E., Malenka, R.C., and Nestler, E.J. (2006a). Neural mechanisms of addiction: the role of reward-related learning and memory. Annu Rev Neurosci *29*, 565-598.

Hyman, S.E., Malenka, R.C., and Nestler, E.J. (2006b). Neural mechanisms of addiction: the role of reward-related learning and memory. Annual review of neuroscience *29*, 565-598.

Iino, Y., Sawada, T., Yamaguchi, K., Tajiri, M., Ishii, S., Kasai, H., and Yagishita, S. (2020). Dopamine D2 receptors in discrimination learning and spine enlargement. Nature, 1-26.

Inagaki, H.K., Fontolan, L., Romani, S., and Svoboda, K. (2019). Discrete attractor dynamics underlies persistent activity in the frontal cortex. Nature, 1-30.

Isaac, J.T., Nicoll, R.A., and Malenka, R.C. (1995). Evidence for silent synapses: implications for the expression of LTP. Neuron *15*, 427-434.

Isaac, J.T.R., Ashby, M.C., and McBain, C.J. (2007). The role of the GluR2 subunit in AMPA receptor function and synaptic plasticity. Neuron *54*, 859-871.

Ishikawa, A., Ambroggi, F., Nicola, S.M., and Fields, H.L. (2008). Dorsomedial prefrontal cortex contribution to behavioral and nucleus accumbens neuronal responses to incentive cues. The Journal of neuroscience : the official journal of the Society for Neuroscience *28*, 5088-5098.

Ishikawa, M., Mu, P., Moyer, J.T., Wolf, J.A., Quock, R.M., Davies, N.M., Hu, X.-T., Schlüter, O.M., and Dong, Y. (2009). Homeostatic synapse-driven membrane plasticity in nucleus accumbens neurons. The Journal of neuroscience : the official journal of the Society for Neuroscience *29*, 5820-5831.

Ito, R., and Hayen, A. (2011). Opposing roles of nucleus accumbens core and shell dopamine in the modulation of limbic information processing. The Journal of neuroscience : the official journal of the Society for Neuroscience *31*, 6001-6007.

Ito, R., Robbins, T.W., and Everitt, B.J. (2004). Differential control over cocaine-seeking behavior by nucleus accumbens core and shell. Nature Neuroscience *7*, 389-397.

Ito, R., Robbins, T.W., Pennartz, C.M., and Everitt, B.J. (2008). Functional Interaction between the Hippocampus and Nucleus Accumbens Shell Is Necessary for the Acquisition of Appetitive Spatial Context Conditioning. The Journal of neuroscience : the official journal of the Society for Neuroscience *28*, 6950-6959.

Ito, W., Erisir, A., and Morozov, A. (2015). Observation of Distressed Conspecific as a Model of Emotional Trauma Generates Silent Synapses in the Prefrontal-Amygdala Pathway and Enhances Fear Learning, but Ketamine Abolishes those Effects. Neuropsychopharmacology *40*, 2536-2545.

Ito, W., and Morozov, A. (2019). Prefrontal-amygdala plasticity enabled by observational fear. Neuropsychopharmacology *44*, 1778-1787.

Jadhav, S.P., Kemere, C., German, P.W., and Frank, L.M. (2012). Awake hippocampal sharp-wave ripples support spatial memory. Science *336*, 1454-1458.

Jin, X., Tecuapetla, F., and Costa, R.M. (2014). Basal ganglia subcircuits distinctively encode the parsing and concatenation of action sequences. Nature Neuroscience *17*, 423-430.

Jobes, M.L., Aharonovich, E., Epstein, D.H., Phillips, K.A., Reamer, D., Anderson, M., and Preston, K.L. (2015). Effects of Prereactivation Propranolol on Cocaine Craving Elicited by Imagery Script/Cue Sets in Opioid-dependent Polydrug Users: A Randomized Study. J Addict Med *9*, 491-498.

Joffe, M.E., and Grueter, B.A. (2016). Cocaine Experience Enhances Thalamo-Accumbens N-Methyl-D-Aspartate Receptor Function. Biological Psychiatry.

Johansen, J.P., Cain, C.K., Ostroff, L.E., and LeDoux, J.E. (2011). Molecular mechanisms of fear learning and memory. Cell *147*, 509-524.

Jones, M.W., Errington, M.L., French, P.J., Fine, A., Bliss, T.V., Garel, S., Charnay, P., Bozon, B., Laroche, S., and Davis, S. (2001). A requirement for the immediate early gene Zif268 in the expression of late LTP and long-term memories. Nature Neuroscience *4*, 289-296.

Jonkman, S., and Everitt, B.J. (2011). Dorsal and ventral striatal protein synthesis inhibition affect reinforcer valuation but not the consolidation of instrumental learning. Learning & Memory *18*, 617-624.

Josselyn, S.A., Köhler, S., and Frankland, P.W. (2015). Finding the engram. Nature Reviews Neuroscience *16*, 521-534.

Josselyn, S.A., and Tonegawa, S. (2020). Memory engrams: Recalling the past and imagining the future. Science *367*, eaaw4325.

Ju, H., and Bassett, D.S. (2020). Dynamic representations in networked neural systems. Nature Neuroscience, 1-10.

Kalivas, P., Volkow, N., and Seamans, J. (2005). Unmanageable Motivation in Addiction: A Pathology in Prefrontal-Accumbens Glutamate Transmission. Neuron *45*, 647-650.

Kandel, E.R., Dudai, Y., and Mayford, M.R. (2014). The Molecular and Systems Biology of Memory. Cell *157*, 163-186.

Kasai, H., Fukuda, M., Watanabe, S., Hayashi-Takagi, A., and Noguchi, J. (2010). Structural dynamics of dendritic spines in memory and cognition. Trends in neurosciences *33*, 121-129.

Katz, L.C., and Shatz, C.J. (1996). Synaptic activity and the construction of cortical circuits. Science *274*, 1133-1138.

Kauer, J.A., and Malenka, R.C. (2007). Synaptic plasticity and addiction. Nature Reviews Neuroscience *8*, 844-858.

Kauer, J.A., Malenka, R.C., and Nicoll, R.A. (1988). NMDA application potentiates synaptic transmission in the hippocampus. Nature *334*, 250-252.

Kawaguchi, Y. (1993). Physiological, morphological, and histochemical characterization of three classes of interneurons in rat neostriatum. The Journal of neuroscience : the official journal of the Society for Neuroscience *13*, 4908-4923.

Kawaguchi, Y., Wilson, C.J., Augood, S.J., and Emson, P.C. (1995). Striatal interneurones: chemical, physiological and morphological characterization. Trends in neurosciences *18*, 527-535.

Kelley, A.E. (2004). Memory and addiction: shared neural circuitry and molecular mechanisms. Neuron *44*, 161-179.

Kelley, A.E., and Berridge, K.C. (2002). The neuroscience of natural rewards: relevance to addictive drugs. The Journal of neuroscience : the official journal of the Society for Neuroscience *22*, 3306-3311.

Kelly, A., Laroche, S., and Davis, S. (2003). Activation of mitogen-activated protein kinase/extracellular signal-regulated kinase in hippocampal circuitry is required for consolidation and reconsolidation of recognition memory. The Journal of neuroscience : the official journal of the Society for Neuroscience *23*, 5354-5360.

Kelly, M.P., and Deadwyler, S.A. (2002). Acquisition of a novel behavior induces higher levels of Arc mRNA than does overtrained performance. NSC *110*, 617-626.

Kentros, C., Hargreaves, E., Hawkins, R.D., Kandel, E.R., Shapiro, M., and Muller, R.V. (1998). Abolition of long-term stability of new hippocampal place cell maps by NMDA receptor blockade. Science *280*, 2121-2126.

Kepecs, A., and Fishell, G. (2014). Interneuron cell types are fit to function. Nature *505*, 318-326.

Kerchner, G.A., and Nicoll, R.A. (2008). Silent synapses and the emergence of a postsynaptic mechanism for LTP. Nature Reviews Neuroscience *9*, 813-825.

Khalaf, O., Resch, S., Dixsaut, L., Gorden, V., Glauser, L., and Gräff, J. (2018). Reactivation of recall-induced neurons contributes to remote fear memory attenuation. Science *360*, 1239-1242.

Kim, C.K., Ye, L., Jennings, J.H., Pichamoorthy, N., Tang, D.D., Yoo, A.-C.W., Ramakrishnan, C., and Deisseroth, K. (2017). Molecular and Circuit-Dynamical Identification of Top-Down Neural Mechanisms for Restraint of Reward Seeking. Cell, 1-30.

Kim, H.R., Malik, A.N., Mikhael, J.G., Bech, P., Tsutsui-Kimura, I., Sun, F., Zhang, Y., Li, Y., Watabe-Uchida, M., Gershman, S.J., *et al.* (2020). A Unified Framework for Dopamine Signals across Timescales. Cell, 1-43.

Kim, J., Park, B.-H., Lee, J.H., Park, S.K., and Kim, J.-H. (2011). Cell type-specific alterations in the nucleus accumbens by repeated exposures to cocaine. Biological Psychiatry *69*, 1026-1034.

Kim, J., Schalk, J.C., Koss, W.A., Gremminger, R.L., Taxier, L.R., Gross, K.S., and Frick, K.M. (2019). Dorsal Hippocampal Actin Polymerization Is Necessary for Activation of G-Protein-Coupled Estrogen Receptor (GPER) to Increase CA1 Dendritic Spine Density and Enhance Memory Consolidation. The Journal of neuroscience : the official journal of the Society for Neuroscience *39*, 9598-9610.

Kirson, E.D., and Yaari, Y. (1996). Synaptic NMDA receptors in developing mouse hippocampal neurones: functional properties and sensitivity to ifenprodil. The Journal of physiology *497 (Pt 2)*, 437-455.

Kitamura, T., Ogawa, S.K., Roy, D.S., Okuyama, T., Morrissey, M.D., Smith, L.M., Redondo, R.L., and Tonegawa, S. (2017). Engrams and circuits crucial for systems consolidation of a memory. Science *356*, 73-78.

Klinzing, J.G., Niethard, N., and Born, J. (2019). Mechanisms of systems memory consolidation during sleep. Nature Neuroscience, 1-13.

Knackstedt, L.A., Moussawi, K., Lalumiere, R., Schwendt, M., Klugmann, M., and Kalivas, P. (2010). Extinction training after cocaine self-administration induces glutamatergic plasticity to inhibit cocaine seeking. The Journal of neuroscience : the official journal of the Society for Neuroscience *30*, 7984-7992.

Knierim, J.J., and Zhang, K. (2012). Attractor dynamics of spatially correlated neural activity in the limbic system. Annual review of neuroscience *35*, 267-285.

Knoblauch, A., Körner, E., Körner, U., and Sommer, F.T. (2014). Structural Synaptic Plasticity Has High Memory Capacity and Can Explain Graded Amnesia, Catastrophic Forgetting, and the Spacing Effect. PLoS ONE *9*, e96485-96419.

Knoblauch, A., and Sommer, F.T. (2016). Structural Plasticity, Effectual Connectivity, and Memory in Cortex. Frontiers in neuroanatomy *10*, 99-20.

Knott, G.W., Holtmaat, A., Wilbrecht, L., Welker, E., and Svoboda, K. (2006). Spine growth precedes synapse formation in the adult neocortex in vivo. Nature Neuroscience *9*, 1117-1124.

Koleske, A.J. (2013). Molecular mechanisms of dendrite stability. Nature Neuroscience, 1-15.

Koob, G.F., Fray, P.J., and Iversen, S.D. (1978). Self-stimulation at the lateral hypothalamus and locus coeruleus after specific unilateral lesions of the dopamine system. Brain Research *146*, 123-140.

Koob, G.F., and Volkow, N.D. (2010). Neurocircuitry of addiction. Neuropsychopharmacology *35*, 217-238.

Koos, T., and Tepper, J.M. (1999). Inhibitory control of neostriatal projection neurons by GABAergic interneurons. Nature Neuroscience *2*, 467-472.

Koos, T., Tepper, J.M., and Wilson, C.J. (2004). Comparison of IPSCs evoked by spiny and fast-spiking neurons in the neostriatum. The Journal of neuroscience : the official journal of the Society for Neuroscience *24*, 7916-7922.

Kourrich, S., Rothwell, P.E., Klug, J.R., and Thomas, M.J. (2007). Cocaine experience controls bidirectional synaptic plasticity in the nucleus accumbens. The Journal of neuroscience : the official journal of the Society for Neuroscience *27*, 7921-7928.

Kovács, K.J. (2008). Measurement of immediate-early gene activation- c-fos and beyond. Journal of neuroendocrinology *20*, 665-672.

Koya, E., Cruz, F.C., Ator, R., Golden, S.A., Hoffman, A.F., Lupica, C.R., and Hope, B.T. (2012). Silent synapses in selectively activated nucleus accumbens neurons following cocaine sensitization. Nature Neuroscience *15*, 1556-1562.

Koya, E., Golden, S.A., Harvey, B.K., Guez-Barber, D.H., Berkow, A., Simmons, D.E., Bossert, J.M., Nair, S.G., Uejima, J.L., Marin, M.T., *et al.* (2009). Targeted disruption of cocaine-activated nucleus accumbens neurons prevents context-specific sensitization. Nature Neuroscience *12*, 1069-1073.

Kravitz, A.V., Tye, L.D., and Kreitzer, A.C. (2012). Distinct roles for direct and indirect pathway striatal neurons in reinforcement. Nature Neuroscience *15*, 816-818.

Kreitzer, A.C. (2009). Physiology and pharmacology of striatal neurons. Annual review of neuroscience *32*, 127-147.

Kreitzer, A.C., and Malenka, R.C. (2005). Dopamine modulation of state-dependent endocannabinoid release and long-term depression in the striatum. The Journal of neuroscience : the official journal of the Society for Neuroscience *25*, 10537-10545.

Kreitzer, A.C., and Regehr, W.G. (2001). Retrograde inhibition of presynaptic calcium influx by endogenous cannabinoids at excitatory synapses onto Purkinje cells. Neuron *29*, 717-727.

Krucker, T., Siggins, G.R., and Halpain, S. (2000). Dynamic actin filaments are required for stable long-term potentiation (LTP) in area CA1 of the hippocampus. Proceedings of the National Academy of Sciences *97*, 6856-6861.

Kubota, Y., and Kawaguchi, Y. (2000). Dependence of GABAergic synaptic areas on the interneuron type and target size. The Journal of neuroscience : the official journal of the Society for Neuroscience *20*, 375-386.

Kullmann, D.M. (1994). Amplitude fluctuations of dual-component EPSCs in hippocampal pyramidal cells: implications for long-term potentiation. Neuron *12*, 1111-1120.

Kullmann, D.M., Moreau, A.W., Bakiri, Y., and Nicholson, E. (2012). Plasticity of inhibition. Neuron *75*, 951-962.

Kupchik, Y.M., Brown, R.M., Heinsbroek, J.A., Lobo, M.K., Schwartz, D.J., and Kalivas, P. (2015). Coding the direct/indirect pathways by D1 and D2 receptors is not valid for accumbens projections. Nature Neuroscience *18*, 1230-1232.

Kyriazi, P., Headley, D.B., and Paré, D. (2018). Multi-dimensional Coding by Basolateral Amygdala Neurons. Neuron *99*, 1315-1328.e1315.

Kyriazi, P., Headley, D.B., and Paré, D. (2020). Different Multidimensional Representations across the Amygdalo-Prefrontal Network during an Approach-Avoidance Task. Neuron, 1-20.

Lacagnina, A.F., Brockway, E.T., Crovetti, C.R., Shue, F., McCarty, M.J., Sattler, K.P., Lim, S.C., Santos, S.L., Denny, C.A., and Drew, M.R. (2019). Distinct hippocampal engrams control extinction and relapse of fear memory. Nature Neuroscience, 1-14.

Lai, C.S.W., Adler, A., and Gan, W.-B. (2018). Fear extinction reverses dendritic spine formation induced by fear conditioning in the mouse auditory cortex. Proceedings of the National Academy of Sciences *6*, 201801504-201801506.

Lai, C.S.W., Franke, T.F., and Gan, W.-B. (2012). Opposite effects of fear conditioning and extinction on dendritic spine remodelling. Nature *482*, 87-91.

Langille, J.J., and Gallistel, C.R. (2020). Locating the engram_ Should we look for plastic synapses or information-storing molecules? Neurobiology of Learning and Memory *169*, 107164.

Lansink, C.S., Goltstein, P.M., Lankelma, J.V., Joosten, R.N.J.M.A., McNaughton, B.L., and Pennartz, C.M.A. (2008). Preferential reactivation of motivationally relevant information in the ventral striatum. The Journal of neuroscience : the official journal of the Society for Neuroscience *28*, 6372-6382.

Lansink, C.S., Goltstein, P.M., Lankelma, J.V., McNaughton, B.L., and Pennartz, C.M.A. (2009). Hippocampus leads ventral striatum in replay of place-reward information. PLoS Biology *7*, e1000173.

LaPlant, Q., Vialou, V., Covington, H.E., Dumitriu, D., Feng, J., Warren, B.L., Maze, I., Dietz, D.M., Watts, E.L., Iñiguez, S.D., *et al.* (2010). Dnmt3a regulates emotional behavior and spine plasticity in the nucleus accumbens. Nature Neuroscience *13*, 1137-1143.

Lee, B.R., Ma, Y.-Y., Huang, Y.H., Wang, X., Otaka, M., Ishikawa, M., Neumann, P.A., Graziane, N.M., Brown, T.E., Suska, A., *et al.* (2013). Maturation of silent synapses in amygdala-accumbens projection contributes to incubation of cocaine craving. Nature Neuroscience *16*, 1644-1651.

Lee, H.-K., Takamiya, K., Han, J.-S., Man, H., Kim, C.-H., Rumbaugh, G., Yu, S., Ding, L., He, C., Petralia, R.S., *et al.* (2003). Phosphorylation of the AMPA receptor GluR1 subunit is required for synaptic plasticity and retention of spatial memory. Cell *112*, 631-643.

Lee, J.L.C. (2008). Memory reconsolidation mediates the strengthening of memories by additional learning. Nature Neuroscience *11*, 1264-1266.

Lee, J.L.C., Di Ciano, P., Thomas, K.L., and Everitt, B.J. (2005). Disrupting reconsolidation of drug memories reduces cocaine-seeking behavior. Neuron *47*, 795-801.

Lee, J.L.C., Everitt, B.J., and Thomas, K.L. (2004). Independent cellular processes for hippocampal memory consolidation and reconsolidation. Science *304*, 839-843.

Lee, J.L.C., Milton, A.L., and Everitt, B.J. (2006). Cue-induced cocaine seeking and relapse are reduced by disruption of drug memory reconsolidation. The Journal of neuroscience : the official journal of the Society for Neuroscience *26*, 5881-5887.

Lee, S.-H., Choi, J.-H., Lee, N., Lee, H.-R., Kim, J.-I., Yu, N.-K., Choi, S.-L., Lee, S.-H., Kim, H., and Kaang, B.-K. (2008). Synaptic protein degradation underlies destabilization of retrieved fear memory. Science *319*, 1253-1256.

Lee, S.-H., Ledri, M., Tóth, B., Marchionni, I., Henstridge, C.M., Dudok, B., Kenesei, K., Barna, L., Szabó, S.I., Renkecz, T., *et al.* (2015). Multiple Forms of Endocannabinoid and Endovanilloid Signaling Regulate the Tonic Control of GABA Release. The Journal of neuroscience : the official journal of the Society for Neuroscience *35*, 10039-10057.

Lee, S.-J.R., Escobedo-Lozoya, Y., Szatmari, E.M., and Yasuda, R. (2009). Activation of CaMKII in single dendritic spines during long-term potentiation. Nature *458*, 299-304.

Lee, S.J., Lodder, B., Chen, Y., Patriarchi, T., Tian, L., and Sabatini, B.L. (2020). Cell-type-specific asynchronous modulation of PKA by dopamine in learning. Nature, 1-27.

LeGates, T.A., Kvarta, M.D., Tooley, J.R., Francis, T.C., Lobo, M.K., Creed, M.C., and Thompson, S.M. (2018). Reward behaviour is regulated by the strength of hippocampus–nucleus accumbens synapses. Nature, 1-19.

Lesburguères, E., Gobbo, O.L., Alaux-Cantin, S., Hambucken, A., Trifilieff, P., and Bontempi, B. (2011). Early tagging of cortical networks is required for the formation of enduring associative memory. Science *331*, 924-928.

Levay, M., Krobert, K.A., Wittig, K., Voigt, N., Bermudez, M., Wolber, G., Dobrev, D., Levy, F.O., and Wieland, T. (2013). NSC23766, a Widely Used Inhibitor of Rac1 Activation, Additionally Acts as a Competitive Antagonist at Muscarinic Acetylcholine Receptors. Journal of Pharmacology and Experimental Therapeutics *347*, 69-79.

Levy, S.J., Kinsky, N.R., Mau, W., Sullivan, D.W., and Hasselmo, M.E. (2021). Hippocampal spatial memory representations in mice are heterogeneously stable. Hippocampus *31*, 244-260.

Li, W., Ma, L., Yang, G., and Gan, W.-B. (2017). REM sleep selectively prunes and maintains new synapses in development and learning. Nature Neuroscience, 1-16.

Li, X., DeJoseph, M.R., Urban, J.H., Bahi, A., Dreyer, J.L., Meredith, G.E., Ford, K.A., Ferrario, C.R., Loweth, J.A., and Wolf, M.E. (2013a). Different Roles of BDNF in Nucleus Accumbens Core versus Shell during the Incubation of Cue-Induced Cocaine Craving and Its Long-Term Maintenance. The Journal of neuroscience : the official journal of the Society for Neuroscience *33*, 1130-1142.

Li, X., Venniro, M., and Shaham, Y. (2016). Translational Research on Incubation of Cocaine Craving. JAMA Psychiatry *73*, 1115-1116.

Li, Y., Meloni, E.G., Carlezon, W.A., Milad, M.R., Pitman, R.K., Nader, K., and Bolshakov, V.Y. (2013b). Learning and reconsolidation implicate different synaptic mechanisms. Proceedings of the National Academy of Sciences *110*, 4798-4803.

Li, Z., Van Aelst, L., and Cline, H.T. (2000). Rho GTPases regulate distinct aspects of dendritic arbor growth in Xenopus central neurons in vivo. Nature Neuroscience *3*, 217-225.

Liang, B., Zhang, L., Barbera, G., Fang, W., Zhang, J., Chen, X., Chen, R., Li, Y., and Lin, D.-T. (2018). Distinct and Dynamic ON and OFF Neural Ensembles in the Prefrontal Cortex Code Social Exploration. Neuron, 1-25.

Liao, D., Hessler, N.A., and Malinow, R. (1995). Activation of postsynaptically silent synapses during pairing-induced LTP in CA1 region of hippocampal slice. Nature *375*, 400-404.

Liberti, W.A., Markowitz, J.E., Perkins, L.N., Liberti, D.C., Leman, D.P., Guitchounts, G., Velho, T., Kotton, D.N., Lois, C., and Gardner, T.J. (2016). Unstable neurons underlie a stable learned behavior. Nature Neuroscience, 1-11.

Lin, M.T., Lujan, R., Watanabe, M., Frerking, M., Maylie, J., and Adelman, J.P. (2010). Coupled Activity-Dependent Trafficking of Synaptic SK2 Channels and AMPA Receptors. The Journal of neuroscience : the official journal of the Society for Neuroscience *30*, 11726-11734.

Link, W., Konietzko, U., Kauselmann, G., Krug, M., Schwanke, B., Frey, U., and Kuhl, D. (1995). Somatodendritic expression of an immediate early gene is regulated by synaptic activity. Proceedings of the National Academy of Sciences *92*, 5734-5738.

Lisman, J., Yasuda, R., and Raghavachari, S. (2012). Mechanisms of CaMKII action in long-term potentiation. 1-14.

Lisman, J.E. (1985). A mechanism for memory storage insensitive to molecular turnover: a bistable autophosphorylating kinase. Proceedings of the National Academy of Sciences *82*, 3055-3057.

Liu, X., Ramirez, S., Pang, P.T., Puryear, C.B., Govindarajan, A., Deisseroth, K., and Tonegawa, S. (2012). Optogenetic stimulation of a hippocampal engram activates fear memory recall. Nature *484*, 381-385.

Lobo, M.K., Covington, H.E., Chaudhury, D., Friedman, A.K., Sun, H., Damez-Werno, D., Dietz, D.M., Zaman, S., Koo, J.W., Kennedy, P.J., *et al.* (2010). Cell type-specific loss of BDNF signaling mimics optogenetic control of cocaine reward. Science *330*, 385-390.

Lonergan, M., Saumier, D., Tremblay, J., Kieffer, B., Brown, T.G., and Brunet, A. (2016). Reactivating addiction-related memories under propranolol to reduce craving: A pilot randomized controlled trial. J Behav Ther Exp Psychiatry *50*, 245-249.

Lopez, J., Gamache, K., Schneider, R., and Nader, K. (2015). Memory Retrieval Requires Ongoing Protein Synthesis and NMDA Receptor Activity-Mediated AMPA Receptor Trafficking. The Journal of neuroscience : the official journal of the Society for Neuroscience *35*, 2465-2475.

Losonczy, A., Makara, J.K., and Magee, J.C. (2008). Compartmentalized dendritic plasticity and input feature storage in neurons. Nature *452*, 436-441.

Lovett-Barron, M., Turi, G.F., Kaifosh, P., Lee, P.H., Bolze, F., Sun, X.-H., Nicoud, J.-F., Zemelman, B.V., Sternson, S.M., and Losonczy, A. (2012). Regulation of neuronal input transformations by tunable dendritic inhibition. Nature Neuroscience *15*, 423-430- S421-423.

Loweth, J.A., Li, D., Cortright, J.J., Wilke, G., Jeyifous, O., Neve, R.L., Bayer, K.U., and Vezina, P. (2013). Persistent Reversal of Enhanced Amphetamine Intake by Transient CaMKII Inhibition. The Journal of neuroscience : the official journal of the Society for Neuroscience *33*, 1411-1416.

Loweth, J.A., Reimers, J.M., Caccamise, A., Stefanik, M.T., Woo, K.K.Y., Chauhan, N.M., Werner, C.T., and Wolf, M.E. (2018). mGlu1 tonically regulates levels of calcium-permeable AMPA receptors in cultured nucleus accumbens neurons through retinoic acid signaling and protein translation. The European journal of neuroscience *60*, 308-315.

Loweth, J.A., Scheyer, A.F., Milovanovic, M., LaCrosse, A.L., Flores-Barrera, E., Werner, C.T., Li, X., Ford, K.A., Le, T., Olive, M.F., *et al.* (2014). Synaptic depression via mGluR1 positive allosteric modulation suppresses cue-induced cocaine craving. Nature Neuroscience *17*, 73-80.

Lu, L., Grimm, J.W., Shaham, Y., and Hope, B.T. (2003). Molecular neuroadaptations in the accumbens and ventral tegmental area during the first 90 days of forced abstinence from cocaine self-administration in rats. Journal of Neurochemistry *85*, 1604-1613.

Lu, L., Koya, E., Zhai, H., Hope, B.T., and Shaham, Y. (2006). Role of ERK in cocaine addiction. Trends in neurosciences *29*, 695-703.

Lu, W., Isozaki, K., Roche, K.W., and Nicoll, R.A. (2010). Synaptic targeting of AMPA receptors is regulated by a CaMKII site in the first intracellular loop of GluA1. Proceedings of the National Academy of Sciences of the United States of America *107*, 22266-22271.

Luk, K.C., and Sadikot, A.F. (2001). GABA promotes survival but not proliferation of parvalbumin-immunoreactive interneurons in rodent neostriatum: an in vivo study with stereology. NSC *104*, 93-103.

Lunardi, P., Sachser, R.M., Sierra, R.O., Pedraza, L.K., Medina, C., de la Fuente, V., Romano, A., Quillfeldt, J.A., and de Oliveira Alvares, L. (2018). Effects of Hippocampal LIMK Inhibition on Memory Acquisition, Consolidation, Retrieval, Reconsolidation, and Extinction. 1-10.

Luo, Y.-X., Xue, Y.-X., Liu, J.-F., Shi, H.-S., Jian, M., Han, Y., Zhu, W.-l., Bao, Y.-p., Wu, P., Ding, Z.-B., *et al.* (2015). A novel UCS memory retrieval-extinction procedure to inhibit relapse to drug seeking. Nature Communications *6*, 7675.

Lüscher, C., and Malenka, R.C. (2011). Drug-evoked synaptic plasticity in addiction: from molecular changes to circuit remodeling. Neuron *69*, 650-663.

Lüscher, C., Robbins, T.W., and Everitt, B.J. (2020). The transition to compulsion in addiction. Nature Reviews Neuroscience, 1-17.

Lüthi, A., and Lüscher, C. (2014). Pathological circuit function underlying addiction and anxiety disorders. Nature Neuroscience *17*, 1635-1643.

Lyford, G.L., Yamagata, K., Kaufmann, W.E., Barnes, C.A., Sanders, L.K., Copeland, N.G., Gilbert, D.J., Jenkins, N.A., Lanahan, A.A., and Worley, P.F. (1995). Arc, a growth factor and activity-regulated gene, encodes a novel cytoskeleton-associated protein that is enriched in neuronal dendrites. Neuron *14*, 433-445.

Lynch, W.J., and Taylor, J.R. (2005). Persistent changes in motivation to self-administer cocaine following modulation of cyclic AMP-dependent protein kinase A (PKA) activity in the nucleus accumbens. European Journal of Neuroscience *22*, 1214-1220.

Ma, T., Cheng, Y., Hellard, E.R., Wang, X., Lu, J., Gao, X., Huang, C.C.Y., Wei, X.-Y., Ji, J.-Y., and Wang, J. (2018). Bidirectional and long-lasting control of alcohol- seeking behavior by corticostriatal LTP and LTD. Nature Neuroscience, 1-15.

Ma, Y.-Y., Lee, B.R., Wang, X., Guo, C., Liu, L., Cui, R., Lan, Y., Balcita-Pedicino, J.J., Wolf, M.E., Sesack, S.R., *et al.* (2014). Bidirectional modulation of incubation of cocaine craving by silent synapse-based remodeling of prefrontal cortex to accumbens projections. Neuron *83*, 1453-1467.

Ma, Y.-Y., Wang, X., Huang, Y., Marie, H., Nestler, E.J., Schlüter, O.M., and Dong, Y. (2016). Re-silencing of silent synapses unmasks anti-relapse effects of environmental enrichment. Proceedings of the National Academy of Sciences of the United States of America *113*, 5089-5094.

MacAskill, A.F., Cassel, J.M., and Carter, A.G. (2014). Cocaine exposure reorganizes cell type- and input-specific connectivity in the nucleus accumbens. Nature Neuroscience *17*, 1198-1207.

Madangopal, R., Tunstall, B.J., Komer, L.E., Weber, S.J., Hoots, J.K., Lennon, V.A., Bossert, J.M., Epstein, D.H., Shaham, Y., and Hope, B.T. (2019). Discriminative stimuli are sufficient for incubation of cocaine craving. eLife *8*, 733.

Maddox, S.A., and Schafe, G.E. (2011). The Activity-Regulated Cytoskeletal-Associated Protein (Arc/Arg3.1) Is Required for Reconsolidation of a Pavlovian Fear Memory. The Journal of neuroscience : the official journal of the Society for Neuroscience *31*, 7073-7082.

Madroñal, N., Gruart, A., Sacktor, T.C., and Delgado-García, J.M. (2010). PKMzeta inhibition reverses learning-induced increases in hippocampal synaptic strength and memory during trace eyeblink conditioning. PLoS ONE *5*, e10400.

Magee, J.C., and Grienberger, C. (2020). Synaptic Plasticity Forms and Functions. Annual review of neuroscience *43*, 95-117.

Maldonado-Irizarry, C.S., Swanson, C.J., and Kelley, A.E. (1995). Glutamate receptors in the nucleus accumbens shell control feeding behavior via the lateral hypothalamus. The Journal of neuroscience : the official journal of the Society for Neuroscience *15*, 6779-6788.

Malenka, R.C., and Bear, M.F. (2004). LTP and LTD: an embarrassment of riches. Neuron *44*, 5-21.

Maletic-Savatic, M., Malinow, R., and Svoboda, K. (1999). Rapid dendritic morphogenesis in CA1 hippocampal dendrites induced by synaptic activity. Science *283*, 1923-1927.

Malinow, R., Schulman, H., and Tsien, R.W. (1989). Inhibition of postsynaptic PKC or CaMKII blocks induction but not expression of LTP. Science *245*, 862-866.

Mallet, N., Le Moine, C., Charpier, S., and Gonon, F. (2005). Feedforward inhibition of projection neurons by fast-spiking GABA interneurons in the rat striatum in vivo. The Journal of neuroscience : the official journal of the Society for Neuroscience *25*, 3857-3869.

Mameli, M., Halbout, B., Creton, C., Engblom, D., Parkitna, J.R., Spanagel, R., and Lüscher, C. (2009). Cocaine-evoked synaptic plasticity: persistence in the VTA triggers adaptations in the NAc. Nature Neuroscience *12*, 1036-1041.

Mamou, C.B., Gamache, K., and Nader, K. (2006). NMDA receptors are critical for unleashing consolidated auditory fear memories. Nature Neuroscience *9*, 1237-1239.

Mangiavacchi, S., and Wolf, M.E. (2004). D1 dopamine receptor stimulation increases the rate of AMPA receptor insertion onto the surface of cultured nucleus accumbens neurons through a pathway dependent on protein kinase A. Journal of Neurochemistry *88*, 1261-1271.

Marchant, N.J., Li, X., and Shaham, Y. (2013). Recent developments in animal models of drug relapse. Current Opinion in Neurobiology *23*, 675-683.

Marco, A., Meharena, H.S., Dileep, V., Raju, R.M., Davila-Velderrain, J., Zhang, A.L., Adaikkan, C., Young, J.Z., Gao, F., Kellis, M., *et al.* (2020). Mapping the epigenomic and transcriptomic

interplay during memory formation and recall in the hippocampal engram ensemble. Nature Neuroscience, 1-34.

Mardilovich, K., Baugh, M., Crighton, D., Kowalczyk, D., Gabrielsen, M., Munro, J., Croft, D.R., Lourenco, F., James, D., Kalna, G., *et al.* (2015). LIM kinase inhibitors disrupt mitotic microtubule organization and impair tumor cell proliferation. Oncotarget *6*, 38469-38486.

Marie, H., Morishita, W., Yu, X., Calakos, N., and Malenka, R.C. (2005). Generation of silent synapses by acute in vivo expression of CaMKIV and CREB. Neuron *45*, 741-752.

Markowitz, J.E., Gillis, W.F., Beron, C.C., Neufeld, S.Q., Robertson, K., Bhagat, N.D., Peterson, R.E., Peterson, E., Hyun, M., Linderman, S.W., *et al.* (2018). The Striatum Organizes 3D Behavior via Moment-to- Moment Action Selection. Cell, 1-33.

Marr, D. (1971). Simple memory: a theory for archicortex. Philosophical Transactions of the Royal Society B: Biological Sciences *262*, 23-81.

Marshel, J.H., Kim, Y.S., Machado, T.A., Quirin, S., Benson, B., Kadmon, J., Raja, C., Chibukhchyan, A., Ramakrishnan, C., Inoue, M., *et al.* (2019). Cortical layer–specific critical dynamics triggering perception. Science, eaaw5202-5214.

Mathis, A., Mamidanna, P., Cury, K.M., Abe, T., Murthy, V.N., Mathis, M.W., and Bethge, M. (2018). DeepLabCut: markerless pose estimation of user-defined body parts with deep learning. Nature Neuroscience, 1-12.

Mathur, B.N., Tanahira, C., Tamamaki, N., and Lovinger, D.M. (2013). Voltage drives diverse endocannabinoid signals to mediate striatal microcircuit-specific plasticity. Nature Neuroscience *16*, 1275-1283.

Matsuzaki, M., Ellis-Davies, G.C., Nemoto, T., Miyashita, Y., Iino, M., and Kasai, H. (2001). Dendritic spine geometry is critical for AMPA receptor expression in hippocampal CA1 pyramidal neurons. Nature Neuroscience *4*, 1086-1092.

Matsuzaki, M., Honkura, N., Ellis-Davies, G.C.R., and Kasai, H. (2004). Structural basis of long-term potentiation in single dendritic spines. Nature *429*, 761-766.

Mattson, B.J., Bossert, J.M., Simmons, D.E., Nozaki, N., Nagarkar, D., Kreuter, J.D., and Hope, B.T. (2005). Cocaine-induced CREB phosphorylation in nucleus accumbens of cocaine-sensitized rats is enabled by enhanced activation of extracellular signal-related kinase, but not protein kinase A. Journal of Neurochemistry *95*, 1481-1494.

Maze, I., Covington, H.E., Dietz, D.M., LaPlant, Q., Renthal, W., Russo, S.J., Mechanic, M., Mouzon, E., Neve, R.L., Haggarty, S.J., *et al.* (2010). Essential role of the histone methyltransferase G9a in cocaine-induced plasticity. Science *327*, 213-216.

McClung, C.A., and Nestler, E.J. (2003). Regulation of gene expression and cocaine reward by CREB and ΔFosB. Nature Neuroscience *6*, 1208-1215.

McCutcheon, J.E., Loweth, J.A., Ford, K.A., Marinelli, M., Wolf, M.E., and Tseng, K.Y. (2011a). Group I mGluR activation reverses cocaine-induced accumulation of calcium-permeable AMPA receptors in nucleus accumbens synapses via a protein kinase C-dependent mechanism. The Journal of neuroscience : the official journal of the Society for Neuroscience *31*, 14536-14541.

McCutcheon, J.E., Wang, X., Tseng, K.Y., Wolf, M.E., and Marinelli, M. (2011b). Calcium-permeable AMPA receptors are present in nucleus accumbens synapses after prolonged withdrawal from cocaine self-administration but not experimenter-administered cocaine. The Journal of neuroscience : the official journal of the Society for Neuroscience *31*, 5737-5743.

McFarland, K., and Kalivas, P. (2001). The circuitry mediating cocaine-induced reinstatement of drug-seeking behavior. The Journal of neuroscience : the official journal of the Society for Neuroscience *21*, 8655-8663.

McFarland, K., Lapish, C.C., and Kalivas, P. (2003). Prefrontal glutamate release into the core of the nucleus accumbens mediates cocaine-induced reinstatement of drug-seeking behavior. The Journal of neuroscience : the official journal of the Society for Neuroscience *23*, 3531-3537.

McGinty, V.B., Lardeux, S., Taha, S.A., Kim, J.J., and Nicola, S.M. (2013). Invigoration of Reward Seeking by Cue and Proximity Encoding in the Nucleus Accumbens. Neuron *78*, 910-922.

McHenry, J.A., Otis, J.M., Rossi, M.A., Robinson, J.E., Kosyk, O., Miller, N.W., McElligott, Z.A., Budygin, E.A., Rubinow, D.R., and Stuber, G.D. (2017). Hormonal gain control of a medial preoptic area social reward circuit. Nature Neuroscience, 1-14.

McKendrick, G., and Graziane, N.M. (2020). Drug-Induced Conditioned Place Preference and Its Practical Use in Substance Use Disorder Research. Frontiers in Behavioral Neuroscience *14*, 582147.

McKenzie, S., Huszár, R., English, D.F., Kim, K., Christensen, F., Yoon, E., and Buzsáki, G. (2021). Preexisting hippocampal network dynamics constrain optogenetically induced place fields. Neuron, 1-23.

Medina, C., de la Fuente, V., Dieck, S.t., Nassim-Assir, B., Dalmay, T., Bartnik, I., Lunardi, P., de Oliveira Alvares, L., Schuman, E.M., Letzkus, J.J., *et al.* (2020). LIMK, Cofilin 1 and actin dynamics involvement in fear memory processing. Neurobiology of Learning and Memory *173*, 107275.

Meng, C., Zhou, J., Papaneri, A., Peddada, T., Xu, K., and Cui, G. (2018). Spectrally Resolved Fiber Photometry for Multi- component Analysis of Brain Circuits. Neuron, 1-16.

Meredith, G.E., Agolia, R., Arts, M.P., Groenewegen, H.J., and Zahm, D.S. (1992). Morphological differences between projection neurons of the core and shell in the nucleus accumbens of the rat. NSC *50*, 149-162.

Messaoudi, E., Kanhema, T., Soulé, J., Tiron, A., Dagyte, G., da Silva, B., and Bramham, C.R. (2007). Sustained Arc/Arg3.1 synthesis controls long-term potentiation consolidation through

regulation of local actin polymerization in the dentate gyrus in vivo. The Journal of neuroscience : the official journal of the Society for Neuroscience *27*, 10445-10455.

Meyer, D., Bonhoeffer, T., and Scheuss, V. (2014). Balance and stability of synaptic structures during synaptic plasticity. Neuron *82*, 430-443.

Migaud, M., Charlesworth, P., Dempster, M., Webster, L.C., Watabe, A.M., Makhinson, M., He, Y., Ramsay, M.F., Morris, R.G.M., Morrison, J.H., *et al.* (1998). Enhanced long-term potentiation and impaired learning in mice with mutant postsynaptic density-95 protein. Nature *396*, 433-439.

Migues, P.V., Hardt, O., Wu, D.C., Gamache, K., Sacktor, T.C., Wang, Y.T., and Nader, K. (2010). PKMζ maintains memories by regulating GluR2-dependent AMPA receptor trafficking. Nature Neuroscience *13*, 630-634.

Milad, M.R., and Quirk, G.J. (2012). Fear extinction as a model for translational neuroscience: ten years of progress. Annual review of psychology *63*, 129-151.

Milekic, M.H., Pollonini, G., and Alberini, C.M. (2007). Temporal requirement of C/EBPbeta in the amygdala following reactivation but not acquisition of inhibitory avoidance. Learning & memory (Cold Spring Harbor, NY) *14*, 504-511.

Millan, E.Z., Furlong, T.M., and McNally, G.P. (2010). Accumbens Shell-Hypothalamus Interactions Mediate Extinction of Alcohol Seeking. The Journal of neuroscience : the official journal of the Society for Neuroscience *30*, 4626-4635.

Miller, C.A., and Marshall, J.F. (2005). Molecular substrates for retrieval and reconsolidation of cocaine-associated contextual memory. Neuron *47*, 873-884.

Milstein, A.D., Bloss, E.B., Apostolides, P.F., Vaidya, S.P., Dilly, G.A., Zemelman, B.V., and Magee, J.C. (2015). Inhibitory Gating of Input Comparison in the CA1 Microcircuit. Neuron *87*, 1274-1289.

Milton, A.L., and Everitt, B.J. (2012). The persistence of maladaptive memory: Addiction, drug memories and anti-relapse treatments. Neuroscience and biobehavioral reviews *36*, 1119-1139.

Milton, A.L., Merlo, E., Ratano, P., Gregory, B.L., Dumbreck, J.K., and Everitt, B.J. (2013). Double dissociation of the requirement for GluN2B- and GluN2A-containing NMDA receptors in the destabilization and restabilization of a reconsolidating memory. The Journal of neuroscience : the official journal of the Society for Neuroscience *33*, 1109-1115.

Mogenson, G.J., Jones, D.L., and Yim, C.Y. (1980). From motivation to action: functional interface between the limbic system and the motor system. Progress in neurobiology *14*, 69-97.

Moghaddam, B., and Bunney, B.S. (1989). Differential effect of cocaine on extracellular dopamine levels in rat medial prefrontal cortex and nucleus accumbens: comparison to amphetamine. Synapse (New York, NY) *4*, 156-161.

Mohebi, A., Pettibone, J.R., Hamid, A.A., Wong, J.-M.T., Vinson, L.T., Patriarchi, T., Tian, L., Kennedy, R.T., and Berke, J.D. (2019). Dissociable dopamine dynamics for learning and motivation. Nature, 1-18.

Monfils, M.-H., Cowansage, K.K., Klann, E., and LeDoux, J.E. (2009). Extinction-reconsolidation boundaries: key to persistent attenuation of fear memories. Science *324*, 951-955.

Montijn, J.S., Meijer, G.T., Lansink, C.S., and Pennartz, C.M.A. (2016). Population-Level Neural Codes Are Robust to Single- Neuron Variability from a Multidimensional Coding Perspective. Cell reports *16*, 2486-2498.

Monyer, H., Burnashev, N., Laurie, D.J., Sakmann, B., and Seeburg, P.H. (1994). Developmental and regional expression in the rat brain and functional properties of four NMDA receptors. Neuron *12*, 529-540.

Morales, M., and Margolis, E.B. (2017). Ventral tegmental area: cellular heterogeneity, connectivity and behaviour. Nature Reviews Neuroscience *18*, 73-85.

Morita, D., Rah, J.C., and Isaac, J.T.R. (2013). Incorporation of inwardly rectifying AMPA receptors at silent synapses during hippocampal long-term potentiation. Philosophical Transactions of the Royal Society B: Biological Sciences *369*, 20130156-20130156.

Morris, R.G.M., Anderson, E., Lynch, G.S., and Baudry, M. (1986). Selective impairment of learning and blockade of long-term potentiation by an N-methyl-D-aspartate receptor antagonist, AP5. Nature *319*, 774-776.

Morris, R.G.M., Inglis, J., Ainge, J.A., Olverman, H.J., Tulloch, J., Dudai, Y., and Kelly, P.A.T. (2006). Memory reconsolidation: sensitivity of spatial memory to inhibition of protein synthesis in dorsal hippocampus during encoding and retrieval. Neuron *50*, 479-489.

Morrison, S.E., and Nicola, S.M. (2014). Neurons in the nucleus accumbens promote selection bias for nearer objects. The Journal of neuroscience : the official journal of the Society for Neuroscience *34*, 14147-14162.

Mu, P., Moyer, J.T., Ishikawa, M., Zhang, Y., Panksepp, J., Sorg, B.A., Schluter, O.M., and Dong, Y. (2010a). Exposure to cocaine dynamically regulates the intrinsic membrane excitability of nucleus accumbens neurons. J Neurosci *30*, 3689-3699.

Mu, P., Moyer, J.T., Ishikawa, M., Zhang, Y., Panksepp, J., Sorg, B.A., Schlüter, O.M., and Dong, Y. (2010b). Exposure to cocaine dynamically regulates the intrinsic membrane excitability of nucleus accumbens neurons. The Journal of neuroscience : the official journal of the Society for Neuroscience *30*, 3689-3699.

Müller, U.J., Voges, J., Steiner, J., Galazky, I., Heinze, H.-J., Möller, M., Pisapia, J., Halpern, C., Caplan, A., Bogerts, B., *et al.* (2013). Deep brain stimulation of the nucleus accumbens for the treatment of addiction. Annals of the New York Academy of Sciences *1282*, 119-128.

Murakoshi, H., Shin, M.E., Parra-Bueno, P., Szatmari, E.M., Shibata, A.C.E., and Yasuda, R. (2017). Kinetics of Endogenous CaMKII Required for Synaptic Plasticity Revealed by Optogenetic Kinase Inhibitor. Neuron, 1-23.

Murakoshi, H., Wang, H., and Yasuda, R. (2011). Local, persistent activation of Rho GTPases during plasticity of single dendritic spines. Nature *472*, 100-104.

Murphy, D.D., and Segal, M. (1997). Morphological plasticity of dendritic spines in central neurons is mediated by activation of cAMP response element binding protein. Proceedings of the National Academy of Sciences *94*, 1482-1487.

Murugan, M., Jang, H.J., Park, M., Miller, E.M., Cox, J., Taliaferro, J.P., Parker, N.F., Bhave, V., Hur, H., Liang, Y., *et al.* (2017). Combined Social and Spatial Coding in a Descending Projection from the Prefrontal Cortex. Cell, 1-32.

Nabavi, S., Fox, R., Proulx, C.D., Lin, J.Y., Tsien, R.Y., and Malinow, R. (2014). Engineering a memory with LTD and LTP. Nature *511*, 348-352.

Nader, K. (2015). Reconsolidation and the Dynamic Nature of Memory. Cold Spring Harbor Perspectives in Biology *7*, a021782.

Nader, K., and Einarsson, E.O. (2010). Memory reconsolidation: an update. Ann N Y Acad Sci *1191*, 27-41.

Nader, K., and Hardt, O. (2009). A single standard for memory: the case for reconsolidation. Nat Rev Neurosci *10*, 224-234.

Nader, K., Schafe, G.E., and LeDoux, J.E. (2000). Fear memories require protein synthesis in the amygdala for reconsolidation after retrieval. Nature *406*, 722-726.

Nakayama, A.Y., Harms, M.B., and Luo, L. (2000). Small GTPases Rac and Rho in the maintenance of dendritic spines and branches in hippocampal pyramidal neurons. The Journal of neuroscience : the official journal of the Society for Neuroscience *20*, 5329-5338.

Nakayama, K., Kiyosue, K., and Taguchi, T. (2005). Diminished neuronal activity increases neuron-neuron connectivity underlying silent synapse formation and the rapid conversion of silent to functional synapses. The Journal of neuroscience : the official journal of the Society for Neuroscience *25*, 4040-4051.

Nakazawa, K., Quirk, M.C., Chitwood, R.A., Watanabe, M., Yeckel, M.F., Sun, L.D., Kato, A., Carr, C.A., Johnston, D., Wilson, M.A., *et al.* (2002). Requirement for hippocampal CA3 NMDA receptors in associative memory recall. Science *297*, 211-218.

Nestler, E.J., Barrot, M., DiLeone, R.J., Eisch, A.J., Gold, S.J., and Monteggia, L.M. (2002). Neurobiology of depression. Neuron *34*, 13-25.

Nestler, E.J., and Lüscher, C. (2019). The Molecular Basis of Drug Addiction: Linking Epigenetic to Synaptic and Circuit Mechanisms. Neuron *102*, 48-59.

Neumann, P.A., Wang, Y., Yan, Y., Wang, Y., Ishikawa, M., Cui, R., Huang, Y.H., Sesack, S.R., Schluter, O.M., and Dong, Y. (2016a). Cocaine-Induced Synaptic Alterations in Thalamus to Nucleus Accumbens Projection. Neuropsychopharmacology.

Neumann, P.A., Wang, Y., Yan, Y., Wang, Y., Ishikawa, M., Cui, R., Huang, Y.H., Sesack, S.R., Schlüter, O.M., and Dong, Y. (2016b). Cocaine-Induced Synaptic Alterations in Thalamus to Nucleus Accumbens Projection. Neuropsychopharmacology *41*, 2399-2410.

Nicola, S.M. (2007). The nucleus accumbens as part of a basal ganglia action selection circuit. Psychopharmacology *191*, 521-550.

Nicola, S.M., Yun, I.A., Wakabayashi, K.T., and Fields, H.L. (2004). Cue-Evoked Firing of Nucleus Accumbens Neurons Encodes Motivational Significance During a Discriminative Stimulus Task. Journal of neurophysiology *91*, 1840-1865.

Nishiyama, J., and Yasuda, R. (2015). Biochemical Computation for Spine Structural Plasticity. Neuron *87*, 63-75.

O'Connor, E.C., Kremer, Y., Lefort, S., Harada, M., Pascoli, V., Rohner, C., and Lüscher, C. (2015). Accumbal D1R Neurons Projecting to Lateral Hypothalamus Authorize Feeding. Neuron *88*, 553-564.

Obashi, K., Matsuda, A., Inoue, Y., and Okabe, S. (2019). Precise Temporal Regulation of Molecular Diffusion within Dendritic Spines by Actin Polymers during Structural Plasticity. Cell reports *27*, 1503-1515.e1508.

Oby, E.R., Golub, M.D., Hennig, J.A., Degenhart, A.D., Tyler-Kabara, E.C., Yu, B.M., Chase, S.M., and Batista, A.P. (2019). New neural activity patterns emerge with long-term learning. Proceedings of the National Academy of Sciences of the United States of America *116*, 15210-15215.

Okamoto, K.-I., Nagai, T., Miyawaki, A., and Hayashi, Y. (2004). Rapid and persistent modulation of actin dynamics regulates postsynaptic reorganization underlying bidirectional plasticity. Nature Neuroscience *7*, 1104-1112.

Okamoto, K.-I., Narayanan, R., Lee, S.H., Murata, K., and Hayashi, Y. (2007). The role of CaMKII as an F-actin-bundling protein crucial for maintenance of dendritic spine structure. Proceedings of the National Academy of Sciences of the United States of America *104*, 6418-6423.

Ólafsdóttir, H.F., Bush, D., and Barry, C. (2018). The Role of Hippocampal Replay in Memory and Planning. Current Biology *28*, R37-R50.

Olds, J. (1958). Self-Stimulation of the Brain. Science *127*, 1-11.

Ortinski, P.I., Briand, L.A., Pierce, R.C., and Schmidt, H.D. (2015). Cocaine-seeking is associated with PKC-dependent reduction of excitatory signaling in accumbens shell D2 dopamine receptor-expressing neurons. Neuropharmacology *92*, 80-89.

Ortinski, P.I., Vassoler, F.M., Carlson, G.C., and Pierce, R.C. (2012). Temporally dependent changes in cocaine-induced synaptic plasticity in the nucleus accumbens shell are reversed by D1-like dopamine receptor stimulation. Neuropsychopharmacology *37*, 1671-1682.

Otis, J.M., Dashew, K.B., and Mueller, D. (2013). Neurobiological Dissociation of Retrieval and Reconsolidation of Cocaine-Associated Memory. The Journal of neuroscience : the official journal of the Society for Neuroscience *33*, 1271-1281.

Otis, J.M., Namboodiri, V.M.K., Matan, A.M., Voets, E.S., Mohorn, E.P., Kosyk, O., McHenry, J.A., Robinson, J.E., Resendez, S.L., Rossi, M.A., *et al.* (2017). Prefrontal cortex output circuits guide reward seeking through divergent cue encoding. Nature, 1-19.

Otis, J.M., Zhu, M., Namboodiri, V.M.K., Cook, C.A., Kosyk, O., Matan, A.M., Ying, R., Hashikawa, Y., Hashikawa, K., Trujillo-Pisanty, I., *et al.* (2019). Paraventricular Thalamus Projection Neurons Integrate Cortical and Hypothalamic Signals for Cue- Reward Processing. Neuron, 1-14.

Ottenheimer, D., Richard, J.M., and Janak, P.H. (2018). Ventral pallidum encodes relative reward value earlier and more robustly than nucleus accumbens. Nature Communications, 1-14.

Pachitariu, M., Stringer, C., and Harris, K.D. (2018). Robustness of Spike Deconvolution for Neuronal Calcium Imaging. The Journal of neuroscience : the official journal of the Society for Neuroscience *38*, 7976-7985.

Pan, B., Hillard, C.J., and Liu, Q.-s. (2008). Endocannabinoid signaling mediates cocaine-induced inhibitory synaptic plasticity in midbrain dopamine neurons. The Journal of neuroscience : the official journal of the Society for Neuroscience *28*, 1385-1397.

Pardo-Garcia, T.R., Garcia-Keller, C., Penaloza, T., Kalivas, P., and Heinsbroek, J.A. (2019). Ventral pallidum is the primary target for accumbens D1 projections driving cocaine seeking. The Journal of neuroscience : the official journal of the Society for Neuroscience, 2822-2818-2811.

Park, A.J., Harris, A.Z., Martyniuk, K.M., Chang, C.-Y., Abbas, A.I., Lowes, D.C., Kellendonk, C., Gogos, J.A., and Gordon, J.A. (2021). Reset of hippocampal–prefrontal circuitry facilitates learning. Nature, 1-23.

Park, M., Weller, J.P., Horwitz, G.D., and Pillow, J.W. (2014). Bayesian active learning of neural firing rate maps with transformed gaussian process priors. Neural computation *26*, 1519-1541.

Park, P., Sanderson, T.M., Amici, M., Choi, S.-L., Bortolotto, Z.A., Zhuo, M., Kaang, B.-K., and Collingridge, G.L. (2016). Calcium-Permeable AMPA Receptors Mediate the Induction of the Protein Kinase A-Dependent Component of Long-Term Potentiation in the Hippocampus. The Journal of neuroscience : the official journal of the Society for Neuroscience *36*, 622-631.

Parkhurst, C.N., Yang, G., Ninan, I., Savas, J.N., Yates III, J.R., Lafaille, J.J., Hempstead, B.L., Littman, D.R., and Gan, W.-B. (2013). Microglia Promote Learning-Dependent Synapse Formation through Brain-Derived Neurotrophic Factor. Cell *155*, 1596-1609.

Parkinson, J.A., Olmstead, M.C., Burns, L.H., Robbins, T.W., and Everitt, B.J. (1999). Dissociation in effects of lesions of the nucleus accumbens core and shell on appetitive pavlovian approach behavior and the potentiation of conditioned reinforcement and locomotor activity by D-amphetamine. The Journal of neuroscience : the official journal of the Society for Neuroscience *19*, 2401-2411.

Parvaz, M.A., Moeller, S.J., and Goldstein, R.Z. (2016). Incubation of Cue-Induced Craving in Adults Addicted to Cocaine Measured by Electroencephalography. JAMA Psychiatry *73*, 1127-1128.

Pascoli, V., Terrier, J., Espallergues, J., Valjent, E., O'Connor, E.C., and Lüscher, C. (2014). Contrasting forms of cocaine-evoked plasticity control components of relapse. Nature *509*, 459-464.

Pascoli, V., Terrier, J., Hiver, A., and Lüscher, C. (2015). Sufficiency of Mesolimbic Dopamine Neuron Stimulation for the Progression to Addiction. Neuron *88*, 1054-1066.

Pascoli, V., Turiault, M., and Lüscher, C. (2013). Reversal of cocaine-evoked synaptic potentiation resets drug-induced adaptive behaviour. Nature *481*, 71-75.

Passafaro, M., Piëch, V., and Sheng, M. (2001). Subunit-specific temporal and spatial patterns of AMPA receptor exocytosis in hippocampal neurons. Nature Neuroscience *4*, 917-926.

Pastalkova, E., Serrano, P., Pinkhasova, D., Wallace, E., Fenton, A.A., and Sacktor, T.C. (2006). Storage of spatial information by the maintenance mechanism of LTP. Science *313*, 1141-1144.

Pavlov, I. (1927). Conditioned Reflexes: an Investigation of the Physiological Activity of the Cerebral Cortex (Oxford University Press).

Pedreira, M.E., Pérez-Cuesta, L.M., and Maldonado, H. (2004). Mismatch between what is expected and what actually occurs triggers memory reconsolidation or extinction. Learning & Memory *11*, 579-585.

Penke, Z., Morice, E., Veyrac, A., Gros, A., Chagneau, C., LeBlanc, P., Samson, N., Baumgärtel, K., Mansuy, I.M., Davis, S., *et al.* (2014). Zif268/Egr1 gain of function facilitates hippocampal synaptic plasticity and long-term spatial recognition memory. Philosophical transactions of the Royal Society of London Series B, Biological sciences *369*, 20130159.

Penn, A.C., Zhang, C.L., Georges, F., Royer, L., Breillat, C., Hosy, E., Petersen, J.D., Humeau, Y., and Choquet, D. (2017). Hippocampal LTP and contextual learning require surface diffusion of AMPA receptors. Nature, 1-22.

Pennartz, C.M., Groenewegen, H.J., and Lopes da Silva, F.H. (1994). The nucleus accumbens as a complex of functionally distinct neuronal ensembles: an integration of behavioural, electrophysiological and anatomical data. Progress in neurobiology *42*, 719-761.

Pennartz, C.M.A., Lee, E., Verheul, J., Lipa, P., Barnes, C.A., and McNaughton, B.L. (2004). The ventral striatum in off-line processing: ensemble reactivation during sleep and modulation by

hippocampal ripples. The Journal of neuroscience : the official journal of the Society for Neuroscience *24*, 6446-6456.

Penzo, M.A., Robert, V., Tucciarone, J., De Bundel, D., Wang, M., Van Aelst, L., Darvas, M., Parada, L.F., Palmiter, R.D., He, M., *et al.* (2015). The paraventricular thalamus controls a central amygdala fear circuit. Nature *519*, 455-459.

Peoples, L.L., and West, M.O. (1996). Phasic firing of single neurons in the rat nucleus accumbens correlated with the timing of intravenous cocaine self-administration. The Journal of neuroscience : the official journal of the Society for Neuroscience *16*, 3459-3473.

Peron, S., Pancholi, R., Voelcker, B., Wittenbach, J.D., Ólafsdóttir, H.F., Freeman, J., and Svoboda, K. (2020). Recurrent interactions in local cortical circuits. Nature *579*, 256-259.

Peters, A.J., Chen, S.X., and Komiyama, T. (2014). Emergence of reproducible spatiotemporal activity during motor learning. Nature *510*, 263-267.

Peters, J., LaLumiere, R.T., and Kalivas, P. (2008a). Infralimbic Prefrontal Cortex Is Responsible for Inhibiting Cocaine Seeking in Extinguished Rats. The Journal of neuroscience : the official journal of the Society for Neuroscience *28*, 6046-6053.

Peters, J., LaLumiere, R.T., and Kalivas, P.W. (2008b). Infralimbic prefrontal cortex is responsible for inhibiting cocaine seeking in extinguished rats. J Neurosci *28*, 6046-6053.

Petralia, R.S., Esteban, J.A., Wang, Y.X., Partridge, J.G., Zhao, H.M., Wenthold, R.J., and Malinow, R. (1999). Selective acquisition of AMPA receptors over postnatal development suggests a molecular basis for silent synapses. Nature Neuroscience *2*, 31-36.

Phillips, A.G., and Fibiger, H.C. (1978). The role of dopamine in maintaining intracranial self-stimulation in the ventral tegmentum, nucleus accumbens, and medial prefrontal cortex. Canadian journal of psychology *32*, 58-66.

Phillips, P.E.M., Stuber, G.D., Heien, M.L.A.V., Wightman, R.M., and Carelli, R.M. (2003). Subsecond dopamine release promotes cocaine seeking. Nature *422*, 614-618.

Pickens, C.L., Airavaara, M., Theberge, F., Fanous, S., Hope, B.T., and Shaham, Y. (2011). Neurobiology of the incubation of drug craving. Trends in neurosciences *34*, 411-420.

Pierce, R.C., Bell, K., Duffy, P., and Kalivas, P. (1996). Repeated cocaine augments excitatory amino acid transmission in the nucleus accumbens only in rats having developed behavioral sensitization. The Journal of neuroscience : the official journal of the Society for Neuroscience *16*, 1550-1560.

Pignatelli, M., Ryan, T.J., Roy, D.S., Lovett, C., Smith, L.M., Muralidhar, S., and Tonegawa, S. (2018). Engram Cell Excitability State Determines the Efficacy of Memory Retrieval. Neuron, 1-17.

Pisanu, A., Lecca, D., Valentini, V., Bahi, A., Dreyer, J.-L., Cacciapaglia, F., Scifo, A., Piras, G., Cadoni, C., and Di Chiara, G. (2015). Impairment of acquisition of intravenous cocaine self-administration by RNA-interference of dopamine D1-receptors in the nucleus accumbens shell. Neuropharmacology *89*, 398-411.

Plant, K., Pelkey, K.A., Bortolotto, Z.A., Morita, D., Terashima, A., McBain, C.J., Collingridge, G.L., and Isaac, J.T.R. (2006). Transient incorporation of native GluR2-lacking AMPA receptors during hippocampal long-term potentiation. Nature Neuroscience *9*, 602-604.

Plath, N., Ohana, O., Dammermann, B., Errington, M.L., Schmitz, D., Gross, C., Mao, X., Engelsberg, A., Mahlke, C., Welzl, H., *et al.* (2006). Arc/Arg3.1 is essential for the consolidation of synaptic plasticity and memories. Neuron *52*, 437-444.

Ploski, J.E., Pierre, V.J., Smucny, J., Park, K., Monsey, M.S., Overeem, K.A., and Schafe, G.E. (2008). The activity-regulated cytoskeletal-associated protein (Arc/Arg3.1) is required for memory consolidation of pavlovian fear conditioning in the lateral amygdala. The Journal of neuroscience : the official journal of the Society for Neuroscience *28*, 12383-12395.

Pnevmatikakis, E.A., and Giovannucci, A. (2017). NoRMCorre: An online algorithm for piecewise rigid motion correction of calcium imaging data. Journal of neuroscience methods *291*, 83-94.

Pnevmatikakis, E.A., Soudry, D., Gao, Y., Machado, T.A., Merel, J., Pfau, D., Reardon, T., Mu, Y., Lacefield, C., Yang, W., *et al.* (2016). Simultaneous Denoising, Deconvolution, and Demixing of Calcium Imaging Data. Neuron *89*, 285-299.

Poncer, J.C., Esteban, J.A., and Malinow, R. (2002). Multiple mechanisms for the potentiation of AMPA receptor-mediated transmission by alpha-Ca2+/calmodulin-dependent protein kinase II. The Journal of neuroscience : the official journal of the Society for Neuroscience *22*, 4406-4411.

Poncer, J.C., and Malinow, R. (2001). Postsynaptic conversion of silent synapses during LTP affects synaptic gain and transmission dynamics. Nature Neuroscience *4*, 989-996.

Poo, M.-m., Pignatelli, M., Ryan, T.J., Tonegawa, S., Bonhoeffer, T., Martin, K.C., Rudenko, A., Tsai, L.-H., Tsien, R.W., Fishell, G., *et al.* (2016). What is memory? The present state of the engram. BMC Biology, 1-18.

Purgianto, A., Scheyer, A.F., Loweth, J.A., Ford, K.A., Tseng, K.Y., and Wolf, M.E. (2013). Different Adaptations in AMPA Receptor Transmission in the Nucleus Accumbens after Short vs Long Access Cocaine Self-Administration Regimens. Neuropsychopharmacology *38*, 1789-1797.

Qi, J., Zhang, S., Wang, H.-L., Barker, D.J., Miranda-Barrientos, J., and Morales, M. (2016). VTA glutamatergic inputs to nucleus accumbens drive aversion by acting on GABAergic interneurons. Nature Neuroscience *19*, 725-733.

Quirk, G.J., and Mueller, D. (2008). Neural mechanisms of extinction learning and retrieval. Neuropsychopharmacology *33*, 56-72.

Quirk, G.J., Paré, D., Richardson, R., Herry, C., Monfils, M.-H., Schiller, D., and Vicentic, A. (2010). Erasing fear memories with extinction training. The Journal of neuroscience : the official journal of the Society for Neuroscience *30*, 14993-14997.

Radiske, A., Rossato, J.I., Gonzalez, M.C., Köhler, C.A., Bevilaqua, L.R., and Cammarota, M. (2017). BDNF controls object recognition memory reconsolidation. Neurobiology of Learning and Memory *142*, 79-84.

Ramanathan, S., Hanley, J.J., Deniau, J.M., and Bolam, J.P. (2002). Synaptic convergence of motor and somatosensory cortical afferents onto GABAergic interneurons in the rat striatum. The Journal of neuroscience : the official journal of the Society for Neuroscience *22*, 8158-8169.

Ramirez, S., Liu, X., Lin, P.-A., Suh, J., Pignatelli, M., Redondo, R.L., Ryan, T.J., and Tonegawa, S. (2013). Creating a false memory in the hippocampus. Science *341*, 387-391.

Ramirez, S., Liu, X., MacDonald, C.J., Moffa, A., Zhou, J., Redondo, R.L., and Tonegawa, S. (2015). Activating positive memory engrams suppresses depression-like behaviour. Nature *522*, 335-339.

Ramon y Cajal, S. (1894). The Croonian Lecture - La fine Structures des Centres Nerveux. Proceedings of the Royal Society of London *55*, 444-468.

Rao-Ruiz, P., Couey, J.J., Marcelo, I.M., Bouwkamp, C.G., Slump, D.E., Matos, M.R., Loo, R.J., Martins, G.J., Hout, M., IJcken, W.F., *et al.* (2019). Engram-specific transcriptome profiling of contextual memory consolidation. Nature Communications, 1-14.

Rao-Ruiz, P., Rotaru, D.C., van der Loo, R.J., Mansvelder, H.D., Stiedl, O., Smit, A.B., and Spijker, S. (2011). Retrieval-specific endocytosis of GluA2-AMPARs underlies adaptive reconsolidation of contextual fear. Nature Neuroscience *14*, 1302-1308.

Rashid, A.J., Yan, C., Mercaldo, V., Hsiang, H.-L.L., Park, S., Cole, C.J., De Cristofaro, A., Yu, J., Ramakrishnan, C., Lee, S.Y., *et al.* (2016). Competition between engrams influences fear memory formation and recall. Science *353*, 383-387.

Rehberg, K., Bergado-Acosta, J.R., Koch, J.C., and Stork, O. (2010). Disruption of fear memory consolidation and reconsolidation by actin filament arrest in the basolateral amygdala. Neurobiology of Learning and Memory *94*, 117-126.

Reijmers, L.G., Perkins, B.L., Matsuo, N., and Mayford, M. (2007). Localization of a stable neural correlate of associative memory. Science *317*, 1230-1233.

Reinert, S., bener, M.H.x.F., Bonhoeffer, T., and Goltstein, P.M. (2021). Mouse prefrontal cortex represents learned rules for categorization. Nature, 1-26.

Resendez, S.L., Jennings, J.H., Ung, R.L., Namboodiri, V.M.K., Zhou, Z.C., Otis, J.M., Nomura, H., McHenry, J.A., Kosyk, O., and Stuber, G.D. (2016). Visualization of cortical, subcortical and deep brain neural circuit dynamics during naturalistic mammalian behavior with head-mounted microscopes and chronically implanted lenses. Nature protocols *11*, 566-597.

Restivo, L., Vetere, G., Bontempi, B., and Ammassari-Teule, M. (2009). The formation of recent and remote memory is associated with time-dependent formation of dendritic spines in the hippocampus and anterior cingulate cortex. The Journal of neuroscience : the official journal of the Society for Neuroscience *29*, 8206-8214.

Rex, C.S., Chen, L.Y., Sharma, A., Liu, J., Babayan, A.H., Gall, C.M., and Lynch, G. (2009). Different Rho GTPase-dependent signaling pathways initiate sequential steps in the consolidation of long-term potentiation. The Journal of cell biology *186*, 85-97.

Rex, C.S., Gavin, C.F., Rubio, M.D., Kramar, E.A., Chen, L.Y., Jia, Y., Huganir, R.L., Muzyczka, N., Gall, C.M., Miller, C.A., *et al.* (2010). Myosin IIb Regulates Actin Dynamics during Synaptic Plasticity and Memory Formation. Neuron *67*, 603-617.

Rich, M.T., Abbott, T.B., Chung, L., Gulcicek, E.E., Stone, K.L., Colangelo, C.M., Lam, T.T., Nairn, A.C., Taylor, J.R., and Torregrossa, M.M. (2016). Phosphoproteomic Analysis Reveals a Novel Mechanism of CaMKII Regulation Inversely Induced by Cocaine Memory Extinction versus Reconsolidation. The Journal of neuroscience : the official journal of the Society for Neuroscience *36*, 7613-7627.

Rich, M.T., Huang, Y.H., and Torregrossa, M.M. (2019a). Calcineurin Promotes Neuroplastic Changes in the Amygdala Associated with Weakened Cocaine-Cue Memories. The Journal of neuroscience : the official journal of the Society for Neuroscience, 0453-0419-0411.

Rich, M.T., Huang, Y.H., and Torregrossa, M.M. (2019b). Plasticity at Thalamo-amygdala Synapses Regulates Cocaine-Cue Memory Formation and Extinction. Cell reports *26*, 1010-1020.e1015.

Richard, J.M., Ambroggi, F., Janak, P.H., and Fields, H.L. (2016). Ventral Pallidum Neurons Encode Incentive Value and Promote Cue-Elicited Instrumental Actions. Neuron *90*, 1165-1173.

Richard, J.M., Stout, N., Acs, D., and Janak, P.H. (2018). Ventral pallidal encoding of reward-seeking behavior depends on the underlying associative structure. eLife *7*, 7957.

Risher, W.C., Kim, N., Koh, S., Choi, J.-E., Mitev, P., Spence, E.F., Pilaz, L.-J., Wang, D., Feng, G., Silver, D.L., *et al.* (2018). Thrombospondin receptor α2δ-1 promotes synaptogenesis and spinogenesis via postsynaptic Rac1. The Journal of cell biology *265*, jcb.201802057-201802019.

Robbe, D., Alonso, G., Duchamp, F., Bockaert, J., and Manzoni, O.J. (2001). Localization and mechanisms of action of cannabinoid receptors at the glutamatergic synapses of the mouse nucleus accumbens. The Journal of neuroscience : the official journal of the Society for Neuroscience *21*, 109-116.

Robbe, D., Kopf, M., Remaury, A., Bockaert, J., and Manzoni, O.J. (2002). Endogenous cannabinoids mediate long-term synaptic depression in the nucleus accumbens. Proceedings of the National Academy of Sciences of the United States of America *99*, 8384-8388.

Roberts Wolfe, D.J., Heinsbroek, J.A., Spencer, S.M., Bobadilla, A.-C., Smith, A.C.W., Gipson, C.D., and Kalivas, P. (2019). Transient synaptic potentiation in nucleus accumbens shell during refraining from cocaine seeking. Addiction Biology *97*, e12759-12710.

Roberts-Wolfe, D., Bobadilla, A.-C., Heinsbroek, J.A., Neuhofer, D., and Kalivas, P. (2018). Drug Refraining and Seeking Potentiate Synapses on Distinct Populations of Accumbens Medium Spiny Neurons. The Journal of neuroscience : the official journal of the Society for Neuroscience *38*, 7100-7107.

Robinson, N.T.M., Descamps, L.A.L., Russell, L.E., Buchholz, M.O., Bicknell, B.A., Antonov, G.K., Lau, J.Y.N., Nutbrown, R., Schmidt-Hieber, C., and Häusser, M. (2020). Targeted Activation of Hippocampal Place Cells Drives Memory-Guided Spatial Behavior. Cell, 1-25.

Robinson, T.E., Gorny, G., Mitton, E., and Kolb, B. (2001). Cocaine self-administration alters the morphology of dendrites and dendritic spines in the nucleus accumbens and neocortex. Synapse *39*, 257-266.

Robinson, T.E., and Kolb, B. (1997). Persistent structural modifications in nucleus accumbens and prefrontal cortex neurons produced by previous experience with amphetamine. The Journal of neuroscience : the official journal of the Society for Neuroscience *17*, 8491-8497.

Robinson, T.E., and Kolb, B. (1999). Alterations in the morphology of dendrites and dendritic spines in the nucleus accumbens and prefrontal cortex following repeated treatment with amphetamine or cocaine. *11*, 1598-1604.

Robison, A.J., Vialou, V., Mazei-Robison, M., Feng, J., Kourrich, S., Collins, M., Wee, S., Koob, G., Turecki, G., Neve, R., *et al.* (2013). Behavioral and Structural Responses to Chronic Cocaine Require a Feedforward Loop Involving FosB and Calcium/Calmodulin-Dependent Protein Kinase II in the Nucleus Accumbens Shell. The Journal of neuroscience : the official journal of the Society for Neuroscience *33*, 4295-4307.

Rodriguez-Ortiz, C.J., Garcia-DeLaTorre, P., Benavidez, E., Ballesteros, M.A., and Bermudez-Rattoni, F. (2008). Intrahippocampal anisomycin infusions disrupt previously consolidated spatial memory only when memory is updated. Neurobiology of Learning and Memory *89*, 352-359.

Roesch, M.R., Singh, T., Brown, P.L., Mullins, S.E., and Schoenbaum, G. (2009). Ventral Striatal Neurons Encode the Value of the Chosen Action in Rats Deciding between Differently Delayed or Sized Rewards. The Journal of neuroscience : the official journal of the Society for Neuroscience *29*, 13365-13376.

Rogan, M.T., Stäubli, U.V., and LeDoux, J.E. (1997). Fear conditioning induces associative long-term potentiation in the amygdala. Nature *390*, 604-607.

Rogerson, T., Cai, D.J., Frank, A., Sano, Y., Shobe, J., Lopez-Aranda, M.F., and Silva, A.J. (2014). Synaptic tagging during memory allocation. Nature Reviews Neuroscience *15*, 157-169.

Roitman, M.F., Wheeler, R.A., and Carelli, R.M. (2005). Nucleus Accumbens Neurons Are Innately Tuned for Rewarding and Aversive Taste Stimuli, Encode Their Predictors, and Are Linked to Motor Output. Neuron *45*, 587-597.

Ron, S., Dudai, Y., and Segal, M. (2012). Overexpression of PKMζ alters morphology and function of dendritic spines in cultured cortical neurons. Cerebral cortex (New York, NY : 1991) *22*, 2519-2528.

Root, D.H., Mejias-Aponte, C.A., Qi, J., and Morales, M. (2014). Role of glutamatergic projections from ventral tegmental area to lateral habenula in aversive conditioning. The Journal of neuroscience : the official journal of the Society for Neuroscience *34*, 13906-13910.

Rossetti, T., Banerjee, S., Kim, C., Leubner, M., Lamar, C., Gupta, P., Lee, B., Neve, R., and Lisman, J. (2017). Memory Erasure Experiments Indicate a Critical Role of CaMKII in Memory Storage. Neuron *96*, 207-216.e202.

Rossi, L.M., Reverte, I., Ragozzino, D., Badiani, A., Venniro, M., and Caprioli, D. (2020). Role of nucleus accumbens core but not shell in incubation of methamphetamine craving after voluntary abstinence. Nature Neuroscience *45*, 256-265.

Roy, D.S., Arons, A., Mitchell, T.I., Pignatelli, M., Ryan, T.J., and Tonegawa, S. (2016). Memory retrieval by activating engram cells in mouse models of early Alzheimer's disease. Nature *531*, 508-512.

Roy, D.S., Kitamura, T., Okuyama, T., Ogawa, S.K., Sun, C., Obata, Y., Yoshiki, A., and Tonegawa, S. (2017a). Distinct Neural Circuits for the Formation and Retrieval of Episodic Memories. Cell, 1-33.

Roy, D.S., Muralidhar, S., Smith, L.M., and Tonegawa, S. (2017b). Silent memory engrams as the basis for retrograde amnesia. Proceedings of the National Academy of Sciences *19*, 201714248-201714248.

Ruff, D.A., Ni, A.M., and Cohen, M.R. (2018). Cognition as a Window into Neuronal Population Space. Annual review of neuroscience *41*, 77-97.

Rule, M.E., O'Leary, T., and Harvey, C.D. (2019). Causes and consequences of representational drift. Current Opinion in Neurobiology *58*, 141-147.

Ryan, T.J., Roy, D.S., Pignatelli, M., Arons, A., and Tonegawa, S. (2015). Memory. Engram cells retain memory under retrograde amnesia. Science *348*, 1007-1013.

Sacktor, T.C. (2011). How does PKMζ maintain long-term memory? Nature Reviews Neuroscience *12*, 9-15.

Saddoris, M.P., and Carelli, R.M. (2014). Cocaine self-administration abolishes associative neural encoding in the nucleus accumbens necessary for higher-order learning. Biological Psychiatry *75*, 156-164.

Saddoris, M.P., Stamatakis, A., and Carelli, R.M. (2011). Neural correlates of Pavlovian-to-instrumental transfer in the nucleus accumbens shell are selectively potentiated following cocaine self-administration. The European journal of neuroscience *33*, 2274-2287.

Sadtler, P.T., Quick, K.M., Golub, M.D., Chase, S.M., Ryu, S.I., Tyler-Kabara, E.C., Yu, B.M., and Batista, A.P. (2014). Neural constraints on learning. Nature *512*, 423-426.

Sanchez, H., Quinn, J.J., Torregrossa, M.M., and Taylor, J.R. (2010). Reconsolidation of a cocaine-associated stimulus requires amygdalar protein kinase A. The Journal of neuroscience : the official journal of the Society for Neuroscience *30*, 4401-4407.

Saneyoshi, T., Matsuno, H., Suzuki, A., Murakoshi, H., Hedrick, N.G., Agnello, E., O'Connell, R., Stratton, M.M., Yasuda, R., and Hayashi, Y. (2019). Reciprocal Activation within a Kinase-Effector Complex Underlying Persistence of Structural LTP. Neuron, 1-19.

Sangha, S., Scheibenstock, A., and Lukowiak, K. (2003). Reconsolidation of a long-term memory in Lymnaea requires new protein and RNA synthesis and the soma of right pedal dorsal 1. The Journal of neuroscience : the official journal of the Society for Neuroscience *23*, 8034-8040.

Sanhueza, M., Fernandez-Villalobos, G., Stein, I.S., Kasumova, G., Zhang, P., Bayer, K.U., Otmakhov, N., Hell, J.W., and Lisman, J. (2011). Role of the CaMKII/NMDA receptor complex in the maintenance of synaptic strength. The Journal of neuroscience : the official journal of the Society for Neuroscience *31*, 9170-9178.

Sartor, G.C., and Aston-Jones, G.S. (2014). Post-retrieval extinction attenuates cocaine memories. Neuropsychopharmacology *39*, 1059-1065.

Saunders, B.T., Richard, J.M., Margolis, E.B., and Janak, P.H. (2018). Dopamine neurons create Pavlovian conditioned stimuli with circuit-defined motivational properties. Nature Neuroscience, 1-17.

Saunders, B.T., and Robinson, T.E. (2012). The role of dopamine in the accumbens core in the expression of Pavlovian-conditioned responses. The European journal of neuroscience *36*, 2521-2532.

Saunders, B.T., Yager, L.M., and Robinson, T.E. (2013). Cue-evoked cocaine "craving": role of dopamine in the accumbens core. The Journal of neuroscience : the official journal of the Society for Neuroscience *33*, 13989-14000.

Schall, T.A., Wright, W.J., and Dong, Y. (2020). Nucleus accumbens fast-spiking interneurons in motivational and addictive behaviors. Molecular psychiatry, 1-13.

Scheuss, V., and Neher, E. (2001). Estimating Synaptic Parameters from Mean, Variance, and Covariance in Trains of Synaptic Responses. Biophysical journal *81*, 1970-1989.

Scheuss, V., Schneggenburger, R., and Neher, E. (2002). Separation of presynaptic and postsynaptic contributions to depression by covariance analysis of successive EPSCs at the calyx

of Held synapse. The Journal of neuroscience : the official journal of the Society for Neuroscience *22*, 728-739.

Scheyer, A.F., Wolf, M.E., and Tseng, K.Y. (2014). A protein synthesis-dependent mechanism sustains calcium-permeable AMPA receptor transmission in nucleus accumbens synapses during withdrawal from cocaine self-administration. The Journal of neuroscience : the official journal of the Society for Neuroscience *34*, 3095-3100.

Schiller, D., Monfils, M.-H., Raio, C.M., Johnson, D.C., LeDoux, J.E., and Phelps, E.A. (2010). Preventing the return of fear in humans using reconsolidation update mechanisms. Nature *463*, 49-53.

Schmidt, H.D., Schassburger, R.L., Guercio, L.A., and Pierce, R.C. (2013). Stimulation of mGluR5 in the accumbens shell promotes cocaine seeking by activating PKC gamma. The Journal of neuroscience : the official journal of the Society for Neuroscience *33*, 14160-14169.

Schoonover, C.E., Ohashi, S.N., Axel, R., and Fink, A.J.P. (2021). Representational drift in primary olfactory cortex. Nature, 1-34.

Schultz, W. (2007). Multiple dopamine functions at different time courses. Annual review of neuroscience *30*, 259-288.

Schultz, W. (2016). Dopamine reward prediction-error signalling: a two-component response. Nature Reviews Neuroscience *17*, 183-195.

Schultz, W., Apicella, P., Scarnati, E., and Ljungberg, T. (1992). Neuronal activity in monkey ventral striatum related to the expectation of reward. The Journal of neuroscience : the official journal of the Society for Neuroscience *12*, 4595-4610.

Schultz, W., Dayan, P., and Montague, P.R. (1997). A neural substrate of prediction and reward. Science *275*, 1593-1599.

Self, D.W., Genova, L.M., Hope, B.T., Barnhart, W.J., Spencer, J.J., and Nestler, E.J. (1998). Involvement of cAMP-dependent protein kinase in the nucleus accumbens in cocaine self-administration and relapse of cocaine-seeking behavior. The Journal of neuroscience : the official journal of the Society for Neuroscience *18*, 1848-1859.

Semon, R. (1921). The Mneme (G. Allen & Unwin Limited).

Serrano, P., Friedman, E.L., Kenney, J., Taubenfeld, S.M., Zimmerman, J.M., Hanna, J., Alberini, C., Kelley, A.E., Maren, S., Rudy, J.W., *et al.* (2008). PKMzeta maintains spatial, instrumental, and classically conditioned long-term memories. PLoS Biology *6*, 2698-2706.

Sesack, S.R., and Grace, A.A. (2010). Cortico-Basal Ganglia reward network: microcircuitry. Neuropsychopharmacology *35*, 27-47.

Setlow, B., Schoenbaum, G., and Gallagher, M. (2003). Neural encoding in ventral striatum during olfactory discrimination learning. Neuron *38*, 625-636.

Sevenster, D., Beckers, T., and Kindt, M. (2012). Retrieval per se is not sufficient to trigger reconsolidation of human fear memory. Neurobiology of Learning and Memory *97*, 338-345.

Sevenster, D., Beckers, T., and Kindt, M. (2013). Prediction error governs pharmacologically induced amnesia for learned fear. Science *339*, 830-833.

Shao, C.Y., Sondhi, R., van de Nes, P.S., and Sacktor, T.C. (2011). PKMζ is necessary and sufficient for synaptic clustering of PSD-95. Hippocampus *22*, 1501-1507.

Shehata, M., Abdou, K., Choko, K., Matsuo, M., Nishizono, H., and Inokuchi, K. (2018). Autophagy enhances memory erasure through synaptic destabilization. The Journal of neuroscience : the official journal of the Society for Neuroscience, 3505-3517-3548.

Shema, R., Haramati, S., Ron, S., Hazvi, S., Chen, A., Sacktor, T.C., and Dudai, Y. (2011). Enhancement of consolidated long-term memory by overexpression of protein kinase Mzeta in the neocortex. Science *331*, 1207-1210.

Shema, R., Sacktor, T.C., and Dudai, Y. (2007). Rapid erasure of long-term memory associations in the cortex by an inhibitor of PKM zeta. Science *317*, 951-953.

Shi, S., Hayashi, Y., Esteban, J.A., and Malinow, R. (2001). Subunit-specific rules governing AMPA receptor trafficking to synapses in hippocampal pyramidal neurons. Cell *105*, 331-343.

Shrestha, P., Ayata, P., Herrero-Vidal, P., Longo, F., Gastone, A., LeDoux, J.E., Heintz, N., and Klann, E. (2019). Cell-type-specific drug-inducible protein synthesis inhibition demonstrates that memory consolidation requires rapid neuronal translation. Nature Neuroscience, 1-26.

Shrestha, P., Shan, Z., Mamcarz, M., Ruiz, K.S.A., Zerihoun, A.T., Juan, C.-Y., Herrero-Vidal, P.M., Pelletier, J., Heintz, N., and Klann, E. (2020). Amygdala inhibitory neurons as loci for translation in emotional memories. Nature, 1-22.

Shukla, A., Beroun, A., Panopoulou, M., Neumann, P.A., Grant, S.G., Olive, M.F., Dong, Y., and Schlüter, O.M. (2017). Calcium-permeable AMPA receptors and silent synapses in cocaine-conditioned place preference. The EMBO Journal, e201695465-201695417.

Shuman, T., Aharoni, D., Cai, D.J., Lee, C.R., Chavlis, S., Page-Harley, L., Vetere, L.M., Feng, Y., Yang, C.Y., Mollinedo-Gajate, I., *et al.* (2019). Breakdown of spatial coding and interneuron synchronization in epileptic mice. Nature Neuroscience, 1-28.

Silver, R.A. (2003). Estimation of nonuniform quantal parameters with multiple-probability fluctuation analysis: theory, application and limitations. Journal of neuroscience methods *130*, 127-141.

Sjulson, L., Peyrache, A., Cumpelik, A., Cassataro, D., and Buzsáki, G. (2018). Cocaine Place Conditioning Strengthens Location- Specific Hippocampal Coupling to the Nucleus Accumbens. Neuron, 1-15.

Skinner, B.F. (1938). The Behavior of Organisms (New York: Appleton-Century-Crofts).

Smith, A.C.W., Kupchik, Y.M., Scofield, M.D., Gipson, C.D., Wiggins, A., Thomas, C.A., and Kalivas, P. (2014). Synaptic plasticity mediating cocaine relapse requires matrix metalloproteinases. Nature Neuroscience *17*, 1655-1657.

Smith, A.C.W., Scofield, M.D., Heinsbroek, J.A., Gipson, C.D., Neuhofer, D., Roberts-Wolfe, D.J., Spencer, S., Stankeviciute, N.M., Smith, R., Allen, N.P., *et al.* (2016). Accumbens nNOS interneurons regulate cocaine relapse. The Journal of neuroscience : the official journal of the Society for Neuroscience, 1-68.

Soundara Rajan, T., Ghilardi, M.F.M., Wang, H.-Y., Mazzon, E., Bramanti, P., Restivo, D., and Quartarone, A. (2017). Mechanism of Action for rTMS: A Working Hypothesis Based on Animal Studies. Frontiers in physiology *8*, 457.

Spencer, S., Garcia-Keller, C., Roberts-Wolfe, D., Heinsbroek, J.A., Mulvaney, M., Sorrell, A., and Kalivas, P. (2016). Cocaine Use Reverses Striatal Plasticity Produced During Cocaine Seeking. Biological Psychiatry.

Squire, L.R., Genzel, L., Wixted, J.T., and Morris, R.G. (2015). Memory consolidation. Cold Spring Harbor Perspectives in Biology *7*, a021766.

Star, E.N., Kwiatkowski, D.J., and Murthy, V.N. (2002). Rapid turnover of actin in dendritic spines and its regulation by activity. Nature Neuroscience *5*, 239-246.

Stefanik, M.T., and Kalivas, P. (2013). Optogenetic dissection of basolateral amygdala projections during cue-induced reinstatement of cocaine seeking. Frontiers in Behavioral Neuroscience *7*, 213.

Stefanik, M.T., Kupchik, Y.M., Brown, R.M., and Kalivas, P. (2013). Optogenetic Evidence That Pallidal Projections, Not Nigral Projections, from the Nucleus Accumbens Core Are Necessary for Reinstating Cocaine Seeking. The Journal of neuroscience : the official journal of the Society for Neuroscience *33*, 13654-13662.

Stefanik, M.T., Moussawi, K., Kupchik, Y.M., Smith, K.C., Miller, R.L., Huff, M.L., Deisseroth, K., Kalivas, P., and LaLumiere, R.T. (2012). Optogenetic inhibition of cocaine seeking in rats. Addiction Biology *18*, 50-53.

Stefanini, F., Kushnir, L., Jimenez, J.C., Jennings, J.H., Woods, N.I., Stuber, G.D., Kheirbek, M.A., Hen, R., and Fusi, S. (2020). A Distributed Neural Code in the Dentate Gyrus and in CA1. Neuron, 1-19.

Steinberg, E.E., Keiflin, R., Boivin, J.R., Witten, I.B., Deisseroth, K., and Janak, P.H. (2013). A causal link between prediction errors, dopamine neurons and learning. Nature Neuroscience *16*, 966-973.

Stephan, A.H., Barres, B.A., and Stevens, B. (2012). The complement system: an unexpected role in synaptic pruning during development and disease. Annual review of neuroscience *35*, 369-389.

Steward, O., Wallace, C.S., Lyford, G.L., and Worley, P.F. (1998). Synaptic activation causes the mRNA for the IEG Arc to localize selectively near activated postsynaptic sites on dendrites. Neuron *21*, 741-751.

Steward, O., and Worley, P.F. (2001). Selective targeting of newly synthesized Arc mRNA to active synapses requires NMDA receptor activation. Neuron *30*, 227-240.

Stopper, C.M., and Floresco, S.B. (2011). Contributions of the nucleus accumbens and its subregions to different aspects of risk-based decision making. Cognitive, affective & behavioral neuroscience *11*, 97-112.

Stratford, T.R., and Kelley, A.E. (1999). Evidence of a functional relationship between the nucleus accumbens shell and lateral hypothalamus subserving the control of feeding behavior. The Journal of neuroscience : the official journal of the Society for Neuroscience *19*, 11040-11048.

Stuber, G.D., Hnasko, T.S., Britt, J.P., Edwards, R.H., and Bonci, A. (2010). Dopaminergic Terminals in the Nucleus Accumbens But Not the Dorsal Striatum Corelease Glutamate. The Journal of neuroscience : the official journal of the Society for Neuroscience *30*, 8229-8233.

Stuber, G.D., Klanker, M., de Ridder, B., Bowers, M.S., Joosten, R.N., Feenstra, M.G., and Bonci, A. (2008). Reward-predictive cues enhance excitatory synaptic strength onto midbrain dopamine neurons. Science *321*, 1690-1692.

Stuber, G.D., Roitman, M.F., Phillips, P.E.M., Carelli, R.M., and Wightman, R.M. (2004). Rapid Dopamine Signaling in the Nucleus Accumbens during Contingent and Noncontingent Cocaine Administration. Neuropsychopharmacology *30*, 853-863.

Stuber, G.D., Sparta, D.R., Stamatakis, A.M., van Leeuwen, W.A., Hardjoprajitno, J.E., Cho, S.L., Tye, K.M., Kempadoo, K.A., Zhang, F., Deisseroth, K., *et al.* (2012). Excitatory transmission from the amygdala to nucleus accumbens facilitates reward seeking. Nature *475*, 377-380.

Stuber, G.D., Wightman, R.M., and Carelli, R.M. (2005). Extinction of cocaine self-administration reveals functionally and temporally distinct dopaminergic signals in the nucleus accumbens. Neuron *46*, 661-669.

Südhof, T.C. (2018). Towards an Understanding of Synapse Formation. Neuron *100*, 276-293.

Sugam, J.A., Saddoris, M.P., and Carelli, R.M. (2014). Nucleus accumbens neurons track behavioral preferences and reward outcomes during risky decision making. Biological Psychiatry *75*, 807-816.

Sugden, A.U., Zaremba, J.D., Sugden, L.A., McGuire, K.L., Lutas, A., Ramesh, R.N., Alturkistani, O., x000F8, K.K.L., Burgess, C.R., and Andermann, M.L. (2020). Cortical reactivations of recent sensory experiences predict bidirectional network changes during learning. Nature Neuroscience, 1-38.

Sun, C., Yang, W., Martin, J., and Tonegawa, S. (2020a). Hippocampal neurons represent events as transferable units of experience. Nature Neuroscience, 1-33.

Sun, X., Bernstein, M.J., Meng, M., Rao, S., Sørensen, A.T., Yao, L., Zhang, X., Anikeeva, P.O., and Lin, Y. (2020b). Functionally Distinct Neuronal Ensembles within the Memory Engram. Cell, 1-32.

Sun, X., Zhao, Y., and Wolf, M.E. (2005). Dopamine receptor stimulation modulates AMPA receptor synaptic insertion in prefrontal cortex neurons. The Journal of neuroscience : the official journal of the Society for Neuroscience *25*, 7342-7351.

Surmeier, D.J., Ding, J., Day, M., Wang, Z., and Shen, W. (2007). D1 and D2 dopamine-receptor modulation of striatal glutamatergic signaling in striatal medium spiny neurons. Trends in neurosciences *30*, 228-235.

Sussillo, D. (2014). Neural circuits as computational dynamical systems. Current Opinion in Neurobiology *25*, 156-163.

Sutton, M.A., Schmidt, E.F., Choi, K.-H., Schad, C.A., Whisler, K., Simmons, D., Karanian, D.A., Monteggia, L.M., Neve, R.L., and Self, D.W. (2003). Extinction-induced upregulation in AMPA receptors reduces cocaine-seeking behaviour. Nature *421*, 70-75.

Suvrathan, A., Bennur, S., Ghosh, S., Tomar, A., Anilkumar, S., and Chattarji, S. (2013). Stress enhances fear by forming new synapses with greater capacity for long-term potentiation in the amygdala. Philosophical Transactions of the Royal Society B: Biological Sciences *369*, 20130151-20130151.

Sweis, B.M., Mau, W., Rabinowitz, S., and Cai, D.J. (2021). Dynamic and heterogeneous neural ensembles contribute to a memory engram. Current Opinion in Neurobiology *67*, 199-206.

Takahashi, T., Svoboda, K., and Malinow, R. (2003). Experience strengthening transmission by driving AMPA receptors into synapses. Science *299*, 1585-1588.

Takehara-Nishiuchi, K., and McNaughton, B.L. (2008). Spontaneous changes of neocortical code for associative memory during consolidation. Science *322*, 960-963.

Tanaka, J.-i., Horiike, Y., Matsuzaki, M., Miyazaki, T., Ellis-Davies, G.C.R., and Kasai, H. (2008). Protein synthesis and neurotrophin-dependent structural plasticity of single dendritic spines. Science *319*, 1683-1687.

Tanaka, K.Z., He, H., Tomar, A., Niisato, K., Huang, A.J.Y., and McHugh, T.J. (2018). The hippocampal engram maps experience but not place. Science *361*, 392-397.

Tang, S., and Yasuda, R. (2017). Imaging ERK and PKA Activation in Single Dendritic Spines during Structural Plasticity. Neuron, 1-14.

Tashiro, A., Minden, A., and Yuste, R. (2000). Regulation of dendritic spine morphology by the rho family of small GTPases: antagonistic roles of Rac and Rho. Cerebral Cortex *10*, 927-938.

Tashiro, A., and Yuste, R. (2004). Regulation of dendritic spine motility and stability by Rac1 and Rho kinase: evidence for two forms of spine motility. Molecular and Cellular Neuroscience *26*, 429-440.

Taubenfeld, S.M., Milekic, M.H., Monti, B., and Alberini, C.M. (2001). The consolidation of new but not reactivated memory requires hippocampal C/EBPbeta. Nature Neuroscience *4*, 813-818.

Taverna, S., van Dongen, Y.C., Groenewegen, H.J., and Pennartz, C.M.A. (2004). Direct physiological evidence for synaptic connectivity between medium-sized spiny neurons in rat nucleus accumbens in situ. Journal of neurophysiology *91*, 1111-1121.

Taylor, J.R., Olausson, P., Quinn, J.J., and Torregrossa, M.M. (2008). Targeting extinction and reconsolidation mechanisms to combat the impact of drug cues on addiction. Neuropharmacology, 1-10.

Tecuapetla, F., Jin, X., Lima, S.Q., and Costa, R.M. (2016). Complementary Contributions of Striatal Projection Pathways to Action Initiation and Execution. Cell *166*, 703-715.

Tecuapetla, F., Patel, J.C., Xenias, H., English, D.F., Tadros, I., Shah, F., Berlin, J., Deisseroth, K., Rice, M.E., Tepper, J.M., *et al.* (2010). Glutamatergic Signaling by Mesolimbic Dopamine Neurons in the Nucleus Accumbens. The Journal of neuroscience : the official journal of the Society for Neuroscience *30*, 7105-7110.

Tepper, J.M., Wilson, C.J., and Koos, T. (2008). Feedforward and feedback inhibition in neostriatal GABAergic spiny neurons. Brain research reviews *58*, 272-281.

Terrier, J., Lüscher, C., and Pascoli, V. (2016). Cell-Type Specific Insertion of GluA2-Lacking AMPARs with Cocaine Exposure Leading to Sensitization, Cue-Induced Seeking, and Incubation of Craving. Neuropsychopharmacology *41*, 1779-1789.

Thalhammer, A., Rudhard, Y., Tigaret, C.M., Volynski, K.E., Rusakov, D.A., and Schoepfer, R. (2006). CaMKII translocation requires local NMDA receptor-mediated Ca2+ signaling. The EMBO Journal *25*, 5873-5883.

Titley, H.K., Brunel, N., and Hansel, C. (2017). Toward a Neurocentric View of Learning. Neuron *95*, 19-32.

Toda, S., Shen, H.-w., Peters, J., Cagle, S., and Kalivas, P. (2006). Cocaine increases actin cycling: effects in the reinstatement model of drug seeking. The Journal of neuroscience : the official journal of the Society for Neuroscience *26*, 1579-1587.

Tolias, K.F., Bikoff, J.B., Burette, A., Paradis, S., Harrar, D., Tavazoie, S., Weinberg, R.J., and Greenberg, M.E. (2005). The Rac1-GEF Tiam1 Couples the NMDA Receptor to the Activity-Dependent Development of Dendritic Arbors and Spines. Neuron *45*, 525-538.

Tominaga-Yoshino, K., Urakubo, T., Okada, M., Matsuda, H., and Ogura, A. (2008). Repetitive induction of late-phase LTP produces long-lasting synaptic enhancement accompanied by synaptogenesis in cultured hippocampal slices. Hippocampus *18*, 281-293.

Tonegawa, S., Liu, X., Ramirez, S., and Redondo, R. (2015). Memory Engram Cells Have Come of Age. Neuron *87*, 918-931.

Tonegawa, S., Morrissey, M.D., and Kitamura, T. (2018). The role of engram cells in the systems consolidation of memory. Nature Reviews Neuroscience, 1-14.

Torregrossa, M.M., and Taylor, J.R. (2013). Learning to forget: manipulating extinction and reconsolidation processes to treat addiction. Psychopharmacology (Berl) *226*, 659-672.

Torregrossa, M.M., and Taylor, J.R. (2016). Neuroscience of learning and memory for addiction medicine: from habit formation to memory reconsolidation. Prog Brain Res *223*, 91-113.

Tovar, K.R., and Westbrook, G.L. (1999). The incorporation of NMDA receptors with a distinct subunit composition at nascent hippocampal synapses in vitro. The Journal of neuroscience : the official journal of the Society for Neuroscience *19*, 4180-4188.

Tritsch, N.X., Ding, J.B., and Sabatini, B.L. (2012). Dopaminergic neurons inhibit striatal output through non-canonical release of GABA. Nature *490*, 262-266.

Tritsch, N.X., and Sabatini, B.L. (2012). Dopaminergic Modulation of Synaptic Transmission in Cortex and Striatum. Neuron *76*, 33-50.

Tronson, N.C., and Taylor, J.R. (2007). Molecular mechanisms of memory reconsolidation. Nature Reviews Neuroscience *8*, 262-275.

Tronson, N.C., Wiseman, S.L., Olausson, P., and Taylor, J.R. (2006). Bidirectional behavioral plasticity of memory reconsolidation depends on amygdalar protein kinase A. Nature Neuroscience *9*, 167-169.

Trouche, S., Koren, V., Doig, N.M., Ellender, T.J., El-Gaby, M., Lopes-dos-Santos, V., Reeve, H.M., Perestenko, P.V., Garas, F.N., Magill, P.J., *et al.* (2019). A Hippocampus-Accumbens Tripartite Neuronal Motif Guides Appetitive Memory in Space. Cell, 1-31.

Trouche, S., Sasaki, J.M., Tu, T., and Reijmers, L.G. (2013). Fear extinction causes target-specific remodeling of perisomatic inhibitory synapses. Neuron *80*, 1054-1065.

Tse, D., Takeuchi, T., Kakeyama, M., Kajii, Y., Okuno, H., Tohyama, C., Bito, H., and Morris, R.G.M. (2011). Schema-dependent gene activation and memory encoding in neocortex. Science *333*, 891-895.

Tu, X., Yasuda, R., and Colgan, L.A. (2020). Rac1 is a downstream effector of PKCα in structural synaptic plasticity. Scientific Reports, 1-9.

Turrigiano, G.G. (2008). The Self-Tuning Neuron: Synaptic Scaling of Excitatory Synapses. Cell *135*, 422-435.

Tye, K.M., Stuber, G.D., de Ridder, B., Bonci, A., and Janak, P.H. (2008). Rapid strengthening of thalamo-amygdala synapses mediates cue–reward learning. Nature *453*, 1253-1257.

Vega-Villar, M., Horvitz, J.C., and Nicola, S.M. (2019). NMDA receptor-dependent plasticity in the nucleus accumbens connects reward-predictive cues to approach responses. Nature Communications, 1-16.

Vetere, G., Restivo, L., Cole, C.J., Ross, P.J., Ammassari-Teule, M., Josselyn, S.A., and Frankland, P.W. (2011). Spine growth in the anterior cingulate cortex is necessary for the consolidation of contextual fear memory. Proceedings of the National Academy of Sciences of the United States of America *108*, 8456-8460.

Volk, L.J., Bachman, J.L., Johnson, R., Yu, Y., and Huganir, R.L. (2013). PKM-ζ is not required for hippocampal synaptic plasticity, learning and memory. Nature *493*, 420-423.

Volkow, N.D., Wise, R.A., and Baler, R. (2017). The dopamine motive system: implications for drug and food addiction. Nature Reviews Neuroscience *18*, 741-752.

von Hertzen, L.S.J., and Giese, K.P. (2005). Memory reconsolidation engages only a subset of immediate-early genes induced during consolidation. The Journal of neuroscience : the official journal of the Society for Neuroscience *25*, 1935-1942.

Vyas, S., Golub, M.D., Sussillo, D., and Shenoy, K.V. (2020). Computation Through Neural Population Dynamics. Annual review of neuroscience *43*, 249-275.

Waites, C.L., Craig, A.M., and Garner, C.C. (2005). Mechanisms of vertebrate synaptogenesis. Annual review of neuroscience *28*, 251-274.

Wang, H.-L., Qi, J., Zhang, S., Wang, H., and Morales, M. (2015). Rewarding Effects of Optical Stimulation of Ventral Tegmental Area Glutamatergic Neurons. The Journal of neuroscience : the official journal of the Society for Neuroscience *35*, 15948-15954.

Wang, J., Ishikawa, M., Yang, Y., Otaka, M., Kim, J.Y., Gardner, G.R., Stefanik, M.T., Milovanovic, M., Huang, Y.H., Hell, J.W., *et al.* (2018). Cascades of Homeostatic Dysregulation Promote Incubation of Cocaine Craving. The Journal of neuroscience : the official journal of the Society for Neuroscience *38*, 4316-4328.

Wang, J., Li, K.-L., Shukla, A., Beroun, A., Ishikawa, M., Huang, X., Wang, Y., Wang, Y.Q., Yue, Y., Bastola, N.D., *et al.* (2020). Cocaine Triggers Astrocyte-Mediated Synaptogenesis. Biological Psychiatry, 1-31.

Wang, S.-H., de Oliveira Alvares, L., and Nader, K. (2009). Cellular and systems mechanisms of memory strength as a constraint on auditory fear reconsolidation. Nature Neuroscience *12*, 905-912.

Wang, X., He, L., Wu, Y.I., Hahn, K.M., and Montell, D.J. (2010). Light-mediated activation reveals a key role for Rac in collective guidance of cell movement in vivo. Nature Neuroscience *12*, 591-597.

Wang, Y.Q., Huang, Y.H., Balakrishnan, S., Liu, L.-D., Wang, Y.T., Nestler, E.J., Schlüter, O.M., and Dong, Y. (2021). AMPA and NMDA Receptor Trafficking at Cocaine-Generated Synapses. The Journal of Neuroscience.

Warren, B.L., Mendoza, M.P., Caprioli, D., Rubio, F.J., Whitaker, L.R., McPherson, K.B., Bossert, J.M., Shaham, Y., and Hope, B.T. (2016). Distinct Fos-Expressing Neuronal Ensembles in the Ventromedial Prefrontal Cortex Mediate Food Reward and Extinction Memories. The Journal of neuroscience : the official journal of the Society for Neuroscience *36*, 6691-6703.

Washbourne, P., Bennett, J.E., and McAllister, A.K. (2002). Rapid recruitment of NMDA receptor transport packets to nascent synapses. Nature Neuroscience *5*, 751-759.

Wells, A.M., Lasseter, H.C., Xie, X., Cowhey, K.E., Reittinger, A.M., and Fuchs, R.A. (2011). Interaction between the basolateral amygdala and dorsal hippocampus is critical for cocaine memory reconsolidation and subsequent drug context-induced cocaine-seeking behavior in rats. Learn Mem *18*, 693-702.

Werner, C.T., Stefanik, M.T., Milovanovic, M., Caccamise, A., and Wolf, M.E. (2018). Protein translation in the nucleus accumbens is dysregulated during cocaine withdrawal and required for expression of incubation of cocaine craving. The Journal of neuroscience : the official journal of the Society for Neuroscience, 2412-2417-2415.

West, E.A., and Carelli, R.M. (2016). Nucleus Accumbens Core and Shell Differentially Encode Reward-Associated Cues after Reinforcer Devaluation. The Journal of neuroscience : the official journal of the Society for Neuroscience *36*, 1128-1139.

Whitaker, L.R., Carneiro de Oliveira, P.E., McPherson, K.B., Fallon, R.V., Planeta, C.S., Bonci, A., and Hope, B.T. (2016). Associative Learning Drives the Formation of Silent Synapses in Neuronal Ensembles of the Nucleus Accumbens. Biological Psychiatry *80*, 246-256.

Whitlock, J.R., Heynen, A.J., Shuler, M.G., and Bear, M.F. (2006). Learning induces long-term potentiation in the hippocampus. Science *313*, 1093-1097.

Wiegert, J.S., and Oertner, T.G. (2013). Long-term depression triggers the selective elimination of weakly integrated synapses. Proceedings of the National Academy of Sciences of the United States of America *110*, E4510-4519.

Wills, T.J., Lever, C., Cacucci, F., Burgess, N., and O'Keefe, J. (2005). Attractor dynamics in the hippocampal representation of the local environment. Science *308*, 873-876.

Willuhn, I., Burgeno, L.M., Everitt, B.J., and Phillips, P.E.M. (2012). Hierarchical recruitment of phasic dopamine signaling in the striatum during the progression of cocaine use. Proceedings of the National Academy of Sciences of the United States of America *109*, 20703-20708.

Wilson, C.J., and Groves, P.M. (1980). Fine structure and synaptic connections of the common spiny neuron of the rat neostriatum: a study employing intracellular inject of horseradish peroxidase. The Journal of comparative neurology *194*, 599-615.

Wilson, C.J., and Kawaguchi, Y. (1996). The origins of two-state spontaneous membrane potential fluctuations of neostriatal spiny neurons. The Journal of neuroscience : the official journal of the Society for Neuroscience *16*, 2397-2410.

Wimmer, K., Nykamp, D.Q., Constantinidis, C., and Compte, A. (2014). Bump attractor dynamics in prefrontal cortex explains behavioral precision in spatial working memory. Nature Neuroscience *17*, 431-439.

Winters, B.D., Krüger, J.M., Huang, X., Gallaher, Z.R., Ishikawa, M., Czaja, K., Krueger, J.M., Huang, Y.H., Schlüter, O.M., and Dong, Y. (2012). Cannabinoid receptor 1-expressing neurons in the nucleus accumbens. Proceedings of the National Academy of Sciences of the United States of America *109*, E2717-2725.

Winters, B.D., Tucci, M.C., and DaCosta-Furtado, M. (2009). Older and stronger object memories are selectively destabilized by reactivation in the presence of new information. Learning & memory (Cold Spring Harbor, NY) *16*, 545-553.

Wise, R.A. (1987). The role of reward pathways in the development of drug dependence. Pharmacology and Therapeutics *35*, 227-263.

Wise, R.A. (2004). Dopamine, learning and motivation. Nature Reviews Neuroscience *5*, 483-494.

Wise, R.A., and Koob, G.F. (2013). The Development and Maintenance of Drug Addiction. Neuropsychopharmacology *39*, 254-262.

Wise, R.A., and Rompre, P.P. (1989). Brain dopamine and reward. Annual review of psychology *40*, 191-225.

Wolf, M.E. (2016a). Synaptic mechanisms underlying persistent cocaine craving. Nat Rev Neurosci.

Wolf, M.E. (2016b). Synaptic mechanisms underlying persistent cocaine craving. Nature Reviews Neuroscience *17*, 351-365.

Wright, W.J., and Dong, Y. (2020). Psychostimulant-Induced Adaptations in Nucleus Accumbens Glutamatergic Transmission. Cold Spring Harbor Perspectives in Medicine, a039255-039221.

Wright, W.J., Graziane, N.M., Neumann, P.A., Hamilton, P.J., Cates, H.M., Fuerst, L., Spenceley, A., MacKinnon-Booth, N., Iyer, K., Huang, Y.H., *et al.* (2020). Silent synapses dictate cocaine memory destabilization and reconsolidation. Nature Neuroscience *23*, 32-46.

Wu, A., Yu, B., Chen, Q., Matthews, G.A., Lu, C., Campbell, E., Tye, K.M., and Komiyama, T. (2020). Context-dependent plasticity of adult-born neurons regulated by cortical feedback. Science advances *6*, eabc8319.

Wu, Y.I., Frey, D., Lungu, O.I., Jaehrig, A., Schlichting, I., Kuhlman, B., and Hahn, K.M. (2009). A genetically encoded photoactivatable Rac controls the motility of living cells. Nature *461*, 104-108.

Xia, S., Yu, J., Huang, X., Sesack, S.R., Huang, Y.H., Schlüter, O.M., Cao, J.-L., and Dong, Y. (2020). Cortical and Thalamic Interaction with Amygdala-to-Accumbens Synapses. The Journal of neuroscience : the official journal of the Society for Neuroscience, JN-RM-1121-1120-1114.

Xiao, M.-Y., Wasling, P., Hanse, E., and Gustafsson, B. (2004). Creation of AMPA-silent synapses in the neonatal hippocampus. Nature Neuroscience *7*, 236-243.

Xie, X., Lasseter, H.C., Ramirez, D.R., Ponds, K.L., Wells, A.M., and Fuchs, R.A. (2012). Subregion-specific role of glutamate receptors in the nucleus accumbens on drug context-induced reinstatement of cocaine-seeking behavior in rats. Addiction Biology *17*, 287-299.

Xu, T., Yu, X., Perlik, A.J., Tobin, W.F., Zweig, J.A., Tennant, K., Jones, T., and Zuo, Y. (2009). Rapid formation and selective stabilization of synapses for enduring motor memories. Nature *462*, 915-919.

Xue, Y.-X., Luo, Y.-X., Wu, P., Shi, H.-S., Xue, L.-F., Chen, C., Zhu, W.-l., Ding, Z.-B., Bao, Y.-p., Shi, J., *et al.* (2012). A memory retrieval-extinction procedure to prevent drug craving and relapse. Science *336*, 241-245.

Yang, G., Lai, C.S.W., Cichon, J., Ma, L., Li, W., and Gan, W.-B. (2014). Sleep promotes branch-specific formation of dendritic spines after learning. Science *344*, 1173-1178.

Yang, G., Pan, F., and Gan, W.-B. (2009). Stably maintained dendritic spines are associated with lifelong memories Nature *462*, 920-924.

Yang, H., de Jong, J.W., Tak, Y., Peck, J., Bateup, H.S., and Lammel, S. (2017). Nucleus Accumbens Subnuclei Regulate Motivated Behavior via Direct Inhibition and Disinhibition of VTA Dopamine Subpopulations. Neuron, 1-21.

Yasuda, R. (2017). Biophysics of Biochemical Signaling in Dendritic Spines: Implications in Synaptic Plasticity. Biophysical journal *113*, 2152-2159.

Yin, H.H., and Lovinger, D.M. (2006). Frequency-specific and D2 receptor-mediated inhibition of glutamate release by retrograde endocannabinoid signaling. Proceedings of the National Academy of Sciences of the United States of America *103*, 8251-8256.

Yin, H.H., Ostlund, S.B., and Balleine, B.W. (2008). Reward-guided learning beyond dopamine in the nucleus accumbens: the integrative functions of cortico-basal ganglia networks. The European journal of neuroscience *28*, 1437-1448.

Yokose, J., Okubo-Suzuki, R., Nomoto, M., Ohkawa, N., Nishizono, H., Suzuki, A., Matsuo, M., Tsujimura, S., Takahashi, Y., Nagase, M., *et al.* (2017). Overlapping memory trace indispensable for linking, but not recalling, individual memories. Science *355*, 398-403.

Yoon, K., Buice, M.A., Barry, C., Hayman, R., Burgess, N., and Fiete, I.R. (2013). Specific evidence of low-dimensional continuous attractor dynamics in grid cells. Nature Neuroscience, 1-11.

Yu, J., Yan, Y., Li, K.-L., Wang, Y., Huang, Y.H., Urban, N.N., Nestler, E.J., Schlüter, O.M., and Dong, Y. (2017). Nucleus accumbens feedforward inhibition circuit promotes cocaine self-administration. Proceedings of the National Academy of Sciences of the United States of America *56*, 201707822.

Yusifov, R., Tippmann, A., Staiger, J.F., Schlüter, O.M., and Löwel, S. (2021). Spine dynamics of PSD-95-deficient neurons in the visual cortex link silent synapses to structural cortical plasticity. Proceedings of the National Academy of Sciences of the United States of America *118*.

Yuste, R. (2015). From the neuron doctrine to neural networks. 1-11.

Zagha, E., Ge, X., and McCormick, D.A. (2015). Competing Neural Ensembles in Motor Cortex Gate Goal-Directed Motor Output. Neuron *88*, 565-577.

Zell, V., Steinkellner, T., Hollon, N.G., Warlow, S.M., Souter, E., Faget, L., Hunker, A.C., Jin, X., Zweifel, L.S., and Hnasko, T.S. (2020). VTA Glutamate Neuron Activity Drives Positive Reinforcement Absent Dopamine Co-release. Neuron, 1-15.

Zhang, X., Kim, J., and Tonegawa, S. (2020). Amygdala Reward Neurons Form and Store Fear Extinction Memory. Neuron, 1-25.

Zheng, T., and Wilson, C.J. (2002). Corticostriatal combinatorics: the implications of corticostriatal axonal arborizations. Journal of neurophysiology *87*, 1007-1017.

Zhou, J., Jia, C., Montesinos-Cartagena, M., Gardner, M.P.H., Zong, W., and Schoenbaum, G. (2020). Evolving schema representations in orbitofrontal ensembles during learning. Nature, 1-21.

Zhou, L., Furuta, T., and Kaneko, T. (2003). Chemical organization of projection neurons in the rat accumbens nucleus and olfactory tubercle. NSC *120*, 783-798.

Zhou, P., Resendez, S.L., Rodriguez-Romaguera, J., Jimenez, J.C., Neufeld, S.Q., Giovannucci, A., Friedrich, J., Pnevmatikakis, E.A., Stuber, G.D., Hen, R., *et al.* (2018). Efficient and accurate extraction of in vivo calcium signals from microendoscopic video data. eLife *7*.

Zhou, Q., Xiao, M., and Nicoll, R.A. (2001). Contribution of cytoskeleton to the internalization of AMPA receptors. Proceedings of the National Academy of Sciences *98*, 1261-1266.

Zhou, Y., Zhu, H., Liu, Z., Chen, X., Su, X., Ma, C., Tian, Z., Huang, B., Yan, E., Liu, X., *et al.* (2019). A ventral CA1 to nucleus accumbens core engram circuit mediates conditioned place preference for cocaine. Nature Neuroscience, 1-14.

Zhou, Z., Liu, A., Xia, S., Leung, C., Qi, J., Meng, Y., Xie, W., Park, P., Collingridge, G.L., and Jia, Z. (2017). The C-terminal tails of endogenous GluA1 and GluA2 differentially contribute to hippocampal synaptic plasticity and learning. Nature Neuroscience, 1-19.

Zhu, J.J., Qin, Y., Zhao, M., Van Aelst, L., and Malinow, R. (2002). Ras and Rap control AMPA receptor trafficking during synaptic plasticity. Cell *110*, 443-455.

Zhu, Y., Wienecke, C.F.R., Nachtrab, G., and Chen, X. (2016). A thalamic input to the nucleus accumbens mediates opiate dependence. Nature *530*, 219-222.

Ziminski, J.J., Hessler, S., Margetts-Smith, G., Sieburg, M.C., Crombag, H.S., and Koya, E. (2017). Changes in Appetitive Associative Strength Modulates Nucleus Accumbens, But Not Orbitofrontal Cortex Neuronal Ensemble Excitability. The Journal of neuroscience : the official journal of the Society for Neuroscience *37*, 3160-3170.

Ziminski, J.J., Sieburg, M.C., Margetts-Smith, G., Crombag, H.S., and Koya, E. (2018). Regional Differences in Striatal Neuronal Ensemble Excitability Following Cocaine and Extinction Memory Retrieval in Fos-GFP Mice. Nature Neuroscience *43*, 718-727.

Zito, K., Knott, G., Shepherd, G.M.G., Shenolikar, S., and Svoboda, K. (2004). Induction of spine growth and synapse formation by regulation of the spine actin cytoskeleton. Neuron *44*, 321-334.

Ziv, N.E., and Brenner, N. (2017). Synaptic Tenacity or Lack Thereof: Spontaneous Remodeling of Synapses. Trends in neurosciences, 1-11.

Ziv, Y., Burns, L.D., Cocker, E.D., Hamel, E.O., Ghosh, K.K., Kitch, L.J., El Gamal, A., and Schnitzer, M.J. (2013). Long-term dynamics of CA1 hippocampal place codes. Nature Neuroscience *16*, 264-266.

Zovkic, I.B., Paulukaitis, B.S., Day, J.J., Etikala, D.M., and Sweatt, J.D. (2014). Histone H2A.Z subunit exchange controls consolidation of recent and remote memory. Nature *515*, 582-586.